(CA)₁₅

(GA)₁₅

(CAA)₁₀

COVER: figure from the article inside by Kamika Sribenja, Alongklod Tanomtong, Nuntaporn Getlekha. "Chromosome Mapping of Repetitive DNAs in the Picasso Triggerfish (*Rhinecanthus aculeatus* (Linnaeus, 1758)) in Family Balistidae by Classical and Molecular Cytogenetic Techniques".

Caryologia

International Journal of Cytology, Cytosystematics and Cytogenetics

Volume 75, Issue 3 - 2022

Chromosome Mapping of Repetitive DNAs in the Picasso Triggerfish (*Rhinecanthus aculeatus* (Linnaeus, 1758)) in Family Balistidae by Classical and Molecular Cytogenetic Techniques

Kamika Sribenja[1], Alongklod Tanomtong[1], Nuntaporn Getlekha[2,*]

[1] Department of biology, Faculty of Science, Khon Kaen University, Muang, KhonKaen 40002, Thailand
[2] Department of Biology, Faculty of Science and Technology, Muban Chombueng Rajabhat University, Chombueng, Ratchaburi 70150, Thailand
*Corresponding author. E-mail: nanthaphonket@mcru.ac.th

Abstract. This work presents the cytogenetic analysis conducted on the Picasso triggerfish (*Rhinecanthus aculeatus* (Linnaeus, 1758)) from Thailand. Mitotic chromosomes were prepared from the anterior kidney. The cell suspensions were harvested by *in vivo* colchicine treatment. The present study includes the chromosomal investigation on *R. aculeatus*, using conventional (Giemsa staining, Ag-NOR and C-banding) and molecular approaches (*in situ* mapping of five different repetitive DNA classes including 18S rDNA, 5S rDNA, $(CA)_{15}$, $(GA)_{15}$ and $(CAA)_{10}$ as markers.) The results showed that *R. aculeatus* has karyotypes formed exclusively by telocentric chromosomes (44t; NF=44). The C-positive heterochromatic blocks are preferentially located in the centromeric and telomeric regions of some chromosomal pairs. The Ag-NOR sites occupy the interstitial position of the long arms of the largest telocentric pair (pair 1). The exclusive location of the major ribosomal sites in these pairs was confirmed by hybridization with 18S rDNA probes. However, the 5S rDNA genes are not located on 18S rDNA-bearing chromosomes, but instead located exclusively in the subcentromeric region of pair 4. The mapping of $(CA)_{15}$, $(GA)_{15}$ and $(CAA)_{10}$ microsatellites are sparsely dispersed along all the chromosomes. The karyotype formula of *R. aculeatus* is 2n (44) = 44t.

Keywords: Triggerfish, Chromosome, Repetitive sequences, Fish cytogenetics.

INTRODUCTION

The family Balistidae belongs to order Tetraodontiformes which includes the triggerfish of often brightly colored fish (Nelson et al., 2016). Around 40 species distributed in 12 genera are classified in this family (Allen et al., 2017). Triggerfish fishes are usually found in tropical and subtropical oceans throughout the world, with the greatest species richness in the Indo-Pacific.

The most abundance of species are found in relatively shallow, coastal habitats, especially at coral reefs (Allen et al., 2017). In the present, several species from this family are popular in the marine aquarium trade.

Out of 40 described species of Balistidae, only 15 species have been karyologically investigated: *Balistapus undulates*, *Sufflamen fraenatus* (Takai and Ojima, 1987), *Balistes capriscus* (Vitturi et al., 1988), *Balistes carolinensis* (Vitturi et al., 1992; Thode et al., 1994), *Balistes vetula* (Gustavo and Molina, 2005), *Balistoides conspicillus* (Takai and Ojima, 1987; Gustavo and Molina, 2004), *Balistoides viridescens* (Takai and Ojima, 1988), *Pseudobalistes flavimarginatus*, *Rhinecanthus verrucosus*, *Sufflamen chrysopterus* (Arai and Nagaiwa, 1976), *Rhinecanthus aculeatus* (Arai and Nagaiwa, 1976; Kitayama and Ojima, 1984), *Rhinecanthus echarpe* (Kitayama and Ojima, 1984), *Melichthys niger* (Gustavo and Molina, 2005) and *Melichthys vidua*, *Odonus niger* (Kitayam and Ojima, 1984). The members of the family Balistidae have 2n ranging from 40 to 46, and most species have the karyotype present as acrocentric and telocentric chromosomes except *B. viridescens* and *P. flavimarginatus*, which are comprised of metacentric and submetacentric chromosomes (Table 1).

The study aims to investigate the evolutionary events associated with the chromosomal diversification in the Picasso triggerfish (*Rhinecanthus aculeatus*). The chromosomal investigation was conducted by obtaining the standard karyotype and idiogram using conventional (Giemsa staining, Ag-NOR and C-banding) and molecular analyses to identify the chromosomal patterns and organization of five classes of repetitive DNAs [18S rDNA, 5S rDNA, $(CA)_{15}$, $(GA)_{15}$, and $(CAA)_{10}$]. Since there were only three previous cytogenetic studies of the genus *Rhinecanthus* showing a diploid chromosome number of 2n=44 (Arai and Nagaiwa, 1976; Kitayama and Ojima, 1984), the results obtained from this study will increase our basic knowledge of the cytogenetics of *R. aculeatus*, which could form the basis for future research and support taxonomy of genus *Rhinecanthus*.

MATERIAL AND METHODS

Specimens collected and conventional methods

Cytogenetic analyses were conducted on the Picasso triggerfish, *Rhinecanthus aculeatus* (4 males and 4 females) from Thailand Gulf (Figure 1). The specimens were caught using a hand-net, placed in sealed plastic bags containing oxygen and clean water and transported to the research station. The experiments followed ethical protocols and

Table 1. Cytogenetic reviews of the family Balistidae (8 genera).

No.	Subfamily/Species	2n	NF	NORs	Formula	References
1	*Balistapus undulates*	42	42	2	42a/t	Takai and Ojima (1987)
2	*Balistes capriscus*	44	44	2	44t	Vitturi et al. (1988)
3	*B. carolinensis*	44	44	2	44t	Vitturi et al. (1992)
		44	44	2	44t	Thode et al. (1994)
4	*B. vetula*	44	44	2	44t	Gustavo and Molina (2005)
5	*Balistoides conspicillus*	44	44	2	44t	Takai and Ojima (1987)
		44	44	2	44t	Gustavo and Molina (2004)
6	*B. viridescens*	44	48	2	2m+2sm+40a/t	Takai and Ojima (1988)
		44	60	3	2m+14a+28t	Supiwong et al. (2013)
7	*Melichthys niger*	40	40	2	40t	Gustavo and Molina (2005)
		40	40	2	40a/t	de Lima et al. (2011)
8	*M. vidua*	40	40	2	40a/t	Kitayama and Ojima (1984)
9	*Odonus niger*	42	–	–	42a/t	Kitayama and Ojima (1984)
10	*Pseudobalistes flavimarginatus*	44	–	–	2m+42a/t	Arai and Nagaiwa (1976)
11	*Rhinecanthus aculeatus*	44	44	2	44t	Arai and Nagaiwa (1976)
		44	44	2	44t	Kitayama and Ojima (1984)
12	*R. echarpe*	44	–	2	44a/t	Kitayama and Ojima (1984)
13	*R. verrucosus*	44	44	2	44t	Arai and Nagaiwa (1976)
14	*Sufflamen chrysopterus*	46	46	–	46a/t	Arai and Nagaiwa (1976)
15	*S. fraenatus*	46	46	2	46a/t	Takai and Ojima (1987)

Remarks: 2n = diploid chromosome number, NF = fundamental number (number of chromosome arm), m = metacentric, sm = submetacentric, a = acrocentric, t = telocentric chromosome, NORs = nucleolar organizer regions and – = not available.

Figure 1. General characteristic of *Rhinecanthus aculeatus*, its respective collection sites in the Indian (Andaman Sea) and Pacific Oceans (Gulf of Thailand).

anesthesia with clove oil prior to sacrificing the animals to minimize suffering. The process was approved by the Ethics Committee of Khon Kaen University and by the RGJ Committee under no. PHD/K0081/2556. Mitotic chromosomes were obtained from cell suspensions of the anterior kidney, using the conventional air-drying method. The C-banding method was also employed to detect the distribution of C-positive heterochromatin and silver staining to detect the Ag-NOR location on chromosomes. The specimens were deposited in the fish collection of the Cytogenetic Laboratory, Department of Biology, Faculty of Science, Khon Kaen University.

Chromosome probes and FISH experiments

Two tandemly arrayed DNA sequences isolated from the genome of an Erythrinidae fish species, *Hoplias malabaricus*, were used as probes. The first probe contained a 5S rDNA repeat and included 120 base pairs (bp) of the 5S rRNA transcribed gene and 200 bp of the non-transcribed spacer (NTS) sequence. The second probe contained a 1400 bp segment of the 18S rRNA gene obtained via PCR from the nuclear DNA. The 5S and 18S rDNA probes were cloned into plasmid vectors and propagated in DH5a *Escherichia coli* competent cells (Invitrogen, San Diego, CA, USA). The 5S and 18S rDNA probes were labeled with Spectrum Green-dUTP and Spectrum Orange-dUTP, respectively, using nick translation according to the manufacturer's recommendations (Roche, Mannheim, Germany).

The microsatellites $(CA)_{15}$, $(GA)_{15}$, and $(CAA)_{10}$ were synthesized. These sequences were directly labeled with Cy3 at the 5' terminus during synthesis by Sigma (St. Louis, MO, USA).

Fluorescence *in situ* hybridization (FISH) was performed under high stringency conditions (Yano et al., 2017). Metaphase chromosome slides were incubated with RNAse (40 μg/ml) for 1.5 h at 37°C. After the denaturation of the chromosomal DNA in 70% formamide/2x SSC at 70°C for 4 min, 20 μl of the hybridization mixture (2.5 ng/μl probes, 2 μg/μl salmon sperm DNA, 50% deionized formamide, 10% dextran sulphate) was dropped on the slides, and the hybridization was performed overnight at 37°C in a moist chamber containing 2x SSC. The first post-hybridization wash was performed with 2x SSC for 5 min at 65°C, and a final wash was performed at room temperature in 1x SSC for 5 min. Finally, the slides were counterstained with DAPI and mounted in an antifade solution (Vectashield from Vector Laboratories).

Image processing

Approximately 20 metaphase spreads were analyzed to confirm the diploid chromosome number, karyotype structure and FISH results. Images were captured using an Olympus BX50 microscope (Olympus Corporation, Ishikawa, Japan) with CoolSNAP and the Image Pro Plus 4.1 software (Media Cybernetics, Silver Spring, MD, USA). Chromosomes were classified according to their arm ratios as metacentric (m), submetacentric (sm), acrocentric (a) or telocentric (t).

RESULTS

The Picasso triggerfish (*Rhinecanthus aculeatus*) have 2n=44. Its karyotype is formed exclusively by telocentric chromosomes (44t) and a fundamental number (NF=44) (Figure 2). The C-positive heterochromatic blocks are preferentially located in the centromeric regions, with some pairs exhibiting blocks in the telomeric ones (Figure 2). The Ag-NOR sites are located in the interstitial region of the long arms of the largest telocentric pair (pair 1), the exclusive location of major ribosomal sites in these regions was confirmed by *in situ* hybridization with 18S rDNA probes (Figure 2). However, the 5S rDNA genes are not located on 18S rDNA-bearing chromosomes, but instead located exclusively in the subcentromeric region of pair 4, while the 18S rDNA sites are instead located on the interstitial position of the long arms of pair 1 (Figure 2).

The chromosomal mapping of all microsatellite sequences indicates a weak and dispersed distribution, without preferential accumulations in any of the chromosomal pairs (Figure 3). The $(CA)_{15}$ $(GA)_{15}$ and $(CAA)_{10}$
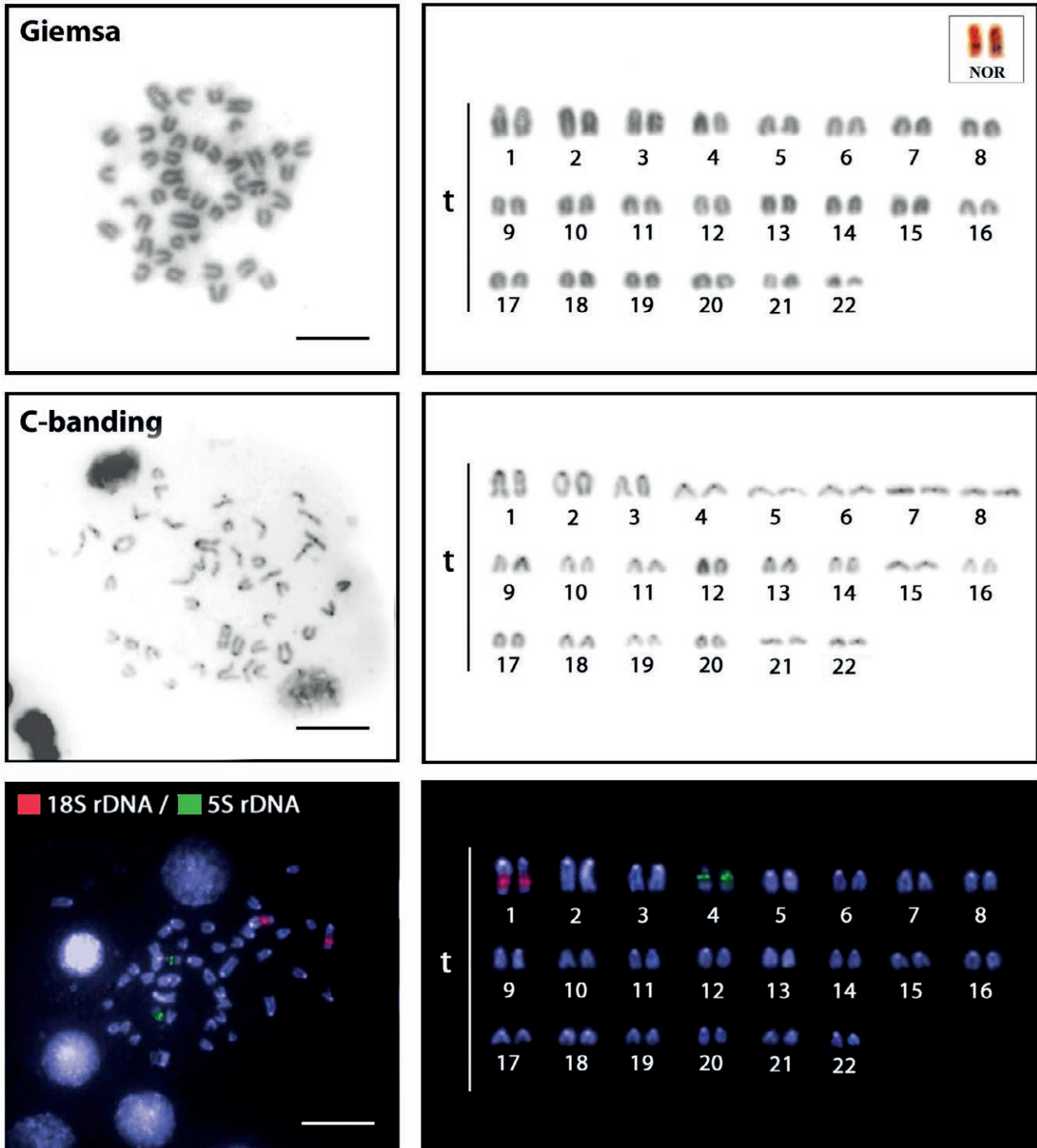
Figure 2. Mataphase and karyotypes of *Rhinecanthus aculeatus* arranged from conventionally Giemsa-stained, Ag-stained (highlighted in the boxes), C-banded and after fluorescence *in situ* hybridization with 5S and 18S rDNA probes. Bar 5 μm.

microsatellites are sparsely dispersed in most chromosomes though they can still form conspicuous clusters. They however exhibit less defined clusters in some chromosome pairs (Figure 3). These clusters occupy the centromeric regions of chromosomes but at rather low frequency. For all the chromosomal markers, no differential hybridization patterns were detected between males and females.
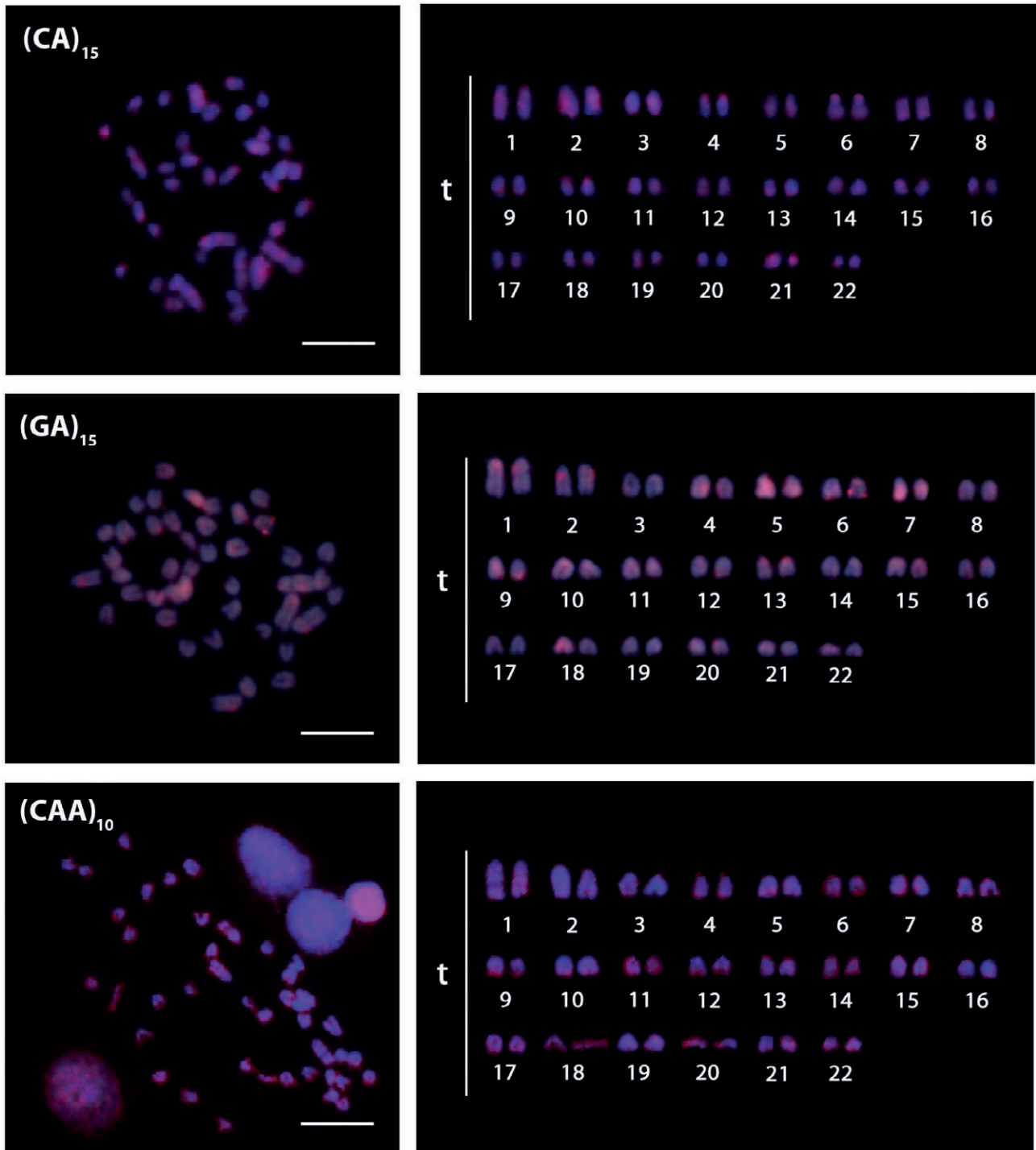
Figure 3. Chromosomal mapping of di- and tri-nucleotide microsatellites in the chromosomes of *Rhinecanthus aculeatus* by fluorescence *in situ* hybridization. The general distribution pattern of $(CA)_{15}$, $(GA)_{15}$ and $(CAA)_{10}$ microsatellites is mainly diffuse, with the occurrence of few conspicuous clusters in some centromeric and chromosome arm regions. Bar = 5 μm.

The idiogram of *R. aculeatus* represents gradually declining length of the chromosomes (Figure 4). The karyotype is notably attributed solely to telocentric chromosomes. The karyotype formula of *R. aculeatus* is as follow: 2n (44) = 44t
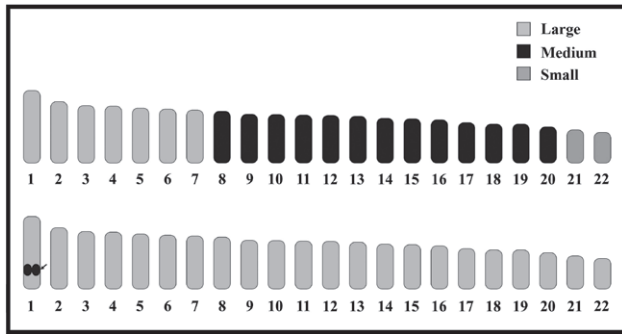
Figure 4. Standardized idiogram showing lengths and shapes of chromosomes of *Rhinecanthus aculeatus* (2*n*=44) by conventional staining and Ag-NOR banding techniques. The arrow indicates nucleolarnucleolar organizer regions.

DISCUSSIONS

Karyotype uniformity among Rhinecanthus *species*

Cytogenetic analyses were conducted on *Rhinecanthus aculeatus* from the Gulf of Thailand (Indo-Pacific). The 2n of *R. aculeatus* is 44 chromosomes in all specimens, with karyotypes predominantly formed by telocentric chromosomes (Figure 2, 3 and Table 2). However, considerable cytogenetic research has been conducted on a number of species in the family Balistidae (Table 1). The karyotype of *Rhinecanthus aculeatus* is 44t; this finding is consistent with that of other species in the genera *Rhinecanthus*, *Balistes*, and *Balistoides*, particularly *Balistes capriscus*, *B. carolinensis*, *B. vetula*, *Balistoides conspicillus*, *Rhinecanthus aculeatus*, *R. echarpe*, and *R. verrucosus*, which still have 2n=44t. It suggests that even after speciation, their karyotypes remain conserved. Although *B. viridescens* and *Pseudobalistes flavimarginatus* have the same number of chromosomes (2n=44) with above species but exhibit an asymmetrical karyotype due to both species are the high variability of chromosomal rearrangements and their higher adaptive divergence. Moreover, like all other species in the family Balistidae, in which the morphologically differentiated sex chromosome could not be observed (Arai and Nagaiwa, 1976; Kitayama and Ojima, 1984).

In addition, *Rhinecanthus* species exhibited karyotypes which are broadly similar in structural patterns, with all of them displaying 2n = 44 and a high number of telocentric chromosomes. These characteristics present in all of the *Rhinecanthus* species analyzed so far (Arai and Nagaiwa, 1976; Kitayama and Ojima, 1984; Montanari et al. 2016; present study).

Chromosome markers of R. aculeatus

The only one pair which bear Ag-NOR/18S rDNA sites are useful chromosomal markers shared among the *Rhinecanthus* species. The result here is also similar to the chromosome bearing nucleolar organizer region in previous studies (Table 1) except *Balistoides viridescens* that found tree NORs (Supiwong et al., 2013) this suggests that this event may be related to chromosomal change during evolution.

Furthermore, the interstitial region of the largest telocentric chromosome pair 1 of *R. aculeatus* showed clearly observable nucleolar organizer regions. This is quite consistent with the report by de Lima et al. (2011) on the karyotype of *Melichthys niger* in the same family. Their study reported the presence of a conspicuous secondary constriction in the interstitial position on the long arm of the chromosome pair No. 2 which was, corresponding to the nucleolar organizer regions, identified by Ag-NOR sites and by *in situ* hybridization with an 18S rDNA ribosomal probe.

Normally, most fishes have only one pair of NORs on chromosomes. Only some fishes have more than two NORs, which may be caused by the translocation between some parts of the chromosomes that have NOR and another chromosome (Sharma et al., 2002). The present study shows that the species analyzed presents NOR site on a single chromosome pair. This is considered a simple isomorphic condition in fish (Almeida-Toledo, 1985). Another peculiar cytogenetic aspect of Tetraodontiformes is the small quantity of heterochromatic regions, localized in telomeric or centromeric positions on most of the chromosome pairs (Supiwong et al., 2013).

Organization of repetitive DNAs in the chromosomes of R. aculeatus

The C-positive heterochromatins in the chromosomes of *R. aculeatus* are distributed in centromeric and telomeric positions in most of the chromosomes (Figure 2). This recurring distribution pattern is similar to those reported for species of other *Balistidae* genera, such as *Melichthys* (de Lima et al., 2011).

The 18S rDNA sites are equally located on the interstitial position of pair 1, whereas 5S rDNA sites occur in the subcentromeric region of pair 4. The non-syntenic organization of these genes is frequent and it could be a plesiomorphic condition in Balistidae.

This is the first report of the presence of microsatellite sequences in the heterochromatin of *R. aculeatus* which show recognizable organizational patterns.

Table 2. Mean length of short arm chromosome (Ls), length long arm chromosome (Ll), length total arm chromosome (LT), relative length (RL), centromeric index (CI) and standard deviation (SD) of RL, CI from 20 metaphase cells of the male and female the Picasso triggerfish (*Rhinecanthus aculeatus*), 2*n*=44.

Chromosome pair	Ls	Ll	LT	RL±SD	CI±SD	Chromosome type
1*	0.00	2.60	2.60	0.070±0.009	1.000±0.000	telocentric
2	0.00	2.20	2.20	0.059±0.004	1.000±0.000	telocentric
3	0.00	2.06	2.06	0.056±0.005	1.000±0.000	telocentric
4	0.00	2.04	2.04	0.055±0.004	1.000±0.000	telocentric
5	0.00	1.97	1.97	0.052±0.003	1.000±0.000	telocentric
6	0.00	1.93	1.93	0.051±0.003	1.000±0.000	telocentric
7	0.00	1.90	1.90	0.051±0.005	1.000±0.000	telocentric
8	0.00	1.86	1.86	0.049±0.003	1.000±0.000	telocentric
9	0.00	1.75	1.75	0.047±0.003	1.000±0.000	telocentric
10	0.00	1.74	1.74	0.047±0.004	1.000±0.000	telocentric
11	0.00	1.72	1.72	0.046±0.005	1.000±0.000	telocentric
12	0.00	1.71	1.71	0.045±0.003	1.000±0.000	telocentric
13	0.00	1.68	1.68	0.044±0.003	1.000±0.000	telocentric
14	0.00	1.61	1.61	0.043±0.003	1.000±0.000	telocentric
15	0.00	1.59	1.59	0.042±0.003	1.000±0.000	telocentric
16	0.00	1.55	1.55	0.041±0.003	1.000±0.000	telocentric
17	0.00	1.45	1.45	0.038±0.003	1.000±0.000	telocentric
18	0.00	1.40	1.40	0.036±0.005	1.000±0.000	telocentric
19	0.00	1.40	1.40	0.036±0.006	1.000±0.000	telocentric
20	0.00	1.30	1.30	0.034±0.006	1.000±0.000	telocentric
21	0.00	1.19	1.19	0.030±0.007	1.000±0.000	telocentric
22	0.00	1.10	1.10	0.028±0.007	1.000±0.000	telocentric

Remark: * NOR-bearing chromosome.

The $(CA)_{15}$ $(GA)_{15}$ and $(CAA)_{10}$ microsatellites present a weak and diffuse distribution on all chromosomes, but they also present a small number of conspicuous clusters characterized by intense signs in some parts of chromosomes (Figure 3). Thus, this data is useful for comparing the phylogenetic proximity of this genus that may share the same distribution pattern of the microsatellite sequences which points to independent evolutionary pathways, constituting homoplastic chromosomal characters. However, since these sequences are subject to high rates of change, their distribution may show marked evolutionary differentiation (Cioffi et al., 2011; Molina et al., 2014a; 2014b). In fact, the organization of microsatellite sequences demonstrates the particular arrangements that repetitive DNAs can be achieved in different species.

Chromosome evolution of the family Balistidae

Chromosomal rearrangements represent the main cause of karyotype diversification among several Perci-formes species (Arai, 2011; Molina and Galetti, 2002). The different Balistidae species underwent an extremely diversified karyotype evolution, considering the numerical and structural aspects of their complements, with diploid chromosome number varying from 2n=40 to 46, and marked differences in the NF that varied from 40 to 60, possibly due to the occurrence of pericentric inversions (Getlekha et al., 2018). Analyses performed highlight the combined importance of the different chromosome rearrangements in the evolutionary modelling of their karyotypes, such as centric fission fusion, and especially pericentric inversions (Getlekha et al., 2016a; 2016b).

The family Balistidae has 2n values lower than 2n=48 with most of their representatives presenting acrocentric and telocentric chromosomes. This karyotypic pattern was also observed in the present study in *R. aculeatus* (2n=44). The origin of the reduced diploid chromosome numbers in these species seems to be centric fissions but chromosome lost in tandem, which seems to be common in other species of the family (Arai and Nagaiwa 1976; Marques et al., 2016).

CONCLUSION

Based on the chromosome study of the Picasso triggerfish (*R. aculeatus*) using conventional analyses (Giemsa staining, Ag-NOR and C-banding) and molecular analysis (*in situ* mapping of five different repetitive DNA classes including 18S rDNA, 5S rDNA, $(CA)_{15}$, $(GA)_{15}$ and $(CAA)_{10}$ as markers), this research can verify diploid chromosome, fundamental number and distribution patterns of microsatellites on the chromosomes. The results show that *R. aculeatus* has 2n=44 with predominantly telocentric chromosome. The fundamental number (NF) was 44. The C-positive heterochromatic blocks are preferentially located in the centromeric and telomeric regions of some chromosomal pairs. The Ag-NORs sites were located on the interstitial region of long arms of the telocentric chromosome pair 1. The exclusive location of the major ribosomal sites in these pairs was confirmed by *in situ* hybridization with 18S rDNA probes. However, the 5S rDNA genes are not located on 18S rDNA-bearing chromosomes, but instead located exclusively in the subcentromeric region of pair 4. The mapping of $(CA)_{15}$, $(GA)_{15}$ and $(CAA)_{10}$ microsatellites are sparsely dispersed along all the chromosomes.

The idiogram of *R. aculeatus* represents gradually declining length of the chromosomes. The karyotype is notably attributed solely to telocentric chromosomes Like in common ancestor of marine fish, the high ability of distribution results in high gene flow and low chromosome evolution. The karyotype formula of *R. aculeatus* is 2n (44) = 44t.

Up to the present, there are 3 species of the Genus *Rhinecanthus* that were cytogenetically analyzed. *Rhinecanthus* species provides remarkable karyotype features for chromosomal and genetic conservatism discussion. Further studies of other species as well as additional information from molecular chromosome analyses are expected to explain the karyotype pattern and chromosome evolution in these fishes.

REFERENCES

Allen, G.R., Erdmann, M.V. & Purtiwi, P.D. (2017). Descriptions of four new species of damselfishes (Pomacentridae) in the Pomacentrus philippinus complex from the tropical western Pacific Ocean. Journal of the Ocean Science Foundation 25:47–76.

Almeida-Toledo, L.F. (1985). As regiões organizadoras do nucléolo em peixes. Cienc. Cult. 37: 448–453.

Arai, R. (2011). Fish Karyotypes: a check list. Tokyo: Springer.

Arai, R. & Nagaiwa, K. (1976). Chromosomes of tetraodontiform fishes from Japan. Bull. Natl. Sci. Mus. Tokyo 2: 59–72.

Cioffi, M.B., Molina, W.F., Moreira-Filho, O., & Bertollo, L.A.C. (2011). Chromosomal distribution of repetitive DNA sequences high- lights the independent differentiation of multiple sex chromo- somes in two closely related fish species. Cytogenet Genome Res 134:295–302.

de Lima, L.C.B., Martinez, P.A. & Molina, W.F. (2011). Cytogenetic characterization of three Balistoidea fish species from the Atlantic with inferences on chromosomal evolution in the families Monacanthidae and Balistidae. Comparative Cytogenetics 5(1): 61–69.

Getlekha, N., Molina, W.F., Cioffi, M.B., Yano, C.F., Maneechot, N., Bertollo, L.A.C., Supiwong, W. & Tanomtong, A. (2016a). Repetitive DNAs highlight the role of chromosomal fusions in the karyotype evolution of Dascyllus species (Pomacentridae, Perciformes). Genetica 144:203–211.

Getlekha, N., Cioffi, M.B., Yano, C.F., Maneechot, N., Bertollo, L.A.C., Supiwong, W., Tanomtong, A. & Molina, W.F. (2016b). Chromosome mapping of repetitive DNAs in sergeant major fishes (Abudefdufinae, Pomacentridae): a general view on the chromosomal conservatism of the genus. Genetica 144:567–576.

Getlekha, N., Cioffi, M.B., Maneechot, N., Bertollo, L.A.C., Supiwong, W., Tanomtong, A.and Molina, W.F. (2018). Contrasting Evolutionary Paths Among Indo-Pacific Pomacentrus Species Promoted by Extensive Pericentric Inversions and Genome Organization of Repetitive Sequences. Zebrafish. 15(1): 45–54.

Gustavo, S. L. & Molina, W. F. (2004). Inferências sobre a evolução cariotípica em Balistidae, Diodontidae, Monacanthidae e Tetraodontidae (Pisces, Tetraodontiformes). Exemplo de extensa diversificação numérica. M.Sc. Thesis. Universidade Federal do Rio Grande do Norte, Brazil.

Gustavo, S. L. & Molina, W. F. (2005). Karyotype diversification in fishes of the Balistidae, Diodontidae and Tetraodontidae (Tetraodontiformes). Caryologia 58: 229–237.

Kitayama, E. & Ojima, Y. (1984). A preliminary report on the phylogeny of five balistid fish in terms of several chromosome banding techniques in combination with a statistical analysis. Proc. Jpn. Acad., Ser. B, Phys. Biol. Sci. 60: 58–61.

Marques, D.A., Lucek, K., Meier, J.I,. Mwaiko, S., Wagner, C.E., Excoffier, L. & Seehausen, O. (2016). Genomics of rapid incipient speciation in sympatric threespine stickleback. PLOS Genetics 12:2:e1005887.

Molina, W.F. & Galetti, P.M. (2002). Robertsonian rearrangements in the reef fish Chromis (Perciformes, Pomacentridae) involving chromosomes bearing 5S rRNA genes. Genet Mol Biol 25:373–377.

Molina, W.F., Martinez, P.A., Bertollo, L.A. & Bidau, C.J. (2014a). Evidence for meiotic drive as an explanation for karyotype changes in fishes. Mar Genomics 15:29–34.

Molina, W.F., Martinez, P.A., Bertollo, L.A. & Bidau, C.J. (2014b) Preferential accumulation of sex and Bs chromosomes in biarmed karyotypes by meiotic drive and rates of chromosomal changes in fishes. An Acad Bras Ciênc 2014b;86:4:1801–1812.

Montanari, S.R., Hobbs, J.P., Pratchett, M.S. and van Herwerden, L. (2016). The importance of ecological and behavioural data in studies of hybridisation among marine fishes. Reviews in Fish Biology and Fisheries 26:181–198.

Nelson, J.S., Grande, T.C. & Wilson, M.V.H. (2016) Fishes of the World. 5th ed. Hoboken : John Wiley and Sons, Inc.

Sharma, O.P., Tripathi, N.K. & Sharma, K.K. (2002). A review of chromosome banding in fishes. In: Sobti, R. C., ed. Some aspects of chromosome structure and functions. Narosa Publishing House, New Delhi.

Supiwong, W., Tanomtong, A. Jumrusthanasan, S. & Sanoamuang, L. (2013). Standardized Karyotype and Idiogram of Titan Triggerfish, Balistoides viridescens (Tetraodontiformes, Balistidae) in Thailand. CYTOLOGIA 78(4):345–351.

Takai, A. & Ojima, Y. (1988). Karyotype and banding analyses in a balisted fish, Balistoides viridescens "gomamongara." Chromosome. Inform. Serv. 45: 25–27.

Takai, A. & Ojima, Y. (1987). Comparative chromosomal studies in three balistid fishes. La Kromosomo, II 47/48: 1545–1550.

Thode, G., Amores, A., & Martinez, G. (1994). The karyotype of Balistes carolinensis Gmelin (Pisces, Tetraodontiformes), a specialized species. Caryologia 47: 257–263.

Vitturi, R., Catalano, E., & Colombera, D. (1992). Karyotype analyses of the teleostean fish Balistes carolinensis and Lophius piscatorius suggest the occurrence of two different karyoevolutional pathways. Biol. Zent. Bl. 111: 215–222.

Vitturi, R., Zava, B., Catalano, E., Maiorca, A. & Macaluso, M. (1988). Karyotypes in five Mediterranean teleostean fishes. Biol. Zent. Bl. 107: 339–344.

Yano, C.F, Bertollo, L.A.C. & Cioffi, M.B. (2017). Fish-FISH: Molecular Cytogenetics in Fish Species. In: Fluorescence in situ Hybridization (FISH)- Application Guide. 2nd edn, Liehr, T. (ed) Springer, Berlin, pp. 429–444.

Caryologia

International Journal of Cytology,
Cytosystematics and Cytogenetics

Chromosome number of some *Satureja* species from Turkey

Esra Kavcı[1], Esra Martin[1], Halil Erhan Eroğlu[2,*], Fatih Serdar Yıldırım[3]

[1] Necmettin Erbakan University, Faculty of Science, Department of Biotechnology, Konya, Turkey
[2] Yozgat Bozok University, Faculty of Science and Arts, Department of Biology, Yozgat, Turkey
[3] Akdeniz University, Faculty of Education, Department of Science Education, Antalya, Turkey
*Corresponding author: herhan.eroglu@bozok.edu.tr

Abstract. The genus *Satureja* belonging to the Lamiaceae family includes about 200 species, generally aromatic, distributed in the Mediterranean basin. In genus *Satureja*, the chromosomal data were reported from only 26 species. In this study, it is aimed to eliminate the deficiencies in the chromosomal data of *Satureja* species, which are distributed in Turkey, which is center of origin and diversity of the genus *Satureja*. It was reported only one chromosome number ($2n = 30$), the first report for chromosome numbers of three taxa, the same chromosome count (excluding B-chromosomes) with previous report in only one species, and the new chromosome number in only one species. In conclusion, this study presented new data into the chromosomal records of genus *Satureja* that might be useful for interpreting or understanding relationships among the species. In addition, dysploidy and polyploidy variations might probably have played an important role in speciation. In this regard, the results contributed to some missing data in *Satureja* cytotaxonomy.

Keywords: *Satureja*, chromosome, dysploidy, polyploidy, Turkey.

INTRODUCTION

The genus *Satureja* L. belonging to the Lamiaceae family includes about 200 species, generally aromatic, distributed in the Mediterranean basin. *Satureja* species are distributed in Morocco, Libya, Saudi Arabia, Caucasus, Iran, Iraq and Turkey, which are mostly Mediterranean countries from Europe, Asia and North Africa. Turkey is center of origin and diversity of the genus *Satureja* (Harley et al. 2004; Dirmenci et al. 2019).

According to Flora of Turkey records, the genus *Satureja* is represented by a total of 15 species, five of which are endemic. *Satureja* species, popularly known as "pointed thyme" or "stone thyme", have a wide range of uses in the food, pharmaceutical and cosmetic industries due to high amounts of thymol

and carvacrol (Momtaz and Abdollahi 2010; Dirmenci et al. 2019). The dried leaves of *Satureja* species are used as spice, food additive and herbal tea (Babajafari et al. 2014). The genus *Satureja* has been the focus of many studies due to its biological activities such as antimicrobial, antioxidant and anti-HIV-1. It has been stated that the rich essential oil (eg mono- and sesquiterpenes) and phenolic content (eg phenolic acids, catechins, and flavonoids) of *Satureja* species are responsible for these activities (Eminağaoğlu et al. 2007; Bektaş 2020).

Cytotaxonomy is a branch of taxonomy that uses karyological parameters to classify organisms. In cytotaxonomy, chromosomal configuration is the most widely used parameter to understand the relationship between organisms. Inference of species relationships is based on the assumption that closely related species share similar features in their chromosomal arrangement. By analyzing similarities and differences in chromosomes, karyotype evolution and species evolution can be reconstructed. The number, structure and behaviour of chromosomes are very valuable in taxonomy and the chromosome numbers (x, $2n$) are the most commonly used characters (Guerra 2008; Eroğlu et al. 2020; Martin et al. 2020; Eroğlu et al. 2021). In genus *Satureja*, the chromosomal data were reported from only 26 species. Eighteen species were only diploid; however, they revealed two different basic numbers: $x = 13$ ($2n = 26$) and $x = 15$ ($2n = 30$). Seven species were polyploid and revealed two different polyploidy levels: tetraploidy ($2n = 4x = 24$, 28, 44, and 60) and hexaploidy ($2n = 6x = 48$). The polyploid species revealed four different basic numbers such as $x = 6$, 7, 11, and 15. *Satureja sahendica* Bornm. had diploid and polyploid records. In addition, *S. hortensis* L. presented dysploidy, which is an alteration in basic number, generally by fusion, without the significant loss or gain of genetic material (Shariat et al. 2013; Irani et al. 2014; Bordbar et al. 2021; Chromosome Counts Database 2022; Vozhdehnazari et al. 2022).

In Turkish *Satureja*, the chromosomal data were reported from eight species, which were *S. macrantha* C.A. Mey. ($2n = 24$), *S. coerulea* Janka, *S. cuneifolia* Ten., *S. pilosa* Velen. *S. thymbra* L. ($2n = 30$), *S. spinosa* L. ($2n = 30 + 2B$), *S. spicigera* Boiss. ($2n = 44$, 60), and *S. hortensis* ($2n = 45$-48) (Shariat et al. 2013; Irani et al. 2014; Chromosome Counts Database 2022; Vozhdehnazari et al. 2022). There was no record of the chromosome number of seven species, which were *S. aintabensis* P.H.Davis, *S. amani* P.H.Davis, *S. boissieri* Hausskn. ex Boiss., *S. cilicica* P.H.Davis, *S. icarica* P.H.Davis, *S. parnassica* Heldr. & Sartori ex Boiss., and *S. wiedemanniana* Lall. ex Velen. Therefore, the lack of some chromosomal reports from Turkey, which is located in the Mediterranean Basin, may lead to some uncertainties in the cytotaxonomy. In this study, it is aimed to eliminate the deficiencies in the chromosomal data of *Satureja* species, which are distributed in Turkey, which is center of origin and diversity of the genus.

MATERIALS AND METHODS

Plant material

Within the scope of this study, *S. aintabensis*, *S. boissieri*, *S. icarica*, *S. macrantha* and *S. spinosa* distributed in different localities of Turkey were examined by chromosome numbers. The examined plant samples were collected from their natural habitats and identified by Prof. Dr. Tuncay Dirmenci et al (Figure 1). The collected plant samples were preserved in Balıkesir University, Necatibey Faculty of Education, Department of Biology Education. The distribution regions and collection information are given in Figure 2 and Table 1.

Cytogenetic procedure

The seeds of the collected plant samples were kept at -40°C for 1 month and then planted in petri dishes. The samples were kept in the dark at 4°C for 21 days, and at the end of 21 days, the samples placed in the climate cabinet were kept until the root tip tissue reached a few centimeters in length. Germinated root tips were kept in α-monobromonaphthalene for 16 hours at 4°C for the first treatment. Afterwards, root tips were fixed in 3:1 absolute alcohol:glacial acetic acid and stored in 70% alcohol in the refrigerator. The root tips were removed from the refrigerator, hydrolyzed in 1N HCl at room temperature for 10 minutes and stained with 2% aceto-orcein for 2 hours at room temperature. Then, squash preparations were prepared with 45% acetic acid. After the preparations were frozen in liquid nitrogen, they were dried at room temperature and stabilized with Depex medium (Martin et al. 2018; Eroğlu et al. 2021).

Ten metaphase plates were used for counting the somatic chromosomes of each species. After the mitotic chromosomes, which were well distributed, had good morphology, and were on the same plane, were detected, their photographs were taken at 1000× magnification with a camera attached to the microscope (Olympus BX51). The chromosome photographs were analyzed using the Image Analysis System (Bs200ProP).
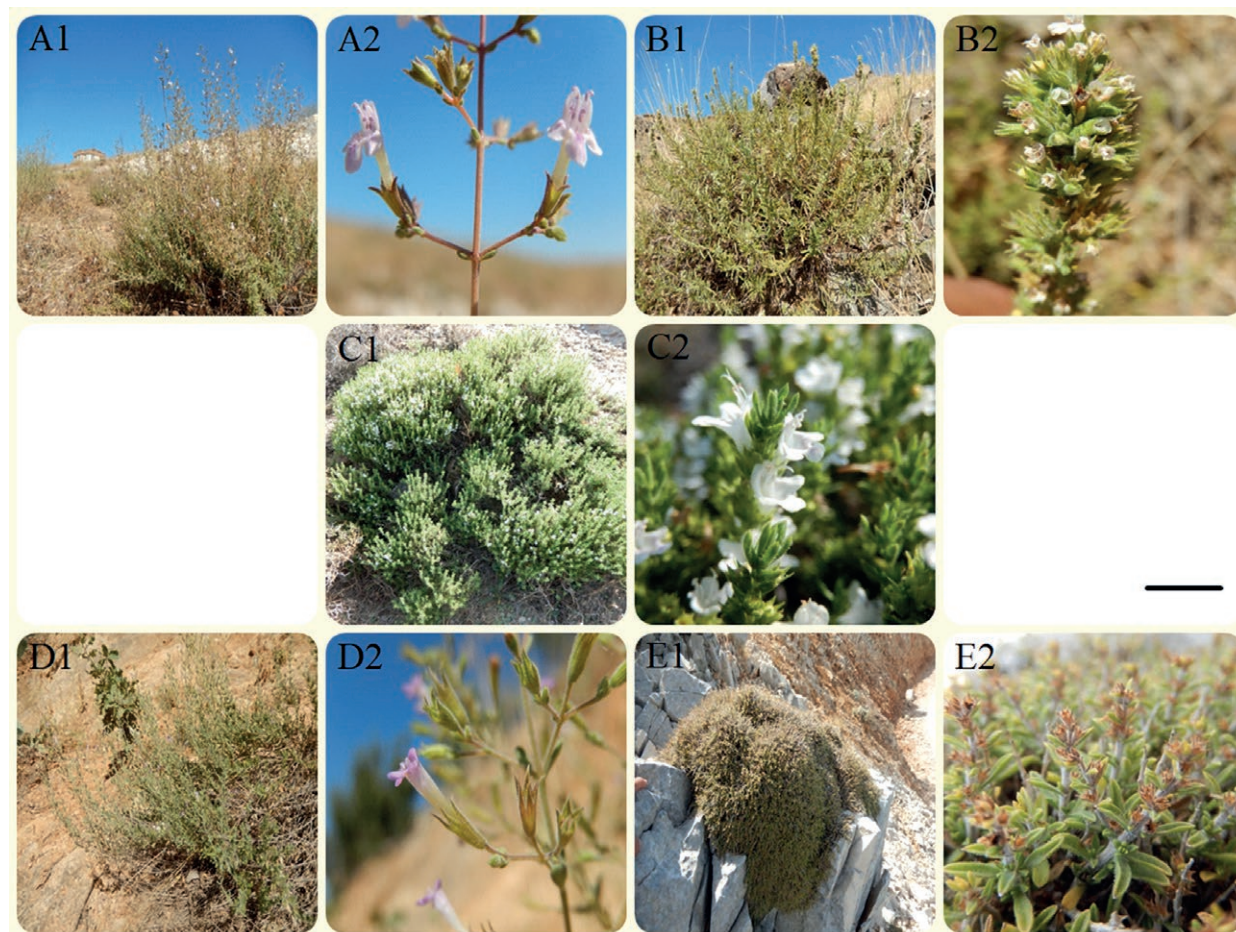
Figure 1. Habitat (1) and flowers (2) of *Satureja* species. (A) *S. aintabensis*; (B) *S. boissieri*; (C) *S. icarica*; (D) *S. macrantha*; and (E) *S. spinosa*. Scale bar, 10 cm for habitat (1) and 5 mm for flowers (2).
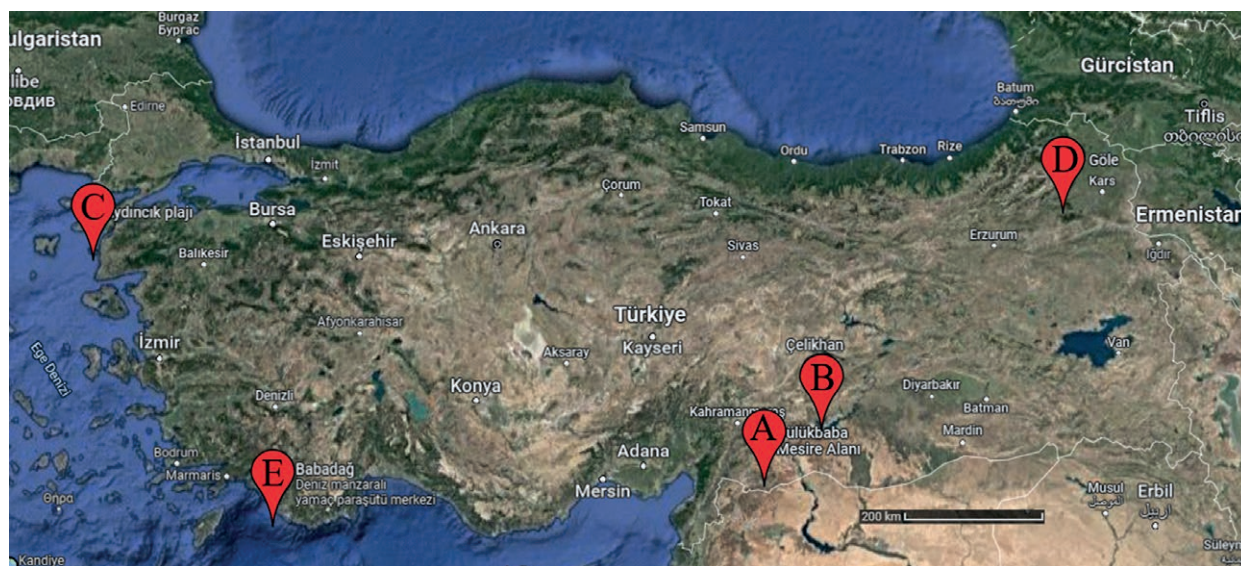
Figure 2. Distribution map of the studied species in Turkey. (A) *S. aintabensis*; (B) *S. boissieri*; (C) *S. icarica*; (D) *S. macrantha*; and (E) *S. spinosa*.

Table 1. The collection information and localities of studied *Satureja* species.

Species	Collection cite	Altitude	Date	Voucher number
S. aintabensis	Gaziantep, Samköy, Behind Dülükbaba promenade.	1000 m	03.09.2018	Dirmenci 5210 & Arabacı
S. boissieri	Adıyaman, Çelikhan, between Yazıbaşı village and Ulubaba mountain, 8th km.	1700 m	02.09.2018	Dirmenci 5207 & Arabacı
S. icarica	Çanakkale, between Gökçeada and Aydıncık, 2nd-3rd km.	300 m	15.08.2018	Dirmenci 5166
S. macrantha	Ardahan, between Göle and Şenkaya, 10th km.	1800 m	31.08.2018	Dirmenci 5196 & Arabacı
S. spinosa	Muğla, Fethiye, Babadağ, above telpher.	1900 m	11.09.2018	Dirmenci 5224 & Yıldız
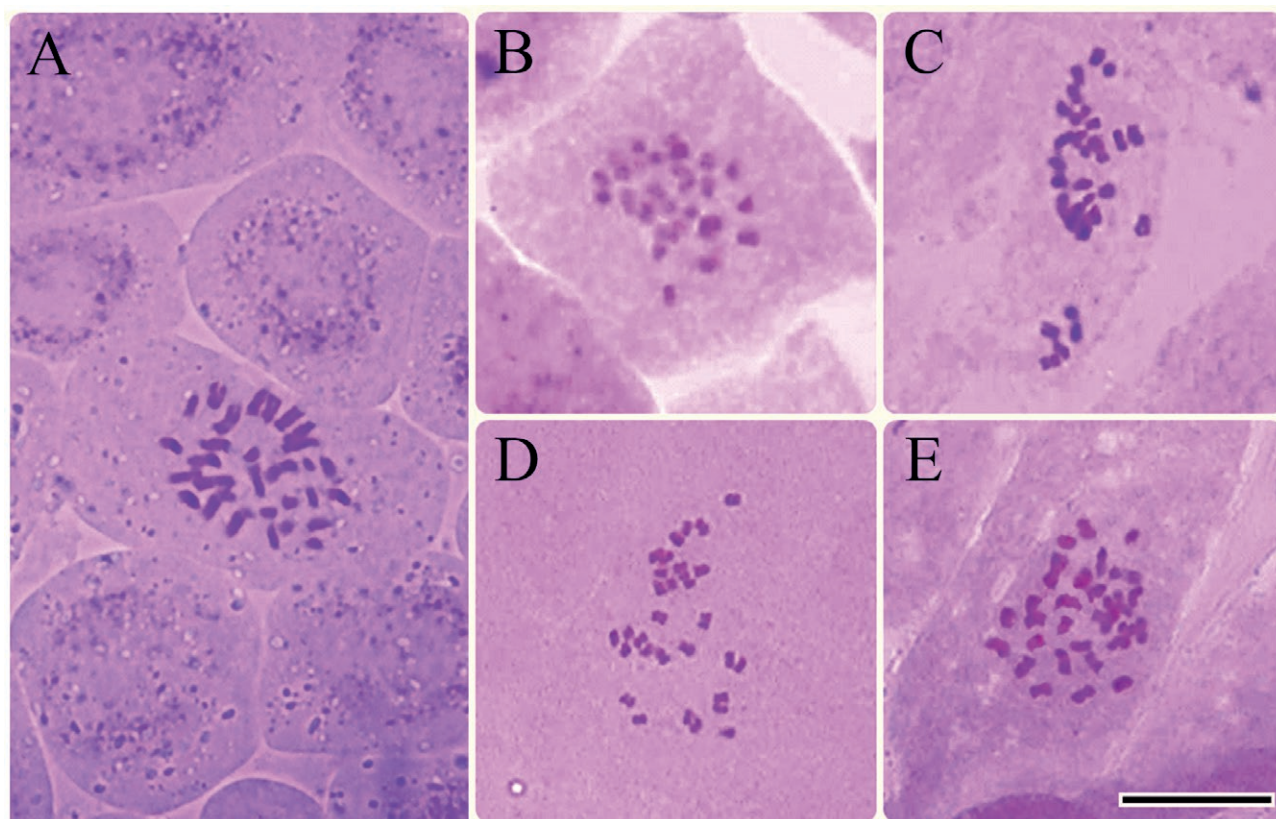
Figure 3. Metaphase chromosomes of *Satureja* species. (A) *S. aintabensis*; (B) *S. boissieri*; (C) *S. icarica*; (D) *S. macrantha*; and (E) *S. spinosa*. Scale bar 10 μm.

RESULTS

Figure 3 presented the mitotic metaphase chromosomes of five *Satureja* species. The chromosome numbers of studied *Satureja* species were given in Table 2. In all species, the diploid number was $2n = 30$, three of which were reported for the first time and the basic number was $x = 15$. In genus *Satureja*, because the chromosomes were very small and the centromere region is unclear, detailed chromosomal measurements were not made.

Table 2. The chromosome numbers of studied *Satureja* species.

Species	x = basic number, $2n$ (ploidy level)
S. aintabensis	$x = 15$, $2n = 30$ (diploid)
S. boissieri	$x = 15$, $2n = 30$ (diploid)
S. icarica	$x = 15$, $2n = 30$ (diploid)
S. macrantha	$x = 15$, $2n = 30$ (diploid)
S. spinosa	$x = 15$, $2n = 30$ (diploid)

Table 3. The chromosome numbers of Turkish *Satureja* in present and previous studies.

Species (alphabetically)	x = basic number, $2n$ (ploidy level)	References	Observation
S. aintabensis	$x = 15$, $2n = 30$ (diploid)	Present study	First report
S. boissieri	$x = 15$, $2n = 30$ (diploid)	Present study	First report
S. coerulea	$x = 15$, $2n = 30$ (diploid)	Chromosome Count Database 2022	Previous report
S. cuneifolia	$x = 15$, $2n = 30$ (diploid)	Chromosome Count Database 2022	Previous report
S. hortensis	$x = 12$, $2n = 48$ (tetraploid) 45-47 (probably dysploidy)	Chromosome Count Database 2022	Previous report
S. icarica	$x = 15$, $2n = 30$ (diploid)	Present study	First report
S. macrantha	$x = 15$, $2n = 30$ (diploid) $x = 12$, $2n = 24$ (diploid)	Present study Vozhdehnazari et al. 2022	New count
S. pilosa	$x = 15$, $2n = 30$ (diploid)	Chromosome Count Database 2022	Previous report
S. spicigera	$x = 15$, $2n = 60$ (tetraploid) $x = 11$, $2n = 44$ (tetraploid)	Shariat et al. 2013 Irani et al. 2014	Previous report
S. spinosa	$x = 15$, $2n = 30$ (diploid) $x = 15$, $2n = 30 + 2B$ (diploid)	Present study Chromosome Count Database 2022	B-chromosomes not observed
S. thymbra	$x = 15$, $2n = 30$ (diploid)	Chromosome Count Database 2022	Previous report

DISCUSSION

The genus *Satureja* was represented by a total of 15 species in Turkey. Eleven Turkish *Satureja* whose chromosome numbers had been reported with present and previous studies were given in the Table 3 for comparison. In the present study, the diploid number of all species was $2n = 30$, three of which were reported for the first time: *S. aintabensis*, *S. boissieri*, and *S. icarica*. The chromosome number represented new cytotype in only one species, which was *S. macrantha* ($2n = 30$). Vozhdehnazari et al. (2022) reported that the chromosome number of *S. macrantha* was $2n = 24$. The chromosome number of *S. spinosa* agreed with the previous report excluding B-chromosomes.

In Turkish *Satureja*, five different chromosome numbers were recorded such as $2n = 24$, 30, 44, 48, 60 and $2n = 30$ was the most common diploid number. *S. spinosa* was the only species to have B-chromosomes. Montmollin (1986) reported that the karyotype of *S. spinosa* was $2n = 30 + 2B$, which were small supernumerary chromosomes other than A-chromosomes. B-chromosomes originated from the A-chromosomes and were a basic source of intraspecific variations of nuclear DNA (Heneidak et al. 2019). Although we obtained the same diploid number, we did not observe B-chromosomes. This was probably due to the locality difference.

In Table 3, *Satureja* was a polybasic genus by $x = 11$, 12, 15 with ploidy levels of $2x$ and $4x$. Nine species were diploid with $2n = 2x = 30$. *S. hortensis* and *S. spinosa* were polyploid, which revealed only one polyploidy level of tetraploidy ($2n = 4x = 44$, 48, and 60).

A basic number of $x = 15$ dominated in reported *Satureja* species (all species excluding *S. hortensis* in Table 3), which were *S. aintabensis*, *S. boissieri*, *S. coerulea*, *S. cuneifolia*, *S. icarica*, *S. macrantha* (only in this study), *S. pilosa*, *S. spicigera* (only in this study), *S. spinosa*, and *S. thymbra*. In addition, the basic numbers of $x = 11$ and 12 were recorded. However, different basic numbers were reported, such as $x = 6$ for *S. multiflora* Briq. and $x = 7$ for *S. sahendica* (Krogulevich 1978; Irani et al. 2014). In detecting karyotype evolution and speciation processes, basic chromosome number is one of the most important parameter. In genus *Satureja*, basic number variations were probably caused by descending or ascending dysploidy and dibasic polyploidy.

In Table 3, nine species were diploid with $2x = 30$ (81.82% of the species) and two species were polyploid with $4x = 44$, 48, and 60 (18.18% of the species). Polyploidy was probably one of the important mechanisms in the karyotype evolution of the genus, as it occurred at a non-negligible rate (Chromosome Counts Database 2022) in the genus *Satureja*.

In the present study, it was reported only one chromosome number ($2n = 30$), the first report for chromosome numbers of three taxa, the same chromosome count (excluding B-chromosomes) with previous report in only one species, and the new chromosome number in only one species. In conclusion, this study presented new data into the chromosomal records of genus *Satureja* that might be useful for interpreting or understanding relationships among the species. In addition, dysploidy and polyploidy variations might probably have played an important role in speciation. In this regard, the results contributed to some missing data in *Satureja* cytotaxon-

omy. However, all taxa should be investigated to elucidate the relationships between *Satureja* species and the chromosomal data should be supported by molecular data.

ACKNOWLEDGMENTS

REFERENCES

Babajafari S, Nikaein F, Mazloomi SM, Zibaeenejad MJ, Zargaran A. 2014. A review of the benefits of *Satureja* species on metabolic syndrome and their possible mechanisms of action. J Evid Based Complementary Altern Med. 20:212–223.

Bektaş E. 2020. Changes in essential oil composition, phenylalanine ammonia lyase gene expression and rosmarinic acid content during shoot organogenesis in cytokinin-treated *Satureja spicigera* (C. Koch) boiss. Shoots. J Plant Biochem Biotechnol. 29:450–460.

Bordbar F, Mahani ZE, Mirtadzadini M. 2021. New chromosome counts in Lamiaceae from flora of Iran - I. J Appl Biol Sci. 15:310–317.

Chromosome Counts Database (CCDB, version 1.59). 2022. *Satureja* [accessed 2022 March 4]. http://ccdb. tau.ac.il/

Dirmenci T, Yıldız B, Öztekin M. 2019. Türkiye florası için yeni bir tür kaydı: *Satureja metastasiantha* Rech. f. (Ballıbabagiller / Lamiaceae). Bağbahçe Bilim Dergisi. 6:54–58.

Eminağaoğlu O, Tepe B, Yumrutas O, Akpulat HA, Daferera D, Polissiou M. 2007. The in vitro antioxidative properties of the essential oil and methanol extracts of *Satureja spicigera* (K. Koch.) Boiss. and *Satureja cuneifolia* ten. Food Chem. 100:339–343.

Eroğlu HE, Altay D, Budak Ü, Martin E. 2020. Karyotypic phylogeny and polyploidy variations of *Paronychia* (Caryophyllaceae) taxa in Turkey. Turk J Bot. 44:245–254.

Eroğlu HE, Martin E, Kahraman A, Gezer Aslan E. 2021. The new chromosomal data and karyotypic variations in genus *Salvia* L. (Lamiaceae): dysploidy, polyploidy and symmetrical karyotypes. Caryologia 74:21–28.

Guerra M. 2008. Chromosome numbers in plant cytotaxonomy: concepts and implications. Cytogenet Genome Res. 120:339–350.

Harley RM, Atkins S, Budantsev A, Cantino PH, Conn B, Grayer R, Harley MM, Kok R, Krestovskaja T, Morales A, et al. 2004. Labiatae. In: Kadereit JW, editor. The Families and Genera of Vascular Plants. Berlin: Springer; 2004. p. 167–275.

Heneidak S, Martin E, Altınordu F, Badr A, Eroğlu HE. 2019.Chromosome counts and karyotype analysis of species of family Apocynaceae from Egypt. Caryologia. 72:69–78.

Irani P, Hejazi SMH, Aghdaei SRT. 2014. Karyological study on four species of *Satureja* (Lamiaceae) in Iran. Int J Biosci. 4:229–240.

Krogulevich RE. 1978. Karyological analysis of the species of the flora of eastern Sayana. In: Malyshev LI, Peshlcova GA, editors. Flora of the Prebaikal. Novosibirsk: Sibirskoe Otdelenie; p.19–48.

Martin E, Kahraman A, Dirmenci T, Bozkurt H, Eroğlu HE. 2020. Karyotype evolution and new chromosomal data in *Erodium*: chromosome alteration, polyploidy, dysploidy, and symmetrical karyotypes. Turk J Bot. 44:255–268.

Martin E, Kahraman A, Dirmenci T, Bozkurt H, Eroğlu HE. Forthcoming 2022. New chromosomal data and karyological relationships in *Geranium*: basic number alterations, dysploidy, polyploidy, and karyotype asymmetry. Braz Arch Biol Technol. 65.

Martin E, Yıldız HK, Kahraman A, Binzat OK, Eroğlu HE. 2018. Detailed chromosome measurements and karyotype asymmetry of some *Vicia* (Fabaceae) taxa from Turkey. Caryologia. 71:224–232.

Momtaz S, Abdollahi M. 2010. An update on pharmacology of *Satureja* species; from antioxidant, antimicrobial, antidiabetes and anti-hyperlipidemic to reproductive stimulation. Int J Pharmacol. 6:346–353.

Montmollin BD. 1986. étude cytotaxonomique de la flore de la Crète. III. Nombres chromosomiques. Candollea. 41:431–439.

Shariat A, Karimzadeh G, Assareh MH. 2013. Karyology of Iranian endemic *Satureja* (Lamiaceae) species. Cytologia. 78:305–312.

Vozhdehnazari MS, Hejazi SMH, Sefidkon F, Jahromi MG, Mousavi A. Forthcoming 2022. Karyotype analysis of populations in five *Satureja* species from Iran. J. medicinal plants by- products.

OPEN ACCESS

L-Ascorbic acid modulates the cytotoxic and genotoxic effects of salinity in barley meristem cells by regulating mitotic activity and chromosomal aberrations

Selma Tabur[1,*], Naîme Büyükkaya Bayraktar[2], Serkan Özmen[1]

[1] *Department of Biology, Faculty of Arts and Science, Süleyman Demirel University, 32260 Isparta, Turkey*
[2] *Süleyman Demirel Education Complex, 32260 Isparta, Turkey*
*Corresponding author. E-mail: taburs@gmail.com

Abstract. The objective of the present study was to with all details explain of the effi-ciency of L-ascorbic acid (L-AsA) also known as vitamin C on cytotoxicity and geno-toxicity induced by salt stress in the barley apical meristems. As a result of the sta-tistical analysis salt stress caused a significant ($P \leq 0.05$) decrease in mitotic index of barley seeds depending on concentration increase, while the frequency of chromosom-al aberration (CA) increased. In addition, it was determined that mitotic index value was decreased by 46% with 1 μM L-AsA supplementation as compared to control and chromosomal abnormalities were increased by 8.96% as well as. However, in the case of simultaneously application of 1 μM L-AsA and different salt concentrations, the high salt concentrations exhibited an excellent success according to low salt concentra-tions in alleviating the mitodepressive effect of salt stress. Moreover, the frequency of chromosomal aberrations in the root meristem cells of those seeds with 1 μM L-AsA supplementation germinated at different salt concentrations was substantially reduced compared to own control group (alone 1 μM L-AsA pretreatment). The 1 μM L-AsA pretreatment at the highest salt concentration (at 0.40 M) was showed an excellent suc-cess by reducing the frequency of the chromosomal aberrations by approximately 90 %. Different salt concentrations and/or 1 μM L-AsA supplementation caused micro-nuclei and granulation as well as various chromosomal aberrations in prophase, meta-phase, anaphase and telophase.

Keywords: cytotoxicity, genotoxicity, *Hordeum vulgare* L., mitotic index, ascorbic acid, salinity.

INTRODUCTION

Together the global climate change, which is starting to make its pres-ence felt more and more, plants are becoming more frequently subjected to adverse abiotic stresses, such as extreme temperatures, cold, high salin-ity, and drought, which limiting plant growth and crop productivity. Salin-ity is one of the major environmental factors that reduce plant productivity

(Tobe et al. 2003; Sabagh et al., 2019). Nearly 20% of the world's cultivated land and also five-hundred thousand hectares of irrigation area in Turkey are threatened by salinity (FAO 2016). Salt stress inhibits or delay growth and development of plants by negatively affects plant growth via oxidative stress, especially ion toxicity, nutritional and hormonal imbalance, and osmotic stress (Parida and Das 2005; Ashraf, 2009; Elsheery et al. 2020a). Moreover, the retardant effects of salinity stress on growth, physiological aspects, productivity and cellular activity were also recorded on other different many plants species (Bargaz et al. 2016; Nassar et al. 2016; Elsheery 2020b; Tabur et al. 2021). However, plants develop highly complex mechanisms for tolerate salinity. Tolerance to salt stress of plants is of three types: osmotic stress tolerance, Na+ or Cl- exclusion, and the tolerance of tissue to accumulated Na+ or Cl- (Munns and Tester 2008; Zvanarou et al. 2020). Since the mechanisms behind salinity are quite complex and difficult to understand, impact of salinity on plants, type and causes of salinity, and salt tolerance strategies of plants are still discussed in level cellular and molecular (Zhu et al. 2016). The common view of many researchers in combating salinity is the development of high salt-tolerant plant varieties. However, this method, which is one of the economical ways to eliminate the negative effects of salinity on plants, shows inconsistency between different crops. Therefore, there is a great scientific burden on researchers to cope with this important environmental stress that also limit crop productivity. For all these reasons, most of the researchers contributed to overcome the disadvantages of salt stress and to develop salt tolerant varieties by using various hormones, plant growth regulators, leaf extracts, vitamins biofertilizer and amino acids (Tabur and Demir 2010 a,b; Mohsen et al. 2014; Çavuşoğlu et al. 2016 a,b; Naser et al. 2016; Mahfouz and Rayan 2017; Farheen et al. 2018; Özmen and Tabur 2020; Tabur et al. 2021).

In recent studies, it has been reported that some vitamins may be effective to alleviate the negative effects of salinity by increase resistance to salt stress (Shalata and Neumann 2001), plant growth and yield quality (El-Bassiouny et al. 2005; Bassuony et al. 2008), seed germination, seedling growth (Emam and Helal, 2008), mitotic activity (Özmen and Tabur 2020) some metabolic changes.

Ascorbic acid (AsA) is a naturalist product that acts as an antioxidant and enzyme and also improves cofactor. It acts as an essential substrate in the cyclic pathway of enzymatic detoxification of hydrogen peroxide. There are various isomers of ascorbic acid or vitamin C (L-AsA, D-AsA, D-izoAsA). D-AsA and D-isoAsA do not have

vitamin C function. Therefore, when ascorbic acid is mentioned, L-ascorbic acid (3-keto-L-gulofuranolaktan) comes to mind from these isomers because of the only isomer with biological activity (Dizlek and Gül, 2007). The stimulatory roles of L-AsA, a minor, water-soluble antioxidant, in plant growth and other developmental processes are well documented (Gallie 2013; Hossain et al. 2017; Gaafar et al. 2020). In plants L-AsA serves as a major redox buffer and regulates various physiological processes controlling growth, development, and stress tolerance. Being a major component of the ascorbate-glutathione (AsA-GSH) cycle, L-AsA helps to modulate oxidative stress in plants by controlling ROS detoxification alone and in co-operation with glutathione. Any fluctuations, increases or decreases, in cellular L-AsA levels can have profound effects on plant growth and development, as L-AsA is associated with the regulation of the cell cycle, redox signaling, enzyme function and defense gene expression (Hossain et al. 2017).

The ascorbic acid concentration increases in plant cells exposed to stress conditions and plays a role in providing tolerance against oxidative stress by playing a role in the direct clearance of O^{-2} and OH^-. As a result of enzyme and gene expression analyzes carried out under different abiotic conditions in many plants, it was determined that ascorbic acid-related gene expression levels increased and these increases were given as a defense response against stress. On account of this, it is emphasized that higher L-AsA levels are important to minimize oxidative stress and regulate plant metabolic processes. (Athar et al. 2008, 2009; Akram et al. 2017). The cellular AsA pool size in plants can be regulated by the coordinated action of many related enzymes. Numerous recent studies have confirmed that AsA level increases the tolerance and adaptation of crops to many abiotic stresses such as cold, drought, salinity, heavy metal toxicity and ozone stresses (Xie et al. 2009; Çavuşoğlu and Bilir 2015; Akram et al. 2017; Xu 2017; Sabagh et al. 2019; Gaafar et al. 2020; Nunes et al. 2020; Wang et al., 2020; Chen et al. 2021).

As mentioned above, there are many studies on the effects of AsA on seed germination, seedling growth, plant resistance, plant growth and yield quality, antioxidant enzyme activity, and some biochemical and metabolic changes under various abiotic stress conditions. In addition, it has been known for few decades that AsA plays an important role in plant growth and development by regulating cell division (Smirnoff 1996; Gallie 2013). However, a rather limited number of studies have been found on the response of ascorbic acid to cytotoxicity and genotoxicity caused by various abiotic stresses, including salinity (Barakat 2003; Yu et al. 2014; El-Araby

et al. 2020). For this reason, this work was designed to comprehensively test of the efficiency level of exogenous L-AsA against effects cytotoxic and genotoxic in caused by salt stress in barley meristem cells and to contribute to the gap in the literature. Namely, it is aimed at clarifying to what extent exogenous L-AsA is able to tolerate salt stress, whether it encourages cells to enter the mitosis division, and whether it causes any changes in the structure and behavior of chromosomes.

MATERIALS AND METHODS

The barley cultivar (*Hordeum vulgare* cv. 'Bülbül 89') used in this study was requested from the Field Crops Research Institute, Ankara, Turkey. NaCl and ascorbic acid (L-AsA) used in the experiments were obtained from Merk and Sigma-Aldrich, respectively. Primarily, to prevent fungal contamination, the barley seeds were surface sterilized by immersion in 1% (w/v) NaClO solution for 10 min, rinsed thoroughly five times with sterile distilled water and dried on filter papers at room temperature prior to experimental procedure. The sterilized seeds were divided into two groups and soaked in constant volumes (50 ml) of distilled water (control, C) and L-AsA (1 μM, micromolar) for 24 h at 20 ± 1ºC. The solutions were filtered at the end of this pretreatment session and 20-25 barley seeds which uniform sized were placed in Petri dishes covered with two sheets filter papers moistened with 7 ml of distilled water or three different NaCl (0.32, 0.35 and 0.40 M, molar) concentrations. After, Petri dishes were transferred to incubators at constant temperature (20 ± 1 °C) for germination for several days. These salt levels hindering germination of seeds on a large scale and the most proper concentration of L-AsA level in alleviation of the salt inhibition at the germination were determined in a preliminary investigation conducted by us.

To cytogenetic analyses after 3 or 4 days, the root tips reached to 0.5-1 cm were excised, pretreated with a saturated solution of paradichlorobenzene for 4 h at 20ºC, fixed with Carnoy's Fluid I (absolute ethanol: glacial acetic acid, 3:1, v/v) for 24 h, and stored in 70% ethanol at 4ºC until required. Then, root tips were hydrolyzed in 1 N HCl at 60ºC for 15-18 min, stained for 1-1.5 h in accordance with the standard procedure for Feulgen staining, and squashed in 45 % acetic acid (Sharma and Gupta 1982; Elçi and Sancak 2013). After one day, microscopic slides were made permanent in by mounting Canada balsam by alcohol vapor exchange method. The best mitosis phases and aberrances were observed in permanent slides and photographed (100X) with a digi-

tal camera (Olympus C-5060) mounted on an Olympus CX41 microscope.

The prepared slides were examined under the microscope at 100X magnification, and mitotic index, i.e. percentage of dividing cells were accounted by counting approximately 15000 cells (three repeat, 5000 per slide) for all per-application. The mitotic index (MI) was calculated using the following the equation:

$$MI\ (\%) = \frac{\text{total number of dividing cells}}{\text{total number of analyzed cells}} \times 100$$

In addition, chromosomal aberrations (CA) occurring at all stages of mitosis during microscopic observation of the slides were calculated according to the following the equation for each per-application as the percentage of 350 dividing cells counted.

$$CA\ (\%) = \frac{\text{total number of abnormal cells}}{\text{total number of dividing cells}} \times 100$$

All experiments were repeated three times. Statistical evaluations of obtained data were actualized using the SPSS 14.0 program and Duncan's multiple range test (Duncan, 1955).

RESULTS

The mitotic index (MI) data obtained from the cytological analysis of barley root tips treated with different NaCl levels and 1 μM L-AsA (vitamin C) are summarized in Table 1. Based on these data, MI gradually drastic reduced with parallel to increasing NaCl levels as compared to the control group. At the highest salt level (at 0.40 M, molar), the mitotic index was reached to the lowest value by reducing from 7.0 ± 1.5 (control, in distilled water) to 1.6 ± 0.07 (77%). In the root meristem cells exposed to 1 μM L-AsA alone, a mitotic index reduction of about 46% was recorded according to control group. When samples with L-AsA treated germinated at different salt levels were compared with their selves control group (L-AsA alone), it was determined that the mitotic index increased statistically a little except for 0.32 M NaCl. 0.35 and 0.40 M NaCl levels exhibited major successful compared as each other the mitotic index values of L-AsA pre-treated and untreated samples at the same salt concentrations (Table 1). Especially, it was recorded that at the highest salt concentration (0.40 M NaCl) the mitotic index value was increases approximately two and a half times (from 1.6 ± 0.07 in control group to 4.0 ± 0.3 in 1 μM AsA).

Table 1. Mitotic index scores and frequency of chromosome aberrations in meristem cells of *H. vulgare* L. exposed to different NaCl concentrations after 1 μM L-AsA supplementation

NaCl (M, mol/L) and L-AsA (μM) Concentrations	Mitotic Index (%)	Chromosome Aberrations (%)
Control (0.00, Distilled Water)	*7.0±1.5[c]	*0.00±0.0[a]
1 μM L-AsA	3.8±0.4[b]	8.96±2.5[b]
0.32 M NaCl	6.3±0.4[c]	2.30±1.0[a]
0.32 M NaCl + 1 μM L-AsA	3.3±0.7[b]	2.50±2.0[a]
0.35 M NaCl	2.8±0.1[b]	8.96±2.5[b]
0.35 M NaCl + 1 μM L-AsA	4.0±0.2[b]	1.70±0.6[a]
0.40 M NaCl	1.6±0.07[a]	21.2±2.5[c]
0.40 M NaCl + 1 μM L-AsA	4.0±0.3[b]	2.00±2.0[a]

*Values with insignificant difference (P ≤ 0.05) for each column are indicated with same letters (± Standard deviation). As test solution, 1 μM ascorbic acid (L-AsA) was used. Concentrations of NaCl were 0.32, 0.35, 0.40 M (mol/L). The pretreatment process of seeds was performed by soaking 24 h in constant volumes of distilled water (control) or L-AsA. Different concentrations of salt were added to germination medium. All data were evaluated as three replicates

The chromosomal aberration frequencies data obtained from barley root tips germinated both distilled water and different NaCl levels in the absence or presence of 1 μM L-AsA are summarized in Table 1. In parallel with the increasing salt concentrations, a very high rate of chromosomal aberrations observed in the root meristem cells of barley seeds. That is, while the chromosomal aberration frequency was 0.00±0.0 in the control seeds germinated in distilled water medium, it was recorded as 2.30±1.0 at 0.32 M salinity, 8.96±2.5 at 0.35 M salinity, and 21.2±2.5 at 0.40 M salinity. On the other hand, the frequency of chromosomal aberrations in seeds germinated in salt stress-free medium after 1 μM L-AsA supplementation alone was remarkably higher than that in the control group (distilled water, 0.00 M NaCl) and was also statistically significant. However, the frequency of chromosomal aberrations of seeds germinated at different salt concentrations after 1 μM L-AsA supplementation has exhibited a statistically significant decrease compared to the percentage of seeds treated with 1 μM L-AsA alone. When these values are compared with the frequencies of seeds germinated only at different salt concentrations, although 1 μM L-AsA supplementation partially increased the chromosome aberration rate at the lowest salt level studied, it significantly reduced the negative effect of salt stress on this parameter, especially at high salt levels (at 0.35 and 0.40 M salinity). In other words, while the chromosomal aberration rate was 8.96 % at 0.35 M salinity and 21.2 % at 0.40 M salinity, the application of 1 μM L-AsA showed
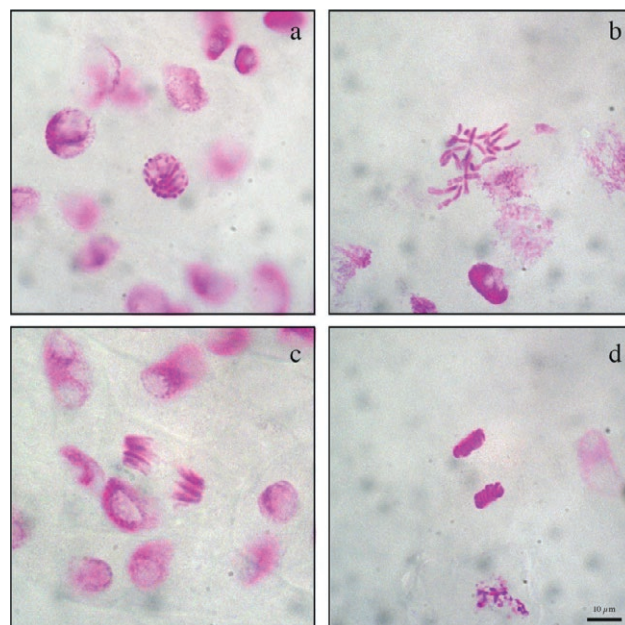
Figure 1. Normal mitosis stages in meristem cells of *H. vulgare* L. germinated in distilled water (Control). **a-** Prophase **b-** Metaphase (2n = 14) **c-** Anaphase **d-** Telophase. Scale bar = 10μm.
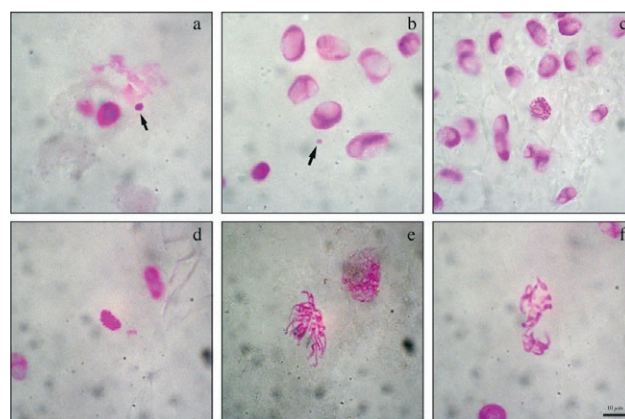
Figure 2. Aberrations observed in pre-prophase and prophase stage in meristem cells of *H. vulgare* L. germinated at different NaCl concentrations after 1 μM L-AsA supplementation for 24 h. **a-b-** micronuclei, **c-d-** chromatin granulation in interphase, **e-f-** disorderly prophase. Scale bar = 10μm.

an excellent success, reducing these aberration rates to 1.70% and 2.00%, respectively (Table 1).

As a result of scans in mitosis slides, no abnormality was found in the meristem cells of the control group barley seeds germinated in distilled water and at 20°C, and all stages of mitosis were observed normally (Figure 1). Microscopic images of a wide range of chromosome aberrances observed in the preparations prepared with
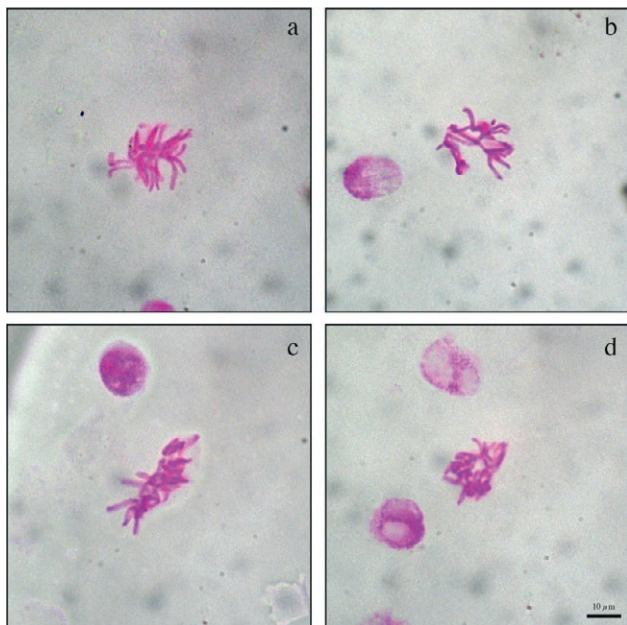
Figure 3. Aberrations observed in metaphase stage in meristem cells of *H. vulgare* L. germinated at different NaCl concentrations after 1 μM L-AsA supplementation for 24 h. **a-b-** uncoiling chromosomes, **c-d-** sticky chromosomes. Scale bar = 10μm.
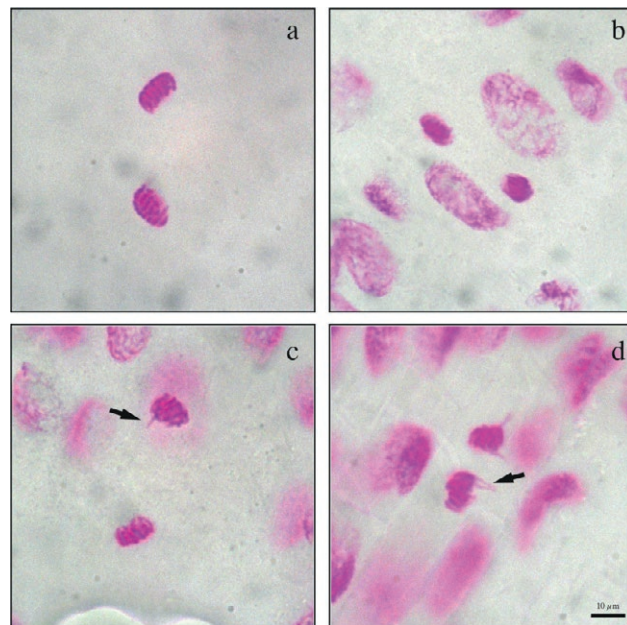
Figure 5. Aberrations observed in telophase stage in meristem cells of *H. vulgare* L. germinated at different NaCl concentrations after 1 μM L-AsA supplementation for 24 h. **a-b-** false polarization in telophase, **c-d-** false polarization in telophase and vagrant chromosomes (arrows). Scale bar = 10μm.
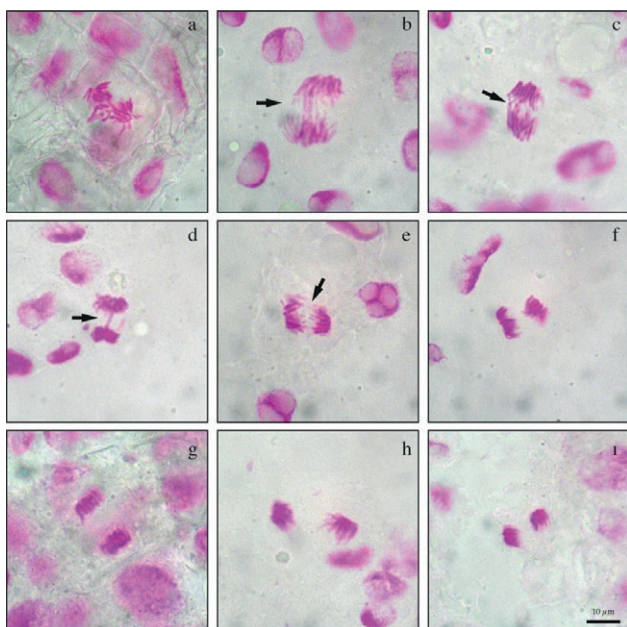
Figure 4. Aberrations observed in anaphase stage in meristem cells of *H. vulgare* L. germinated at different NaCl concentrations after 1 μM L-AsA supplementation for 24 h. **a-** disorderly anaphase, **b-d-** bridges in anaphase (arrows), **e-** laggard chromosome (arrow), **f-g-** alignment anaphase, **h-ı-** false polarization in anaphase. Scale bar = 10μm.

root tips belonging to all other application groups are shown in Figure 2-5. The most common chromosome abnormalities observed in all application were micronucleus, disorderly prophase and anaphase, uncoiling chromosome, sticky chromosome, bridges in anaphase, and false polarization in anaphase and telophase. The abnormalities such as alignment anaphase and vagrant chromosomes were observed in the minimal level.

DISCUSSION

In the present work, effect cytotoxic and genotoxic in the apical meristem cells of barley seeds exposed salt stress of exogenous 1 μM L-AsA supplementation were investigated comprehensive.

Although its mechanism has not been fully explained yet, the effects of salinity stress one of the most important abiotic stresses have been known for a long time by many researchers at cellular and chromosomal levels (Lutsenko et al. 2005; Tabur and Demir 2010 a,b; Pekol et al. 2016; Kiełkowska et al. 2017; El-Araby et al. 2020). All these researchers agree that salt stress causes chromotoxic actions and total inhibition of mitotic processes on meristematic cells, just as in our study. In addition to, Zvanarou et al. (2020) reported

that dividing root meristem cells are more sensitive to NaCl than other tissues since remains in direct contact with abiotic stress factors. However, salt damage extent depends upon plant species, stages of plant development, genotype, salinity concentration, and exposure time (Vicente et al. 2004; Tabur et al. 2021).

To date, many studies have been conducted on the effect of ascorbic acid on morpho-physiological, biochemical and metabolic changes under both normal and various stress conditions using various plant species (Khan et al. 2006; Dolatabadian ve Jouneghani 2009; Fatemi 2014; Mohsen et al. 2014; Gaafar et al., 2020; Nunes et al. 2020; Chen et al. 2021). However, studies on the protective role of exogenous L-AsA supplementation against the cytotoxic effects of various abiotic stresses and its effect on mitotic activity and chromosomal abnormalities, especially against salt stress, are quite insufficient (Barakat 2003; Yu et al. 2014; El-Araby et al. 2020). Therefore, first of all, it was found appropriate to compare the effects of L-AsA during germination in distilled water at 20°C before proceeding to its effects on these parameters under salt stress conditions.

As mentioned in the research findings section, the mitotic index value of barley seeds that were not pretreated with L-AsA (0.00 control, C) was 7.0±1.5, while this value was 3.8±0.4 in seeds that were pretreated. In other words, L-AsA supplementation alone caused a decrease of approximately 46% on the mitotic index compared to the control group (see Table 1). Mitotic index, as known is one of the most important indicators reliably identified the presence of cytotoxicity (Fiskesjö 1985). The decrease of the mitotic index value below 50% compared to the control variant leads to a sublethal effect, while below 22% it can cause lethal effects on test organisms (Mesi and Kopliku 2013). Undoubted, in this case 1μM L-AsA supplementation alone has a potential for sublethal effects. In addition, L-AsA application alone increased the rate of chromosomal aberrations by 8.96% compared to distilled water (see Table 1). As a result of this study, it was revealed that 1μM L-AsA supplementation alone reduced the mitotic index value and had a negative effect on chromosomal aberrations in barley seeds germinated in distilled water environment. Our findings regarding mitotic index and chromosomal abnormalities are in agreement with the study reported in *Allium cepa* by Asita et al, (2017). However, Cenanovic and Durakovic (2016) reported that ascorbic acid treatment at different concentrations (250, 500 and1000 μg/ml) increased the mitotic index in *Allium cepa* root meristems. It is thought that this difference may have occurred depending on the plant species studied and/or the dose and application time of the ascorbic acid used.

As for the effect of L-AsA application on the mitotic index and chromosomal aberrations of barley seeds germinated in saline conditions, the data obtained from our study on the mentioned parameters will be presented for the first time for barley plant. As a result of our literature research, only three previously reported studies were found that were more or less close to the subject. Firstly, Barakat (2003) reported that high salt concentrations significantly reduced mitotic activity and increased chromosomal aberrations in *Allium cepa* L. However, the researcer has determined that the ascorbic acid supplementation significantly increased the mitotic index and reduced chromosomal aberrations by reducing inhibitory effect of salt. Secondly, Yu et al. (2014) emphasized that the application of the AsA (0, 0.5, 1, 2, 4 mM) decreased markedly chromosome aberrations frequency, and increased mitotic index on *Vicia faba* roots exposed to different concentration of $Pb(NO_3)_2$. Finally, El-Araby et al. (2020) has been researched the effects of two concentrations of ASA (50 and 100 ppm) on the cytological parameters of pea seedlings under salinity stress. They reported that ASA (100 ppm) treatments significantly reduced the damaging effect of salinity stress on mitotic index and chromosomal abnormalities percentage. Similarly, also in our study, 1μM L-AsA showed an excellent performance on the mitotic index of barley seeds under high salt stress conditions. For example, 1μM L-AsA supplementation has increased mitotic index by approximately two and a half times at the highest salt stress condition (at 0.40 M salinity), (see Table 1). In addition, L-AsA supplementation under especially high salt stress conditions showed statistically positive effects on chromosomal aberrations in root meristems of barley seeds too. Although the application of 1μM L-AsA alone caused a significant increase of chromosomal aberrations in root meristem cells of seeds germinated in distilled water, in parallel with the increasing of the salt concentrations, the detrimental effect of supplementation 1μM L-AsA has seriously reduced, from 8.96 ± 2.5% abnormal cells (at distilled water, control) to 2.00 ± 2.0% (at 0.40 M). Moreover, while ratio of the chromosomal aberrations in the highest salt level studied (at 0.40 M) was 21.2 ± 2.5%, it was reduced to 2.00 ± 2.0% with the application of 1μM L-AsA. In other words, 1μM AsA application at 0.40 M salinity has shown an excellent success by almost zeroing the detrimental effect of salt stress (see Table 1). That is, we can say that L-AsA application may be more successful in high salt levels than in low salt levels in alleviating the detrimental effect of salt stress on chromosome structure and behaviors. From here, it can be concluded that effective in including the adaptive response to genotoxic stress since L-AsA at

high salt concentrations significantly reduces the clastogenic effects induced by salinity. Also, it is important to point out that L-AsA, known as vitamin C, have the ability to reduce the toxic effect of various genotropic toxicants if used in appropriate doses and at the convenient stage of growth and development. In unstressed conditions, administration of L-AsA alone might have been function as a stimulator, slowing down the mitotic cycle by suppressing the synthesis of proteins required for normal cell division (Tabur et al. 2021). The slowdown in the mitotic cycle might have triggered mitodepressive effects during cell division, thus causing a significant increase (8.96%) of chromosomal aberrations. It has been known for a long time that external stimulatory growth regulator applications are useless and even harmful under normal conditions without stress (Tabur ve Demir 2010a). Therefore, it is not surprising that L-AsA application alone in distilled water reduces the mitotic index and increases chromosome aberrations. Then, we can say that L-AsA supplementation under stress conditions, especially at high salt concentrations (at 0.35 M and 0.40 M salinity), may have accelerated mitotic activity and consequently reduced chromosomal aberrations caused by stress. Undoubtedly, these results supported that exogenous L-AsA may play a protective role against the harmful effect of salt stress on chromosomes by eliminating the mitodepressive effects that occur under stress conditions.

Chromosomal abnormalities that occur spontaneously or as a result of exposure to environmental stresses are indicate the harmful effect of a toxic agent on plant cells (Nag et al. 2013). Many biotic and abiotic toxic agents can promote the occurrence of chromosome aberrations by different mechanisms, including aneugenic (changes in total chromosome number) and clastogenic (changes in chromosome structure) actions. Feretti et al. (2007) sugessted that if toxic ajans cause damage to plant cell chromosomes, they may also be potentially harmful for mammalian cell chromosomes. Micronucleus (MN) assay is accepted as the most effective endpoint to analyze the mutagenic effect of the toxic agents. The large MN in the cell indicates aneugenic effect resulting from chromosome loss while small MN indicates clastogenic effect due to chromosome breaks (Kontek et al. 2007). Briand and Kapoor (1989) have reported that the micronuclei (Figure 2 a, b) are probably the result of vagrant chromosomes and fragments. Dane and Dalgıç (2005) reported that chromatin granulation is related to the inhibition of enzymes and histone proteins. It emphasized by many researchers that several chromatin regulation-related factors, such as histone modification enzymes, linker histone H1, HMG proteins and

ATP-dependent chromatin remodeling factors have been functioned in plant abiotic stress responses (Kim et al. 2010; Asensi-Fabado et al. 2017). Chromatin granulation at interphase (Figure 2 c, d), most likely caused to deformation of the nuclear material by toxic agents, might be a consequence of all these reasons and abnormal chromatin condensation and indicative of many abnormalities that may occur in future mitosis phases. Uncoiling chromosomes (Figure 3 a, b) and disorderly prophase (Figure 2 e, f) may be the result of a weak mitotic effect and irregular chromosome contractions (Tabur et al. 2021). Sticky chromosomes (Figure 3 c, d) could be originated from abnormal DNA condensation, abnormal chromosomal wrapping and inactivation of the axes (Asita and Mokhobo 2013). At the same time it has been asserted that such aberrations may be a result of improper folding of the chromatin fibers (Klášterská et al. 1976). According to some researchers, sticky chromosomes are a marker of high toxic effect on chromatin and irreversibility of the change (Fiskesjö and Levan 1993; Türkoğlu 2007). In the current study, all of mitoclassic impacts in anaphase and telophase (Figure 4-5) that form an important portion of chromosomal abnormalities might have been largely resulted from spindle dysfunction. Fiskesjö (1997) have informed that bridges (Figure 4 b-d) are clastogenic effects, both resulting from chromosome and chromatid breaks. According to Tabur and Demir (2010 b) the bridges in anaphase and telophase might have been the result of inversions. Moreover, Bonciu et al. (2018) have asserted that nucleoplasmic bridges originate from dicentric chromosomes or occur as a result of as faulty longitudinal break of sister chromatids during anaphase. The disorganizations in mitosis such as disorderly anaphase (Figure 4 a), fault polarization at ana-telophases (Figure 4 h, ı; Figure 5 a-d), alignment anaphase (Figure 4 f, g) and bridges may be mainly the result of faulty kinetochore attachment or of spindle dysfunction (Rieder and Salmon 1998). Such irregularities constitute a significant portion of chromosomal aberrations. Vagrant (Figure 5 c, d) and lagging chromosomes (Figure 4 e) occurs during the anaphase where one or more chromatids gets detached from the rest of the chromatids and is incapable of moving towards the poles. Patil and Bhat (1992) have suggested that laggard chromosomes could be originate from the failure of spindle apparatus to organize in normal way. Also, the laggard of chromosomes may have occurred due to a weak mitotic impress. It known that salt stress, particularly NaCl caused too many c-mitotic reactions (Fiskesjö 1997). Therefore, increasing salt concentrations may have been reason to the formation of laggard chromosomes at high rates. Briefly, L-AsA alone and/or dif-

ferent salt levels used in our study may have been caused to all these abnormalities mentioned above by triggering the stimulation/ inhibition of enzymes and proteins necessary for the normal cell division, by disturbing the spindle mechanism.

CONCLUSION

In the present work, it has been compared the interactions between the mitotic index and chromosome behaviors of L-AsA under normal and salt stress using barley seeds. As known, the mechanisms by which salinity affections plant growth and development are rather complex and also controversial since a long time. Unfortunately, although the causes of salinity have been characterized, our understanding of the mechanisms by which salinity prevents plant growth is still rather poor. In summary, it was determined that L-AsA supplementation alone significantly reduced mitotic activity (46%) and caused a very high (8.96%) abnormality on chromosome behaviors in this study. In this case, L-AsA supplementation alone can create various types of mutations over time. However, this study supports that exogenous L-AsA pretreatment, especially at high salt concentrations, can eliminate the negative effects of salinity on the mentioned parameters in barley plant. The obtained results in our work may provide new conceptual tools for designing the hypotheses of different salt tolerance in plants and to brighten many contradictions particularly in relation to effects of L-AsA and high salt stress on mitotic activity and chromosomal abnormalities. Surely! Further investigation is needed to confirm these findings. Consequently, surveying the effects of L-AsA on principal metabolic events, which can be directly or indirectly effective on cell division and chromosome configuration will contribute to clarify of this mechanism.

REFERENCES

Akram NA, Shafiq F, Ashraf M. 2017. Ascorbic acid- a potential oxidant scavenger and its role in plant development and abiotic stress tolerance. Front Plant Sci. 8:613.

Asensi-Fabado MA, Amtmann A, Perrella G. 2017. Plant responses to abiotic stress: The chromatin context of transcriptional regulation. Biochim Biophys Acta. 1860:106-122.

Ashraf M. 2009. Biotechnological approach of improving plant salt tolerance using antioxidants as markers. Biotechnol Adv. 27:84-93.

Asita AO, Mokhobo MM. 2013. Clastogenic and cytotoxic effects of four pesticides used to control insect pests of stored products on root meristems of *Allium cepa*. Environ Nat Resour Res. 3(2):133–145.

Asita AO, Moramang S, Rantśo T, Magama S. 2017. Modulation of mutagen-induced genotoxicity by vitamin C and medicinal plants in *Allium cepa* L. Caryologia. 70:151-165.

Athar HR, Khan A, Ashraf M. 2008. Exogenously applied ascorbic acid alleviates salt-induced oxidative stress in wheat. Environ Exp Bot. 63:224-231.

Athar HR, Khan A, Ashraf M. 2009. Inducing salt tolerance in wheat by exogenously applied ascorbic acid through different modes. J Plant Nutr. 32:1799-1817.

Barakat H. 2003. Interactive effects of salinity and certain vitamins on gene expression and cell division. Int J Agric Biol. 3:219-225.

Bargaz A, Nassar RMA, Rady MM, Gaballah MS, Thompson SM, Brestic M, Schmidhalter U, Abdelhamid MT. 2016. Improved salinity tolerance by phosphorus fertilizer in two *Phaseolus vulgaris* recombinant inbred lines contrasting in their P-efficiency. J Agron Crop Sci. 202:497-507.

Bassuony FM, Hassanein RA, Baraka DM, Khalil RR. 2008. Physiological effects of nicotinamide and ascorbic acid on *Zea mays* plant grown under salinity stress II-changes in nitrogen constituents, protein profiles, protease enzyme and certain inorganic cations. Aust J Basic & Appl Sci. 2(3):350-359.

Bonciu E, Firbas P, Fontanetti CS, Wusheng J, Karaismailoğlu MC, Liu D, Menicucci F, Pesnya DS, Popescu A, Romanovsky AV, Schiff S, Ślusarczyk J, Souza CP, Srivastava A, Sutan A, Papini A. 2018. An evaluation for the standardization of the *Allium cepa* test as cytotoxicity and genotoxicity assay. Caryologia. 71(3):191-209.

Briand CH, Kapoor BM. 1989 The cytogenetic effects of sodium salicylate on the root meristem cells of *Allium sativum* L. Cytologia 54:203–209.

Cenanovic M, Durakovic C. 2016. In vivo genotoxicity testing of vitamin C and naproxen sodium using plant bioassay. Southeast Europe J Soft Comput 4(2):66-71.

Chen X, Zhou Y, Cong Y, Zhu P, Xing J, Cui J, Xu W, Shi Q, Diao M, Liu HY. 2021. Ascorbic acid-induced photosynthetic adaptability of processing tomatoes to salt stress probed by fast OJIP fluorescence rise. Front Plant Sci. 12:594400.

Çavuşoğlu K, Bilir G. 2015. Effects of ascorbic acid on the seed germination, seedling growth and leaf anatomy of barley under salt stress. ARPN J Agric Biol Sci. 10(4):124-129.

Çavuşoğlu D, Tabur S, Çavuşoğlu K. 2016a. The effects of *Aloe vera* L. leaf extract on some physiological and cytogenetical parameters in *Allium cepa* L. seeds germinated under salt stress. Cytologia. 81(1):103-110.

Çavuşoğlu D, Tabur S, Çavuşoğlu K. 2016b. Role of *Ginkgo biloba* L. leaf extract on some physiological and cytogenetical parameters in *Allium cepa* L. seeds exposed to salt stress. Cytologia. 81(2):207-213.

Dane F, Dalgıç Ö. 2005. The Effect of fungicide benomyl (benlate) on growth and mitosis in onion (*Allium cepa* L.) root apical meristem. Acta Biol Hung. 56 (1-2):119-128.

Dizlek H, Gül H. 2007. L-ascorbic acid and its functions at bread making. Süleyman Demirel Univ J Fac Agric. 2(1):26-34.

Dolatabadian A, Jouneghani RS. 2009. Impact of exogenous ascorbic acid on antioxidant activity and some physiological traits of common bean subjected to salinity stress. Not Bot Horti Agrobot Cluj-Napoca. 37(2):165-172.

Duncan DB. 1955. Multiple range and multiple F tests. Biometrics 11:1-42.

El-Araby HG, El Hefnawy SFM, Nassar MA, Elsheery NI. 2020. Comparative studies between growth regulators and nanoparticles on growth and mitotic index of pea plants under salinity. Afr J Biotech 19(8):564-575.

El-Bassiouny MSH, Gobarah ME, Ramadan AA. 2005. Effect of antioxidants on growth, yield and favism causative agents in seeds of *Vicia faba* L. plants grown under reclaimed sandy soil. J Agron. 4:281-287.

Elçi Ş, Sancak C. 2013. Research methods and observations in cytogenetics. Ankara Univ Publish House. Beşevler/ANKARA, 227p.

Elsheery NI, Helaly MN, Omar SA, John SVS, Zabochnicka-Swiatek M, Kalaji HM, Rastogi A. 2020a. Physiological and molecular mechanisms of salinity tolerance in grafted cucumber. South Afric J Bot. 130: 90-102.

Elsheery NI, Helaly MN, El-Hoseiny HM, Alam-Eldein SM. 2020b. Zinc oxide and silicone nanoparticles to improve the resistance mechanism and annual productivity of salt-stressed mango trees. Agronomy. 10:953-975.

Emam MM, Helal NM. 2008. Vitamins minimize the salt-induced oxidative stress hazards. Aust J Basic & Appl Sci. 2(4):1110- 1119

FAO 2016. FAOSTAT. Food and Agriculture Organization of the United Nations, Rome, Italy. Web. http://faostat.fao.org/default. aspx. Accessed: 12 February 2019.

Farheen J, Mansoor S, Abideen Z. 2018. Exogenously applied salicylic acid improved growth, photosynthetic pigments and oxidative stability in mungbean seedlings (*Vigna radiata*) at salt stress. Pak J Bot. 50:901-912.

Fatemi SN. 2014. Ascorbic acid and its effects on alleviation of salt stress in sunflower. Ann Res Rev Biol. 4(24):3656-3665.

Feretti D, Zerbini I, Zani C, Ceretti, Moretti M, Monarca S. 2007. *Allium cepa* chromosome aberration and micronucleus tests applied to study genotoxicity of extracts from pesticide-treated vegetables and grapes. Food Addit Contam. 24(6):561-572.

Fiskesjö G. 1985. The *Allium* test as a standard in environmental monitoring. Hereditas. 102:99-112.

Fiskesjö G. 1997. *Allium* test for screening chemicals; evaluation of cytological parameters. In: Wang W, Lower WR, Gorsuch JW, Hughes JS (eds) Plant for Environmental Studies. Lewis Publishers, New York, pp 308-333.

Fiskesjö G, Levan A. 1993. Evaluation of the first ten MEIC chemicals in the *Allium* test. Altern Lab Anim. 21:139–149.

Gaafar AA, Ali SI, El-Shawadfy A, Salama ZA, Sekara A, Ulrichs C, Abdelhamid MT. 2020. Ascorbic acid induces the increase of secondary metabolites, antioxidant activity, growth, and productivity of the common bean under water stress conditions. Plants. 9:627.

Gallie DR. 2013. Ascorbic acid: A multifunctional molecule supporting plant growth and development. Scientifca. 795964:1-24.

Hossain MA, Munne-Bosch S, Burritt DJ, Diaz-Vivancos P, Fujita M, Lorence A. 2017. Ascorbic acid in plant growth, development and stress tolerance. Springer, Cham 514p.

Khan MA, Ahmed MZ, Hameed A. 2006. Effect of sea salt and L-ascorbic acid on the seed germination of halophytes. J Arid Environ. 67(3):535-540.

Kiełkowska A. 2017. Cytogenetic effect of prolonged in vitro exposure of *Allium cepa* L. root meristem cells to salt stress. Cytol Genet. 51(6):478-484.

Kim JM, To TK, Nishioka T, Seki M. 2010. Chromatin regulation functions in plant abiotic stress responses. Plant Cell Environ. 33:604-611.

Klášterská I, Natarajan AT, Ramel C. 1976. An interpretation of the origin of subchromatid aberrations and chromosome stickiness as a category of chromatid aberrations. Hereditas. 83:153-162.

Kontek R, Osiecka R, Kontek B. 2007. Clastogenic and mitodepressive effects of the insecticide dichlorvos on root meristems of *Vicia faba*. J Appl Genet.

48(5):359-361.

Lutsenko EK, Marushko EA, Kononenko NV, Leonova TG. 2005. Effects of fusicoccin on the early stages of sorghum growth at high NaCl concentrations. Russ J Plant Physiol. 52:332–337.

Mahfouz H, Rayan WA. 2017. Antimutagenics effects of stigmasterol on two salt stressed *Lupinus termis* cultivars. Egypt J Genet Cytol. 46:253-272.

Mesi A, Kopliku D. 2013. Cytotoxic and genotoxic potency screeningof two pesticides on *Allium cepa* L. Proc Tech. 8:19–26.

Mohsen AA, Ebrahim MKH, Ghoraba WFS. 2014. Role of ascorbic acid on germination indexes and enzyme activity of *Vicia faba* seeds grown under salinity stress. J Stress Physiol Biochem. 10(3):62-77.

Munns R, Tester M. 2008. Mechanisms of salinity tolerance. Annu Rev Plant Biol. 59:651-681.

Nag S, Dutta R, Pal KK. 2013. Chromosomal aberrations induced by acetamiprid in *Allium cepa* L. root meristem cells. Ind J Fund Appl Life Sci. 3(2):1-5.

Naser HM, El-Hosieny H, Elsheery NI, Kalaji HM. 2016. Effect of biofertilizers and putrescine amine on the physiological features and productivity of date palm (*Phoenix dactylifera* L.) grown on reclaimed salinized soil. Trees. 30:1149-1161.

Nassar R, Nermeen T, Reda F. 2016. Active yeast extract counteracts the harmful effects of salinity stress on the growth of leucaena plant. Scienta Hortic. 201:61-67.

Nunes LRL, Pinheiro PR, Silva JB, Dutra AS. 2020. Effects of ascorbic acid on the germination and vigour of cowpea seeds under water stress. Rev Ciênc Agron. 51(2):e20196629.

Özmen S, Tabur S. 2020. Functions of folic acid (vitamin B9) against cytotoxic effects of salt stress in *Hordeum vulgare* L. Pak J Bot. 52(1):17-22.

Parida AK, Das AB. 2005. Salt tolerance and salinity effects on plants: A review. Ecotoxicol Environ Saf. 60:324-349.

Patil BC, Bhat GI. 1992. A comparative study of MH and EMS in the induction of chromosomal aberrations on lateral root meristem in *Clitoria ternetea* L. Cytologia. 57:259–264.

Pekol S, Baloğlu MC, Altınoğlu YÇ. 2016. Evaluation of genotoxic and cytologic effects of environmental stress in wheat species with different ploidy levels. Turk J Biol. 40:580-588.

Rieder CL, Salmon ED. 1998. The vertebrate cell kinetochore and its roles during mitosis. Trends Cell Biol. 8:310–318.

Sabagh AE, Hossain A, Barutçular C, Islam MS, Ratnasekera D, Kumar N, Meena RS, Gharib HS, Saneoka H, Silva JAT. 2019. Drought and salinity stress management for higher and sustainable canola (*Brassica napus* L.) production: A critical review. Aust J Crop Sci. 13(1):88-97.

Shalata A, Neumann PM. 2001. Exogenous ascorbic acid (vitamin C) increases resistance to salt stress and reduces lipid peroxidation. J Exp Bot. 364:2207-2211.

Sharma PC, Gupta PK. 1982. Karyotypes in some pulse crops. Nucleus, 25: 181-185

Smirnoff N. 1996. The function and metabolism of ascorbic acid in plants. Ann Bot. 78(6):661-669.

Tabur S, Demir K. 2010a. Role of some growth regulators on cytogenetic activity of barley under salt stres. Plant Growth Regul. 60:99-104.

Tabur S, Demir K. 2010b. Protective roles of exogenous polyamines on chromosomal aberrations in *Hordeum vulgare* exposed to salinity. Biologia. 65:947-953.

Tabur S, Avcı ZD, Özmen S. 2021. Exogenous salicylic acid application against mitodepressive and clastogenic effects induced by salt stress in barley apical meristems. Biologia. 76:341–350.

Tobe K, Zhang L, Omasa K. 2003. Alleviatory effects of calcium on the toxicity of sodium, potassium and magnesium chlorides to seed germination in three nonhalophytes. Seed Sci Res. 13:47-54.

Türkoğlu S. 2007. Genotoxicity of five food preservatives tested on root tips of *Allium cepa* L., Mut Res. 626:4-14.

Wang M, Ding F, Zhang S. 2020. Mutation of SlSBPASE aggravates chilling-induced oxidative stress by impairing glutathione biosynthesis and suppressing ascorbate-glutathione recycling in tomato plants. Front Plant Sci 11:565701.

Xie JQ, Li GX, Wang XK, Zheng QW, Feng ZZ. 2009. Effect of exogenous ascorbic acid on photosynthesis and growth of rice under O_3 stress. Chin J Eco-Agric. 17:1176-1181.

Xu W. 2017. Alleviative effects and mechanism of exogenous ascorbic acid on chromium (Cr6+) toxicity in wheat. Nanjing: phd, Nanjing Agricultural Univ.

Vicente O, Boscaiu M, Naranjo MA, Estrelles E, Belle's JM, Soriano P. 2004. Responses to salt stress in the halophyte *Plantago crassifolia* (Plantaginaceae). J Arid Environ. 58:463-481.

Yu CM, Xie FD, Ma LJ. 2014. Effects of exogenous application of ascorbic acid on genotoxicity of Pb in *Vicia faba* roots. Int J Agric Biol. 16(4):831-835.

Zhu M, Shabala S, Shabala L, Fan Y, Zhou MX. 2016. Evaluating predictive values of various physiological indices for salinity stress tolerance in wheat. J Agro Crop Sci. 202:115-124.

Zvanarou S, Vágnerová R, Mackievic V, Usnich S,

Smolich I, Sokolik A, Yu M, Huang X, Angelis KJ, Demidchik V. 2020. Salt stress triggers generation of oxygen free radicals and DNA breaks in *Physcomitrella* patens protonema. Environ Exp Bot. 180:104236.

ORCID
KR-M: 0000-0001-6767-1683
EIC-G: 0000-0002-5025-1284
SM-L: 0000-0002-8983-5914
CG-V: 0000-0003-3078-5761

Characterization of the chromosomes of sotol (*Dasylirion cedrosanum* Trel.) using cytogenetic banding techniques

Kristel Ramírez-Matadamas[1], Elva Irene Cortés-Gutiérrez[2], Sergio Moreno-Limón[2], Catalina García-Vielma[1,*]

[1] *Departamento de Citogenética, Centro de Investigación Biomédica del Noreste, Instituto Mexicano del Seguro Social. Monterrey, N.L., México*
[2] *Facultad de Ciencias Biológicas, Universidad Autónoma de Nuevo León, San Nicolás de los Garza, N.L., México*
*Corresponding autor. E-mail: katygarcia2@hotmail.com; catalina.garciav@imss.gob.mx

Abstract. Sotol (*Dasylirion cedrosanum* Trel.) is a perennial species with numerous grayish-to-green leaves that grow symmetrically from the base of the stem outward. Its inflorescences can measure up to 3 m in height and contain membranous bracts that enclose seeds. It is a species that has been scarcely studied at the cytogenetic level, with only one report available in the literature. In Mexico, it has economic importance because it is used to prepare the alcoholic beverage sotol. In the present work, the chromosomes of *Dasylirion cedrosanum* Trel. were obtained and analyzed using different cytogenetic banding techniques and morphometric analysis to construct the first karyotype for this species. Chromosomes were obtained by germinating plant seeds collected in the locality of Las Adjuntas, Santiago, Nuevo León, Mexico. Treatment with colchicine as an antimitotic was performed, followed by enzymatic treatment with pectinase and cellulase, to eliminate the cell walls. Chromosome slides were stained with Giemsa, GTG banding technique, CBW banding, and the 4',6-diamidino-2-phenylindole fluorescence dye, and observed under a microscope. A chromosomal number 2n of 38 chromosomes, as previously reported, was confirmed. Using the different banding techniques, we observed that all chromosomes exhibited a submetacentric morphology with a fundamental number of 76, and it was possible to visualize the pattern of GTG and CBW bands; these findings are reported for the first time for this species. Morphometric analysis established that the average length of the chromosomes was between 5.09 and 9.84 mm.

Keywords: *Dasylirion cedrosanum* Trel., sotol, karyotype, morphology, cytogenetics.

INTRODUCTION

Sotol (*Dasylirion cedrosanum* Trel.) belongs to the *Asparagaceae* family and was first described in 1838. Sotol is perennial and polycarpic in nature, with a semicylindrical and apical morphology (Zuccarini, 1838). The name of the genus means "thick lily" and it has numerous pointed and thorny

grayish-to-green leaves measuring from 30 to 170 cm with a spoon shape in their lower part that grows from the base of the stem outward in a symmetrical way. Its stem is thick and fibrous, and up to 1 m in height (Sierra Tristán, 2008). It presents dioecious inflorescences with a single type of gametes in stamens (male scape) or pistils (female scape) that reach 3 m in height (Flores-Gallegos, 2019) (Figure 1).

The geographic distribution of sotol ranges from the southwestern United States to Oaxaca, Mexico. Sixteen species were originally described, most of which are endemic to Mexico (Bogler, 1995), and additional species were later identified in northeastern Mexico (Bogler, 1998). *Dasylirion cedrosanum* Trel. is the species with the greatest economic importance in Mexico, from which a drink called sotol is prepared via the fermentation of the stem of the plant (Hernández-Quintero, 2015). This drink is used for recreational purposes and as a medicinal remedy for diabetes and stomach ailments (Goverment of Mexico, 2022). The genus *Dasylirion* has rarely been studied at the cytogenetic level. Previous studies reported a diploid chromosome num-

ber of 38 in the species *Dasylirion texanum* and *Dasylirion wheeler* in specimens grown under greenhouse conditions, and also described multiple submetacentric chromosomes and two acrocentric chromosomes exclusively in *Dasylirion texanum* (Sato, 1935). For *Dasylirion cedrosanum* Trel., there is only one report of the gametic (n = 19) and somatic (2n = 38) chromosome number in plants collected in Saltillo, Coahuila, Mexico (Hernández-Quintero, 2015). Moreover, it has not been reported in the plant chromosomal number index (IPCN: Index to Plant Chromosome Numbers) of the Missouri Botanical Garden, USA, where most of the records of the chromosome numbers of various plant species worldwide can be found (Goldblatt, 2021).

Using different cytogenetic staining techniques, the chromosomes of a species can be observed and characterized. The usual Giemsa and 4',6-diamidino-2-phenylindole (DAPI) staining allows the observation of the number and structure of each chromosome. The GTG banding technique (G bands with trypsin and Giemsa) helps to visualize the shape and pattern of the light bands (euchromatin) and dark bands (heterochromatin) present in each chromosome; and the CBW banding technique (C bands with barium and Wright's stain) specifically stains the centromeres and heterochromatic regions of the chromosomes (Barch, 1997).

The morphometric measurements of chromosomes are another important tool in this context. Images of the chromosomes are acquired under a bright-field or fluorescence microscope, and are analyzed using software that reports the results of the measurements in micrometers. The morphometric measurements that can be used are as follows: the total length of the chromosome (TCL), the length of the short (SAL) and long (LAL) arms, and the average length of the short (ASAL) and long (ALAL) arms. The centromere index (CI), which is the relationship between the length of the short arm of the chromosome and the TCL (Peruzzi, 2013), is expressed as a percentage (0%–50%). The relative longitude (RL), which is defined as the TCL divided by the sum of the total length of the karyotype, is also expressed as a percentage (Jabeen, 2012), whereas the fundamental number (FN) is the number of short and long arms present in a karyotype (Matthey, 1945; Matthey, 1965) and helps to determine the type of chromosomes present (Nirchio, 2014). The objective of this study was to obtain and characterize the chromosomes of *Dasylirion cedrosanum* Trel. to develop a karyotype of the species based on the morphological characteristics of its chromosomes.

Figure 1. *Dasylirion cedrosanum* Trel. (Photograph by Arturo Cruz Anaya, https://www.naturalista.mx/observations/21031288)

MATERIALS AND METHODS

Collection site

We used *Dasylirion cedrosanum* Trel. seeds collected in the locality of Las Adjuntas, Santiago, Nuevo León, Mexico (25°18'03.6"N, 100°08'27.3"W) (Figure 2).

Preparation seeds

The seeds were washed and disinfected with 1% sodium hypochlorite (SIGMA-Aldrich, St. Louis, USA), and 10 seeds were placed in each petri dish (Pyrex, Tehama, CA, USA) in triplicate, and transferred to a bioclimatic chamber (Stemcells technologies, Vancouver, Canada) at 25-30°C for approximately 10 days for germination.

Cytogenetics

To obtain chromosomes, the technique of Hernández-Quintero et al. (2015), with some modifications, was used. The apical meristems were cut with a scalpel, preferably between 08:00 and 10:00 am, and incubated in 2% colchicine (Sigma-Aldrich) at 37°C for 48 h, followed by washing for 15 min with distilled water. Farmer's fixative solution (methanol:glacial acetic acid, 3:1) (CTR Scientific, Mexico) was then added, and the solution was incubated for 24 h at 4°C, washed in distilled water for 15 min, vortexed for 5 min, and centrifuged at 7440' *g* for 1 min. Subsequently, the supernatant was decanted and a mixture of pectinase (PlantMedia, Ohio, USA) and cellulase (PlantMedia) at a ratio of 1:1 at 0.2% was added, followed by resuspension of the pellet in distilled water and incubation at 37°C for 2 h. The cell button was dripped onto slides with a layer of glacial acetic acid, and heat was then applied.

Different staining and cytogenetic banding techniques were performed on the chromosomes obtained. 1) Giemsa staining: the chromosomes were incubated in Giemsa solution (Sigma-Aldrich) (1:20) for 5 min, rinsed in distilled water, and allowed to dry. 2) GTG banding: the chromosomes were incubated in 0.025 M trypsin at 37°C for 1 min, stained with Giemsa stain 1:20 for 5 min, rinsed, and allowed to dry. 3) CBW banding: the

Figure 2. *Dasylirion cedrosanum* Trel. seed collection site, Las Adjuntas, Santiago, N.L., Mexico (25°18'03.6"N, 100°08'27.3"W), as indicated by the red globe (INEGI Map, 2021 https://www.inegi.org.mx/app/mapas/).

chromosomes were incubated in 0.2 N HCl (SIGMA-Aldrich) for 60 min at room temperature, rinsed with DNase-free water, and allowed to dry; then they were immersed in 5% BaOH (SIGMA-Aldrich) for 40 min and rinsed, passed through 70% and 100% ethanol, immersed in 2× SSC (3 M Sodium chloride and 300 mM Sodium citrate dihydrate, pH 7.0, SIGMA-Aldrich) for 60 min at 60°C, rinsed, dried, and stained with 1:3 Wright's stain for 2 min. 4) Fluorescent staining with DAPI (SIGMA-Aldrich): 7 µl of DAPI at 2.5 mg/ml were added to chromosomes, which were then incubated for 15 min at 4°C. The slides were observed using an AxioScope A1 microscope (Zeiss, Göttingen, Germany) with a 100× objective and coupled to an Axiocam 502 mono camera (Zeiss) coupled to Zen blue (version 3.3.89.0000) software (Zeiss). Images were acquired with an Axiophot HXP 120 V fluorescence lamp with a DAPI filter (Zeiss). The karyotype was organized based on the size of the chromosomes, from longest to shortest, in descending order, and pairing the homologues based on the observed GTG bands (Levan, 1964).

Morphometry

DRAWID (version 0.26) software (Kirov et al., 2017) was used to perform the morphological measurements of TCL, SAL, LAL, ASAL, ALAL and CI, and for the elaboration of the ideogram of the chromosomes. The images of the metaphases were opened in the software and each chromosome was measured, starting from the long arm toward the middle region, where the position of the centromere was marked (Centromere button), and continuing with the short arm at the lower end, thus ending the measurement. The process was repeated individually for each chromosome. RL was obtained using the formula:

RL = (TCL / STCL) (100); TCL was obtained by adding the measurements of SAL and LAL; ASAL and ALAL were obtained based on the lengths determined for the 38 chromosomes; whereas CI was obtained from the formula: CI = SAL / (SAL + LAL). All measurements were performed individually for each of the 38 chromosomes in each of the cells analyzed. The FN of the karyotype was calculated using as a criterion the presence of two arms in the chromosomes. Descriptive statistics were applied, such as mean and standard deviation, using SPSS Statistics, version 22 (IBM, Armonk, NY, USA).

RESULTS

Cytogenetics

Thirty metaphases were analyzed, which led to the identification of 38 chromosomes (2n) in 100% of the analyzed cells. All chromosomes were of the submetacentric type, that is, with the centromere displaced toward one of the ends, in which the arms differed in length. Using the GTG banding technique, it was possible to establish a pattern of bands in each chromosome, with the presence of dark bands in the telomeric regions of most of them. Based on the GTG banding patterns, the karyotype depicted in Figure 3 was established.

Using CBW banding, the centromere was observed in a displaced position toward one of the ends of the arms of the chromosomes. Concomitantly, heterochromatin regions were observed at the ends of some chromosomes (Figure 4).

Figure 3. Karyotype of *Dasylirion cedrosanum* Trel. stained with GTG banding. The pattern of bands in each chromosome and the dark bands in the telomeric region (arrow) are shown.

Figure 4. Chromosomes of *Dasylirion cedrosanum* Trel. stained with CBW banding, in which the presence of telomeric heterochromatin is confirmed (arrow).
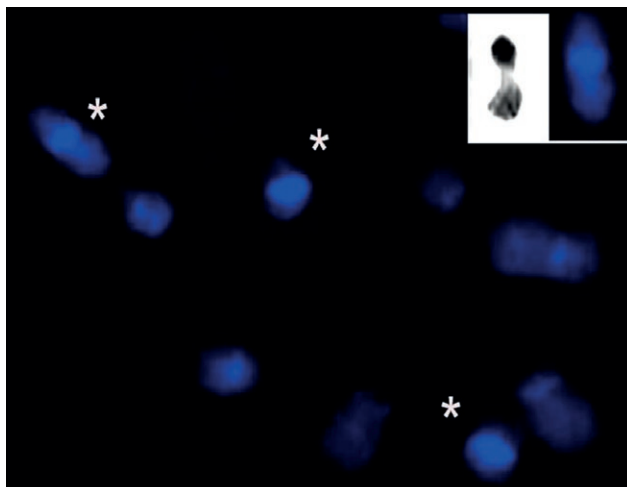
Figure 5. Chromosomes of *Dasylirion cedrosanum* Trel. stained with DAPI. More intensely marked areas of constitutive heterochromatin can be observed (chromosomes marked with an asterisk). In the upper-right corner, the CBW bands can be compared with the zones detected using DAPI, thus confirming the distribution in the chromosomes of the constitutive heterochromatin.

also confirming their number and submetacentric shape (Figure 5).

Morphometry

TCL average of the chromosomes was in the range of 5.09 mm for the shortest chromosome and 9.84 mm for the longest. The remaining chromosomes ranged from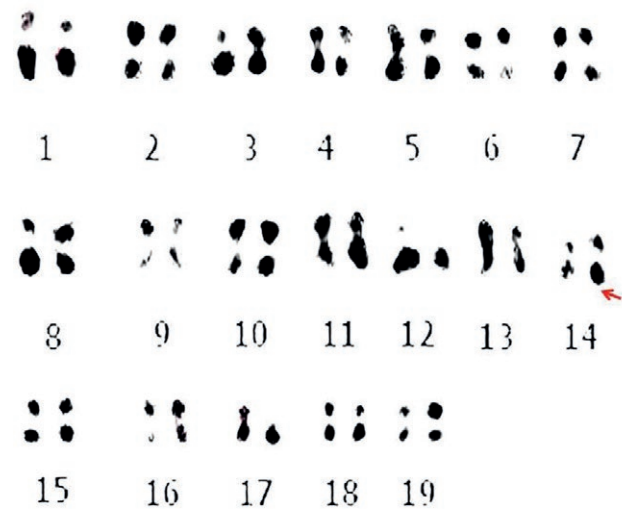 5.47 to 8.62 mm in length. The average of the SAL indicated a length of 2.96 ± 0.58 mm, whereas the average of the LAL was 3.93 ±0.73 mm. The RL average of the 38 chromosomes ranged from 1.94% to 3.76%, whereas the CI average was between 39.98% and 44.66 %. FN of the karyotype of *Dasylirion cedrosanum* Trel. was 76, considering as a criterion that each chromosome had two arms (Table 1).

Based on the results of staining, banding, and previous measurements, and using the image analysis software, an ideogram of the *Dasylirion cedrosanum* Trel. chromosomes was constructed with GTG bands (Figure 6).

Visualization using DAPI allowed us to observe the morphology of the chromosomes in greater detail, while

Table 1. Mean length of short arm chromosome (SAL), long arm chromosome (LAL), total arm chromosome (TCL), relative length (RL), and centromeric index (CI) from 30 metaphases of *Dasylirion cedrosanum* Trel (2n=38).

Chromosome	SAL x̄±SD (µm)	LAL x̄±SD (µm)	TCL x̄ (µm)	RL %	CI %	Type of chromosome
1	4,44±1,42	5,79±1,63	9,84	3,76	44,66	Submetacentric
2	3,66±0,44	5,06±1,44	8,62	3,29	43,76	Submetacentric
3	3,81±1,25	4,54±0,46	8,30	3,17	43,24	Submetacentric
4	3,48±0,83	4,64±0,84	8,01	3,06	42,21	Submetacentric
5	3,48±0,77	4,31±0,68	7,72	2,95	43,31	Submetacentric
6	3,26±0,72	4,32±0,64	7,52	2,87	43,64	Submetacentric
7	3,04±0,84	4,23±0,45	7,19	2,74	43,11	Submetacentric
8	2,77±0,66	4,22±0,51	6,96	2,66	39,98	Submetacentric
9	2,73±0,30	4,07±0,90	6,77	2,59	41,96	Submetacentric
10	2,89±0,49	3,78±0,66	6,64	2,54	44,47	Submetacentric
11	2,81±0,47	3,74±0,66	6,53	2,49	43,34	Submetacentric
12	2,80±0,63	3,63±0,52	6,41	2,45	42,57	Submetacentric
13	2,58±0,27	3,72±0,76	6,26	2,39	42,73	Submetacentric
14	2,70±0,49	3,48±0,57	6,16	2,35	43,12	Submetacentric
15	2,66±0,33	3,38±0,70	5,99	2,29	43,27	Submetacentric
16	2,39±0,10	3,48±1,03	5,84	2,23	41,65	Submetacentric
17	2,31±0,70	3,44±0,34	5,69	2,17	41,64	Submetacentric
18	2,49±0,56	3,02±0,44	5,47	2,09	43,79	Submetacentric
19	2,23±0,60	2,94±0,52	5,09	1,94	43,85	Submetacentric
ASAL= 2.96±0.58		ALAL=3.93±0.73		ΣTCL=261.88		

SD = Standard deviation, ASAL= average short arm, ALAL= average long arms.
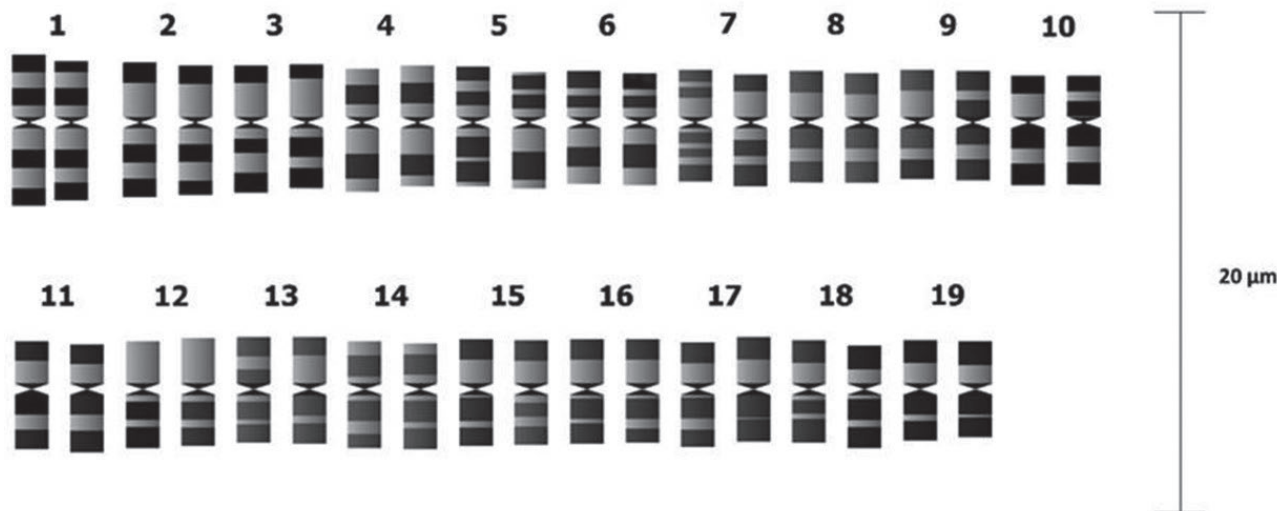
Figure 6. Ideogram of the chromosomes of *Dasylirion cedrosanum* Trel., with GTG bands.

DISCUSSION

In the present work, we found a somatic number of 38 chromosomes in the studied specimens of *Dasylirion cedrosanum* Trel. These results coincide with those reported by Hernández-Quintero et al. (2015), thus reaffirming that the chromosome number is highly conserved among the species of the genus *Dasylirion* (Sato, 1935). In some plant species, there is a natural selection process, karyotypic orthoselection, which consists of the presence of the same type of chromosome rearrangement in specimens of the same species, thus maintaining the chromosome number, which is involved in the process of evolution (Palomino, 2010). This process occurs via the amplification of noncoding regions of DNA at chromosome crossover sites, resulting in a uniform basic number and karyotypes that maintain chromosome number and structure (Flores-Maya et al., 2015). Additional cytogenetic and molecular biology studies are required to determine if the same process is present in *Dasylirion cedrosanum* Trel.

In plants, it is difficult to obtain chromosomal bands because of the presence of a cell wall and the characteristics of the tissue (Chattopadhyay, 1988). In plant chromosomes, the pattern of GTG bands observed in mammals has not been reported. However, in this work, modifications of the original technique allowed the resolution of light and dark chromosomal bands, leading to the identification of seven bands on large chromosomes and five bands on smaller chromosomes. In addition, dark telomeric bands were detected in most of the chromosomes, which represents the first report of a banding

pattern for this species. Previous work on *C. pubescens* indicated the presence of dark bands at the telomere level (Guevara, 2000) and suggested that these bands represent the constitutive heterochromatin—as corroborated here in *Dasylirion cedrosanum* Trel.—with the implementation of the CBW bands. Plant chromosomes contain much more DNA than do vertebrate chromosomes, with a comparable length and with a higher degree of compaction, which explains the presence of these dark bands at the telomere level (Argüelles Saenz, 2018).

Using different cytogenetic banding techniques and morphometric analysis, we established that all chromosomes were of the submetacentric type, which differs from the report of subtelocentric chromosomes previously (Hernández-Quintero et al., 2015). Therefore, it was possible to establish an FN of 76 for *Dasylirion cedrosanum* Trel., and represents the first report defining the FN in this species. The TCL of the chromosomes was significantly higher than those obtained in previous work (Hernández-Quintero et al., 2015). Although hydroxyquinoline is widely used in plants and is especially suitable for species with large chromosomes (Sharma, 2014), in the present work, colchicine was used as an antimitotic agent, with modification of the exposure time and concentration, and afforded more elongated chromosomes, which assisted observation of the bands in each of them. The CI average was between 39.98 % and 44.66 %, and the RL was between 1.94 % and 3.76 % for each chromosome, which can be considered as an approximation of the contribution of each of them to the total content of the *Dasylirion cedrosanum* Trel. genome.

Although all chromosomes present in the karyotype of *Dasylirion cedrosanum* Trel. were of the submetacentric type, in some plant species, transcriptional activity has been observed in nonacrocentric chromosomes. As a future perspective of this study, AgNORs banding or fluorescent *in situ* hybridization using specific probes for the 5S and 45S regions should be carried out.

It is important to determine the number of chromosomes and the ploidy level of a species, especially in those of economic importance. In the case of *Dasylirion cedrosanum* Trel., the lack of cytogenetic studies is well known. To our knowledge, this is the first time that chromosomal characteristics have been reported and a karyotype constructed for this species in specimens from the state of Nuevo León. In addition, these data are very useful in the phylogenetic and taxonomic study of a species to analyze the evolutionary mechanisms involved in speciation and diversity.

AUTHOR'S CONTRIBUTIONS

C.G.V, E.I.C.G and S.M.L designed the study, K.R.M. and C.G.V. performed analyses, K.R.M., C.G.V, E.I.C.G and S.M.L collected data, K.R.M., C.G.V and E.I.C.G led the writing of the manuscript. All authors contributed critically to the drafts and gave final approval for publication.

GEOLOCATION INFORMATION

https://www.journalmap.org/search#list?bounds=57.98481,164.35547|-24.36711,44.47266&precision=1&query=sotol

ACKNOWLEDGMENTS

REFERENCES

Argüelles Saenz, F. V. (2018). *Obtención de cariotipo de Capsicum pubescens R & P (Rocoto).* Retrieved from

Barch, M., Knutsen T, Spurbeck JL. (1997). *AGT Cytogenetics Laboratory Manual.* Philadelphia NY.: Lippincott Williams & Wilkins

Bogler, D. J. (1995). Dasylirion systematics: taxonomy and molecular phylogeny . *Botanical Sciences, 56,* 69-76. doi:https://doi.org/10.17129/botsci.1465

Bogler, D. J. (1998). Three new species of Dasylirion (Nolinaceae) from Mexico and a clarification of the D. longissimum complex. *Brittonia, 50,* 71-86. doi:https://doi.org/10.2307/2807720

Chattopadhyay, D., Sharma, A. K. . (1988). A new technique for orcein banding with acid treatment. . *Stain Technology, 63,* 283-287.

Flores-Gallegos, A. C., Cruz-Requena, M., Castillo-Reyes, F., Rutiaga-Quiñones, O. M., Torre, L. S., Paredes-Ortíz, A., Soto ON, Rodriguez-Herrera, R. . (2019). Sotol, an alcoholic beverage with rising importance in the worldwide commerce. . *Alcoholic Beverages. Elsevier Inc, 7.* doi: https://doi.org/10.1016/B978-0-12-815269-0.00005-2

Flores-Maya, S., Vargas-Jurado, M. Á., Suárez-Mota, M. E., & Barrera-Escorcia, H. (2015). Análisis cariotípico de Agave marmorata y A. peacockii (Agavaceae) ubicados en las terrazas aluviales del río Zapotitlán, Puebla, México. *Polibotánica, 0*(40). doi:10.18387/polibotanica.40.7

Goldblatt, P. (2021). Missouri Botanical Garden. Internet [January, 5] Available: https://www.missouribotanicalgarden.org/plant-science/plant-science/research-staff/article/2561/goldblatt-peter.

Goverment of Mexico. (2022). Secretaria de Agricultura y Desarrollo Rural. Internet [January, 14]. Available https://www.missouribotanicalgarden.org/plant-science/plant-science/research-staff/article/2561/goldblatt-peter.

Guevara, M., Siles, M., & Bracamonte, O. . (2000). Análisis cariotípico de Capsicum pubescens (solanaceae)" rocoto". *Revista Peruana de Biología, 7,* 134-141.

Hernández-Quintero, J., Reyes-Valdés, M., Mendoza-Rodríguez, D., Gómez-Martínez, M., & Rodríguez-Herrera, R. . (2015). Study of the mitotic and meiotic chromosomes of sotol (Dasylirion cedrosanum Trel.). *Phyton, 84*(1), 107-112. doi:10.32604/phyton.2015.84.107

Jabeen, R., Iftikhar, T., Mengal, T., & Iqbal Khattak, M. . (2012). A comparative chromosomal count and morphological karyotyping of three indigenous cultivars of Kalongi (Nigella sativa L.). *Pakistan Journal of Botany,, 44,* 1007-1012.

Kirov, I., Khrustaleva, L., Laere, K. V., Soloviev, A., Sofie, M., Romanov, D., & Fesenko, I. (2017). DRAWID: user-friendly java software for chromosome measurements and idiogram drawing. *Comp Cytogenet, 11*(4), 747-757. doi:10.3897/CompCytogen.v11i4.20830

Levan, A. (1964). Nomenclature for centromeric position on chromosomes. *Hereditas, 52,* 201–220.

Matthey, R. (1945). L'évolution de la formule chromo-somiale chez les vertébrés. *Experientia, 1*, 78–86.

Matthey, R. (1965). Cytogenetic mechanisms and speciations of mammals. *In Vitro, 1*(1).

Nirchio, M. (2014). Citogenética como herramienta taxonómica en peces. *Saber, 26*, 361-372.

Palomino, G., Martínez, J., & Méndez, I. . (2010). Análisis del tamaño del genoma y cariotipo de Agave aktites Gentry (Agavaceae) de Sonora, México. *Revista Mexicana de Biodiversidad,, 81*, 655-662.

Peruzzi, L., & Eroğlu, H. E. . (2013). Karyotype asymmetry: again, how to measure and what to measure? *Comparative Cytogenetics, 7*, 13.

Sato, D. (1935). Analysis of the karyotypes in Yucca, Agave and the related genera with special reference to the phylogenetic significance *The Japanese Journal of Genetics, 11*(5), 272-278. doi:10.1266/jjg.11.272

Sharma, A. K. a. S., A. (2014). *Chromosome Techniques: Theory and Practice* (Oxford Ed.).

Sierra Tristán, J. S., Lara Macías, C. R., Carrillo Romo, R., Melgoza Castillo, A., Morales Nieto, C., & Royo Márquez, M. H. (2008). Los Sotoles (Dasylirion spp) de Chihuahua. . *Folleto técnico INIFAP, 20*, 1-13.

Zuccarini, J. G. (1838). Ueber eine neue Gattung aus der Familie der Bromeliaceae. *Allgemeine Gartenzeitung, 33*, 257-259.

Contributions of species *Rineloricaria pentamaculata* (Loricariidae:Loricariinae) in a karyoevolutionary context

A Cius[1], CA Lorscheider[2], LM Barbosa[1], AC Prizon[1], CH Zawadzki[3], LA Borin-Carvalho[1], FE Porto[4], ALB Portela-Castro[1,4]

[1] *Departamento de Biotecnologia, Genética e Biologia Celular, Universidade Estadual de Maringá, Avenida Colombo, 5790, 87020-900, Maringá – Paraná, Brasil*
[2] *Colegiado de Ciências Biológicas, Universidade Estadual do Paraná, Campus União da Vitória, Praça Coronel Amazônas, s/n, 86400-000, União da Vitória - Paraná, Brasil*
[3] *Departamento de Biologia/Núcleo de Pesquisas em Limnologia, Ictiologia e Aquicultura (Nupélia), Universidade Estadual de Maringá, Avenida Colombo, 5790, 87020-900, Maringá – Paraná, Brasil*
[4] *Departamento de Ciências do Movimento Humano, Campus Regional do Vale do Ivaí, Universidade Estadual de Maringá, Avenida Espanha, s/n, 86870-000 Ivaiporã-Paraná, Brasil*
[5] *Núcleo de Pesquisas em Limnologia, Ictiologia e Aquicultura (Nupélia), Universidade Estadual de Maringá, Avenida Colombo, 5790, 87020-900, Maringá – Paraná, Brasil*
*Corresponding author. E-mail: ferpsaparolli@uem.br

Abstract. Species of *Rineloricaria* demonstrate an interesting evolutionary history from a cytogenetic point of view, due to the occurrence of extensive variation in diploid number (2n=36 -70 chromosomes), with Robertsonian rearrangements mostly responsible for this karyotypic diversity. In this study we present the karyotypic data for a population of *Rineloricaria pentamaculata*, collected in the Itiz stream, a tributary of the Paraná River Basin (Paraná, Brazil), which exhibited 2n=56 chromosomes distributed in 8m/sm+48st/a (number fundamental equal to 64) and simple NOR system revealed by fluorescent *in situ* hybridization (FISH) with 18S rDNA probe, silver nitrate and positive C band, located on the first submetacentric chromosome pair (pair 5). In addition, the NOR pair showed a size heteromorphism for this region, rich in GC composition (positive CMA3). Clusters of 5S rDNA were located in 14 chromosomes and the FISH with a telomeric probe was used to map possible evidence of chromosomal fusions, however, it showed only telomeric sites. These results corroborate the data for the species *R. pentamaculata* and the genus *Rineloricaria*, showing that they are similar to most of the populations analyzed. About the cytogenetic data of *R. pentamaculata*, we reaffirm that most populations were conserved, but in those with derived characteristics, Robertsonian chromosomal rearrangements probably contributed to the karyotypic evolution of the group.

Keywords: *Rineloricaria*, chromosomal rearrangements, cytogenetics, Paraná River Basin, karyotypic evolution.

INTRODUCTION

The subfamily Loricariinae contain 252 valid species distributed by basins of Central and South America, and although morphologically the group is considered monophyletic, taxonomic problems have been reported, for example, the tribe Loricariini several species have similar descriptions (Costa-Silva 2015; Roxo et al. 2019). The genus *Rineloricaria* (Bleeker 1982) is the most numerous genus in the subfamily Loricariinae (Tribe Loricariini), currently consisting of 78 valid species (Fricke and Eschmeyer et al., 2022), distributed throughout the Neotropical region, from the Panama to Argentina, occupying a wide variety of habitats and with restricted information on genetic diversity (Rodriguez and Reis 2008; Vera-Alcaraz et al. 2012). *Rineloricaria* is also considered a monophyletic táxon, however, it presents historical taxonomic problems such as some synonymous species (*Hemiloricaria* Bleeker 1862, *Ixiandria* Regan 1906, *Fonchiichtys* Isbrücker and Michels 2001 and *Leliella* Isbrücker, 2001), species complex (*R. heteroptera* Isbrücker and Nijssen 1976, *R. lima* Kner 1853, *R. cadeae* Hensel 1868, *R. strigilata* Hensel 1868 and *R. lanceolata* Günther 1868) and doubts about the identity of the genus, due to loss of specimen data from the type locality (Costa-Silva 2015; Covain et al. 2016; Venturelli et al. 2021). *Rineloricaria pentamaculata* was described by Langeani and Araújo (1994) from specimens collected in the Turvo River (Ourinhos, SP) in the Upper Paraná River basin and has been collected in different environments of the upper Paraná River basin (Table 1).

Although cytogenetic studies in *Rineloricaria* are scarce and were performed in only 16 species (Giuliano-Caetano 1998; Alves et al. 2003; Maia et al. 2010; Rodrigues 2010; Porto et al. 2011; Rosa et al. 2012; Porto et al. 2014; Ventureli 2014, Primo et al. 2017; Guloski et al 2018, Takagui et al. 2020; Venturelli et al. 2021), these studies have contributed as an important support for studies in species taxonomically complex. Considerable karyotype diversity has been reported in genus, with diploid numbers ranging from 2n=36 in *Rineloricaria latirostris* (Giuliano-Caetano 1998) to 2n=70 in *R. lima* (Rosa et al. 2012). In addition, chromosomal polymorphisms (structural and numerical) were found in six species, called: *R. latirostris* (Giuliano-Caetano 1998), *R. pentamaculata* (Porto et al. 2011; Primo et al. 2017), *R. lima* (Rosa et al. 2012), *R. lanceolata* (Porto et al. 2014).

Robertsoninan chromosomal rearrangements are suggested as the main involved in of karyotypic evolution of *Rineloricaria*, as they would explain the origin of chromosomal polymorphisms and the extensive numerical and structural chromosomal diversity detected in species of genus (Alves et al. 2005; Porto et al. 2011; Porto et al. 2014). This hypothesis has been investigated and supported due to evidence of occurrence of these rearrangements in chromosomes of some species. Cytogenetic techniques have supported this proposition, such as FISH using 5S rDNA and telomeric probes, showed interstitial telomeric sites (ITS) co-located with 5S rDNA sites on specific chromosomes, in addition to detecting transposable elements associated with sequences of 5S rDNA. (Rosa et al. 2012; Porto et al. 2014; Primo et al. 2017; Guloski et al. 2018).

Cytogenetic studies carried out in *Rineloricaria pentamaculata* show that most populations have conserved characteristics, in relation to karyotype, location and simple NOR system and distribution of constitutive heterochromatin. However, in some populations cytogenetic diversity was observed, due to reports of B chromosomes, intrapopulational and interpopulational karyotypic differences, multiple NOR system and variation with respect to the location and amount of chromosomes with 5S rDNA sites 5S (Porto et al. 2010- 2011; Venturelli 2014; Primo et al. 2017).

This study consists of the cytogenetic characterization of *R. pentamaculata* from the Itiz stream (Rio Ivaí sub-basin, Upper Rio Paraná Basin) located in the city of Marialva (Paraná-Brazil), using classical cytogenetic techniques and physical chromosomal mapping of 18S and 5S rDNA, telomeric sequences. Thus, we compile and discuss the cytogenetic data available for the species *R. pentamaculata*, highlighting the similarities and variations found in the different populations with inferences about karyoevolutionary aspects in this group.

MATERIALS AND METHODS

Cytogenetic analysis was conducted on 16 specimens (9 females and 7 males) identified as *Rineloricaria pentamaculata* (NUP 17750 1), collected from the Itiz stream, a small tributary of the Ivaí River (basin of the upper Paraná River, Paraná state, Brazil), Voucher specimens were deposited in the Ichthyological Collection of the Limnology, Ichthyology and Aquaculture Research Center (Nupélia) at Maringá State University, Paraná, Brazil. The protocols used in this study were submitted and reviewed by the Ethics Committee on Animal Experimentation (Protocol 07/2011) of the Maringá State University.

The mitotic chromosomes of *R. pentamaculata* were obtained from kidney cells as described by Bertollo et al. (1978). Chromosomal banding was performed for detection of constitutive heterochromatin by the C-band

technique (Sumner 1972) and double staining using the fluorochromes chromomycin A3 (CMA$_3$) and DAPI, according to Schweizer (1976). Nucleolus organizer regions were labeled by silver nitrate (Ag-NO$_3$) staining as described by Howell and Black (1980). Fluorescent in situ hybridization (FISH) using 18S and 5S rDNA probes was performed based on Pinkel et al (1986).

The 18S rDNA probes were obtained from cloned and amplified fragments of *Prochilodus argenteus* Spix and Agassiz, 1829 (Hatanaka and Galetti 2004), the 5S rDNA probe was isolated from the genomic DNA of *Leporinus elongatus* Valenciennes, 1850 (Martins and Galetti 1999). In this study, we also used a telomeric DNA probe amplified by PCR, free of DNA, from primers (TTAGGG)n and (CCCTAA)n, based on the method of Ijdo et al. (1991). The rDNA probes were labeled by Nick translation with biotin-16-dUTP and 5S and telomeric digoxigenin-11-dUTP. Fluorescent signals were detected with avidin-FITC (for 18S rDNA) and with digoxigenin-rhodamine for 5S rDNA probes and telomeric probe. The metaphases were photographed in an Zeiss Axioskop Microscope with image capture and epifluorescence system. The morphology of the chromosomes was established according to the ratio of arms (RB), according to the proportions proposed by Levan et al. (1964), classifying them as metacentric RB from 1.00 to 1.70), submetacentric (RB from 1.71 to 3.00), subtelocentric (RB from 3.01 to 7.00) and acrocentric (RB greater than 7.00). To calculate the fundamental number (NF), metacentric (m) and submetacentric (sm) chromosomes were considered to have two arms, while subtelocentric (st) and acrocentric (a) chromosomes were single-armed.

RESULTS

The specimens of *Rineloricaria pentamaculata* had a diploid number of 2n= 56 chromosomes, with 8 m/sm+48st/a and fundamental number (NF) of 64, in both sexes (Figure 1a). Ag-NOR sites were found the entire short arm of the first pair of subtelo-acrocentric chromosomes (pair 5), showed a heteromorphism in the size of the secondary constriction (Figure 1a, in box), confirmed by FISH with an 18S rDNA probe (Figure 1b). FISH using 5S rDNA probe revealed 14 subtelo/acrocentric chromosomes with sites (pairs: 6, 7, 8, 10, 11, 12 and 14) located in the terminal regions of these chromosomes (Figure 1b). Hybridization with a telomeric probe revealed markings in the telomeric regions of all chromosomes and absence of interstitial telomeric sites (ITS) (Figure 1c).
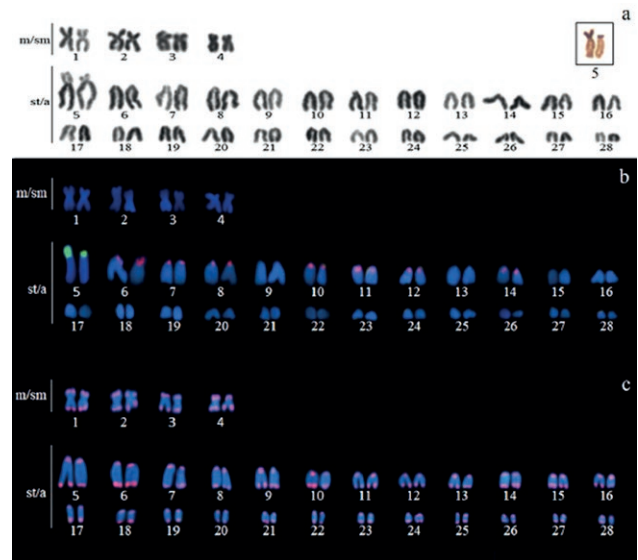
Figure 1. Karyotype for *Rineloricaria pentamaculata* of the Itiz stream after: a) conventional staining by Giemsa and Ag-NOR located on par Nº 5 (in box); b) double-FISH using 18S rDNA (green) and 5S rDNA (red) probes; **c)** FISH with telomeric probe. Note the absence of the ITS.
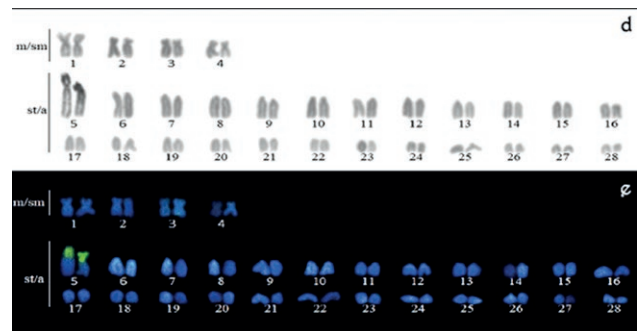
Figure 2. Karyotype of *Rineloricaria pentamaculata* from the Itiz stream showing: d) the heterochromatin distribution pattern after C-banding; **e)** CMA3/DAPI base-specific profile.

Few blocks of heterochromatin were detected in some chromosomes, however, the first pair of subtelo/acrocentric chromosomes presented blocks conspicuous associates the NOR sites (Figure 2d), which also revealed double staining with CMA$_3$/DAPI and, therefore, rich in CG at the sites Ag-NOR (Figure 2e).

DISCUSSION

The data obtained in the present study showed similarities to those observed for most populations of *R.*

pentamaculata, in relation to diploid number (2n=56), karyotypic formula (8m/sm+48st/a), fundamental number (NF=64) and simple NOR system located on the first pair of st/a chromosomes (Table 1). However, divergent karyotypes were found in the populations from the Upper Paraná basin (PR), that is, 2n=58 e 2n=54 and distinct karyotypic formulas (Table 1). In the population of *R. pentamaculata* from the Barra Grande river, Primo et al. (2017) registered a karyomorph B (2n=54) and founded traces of ITS in the centromeric region of a pair of metacentrics (pair 1) suggesting the occurrence of Robertsonian fusion that resulted in the reduction of 2n from 56 to 54 chromosomes. In the population of the Tauá stream (Porto et al. 2011), two karyotypic formulas were detected and the one with 9m/sm +47st/a originated from 8m/sm + 48st/a, and that meiotic nondisjunction and chromosome fusion mechanisms promoted this karyotypic alteration, besides, B microchromosomes (0-3B) were also described for this population, whose origin has been suggested as centric fragments originated from chromosome rearrangements (Porto et al. 2010; Table 1). Therefore, we suggest that the cytogenetic characteristics detected in the present study and in most populations of *R. pentamaculata*, be considered a primitive condition for the species. In the Loricariidae family, from a cytogenetic point of view, the diploid number of 2n=54 chromosomes has been suggested as a plesiomorphic characteristic, and that due possible chromosomal rearrangements such as fusions and fissions occurred throughout the evolution of loricariids, promoted the increase and decrease of diploid numbers (Artoni and Bertollo 2001; Kavalco et al. 2005, Mendes-Neto et al. 2011; Alves et al. 2012).

Possible promoters of chromosomal rearrangements and consequently of chromosomal polymorphisms were investigated in the species of *Rineloricaria*. Interstitial telomeric sites (ITS) have been related to the centric fusion events, corroborating the hypothesis that these rearrangements the involvement with changes in karyotypic formulas, NF and reduction of diploid number in some populations of *Rineloricaria,* such as in *R. lanceolata* (Porto et al. 2014), *R. latirostris* (Primo et al. 2017) and in two species from the Iguaçu River (*R. cubatoni* and *R. maackii*, in preparation). Primo et al. (2017) conducted cytogenetic analysis on a population of *R. pentamaculata* from the Barra Grande River whose specimens showed diploid number of 2n=54 chromosome with the first metacentric chromosome pair bearer of an ITS. The telomeric sequences located in an interstitial position it has been considered traces of centric fusion occurred between acrocentric chromosomes originating metacentric chromosomese with consequent reduction of the diploid number from 56 to 54 chromosomes and alteration of karyotypic formula (table 1; Primo et al. 2017). However, even though ITS were not observed in the population of the Itiz stream and the cytogenetic data show conserved characteristics, this method is not sufficient to postulate the occurrence of centric fusion chromosomal rearrangements. On the other hand, repetitive telomere-like DNA sequences that are components of heterochromatin and located in an interstitial position could be misinterpreted as ITS, these sequences would

Table 1. Cytogenetic data available for *Rineloricaria pentamaculata*.

River/Basin/State	2n (NF)	Karyotype Formula	NOR		rDNA 5S	Ref
			Ag-NOR	rDNA 18S		
Taquaral River/ Paranapanema/ SP	58(62)	4m/sm+54st/a	te (1th st/a)	te (1th st/a pair 3)	10 sites/te	1
Juruba/ Tibagi River/ PR	56(70)	14m/sm+42st/a	-	te (1th st/a, pair 3)	12 sites/te	
Barra Grande River/ Ivaí River / PR	56(70)*	14m/sm+42st/a	-	te (1th st/a, pair 3)	10 sites/te	2
	54(64)**	10m/sm + 44st/a	-	te (1th st/a, pair 4)	8 sites/te	
Tauá Stream/ Alto Paraná River basin / PR	56(65)	9m/sm+47st/a	te (1th st/a)	te (1th st/a)	-	
	56(64)	8m/sm+48st/a	te (1th st/a)	te (1th st/a)	-	3
Tatupeba River/ Alto Paraná River basin PR	56(64)	8m/sm+48st/a	te (1th st/a)	te (1th st/a) and 4th st/a)	-	
Keller River/ Alto Paraná River basin / PR	56(64)	8m/sm+48st/a	te (1th st/a)	te (1th st/a)	-	
Jacucaca River/ Alto Paraná River basin / PR	56(64)	8m/sm+48st/a	te (1th st/a)	te (1th st/a)	12 sites	4
Água do Oito Stream/Tibagi River/ Alto Paraná River	56(64)	8m/sm+48st/a	te (1th st/a)	-	-	5
Quexada River/ Alto Paraná River / PR	56(64)	8m/sm+48st/a	te (1th st/a)	te (1th st/a)	12 sites	6
Itiz stream/ Ivaí River / Alto Paraná River PR	56(64)	8m/sm+48st/a	te (1th st/a)	te (1th st/a)	14 sites/te	7

Subtitles: 2n: diploid number; NF: fundamental number; m: metacentric; sm: submetacentric; st: subtelocentric; a: acrocentric; te: terminal; SP: São Paulo; PR: Paraná; Ref: references: 1- Rodrigues 2010; 2- Primo et al. 2017: * karyomorph A and ** Karyomorph B;.3- Porto et al. 2011; 4- Maia et al. 2010 and Venturelli 2014; 5-Maia et al. 2010; 6-Venturelli 2014; 7- Present study.

not be involved with centric fusion events (Meyne et al. 1990; Ocalewicz 2013; Bolzán 2017).

In addition to ITS, other repetitive DNA sequences are considered hotspot for chromosomal rearrangements, contributing to the understanding of the karyotypic diversity of the genus. In *R. lima*, 5S rDNA sites associated with TTAGGGn were observed in centromeric position in some meta-submetacentric chromosomes suggesting as susceptible sites for chromosomal breaks (Rosa et al. 2012). Glugoski et al. (2018) found transposable elements associated with 5S rDNA sites and TTAGGGn sequences in a population of *R. latirostris* (river of Pedras, Ventania-PR Brazil) and that these elements are probably also involved with chromosomal rearrangements and the karyotypic variability of the species. However, transposable elements were not observed associated with repetitive regions of the genome (5S rDNA and/or TTAGGGn) in populations of *R. latirostris* (Laranjinha river, Ventania-PR Brazil), *R. pentamaculata, R. stellata* and *R. capitonia* (Primo et al. 2018) and this presente study, such analysis was not performed. Thus, the expansion of molecular cytogenetic studies in the genus are essential for the better understanding of the types of rearrangements that caused chromosomal variability, as well as the mechanisms involved in the karyotypic evolution of *Rineloricaria*.

The simple NOR system located in the terminal position of the first pair of subtelo-acrocentric chromosomes is a conserved characteristic among the populations of the species and *Rineloricaria* genus, and was also detected in the present study (Alves et al. 2003; Rodrigues 2010; Maia et al. 2010; Porto et al. 2011; Rosa et al. 2012; Porto et al. 2014; Primo et al. 2017; Venturelli et al. 2021), except for *R. pentamaculata* from the Tatupeba stream, which showed NOR system multiple with two pairs of subtelo-acrocentric chromosomes containing 18S rDNA sites, one of the pairs being the first pair of subtelo-acrocentric chromosomes (Porto et al. 2011; Table 1). The NOR phenotype detected in the present study and in most populations of *R. pentamaculata* and in other species of *Rineloricaria* indicates an origin from a common ancestor. In the Loricariidae most species, showed that the simple NOR system located in terminal position and constitutive heterochromatin generally associated with this region are suggested as an ancestor phenotype. (Júlio-Jr 1994; Artoni and Bertollo 1996; Ribeiro et al. 2015; Prizon et al. 2016; Venturelli et al. 2021). However, in species of Loricariidae with multiple NOR system and the occurrence of B chromosomes, these characteristics were considered apomorphic. (Artoni and Bertolo 1996; Artoni and Bertolo et al. 2001; Kavalco et al. 2005; Porto et al. 2010-2011; Rubert et al. 2016).

Likewise, spécimens of *R. pentamaculata* from the Itiz stream showed similarity to other cytogenetic studies in the pattern of constitutive heterochromatin distribution (Maia et al. 2010; Porto et al. 2011; Venturelli 2014; Primo et al. 2017). The association of constitutive heterochromatin and NOR, detected in the present study, has been frequently reported in fish and shared by all species of *Rineloricaria* has been interpreted as a synapomorphic trait and comes from a common ancestor. (Giuliano-Caetano 1998; Porto et al. 2011; Venturelli et al. 2021). In addition to corroborating the data on the distribution of constitutive heterochromatin in *R. pentamaculata*, we show the composition of CG-rich heterochromatin (CMA3 positive) and emphasize the importance of descriptive and comparative cytogenetics. Furthermore, it is observed that most species of *Rineloricaria*, especially *R. pentamacula*, exhibited low constitutive heterochromatin profiles, with a varied distribution being found in the interstitial and pericentromeric regions, occupying low portions of the long or short chromosome arms (Primo et al. 2017).

Physical mapping of 5S rDNA sequences in species of *Rineloricaria,* especially in *R. pentamaculata*, has increased since 2011 and of the 11 cytogenetically characterized species, seven presented studies of 5S rDNA sites, showing variation in location and quantity (7 to 14 sites, table 1). For the genus *Rineloricari*a, these regions are evidenced in more than one pair of chromosomes (Rosa et al. 2012; Primo et al. 2017; Glugoski et al. 2018; Venturelli et al. 2021), however, it is not possible to establish a pattern, suggesting that these sites is a species-specific character. Information on diploid number and 5S rDNA distribution, has been used as a support to distinguish species of *Rineloricaria* that are morphologically similar, with difficulties in characterizing and validating the taxonomic status of the species. (Venturelli et al, 2021).

A hypothesis that could explain the multiple sites of 5S rDNA detected in species of *Rineloricaria* is that tranposable elements promoted the dispersion of copies of these genes throughout the genomes (Primo et al. 2018; Glugoski et al. 2018). Furthermore, according to Glugoski et al. (2018) in *R. latirostris*, showed multiple degenerate 5S rDNA, would be involved with the insertion of the transposable element hAT. Unequal crossover has been suggested to explain the existence of these degenerate sequences, establishing a breakpoint region susceptible to chromosome breakage, non-homologous recombination and Robertsonian fusion (Rb), and thus corroborating the hypothesis that both 5S rDNA sites and transposable elements may be involved with chromosomal polymorphisms and the karyotypic variability

observed in *Rineloricaria* (Glugoski et al. 2018).

Therefore, the present study contributes to aggregate and stimulate cytogenetic studies in the species *Rineloricaria pentamaculata* and others species of *Rineloricaria.* Futhermore, we postulate that the diploid number of 2n=56, karyotypic formula 8m/sm + 44st/a, NF=64 and simple NOR system located in the first pair of ts/a chromosomes reinforcing this chromosomal structure as representative of this species and probably, a plesiomorphic condition for *R. pentamaculata*. On the other hand, for those populations that presented apomorphic cytogenetic characteristics (Tauá and Tatupeba streams and Barra Grande river, Table 1), Robertsonian rearrangements could have caused these variations, and that 5S rDNA sequences and the transposable elements promoted these rearrangements, contributing for the karyotypic evolution to the species. However, the presence of multiple 5S rDNA sites also seems to be a characteristic of the chromosomal structure of *R. pentamaculata*, constituting an important marker of intraspecific variations in comparative analyzes of this group.

REFERENCES

Alves ALC, Oliveira C, Foresti F. 2003. Karyotype variability in eight species of the subfamilies Loricariinae and Ancistrinae (Teleostei, Siluriformes, Loricariidae). Caryologia. 1:57–63.

Alves AL, Oliveira C, Foresti F. 2005. Comparative cytogenetic analysis of eleven species 308 of subfamilies Neoplecostominae and Hypostominae (Siluriformes: Loricariidae). Genetica. 309(124):127-136.

Alves AL, Borba RS, Oliveira C, Nirchio M, Granado A, Foresti F. 2012. Karyotypic diversity and evolutionary trends in the Neotropical catfish genus *Hypostomus* Lacépède, 1803 (Teleostei, Siluriformes, Loricariidae). Comp Cytogen. Available from: http://www.pensoft. net/journals/compcytogen.

Artoni RF, Bertollo LAC. 2001. Trends in the karyotype evolution of Loricariidae fish (Siluriformes). Hereditas. 134:201–210. Available from: http://doi/10.1111/j.1601-5223.2001.00201.x

Artoni RF, Bertollo LAC. 1996. Cytogenetic studies on Hypostominae (Pisces, 312 Siluriformes, Loricariidae). Considerations on karyotype evolution in the genus *Hypostomus*. Caryologia. 49:81–90.

Bertollo LAC, Takahashi CS, Moreira Filho O. 1978. Cytotaxonomic considerations on *Hoplias lacerda* (Pisces, Erythrinidae). Brazilian Journal of Genetics. 1: 103–120. Bolzán AD. 2017. Interstitial telomeric sequences in vertebrate chromosomes: origin, function, Instability and evolutions. Mutation Research. 1383-5742(16):30153-3. Available from: http://dx.doi. org/doi:10.1016/j.mrrev.

Costa-Silva GJ, Rodriguez MS, Roxo FF, Foresti F, Oliveira C. 2015. Using Different Methods to Access the Difficult Task of Delimiting Species in a Complex Neotropical Hyperdiverse Group. PLoS ONE. 10(9):e0135075. Available from: http://doi/10.1371/ journal. pone.0135075

Covain R, Fish-Muller S, Oliveira C, Mol JH, Montoya-Burgos JI, Dray S. 2016. Molecular phylogeny of the highly diversified catfish subfamily Loricariinae (Siluriformes, Loricariidae) reveals incongruences with morphological classification. Mol Phylogenet Evol. 94:492–517. Available from: https://doi.org/10.1016/j. ympev.2015.10.018

Kavalco KF, Pazza R, Bertollo LAC, Moreira-Filho. 2005. Karyotypic diversity and 370 evolution of Loricariidae (Pisces, Siluriformes). Heredity. 4:180-186.

Fricke R, Eschmeyer WN. 2022. A guide to fish collections in Eschmeyer's catalog of fishes [internet]. San Francisco: California Academy of Science. Accessed [2022-03-02]. Available from: http://researcharchive. calacademy. org/research/ichthyology/catalog/collections.asp.

Giuliano-Caetano L. 1998. Polimorfismo cromossômico Robertosiano em populações de *Rineloricaria latirostris* (Pisces, Loricariidae). [thesi]. Departamento de Genética e Evolução. São Carlos-SP: Universidade Federal de São Carlos.

Glugoski L, Giuliano-Caetano L, MoreiraFilho O, Vicari MR, NogarotoV. 2018. Co-located hAT transposable element and 5S rDNA in an interstitial telomeric sequence suggest the formation of Robertsonian fusion in armored catfish. Gene. 650:49-54. Available from: http://doi/10.1016/ j.gene. 2018.01.099.

Hatanaka T, Galetti Jr PM. 2004. Mapping 18S and 5S ribosomal RNA genes in the fish *Prochilodus argenteus* Agassiz, 1929 (Characiformes, Prochilodontidae). Genetica. 122:239–244. DOI:10.1007/s10709-004-2039-y.

Howell WM, Black DA. 1980. Controlled silver-staining of nucleolus organizer regions with a protective

colloidal developer: a 1-step method. Experientia. 36:1014–1015. DOI:10.1007/ BF01953855.

Ijdo JW, Baldini A, Ward DC, Reeders ST, Wells RA. 1991. Origin of human chromosome 2: an ancestral telomere-telomere fusion. Proc Natl AcadSci USA. 88:9051-9055.

Levan A, Fredga K, Sandberg AA. 1964. Nomenclature for centromeric position on chromosomes. Hereditas. 52:201–220. Available from: DOI:10.1111/j.1601-5223.1964.tb01953.x.

Maia TPA, Giuliano – Caetano L, Rodriguez MS, Rubert M, Takagui FH, Dias AL. 2010. Chromosomal banding in three species of the genus *Rineloricaria* (Siluriformes, Loricariidae, Loricariinae).Ichthyol Res. 57:209–213.

Mendes-Neto EO, Vicari MR, Artoni RF, Moreira-Filho O. 2011. Description of karyotype in *Hypostomus regain* (Ihering, 1905) (Teleostei, Loricariidae) from the Piumhi river in Brazil with comments on karyotype variation found in Hypostomus. Comparative Cytogenetics. 5:133–142. DOI:10.3897/compcytogen. v5i2.964

Meyne J, Baker RJ, Hobart H, Hsu TC, Oliver AR, Ward OG. 1990. Distribution of non-telomeric sites of the (TTAGGG)n telomeric sequences in vertebrate chromosomes. Chromosoma. 99:3–10.

Pinkel D, Straume T, Gray JW. 1986 Cytogenetic analysis using quantitative, high sensitivity, fluorescence hybridization. Proceedings of the National Academy of Sciences of the United States of America. 83:2934–2938. DOI:10.1073/pnas.83.9.2934

Porto FE, Portela-Castro ALB, Martins-Santos IC. 2010. Possible origins of B chromossomes in *Rineloricaria pentamaculata* (Loricariidae, Siluriformes) from the Paraná River basin. Genetic Molecular Research. 9(3):1.654-1659. DOI: 10.4238/vol 9-3gmr859.

Porto FE, Portela-Castro ALB, Martins-Santos IC. 2011. Chromosome polymorphism in *Rineloricaria pentamaculata* (Loricariidae, Siluriformes) of the Paraná River basin. Ichthyologic Research. 58:225–231. DOI:10.1007/s10228-011-0215-5.

Porto FE, Vieira MMR, Barbosa LG, Borin-Carvalho LA, Vicari MR, Portela-Castro ALB, Martins-Santos IC. 2014. Chromosomal polymorphism in *Rineloricaria lanceolata* Günther, 1868 (Loricariidae: Loricariinae) of the Paraguay basin (Matogrosso do Sul, Brazil): evidence of fusions and their consequences in the population. Zebrafish. 11(4):318-24. DOI:10.1089/ zeb.2014.0996.

Primo CC, Glugoski L, Mara C, Almeida MC, Zawadzki CH, Moreira-Filho O, Vicari MR, Nogaroto V. 2017. Mechanisms of chromosomal diversification in species of *Rineloricaria* (Actinopterygii: Siluriformes: Loricariidae). Zebrafish. 14:161-168.

Primo CC, Glugoski L, Vicari MR, Nogaroto V. 2018. Chromosome Mapping and Molecular Characterization of the Tc1/Mariner Element in *Rineloricaria* (Siluriformes: Loricariidae). Braz. Arch. Biol. Technol. DOI:10.1590/1678-4324-2018170623.

Prizon AC, Borin-Carvalho LA, Bruschi DP, Ribeiro MO, Barbosa LM, Ferreira GEB, Cius A, Zawadzki CH, Portela-Castro ALB. 2016. Cytogenetic data on *Ancistrus* sp. (Siluriformes, Loricariidae) of the Paraguay River basin (MS) sheds light on intrageneric karyotype diversification. Comp Cytogen. 10(4): 625–636. Available from: http://doi/10.3897/CompCytogen. v10i4.8532 http://compcytogen.pensoft.net.

Rodrigues RM. 2010. Estudos cromossômicos e moleculares em Loricariinae com ênfase em espécies de *Rineloricaria* (Siluriformes, Loricariidae): uma perspectiva evolutiva. 218p. [dissertation]. São Paulo (SP): Instituto de Biociências da Universidade de São Paulo.

Rodriguez M.S, Reis RE. 2008. Taxonomic Review of *Rineloricaria* (Loricariidae: Loricariinae) from the Laguna dos Patos Drainage, Southern Brazil, with the Descriptions of Two New Species and the Recognition of Two Species Groups. Copeia. 2008:333–49.

Rosa KO, Ziemniczak K, Barros AV, Nogaroto V, Almeida MC, Cestari MM, Artoni, RF, Vicari MR. 2012. Numeric and structural chromosome polymorphism in *Rineloricaria lima* (Siluriformes: Loricariidae): fusion points carrying 5S rDNA or telomere sequence vestiges .Rev Fish Biol Fisheries. DOI:10.1007/s11160-011-9250-6.

Rubert M, Rosa R, Zawadzki CH, Mariotto S, Moreira-Filho O, Giuliano-Caetano L. 2016. Chromosome Mapping of 18S Ribosomal RNA Genes in Eleven *Hypostomus* Species (Siluriformes, Loricariidae): Diversity Analysis of the Sites. Zebrafish. 13(4). DOI:10.1089/zeb.2016.1279.

Scavone MDP, Júlio HF Jr. 1994. Cytogenetic analysis and probable supernumerary chromosomes of *Loricaria prolixa* and *Loricaria* sp. Females (Loricariidae-Siluriformes) from the Parana´ river basin. Rev Ictiol. 2:41–47.

Schweizer D. 1976. Reverse fluorescent chromosome banding with chromomycin and DAPI. Chromossoma. 58: 307–324. DOI: 10.1007/BF00292840.

Sumner AT. 1972. A simple technique for demonstrating centromericheterochromation. Experimental Cell Research. 75:304–306. DOI:10.1016/0014-4827(72)90558-7.

Takagui FH, Baumgartner L, Venturelli NB, Paiz LM, Viana P, Dionısio JF, Pompeo LRS, Margarido VP,

Fenocchio AS, Rosa R, Giuliano-Caetano L. 2020. Unrevealing the Karyotypic Evolution and Cyto-taxonomy of Armored Catfishes (Loricariinae) with Emphasis in *Sturisoma*, *Loricariichthys*, *Loricaria*, *Proloricaria*, *Pyxiloricaria*, and *Rineloricaria*. Zebrafish. 17:5. DOI: 10.1089/zeb.2020.1893.

Venturelli NB. 2014. Mapeamentos dos genes ribossômicos e cromossomos marcadores em nove espécies de *Rineloricaria* (Siluriformes, Loricariidae, Loricariinae) de distintas Bacias hidrográficas. [dissertation]. Londrina (PR): Universidade Estadual de Londrina.

Venturelli NB, Takagui FH, Pompeo LRS, Rodriguez MS, Rosa R, Giuliano-Caetano L. 2021. Cytogenetic markers to understand chromosome diversification and conflicting taxonomic issues in *Rineloricaria* (Loricariidae: Loricariinae) from Rio Grande do Sul coastal drainages. Biologia. Available from: https://doi.org/10.1007/s11756-021-00748-3.

Vera-Alcaraz HS, Pavanelli CS, Zawadzki CH. 2012. Taxonomic revision of the *Rineloricaria* species (Siluriformes: Loricariidae) from the Paraguay River basin. Neotropical Ichthyology. 10:285–311.

Cadmium induced genotoxicity and antioxidative defense system in lentil (*Lens culinaris* Medik.) genotype

Durre Shahwar[1,2,*], Zeba Khan[3], Mohammad Yunus Khalil Ansari[1]

[1] *Cytogenetics and Molecular Biology laboratory, Department of Botany, Aligarh Muslim University, Aligarh, 202002, India*
[2] *Plant Genomics and Molecular Biology laboratory, Department of Horticultural Bioscience, Pusan National University, Miryang 50463, Korea*
[3] *Center for Agricultural Education, Faculty of Agricultural Sciences, Aligarh Muslim University, Aligarh 202002, India*
*Corresponding author. E-mail: khanzeba02@gmail.com

Abstract. Induced mutagenesis is considered a coherent mechanism in crop improvement programmes to produce novel plant varieties. Due to the insufficiency of desired genotypes, plant breeders are supposed to re-associate the gene of interest from the accessible gene pool of the related plant species through hybridization to develop new cultivars with desired traits. The present investigation was performed to evaluate cadmium induced mutagenesis on growth performance, physio-biochemical traits and DNA damage studies in lentil. Growth and morphological parameters exhibited reduction with increasing concentration of cadmium. Maximum devaluation was reported at the highest concentration. Physiological and biochemical traits were also affected by different cadmium concentrations and reduced as concentration increased. Lipid peroxidation activity and antioxidant enzymes increased as mutagenic stress increased caused by cadmium. CAT and SOD concentration was found to increase initially and then decreased gradually at higher cadmium concentrations. SEM analysis of stomatal morphology revealed variation in stomatal shape and size in treated populations. There was a gradual enhancement in the percentage of DNA damage along with variation in morphological traits. The DNA damage was recorded as precocious movement, stray bivalent, laggard, stickiness, disorientation of chromosome, multi-bridge, disturbed polarity and micronuclei. It was concluded that at higher concentrations, cadmium cause DNA damage and these chromosomal alterations causes morpho-physiological and biochemical changes in lentil.

Keywords: Abiotic stress, oxidative stress, antioxidant activity, DNA damage, *Lens culinaris*.

ABBREVIATIONS

Cd	Cadmium
CAT	Catalase activity
SOD	Superoxide dismutase

ROS   Reactive oxygen species
EDTA   Ethyl diamine tetra acetic acid

INTRODUCTION

Nowadays, world is posing a severe threat of malnutrition and food insecurity to human civilization. Scientists are involved in developing new and ingenious approaches to diminish hunger and malnutrition issues which are expanding day by day around the world. Pulses play a significant role in compensating food insecurity, especially for low-income families (Kumar and Pandey 2020).India is one of world's largest producer, importer and consumer of pulses, especially lentils, which have great potential to elucidate the global food crisis. Lentil is highly efficient inadjusting adverse climatic conditions, which resulted in a declaration by United Nations in 2016 as an International Year of Pulses (IYP2016), with interdisciplinary research approaches towards the qualitative and quantitative improvement of pulses.

Lentil is considered as essentially important nutritious crop rich in protein and minerals. *Lens culinaris* is self-pollinated, diploid (2n=14) crop with a genome size of 4063Mbp (Arumuganathan and Earle, 1991). Van Oss *et al.* (1997) suggested that the *Lens* genus has four wild species *L.culinaris*, *L. lamottei, L. nigricans* and *L. ervoides*, whereas (Ferguson et al. 2000) observed that *Lens culinaris* Medikus contain three wild subspecies: *L. culinaris* subsp. Orientalis and *L. culinaris* subsp. *tomentosus* and *L. culinaris* subsp. *Odemensis* of which *L. culinaris* subsp. *orientalis* is considered the ancestor of cultivated lentil. Full knowledge of lentil was given by Barulina (1930), who categorized *Lens culinaris* into two subspecies, of which one is named macrosperma (large seeds with 6-9 mm diameter) and the other microsperma (tiny seeds with 2-6mm diameter). Lentil is known to be a source of protein and high quality fiber among all pulses, because of this property, it is considered an economical food consumed all over the world. Lentil is an accomplished source of essential vitamins and minerals such as foliate vitamin B1, magnesium, phosphorus, potassium, copper complex carbohydrates and vegetable protein and a low amount of fatfree cholesterol (Tharanathan & Mahadevamma, 2003). Lentil contains macronutrients and also poses certain phytochemicals such as; flavonols, phenolic acids, phytic acid, soyasaponins and tannins (Xu & Chang, 2010). It can fix atmospheric nitrogen and increase soil fertility due to increased level of nitrogen in soil and by adding carbon and organic matter. Keeping all these attributes in mind, it becomes necessary to ameliorate len-

til variety to obtain genotype of good nutrient quality and yield-related traits. Induced mutagenesis is a helpful technique in the plant-breeding programme for breeders or biological researchers with the embellishment in knowledge of technique for inducing mutation and mutation process itself to produce new cultivar of better quality by creating variability (Chaudhary *et al.* 2019).Mutagenesis has increased genetic variability for qualitative and quantitative traits and induces desirable mutant alleles, which may not previously present in germplasm in a wide variety of species.Induced mutagenesis has played a significant role in overcoming food scarcity for world population and developed new mutant cultivars with increased nutritional values (Suprasanna *et al.* 2015).

Cd is an anthropogenic genotoxic pollutant that is highly soluble in water (Jiang *et al.* 2001)and is readily absorbed by the plants. Cd toxicity reduces uptake and translocation of nutrients and water, increases oxidative damage, disrupts plant metabolism, and inhibits plant morphology and physiology (Haider *et al.* 2021). In plants, primary effect of metal toxicity is inhibition in root growth and cell division, protein denaturation, altered photosynthesis (Rathore *et al.* 2007; Akinci *et al.* 2010) and increases in the frequency of chromosomal aberrations as studied in different plants such as *Allium* by Liu *et al.*, 1994, *Allium sativum* (Yi and Meng, 2003); *Helianthus annuus* (Kumar and Srivastava, 2006); *Lathyrus sativus* (Kumar and Tripathi, 2007a) etc. Heavy metal can induce reactive oxygen species (ROS) (Qian *et al.* 2009). Plants overcome the damage induced via metals stress by activating defense mechanisms which involve both -enzymatic components such as catalase (CAT), superoxide dismutase (SOD) and peroxidase (POX) to protect themselves from ROS (Ruley *et al.*2004) and non-enzymatic components such as glutathione–S-tranferase and glutathione reductase. An increase in ROS causes overproduction of MDA, therefore MDA in plant cell acts as a markerbetween production and scavenging of free radicals. Production of ROS causes oxidative burst in biological macromolecules such as enzymes, proteins, membrane lipids, DNA, chloroplast and carotenoids (Tripathy and Oelmüller 2012). Cadmium binds strongly to DNA and RNA, and alters the DNA transcription process so that DNA synthesis and mitotic activities are disturbed resulting in depolymerization, DNA strand breaks, generation of abnormal nitrogenous bases, DNA – DNA cross-links and DNA – protein cross-links. The present investigation examines cadmium-induced mutagenicity and related stress in lentils by assessing the growth, yield, cytological, physiological and biochemical traits.

2. MATERIALS AND METHODS

2.1 Seed procurement and treatments

Dry, healthy, certified, uniform and equal size seeds of *Lens culinaris* variety L-4076 were obtained from Indian Agricultural Research Institute, New Delhi. Fresh, uniform and healthy seeds of lentil were presoaked in double-distilled water for 24 hours, and the mutagenic treatment of cadmium nitrate were given according to my previous study related to work (Shahwar *et al.* 2019). The comprehensive knowledge of induced mutagenesis and selection of mutant lines are described in detail in earlier study related to the work (Shahwar *et al.*, 2022). Presoaked seeds were then subjected to different concentrations (20,40,60,80 and 100ppm) of freshly prepared cadmium nitrate solution in double- distilled water at pH 7.0 for 12 hrs with intermittent shaking after an interval of 1 or 2 hours at room temperature of 25± 2°C. After treatment, the seeds were thoroughly washed with tap water to ensure the removal of adhered metal (Cd++) on the surface of the seed coat.Treated seeds of each concentration were sown in replicates with their respective control in earthen pots having soil mixed with farmyard manure and irrigated regularly.

2.2 Growth and morphological study

The experiment was carried out to demonstrate the cadmium stress on the growth and morphology of *Lens culinaris*. Root and shoot length were measured from randomly selected seedlings of each replicate for 30 days. Agronomical parameters such as plant height, number of branches per plant, yield and yield related traits were recorded during the development.

2.3Determination of physiological and biochemical parameters

2.3.1 Estimation of chlorophyll and carotenoid content

The photosynthetic pigments (chlorophyll a, b and carotenoid) were determined by acetone method (Arnon 1949) following pigment extraction. For the purpose,1 g fresh leaves were ground with 80% acetone and the extract was diluted with double distilled water and the final volume was made 10mL. The optical density (O.D) of photosynthetic pigments were measured at wavelengths of 663 and 645nm (Smith and Benitez, 1955) using UV-VISspectrophotometers. Photosynthetic pigment of the sample was calculated using the following formula:

chlorophyll a = 12.7 (O.D.) 663-2.69(O.D.) 645×v/w×1000

chlorophyll b = 22.9 (O.D.) 645-4.68(O.D.) 663×v/w×1000

Total chlorophyll = 20.2 (O.D.) 645+8.02 (O.D.) 663×v/w×1000

carotenoids = 46.95 (O.D. 440.5-0.268× chlorophyll (a+b)
Where W=fresh weight of extracted tissue in grams
V= total volume of extract

2.3.2 Analysis of stomatal morphology and mineral elements

Stomatal morphology was studied using scanning electron microscopy (JEOL, JSM-6510LV, JAPAN). Scanning electron microscopy andenergy dispersive X-ray microanalysis(EDX) of leaf sample were performed following the protocol proposed by Daud*et al.* (2009) with minor changes. The leaf samples were fixed in 2.5 % glutaraldehyde and 2% paraformaldehyde in 0.1M phosphate buffer (pH 7.0) for 4 hrs and washed for 15 min with phosphate buffer thrice at each step. Leaf samples were then re-fixed for 1 hour with OsO_4 (osmium tetraoxide) in 0.1 M of potassium phosphate buffer (pH 7.0) and were again washed for 15 min with the same phosphate buffer thrice at each step. The dehydration was done after fixation using ethanol series (30%, 50%, 70%, 90%, and 100%) for 15-20 min thrice for each cycle and transferred in the mixture of alcohol and isoamyl acetate (1:1) for half an hour and in pure isoamyl acetate for one hour. Dehydration of specimens were done by Zeiss Evo 60 (Carl Zeiss SEM, Germany) critical point dryer using liquid carbon dioxide, the samples were coated with a thin layer of Palladium and observed under SEM at 15 kv with x1500 magnifications. Prepared leaf samples were analyzed through EDX for mineral element analysis.

2.3.3 Estimation of proline content

Leaf sample was homogenized in 10 mL of 3% aqueous sulfosalicylic acid and centrifuged at 9000 rpm for 10 min. 2ml glacial acetic acid was added to 2 mL of supernatant; further 2ml ninhydrin solution in 30ml acetic acid and 20mL of 6M H_3PO_4were added. The solution was incubated at 100ºC for 1 hour and OD was recorded at 520 nm using toluene as blank. Proline content in test sample was calculated using a standard curve (Bates *et al.* 1973).

2.3.4 Determination of lipid peroxidation/MDA content

Malondialdehyde (MDA) content was measured following the protocol proposed by Hodges *et al.* (1999) and expressed as μ moles g $^{-1.}$

2.3.5 Antioxidant enzyme activity assay

Antioxidant enzyme assay was done by the method proposed by Sinha *et al.* (2018) with slight modification. Fresh leaves tissues were grinded in 1 ml extraction buffer having 80 mM sodium phosphate buffer, 1mM EDTA, 1 m Mphenylsulfonylfluride (PMSF), 1% polyvinyl pyrrolidone (PVP), and 0.5% (v/v) Triton X-100 and centrifuged at 11000 rpm for 25 min at 4°C. The supernatant kept at -20°C was used to determine antioxidant enzyme activities such as catalase (CAT) following protocol proposed by Yu and Rengel (1999), superoxide dismutase (SOD), Gallego *et al.* (1996) and peroxidase (POX) Kar and Mishra (1976).

2.3.6 Estimation of protein content

Dry seeds (0.5g) were ground in 10ml water and 1ml of 10%trichloroaceticacid was added to the extract. The sample was kept in an ice bath for 10 min. and the supernatant was collected and centrifuged at 5000 rpm for 10 min at 4°C. 20 ml sodium hydroxide (0.1N) was added to dissolve the protein and the total volume was made the nearest whole number. Seed protein content of the extract was determined by Lowry's method (1951) using BSA (Bovine serum albumin) as standard and absorbance were measured at 650 nm.

2.4 DNA damage Studies

For chromosomal studies, young and small-sized flower buds were collected from treated and control plants, fixed in freshly prepared Carnoy's fluid (1:3:6 ratio of glacial acetic acid, chloroform and alcohol) and were preserved in 70% alcohol. For DNA damage studies,anthers of appropriate size were squashed in 0.5% propionocarmine stain, dehydrated in normal butyl alcohol series and mounted on Canada balsam to prepare permanent slides. Microphotographs of chromosomal lesion or DNA damage were taken from temporary and permanent slides by "Olympus" microphotographic unit.

2.5 Statistical interpretation

The results were analyzed and interpreted statistically using software SPSS version 20 for windows 10 using one-way ANOVA. For determinationof least significant difference (LSD) at 5% and 10% probability ($p < 0.05$, 0.01), data analysis of variance, one-way ANOVA was done using Duncan's Multiple Range Test (DMRT) (Duncan, 1955)

3. RESULTS

3.1 Effect of heavy metal stress on growth and morphological parameter

3.1.1 Germination, survival and pollen fertility

Effects of cadmium stress on seedling growth were investigated on 15 days old seedling. It was observed that plant germination, survival and pollen fertility decreased linearly in dose-dependent manner. The inhibitory effect on germination and related parameters were evident at the highest concentration of heavy metal. Fig. 1A depicts a gradual decrease in these characters as concentration increases. The highest concentration (100 ppm) of mutagen exhibited a maximum reduction in all these parameters.

3.1.2 Effect of Cd heavy metal on root and shoot length (cm)

A more pronounced impact of cadmium stress on root and shoot lengths were observed in treated plants. Fresh weight of the seedlings decreased significantly with increase in cadmium concentration. The decrease was significantat 80 and 100 ppm for root length and in 40-100 $Cd(NO_3)_2$ for shoot length.Inhibitory effect on the seedling growth was higher in the root than in the aerial segment. (Fig. 1B).

3.1.3 Plant height

At maturity plant height was found to be maximum in control 43.26±1.52 and decreased significantly from 39.53±3.24 to 31.80±3.31 in 20 to100 ppm both at 5% ($p < 0.05$) and 1 % level ($p < 0.01$) (Table 1).

3.1.4 Number of branches per plant

Mean for number of branches per plant was found to be 3.86±0.49 in control and decreased significantly at
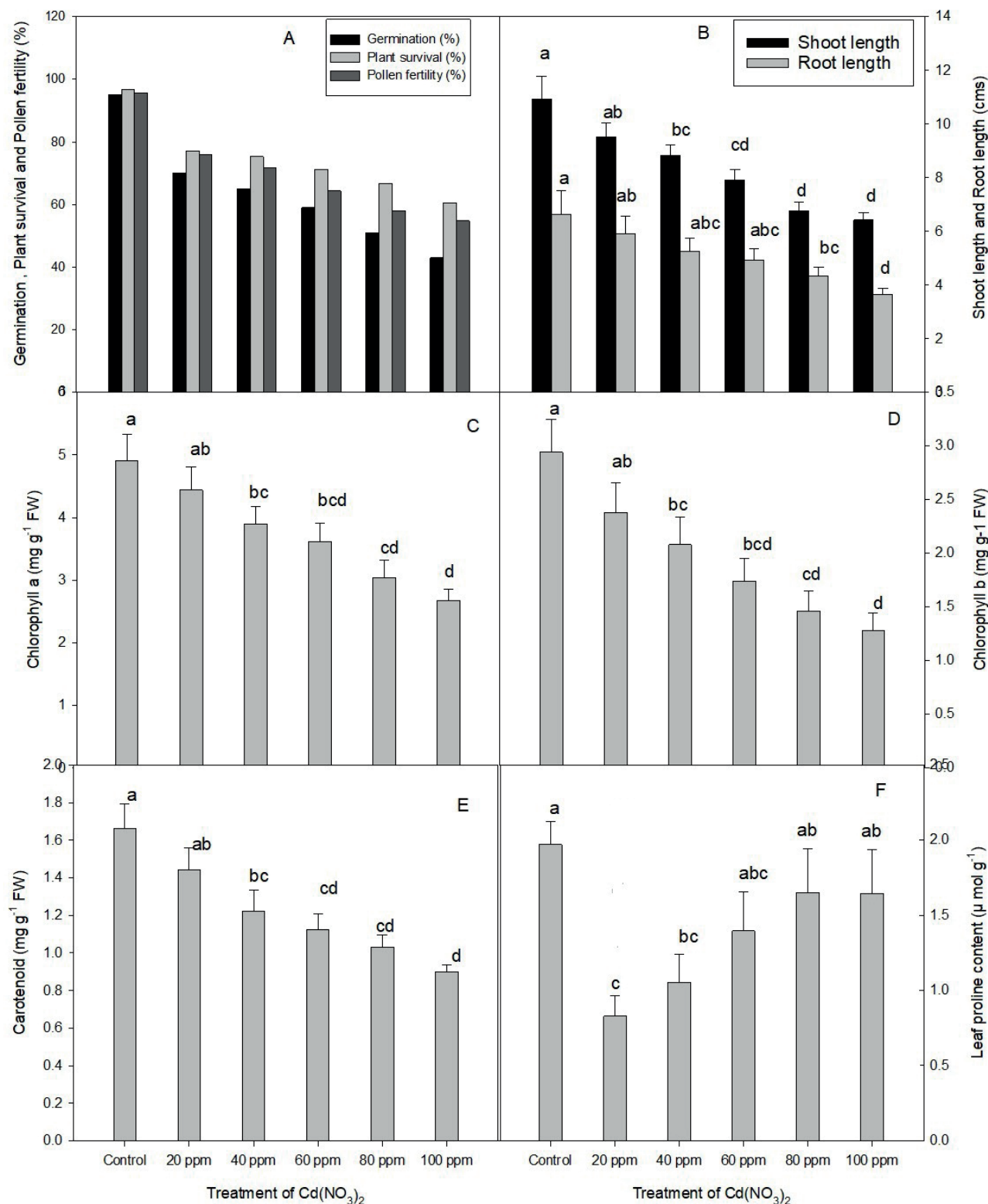
Figure 1. Effect of Cd(NO₃)₂ on germination, survival, and pollen fertility, root and shoot length (cm), photosynthetic pigments and proline content (μmoles/g dry wt) in *Lens culinaris*. Medik L. (M₁ generation). Data means within columns followed by the same letter is not different at the 5% level of significance, based on the Duncan Multiple Range Test.

Table 1. Growth and Yield Studies in $Cd(NO_3)_2$ treated *Lens culinaris* Medik.

Conc. ppm $Cd(NO_3)_2$	Plant Height (cm) Mean±SD CV	No. of Branches/Plant Mean±SD CV	No. of Pods/Plant Mean±SD CV	Length/pod (cm) Mean±SD CV	No. of Seeds/ pod Mean±SD CV	Total no. of Seeds/Plant Mean±SD CV	100-Seeds Weight (g) Mean±SD CV	Total Yield/ plant(g) Mean±SD CV
Control	43.26±1.52 3.51	3.86±0.49 12.69	38.53±1.25 3.24	1.06±0.16 15.09	2.0±0.36 18.0	77.06±2.08 2.69	3.10±0.20 6.45	2.38±0.45 18.90
20	39.53*±3.24 8.25	2.93**±0.57 19.45	37.26±2.48 6.65	1.00±0.23 23.00	1.66±0.44 26.50	61.85**±4.42 7.14	2.94±0.36 12.24	1.81±0.69 38.12
40	38.93*±3.31 8.50	2.73**±0.67 24.54	36.13±2.67 7.38	0.96±0.24 25.00	1.46*±0.48 32.87	52.74**±4.64 8.79	2.88±0.39 13.54	1.51*±0.78 51.65
60	35.00**±4.22 12.05	2.66**±0.73 27.44	34.46**±3.36 9.75	0.92±0.25 27.17	1.33**±0.49 36.84	45.83**±5.15 11.23	2.80±0.41 14.64	1.28**±0.81 63.28
80	32.46**±4.68 14.41	2.40**±0.80 33.33	32.53**±3.79 11.65	0.87±0.27 31.03	1.26**±0.49 38.88	40.98**±5.81 14.17	2.72*±0.46 16.91	1.11**±0.75 67.56
100	31.80**±4.96 15.59	2.26**±0.78 34.51	31.66**±4.09 12.91	0.84*±0.28 33.33	1.20**±0.48 40.00	37.99**±6.09 16.03	2.68*±0.50 18.65	1.01**±0.70 69.30
LSD at 5% (*)	3.37	0.60	2.70	0.20	0.41	4.28	0.34	0.64
LSD at 1% (**)	4.72	0.84	3.78	0.29	0.59	5.99	0.48	0.90

SD= Standard Deviation, CV= Coefficient of Variations, LSD= Least Significant Difference.

1% ($p < 0.01$) from lower to higher concentration. Coefficient of variation increased with the increasing concentration of mutagens (Table 1).

3.1.5 Yield attributing traits

Number of pods per plant, number of seeds per pod, total number of seeds per plant, 100 seed weight and total yield per plant are the yield related traits. All these parameters were found to reduce significantly at 5% ($p < 0.05$) and 1% level ($p < 0.01$) when compared with their respective control (Table-1). Number of pods per plant decreased significantly at 1% level ($p < 0.01$) from 34.46±3.36 to 31.66±4.09 (60-100 ppm) concentration and the number of seeds per pod decreased at 1% level in 60-100 ppm $Cd(NO_3)_2$ (Table-1). Total number of seeds per plant, 100 seed weight and total yield per plant significantly decreased minimally from lower to higher doses of cadmium nitrate. Coefficient of variation increased with increasing concentration of cadmium which means the coefficient of variation is directly proportional to the concentration of mutagen.

3.2 Physiological and biochemical study

3.2.1. Photosynthetic pigment

Estimation of photosynthetic pigments revealed some significant variations in control and treated plants (Fig. 1C-E). Photosynthetic pigments reduced as Cd con-

centration increased. Chlorophyll 'a', 'b' and carotenoid significantly decreased from 40-100 ppm and the maximum reduction was recorded at highest concentrations with minimum chlorophyll contents.

3.2.2 Proline content

Proline content increased remarkably by Cd exposure. Lowest concentration of proline was observed at 20 and 40 ppm, i.e. 2.12 and 2.35 µ moles/g fw, respectively compared to the other treatments, (Fig. 1F) while its production enhanced insignificantly with the increasing concentrations. Maximum significant increase in proline concentration (3.24 µ moles/g fw) was recorded at 100 ppm. Increased proline concentrations are common symptoms of metal stress and served as a non-specific index of Cd-toxicity.

3.2.3 Lipid peroxidation assay

Estimation of lipid peroxidation was done by determining the malondialdehyde content in control and cadmium stressed plants. The MDA content enhanced significantly in all concentrations over the control. The maximum increase of MDA content was 1.10 µ M g^{-1} at 100 ppm of $Cd(NO_3)_2$ (Fig. 2A).
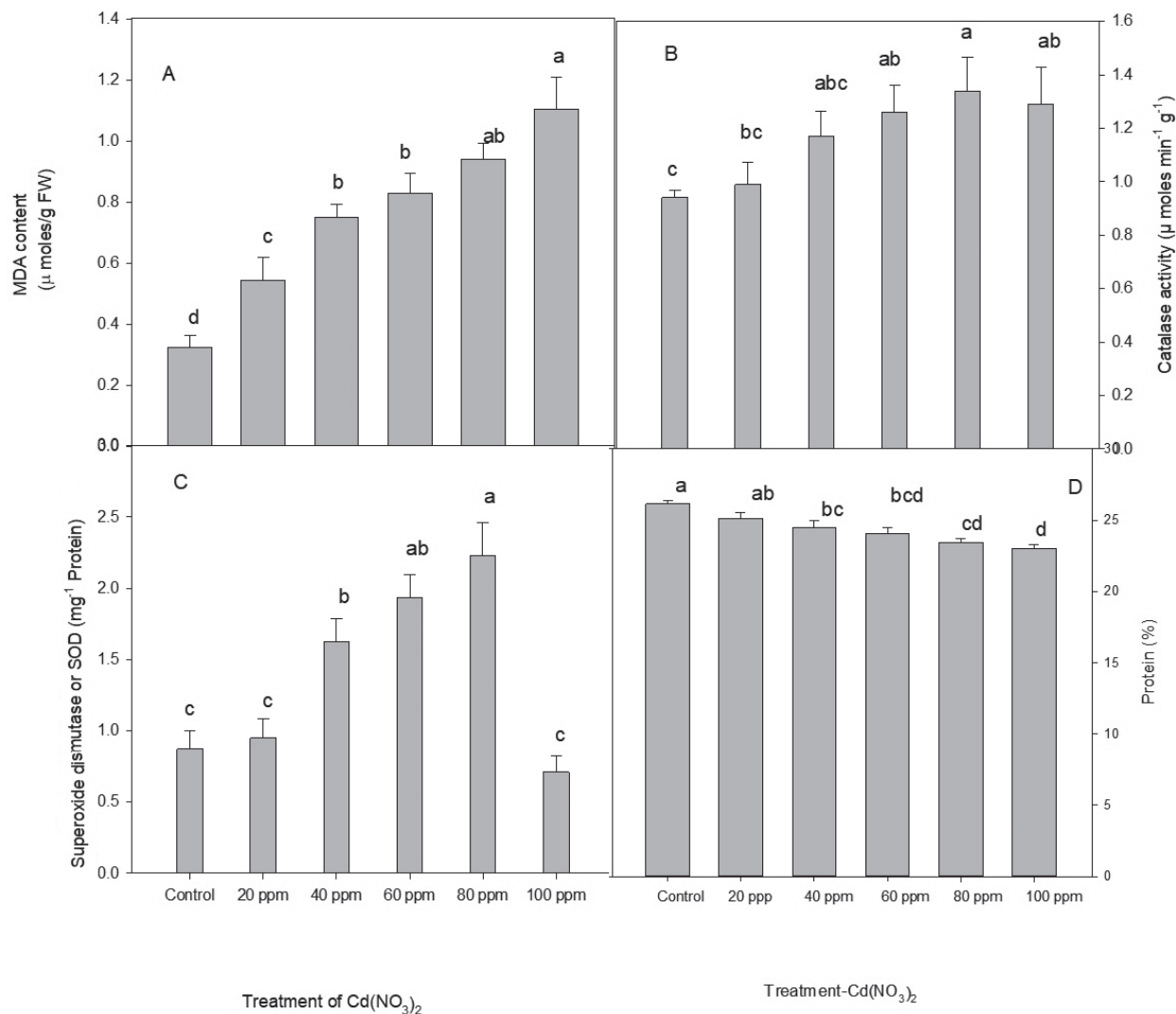
Figure 2. Effect of different concentrations of $Cd(NO_3)_2$ on lipid peroxidation (MDA content µmoles/g FW), catalase activity (CAT) (µmoles min^{-1}g^{-1}) and superoxide dismutase (SOD) (U mg^{-1} Protein) and protein content (%) in *Lens culinaris* Medik. Data means within columns followed by the same letter is not different at the 5% level of significance, based on the Duncan Multiple Range Test.

3.2.4 Antioxidant enzyme activities

Antioxidant activity (CAT, SOD) in leaves were found disturbed under cadmium stress. The antioxidant enzyme activity of lentil was found to be increased initially and then fall at higher doses. The catalase activity increases insignificantly over control in 20 and 40 ppm cadmium whereas it increased significantly in 60-100 ppm (Fig. 2B). On the other hand, SOD activity was significantly enhanced at 40-80 ppm cadmium respectively and thereby decreases (0.71 mg^{-1} protein) with their respective control (0.87 mg^{-1} protein) at 100 ppm (Fig. 2C).

3.2.5 Estimation of protein content

Result of estimation of protein content in *Lens culinaris* is depicted in (Fig. 2D). Protein content decreased as cadmium concentration increased. Highest concentration (100 ppm) showed lower percentage of protein (23.0%) over control. An inverse relationship between cadmium concentration and protein content was observed. Statistical analysis shows a significant difference in each treatment except 20 ppm of Cd at (p < 0.05).
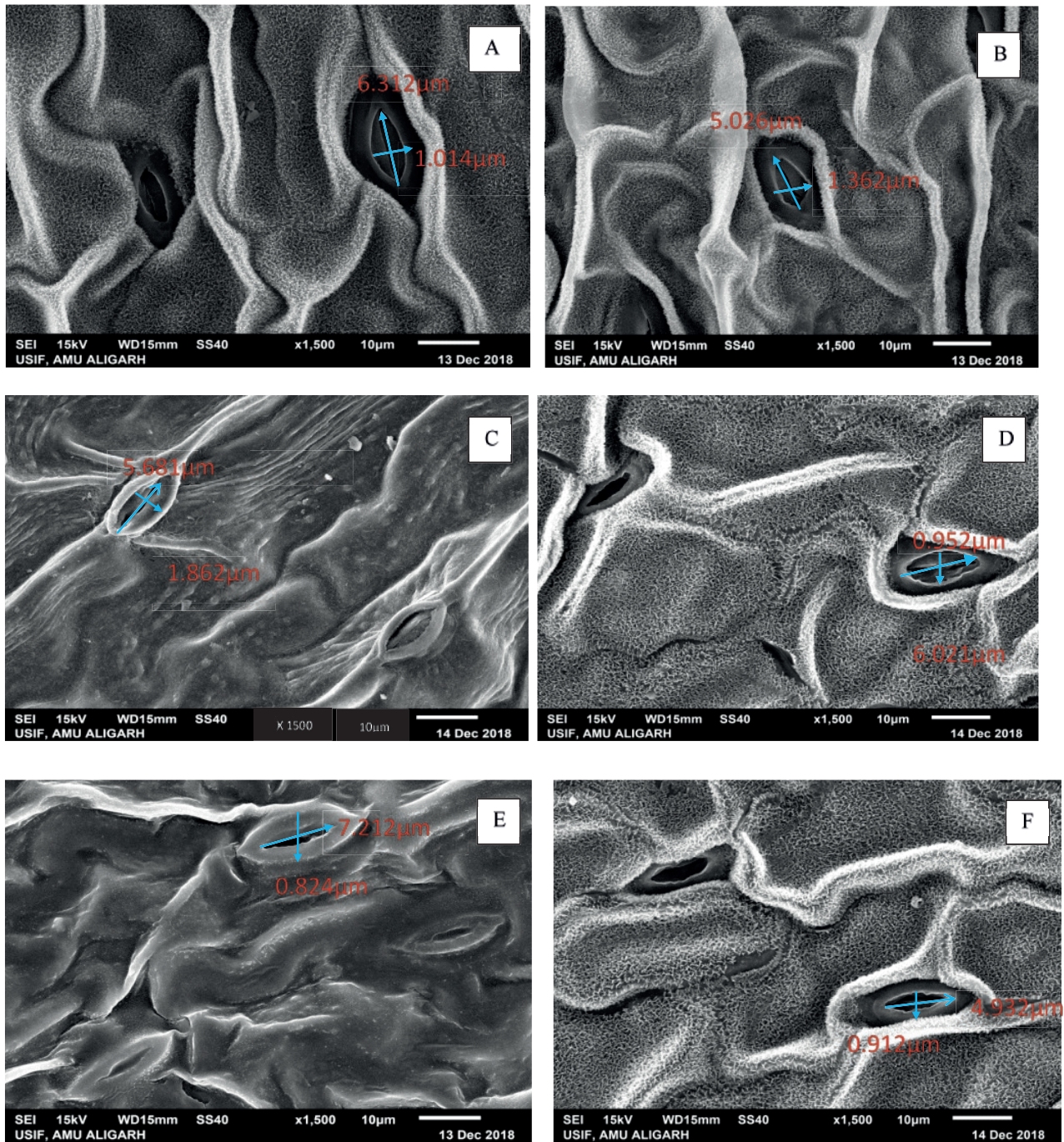
Figure 3. Scanning electron micrographs exhibiting morphology of stomata in control (A) and different shape and size of stomata in various concentrations of cadmium nitrate (20-100 ppm) (B-F).

3.2.6 Stomatal behavior and mineral element analysis

Variation in structure of guard cells in treated populations was determined through scanning electron microscopy (SEM). The SEM image showed variation in shape, length and width of guard cells in treated populations. Cadmium treatment induced partially closed stomata. Stomatal opening slightly increases over control in lower doses while it reduced in higher doses with their respective control (Fig. 3; a-f). EDX profiling of leaf was
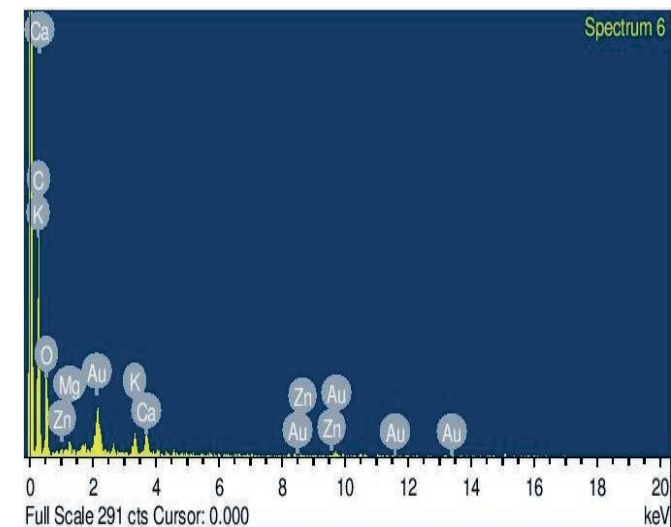
(a)

Element	Weight %	Atomic %
C K	47.80	60.92
O K	37.58	35.96
Mg K	0.89	0.56
K K	1.98	0.78
Ca K	2.44	0.93
Zn K	0.77	0.18
Au M	8.53	0.66
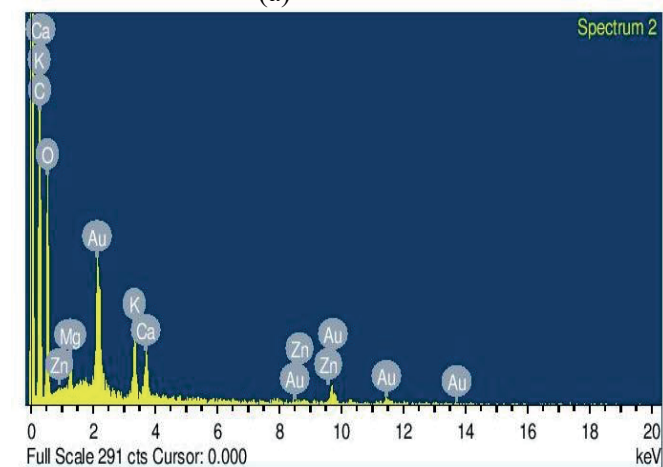
(b)

Element	Weight %	Atomic %
C K	44.04	58.09
O K	38.97	38.58
Mg K	0.95	0.62
K K	2.40	0.97
Ca K	1.99	0.79
Zn K	0.12	0.03
Au M	11.54	0.93
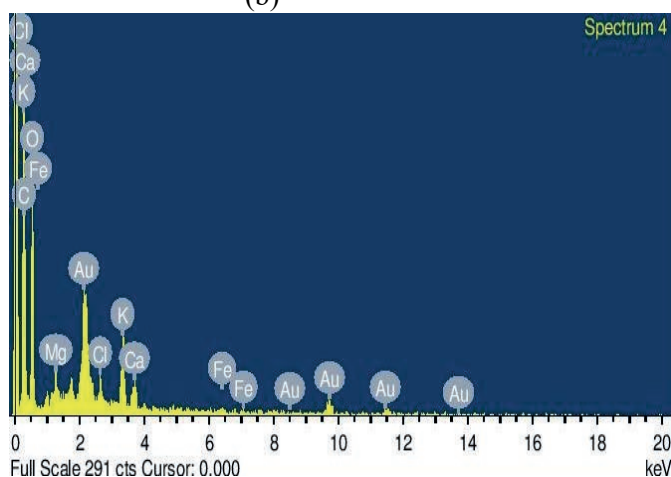
(c)

Element	Weight %	Atomic %
C K	33.56	46.67
O K	46.44	48.48
Mg K	0.93	0.64
Cl K	1.20	0.57
K K	4.35	1.86
Ca K	1.58	0.66
Fe K	0.53	0.16
Au M	11.41	0.97

Figure 4. EDX profiling of mineral content of leaf (a) control; (b) 40 ppm Cd; (c) 80 ppm Cd.

(a)

(b)

(c)
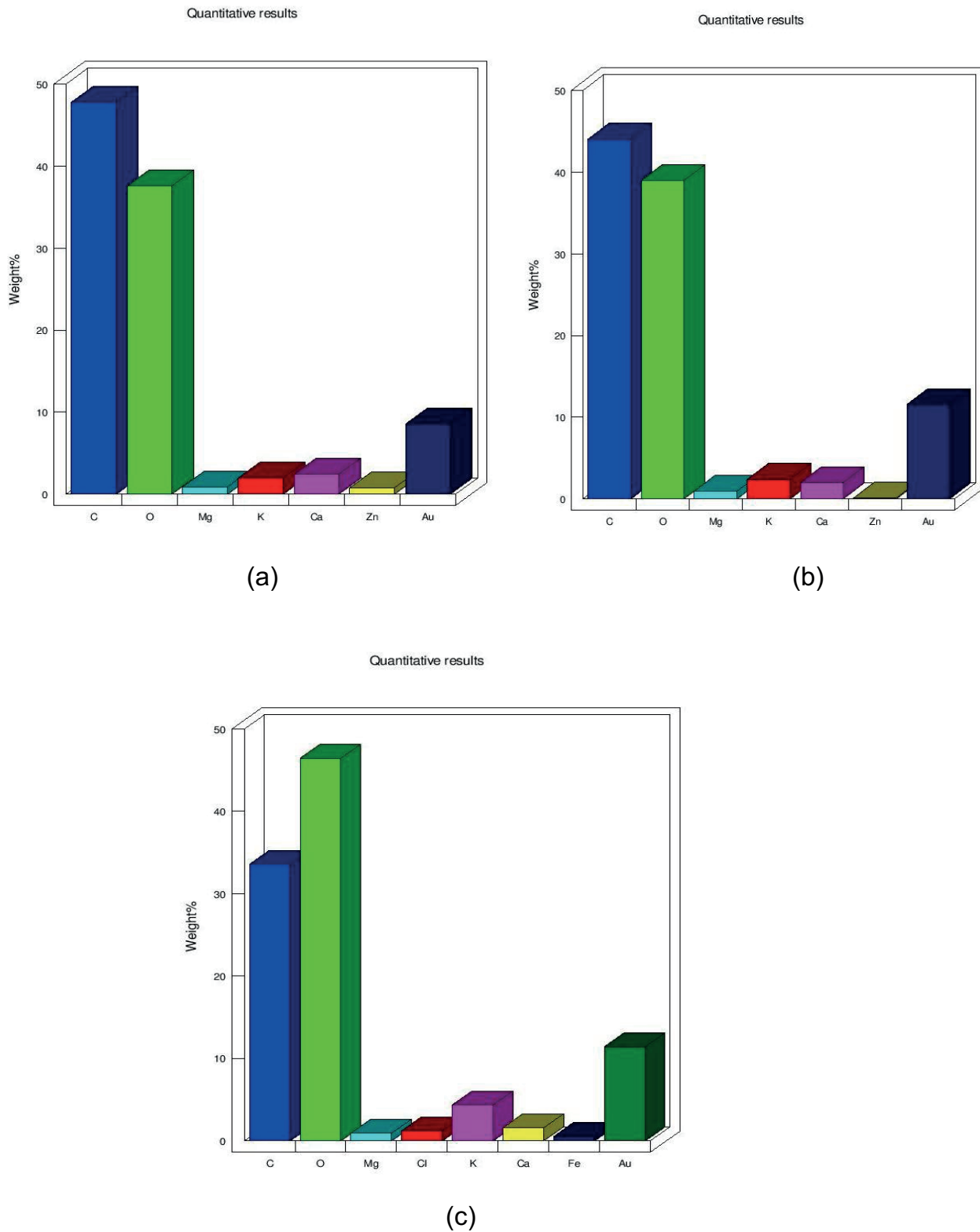
Figure 5. Graphical representation of EDX profiling of mineral content of treated plant of lentil along with control plant.
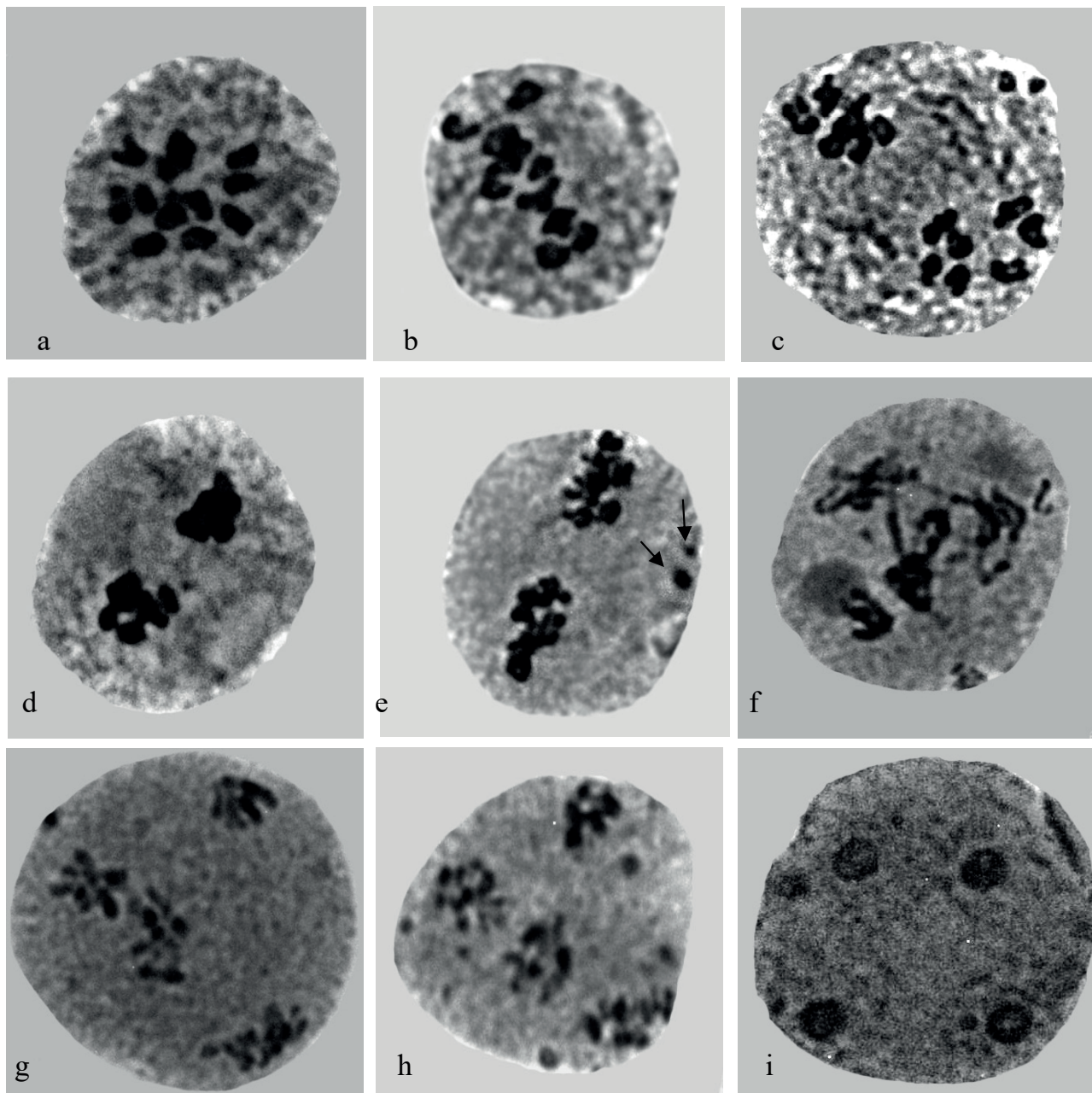
Figure 6. a: Metaphase I (control), b: Metaphase I (precocious movement of chromosome), c: Anaphase I (unequal division with two laggards), d: Telophase I (sticky chromosomes), e: Metaphase II (stray chromosomes), f: Anaphase II (disturbed polarity with multi bridge formation) g, h: Anaphase II (disturbed polarity), i: Telophase II (two micronuclei).

also done via energy dispersive X-ray analyser (EDX)to estimate mineral element of control as well as treated plants. Treated populations exhibited a slight reduction and enhancement in mineral elements as compared to control when expressed in percentage content (Fig. 4 and 5a-c)

3.3 DNA damage

Meiotic studies in pollen mother cells treated with different concentrations of Cd are shown in Fig. 6. The aberrant cells increased as heavy metal concentrations increased. Untreated plants exhibited normal meiotic cells at metaphase I (control) (Fig. 6a).Various chromo-

Table 2. Frequency of chromosomal anomalies induced by Cd(NO₃)₂ in *Lens culinaris* Medik. (M₁Generation).

Conc. of mutagen (ppm)	Total no. of PMCs observed	Prophase-I (Diakinesis)			Metaphase-I/II						Anaphase-I/II				Telophase-I/II									Total No. of Abnoral PMCs observed	Total % of Abnormal PMCs observed A+B+C+D
		Univalents	Multivalents	% of Abn. PMCs (A)	Univalents	Multivalents	Precocious Mov. of chromosomes	Stray chromosomes	Stickiness	% of Abn. PMCs (B)	Laggards	Disturbed polarity	Unequal Sep. of chromosomes	% of Abn. PMCs (C)	Laggards	Bridges	Unequal Sep. of chromosomes	Micro nucleate cells	Multi nucleate cells	Disturbed polarity	Cytomixis	% of Abn. PMCs (D)		
Control	289	-	-	-	-	-	-	-	-	-	-	-	-	-	-	-	-	-	-	-	-	-	-	-
Cd(NO₃)₂ (ppm)																								
20	270	2	2	1.4	1	1	2	1	2	2.59	2	1	2	1.85	2	-	-	2	1	2	1	2.96	24	8.88
40	265	3	2	1.8	3	2	4	3	3	5.66	3	2	4	3.39	3	1	1	3	2	3	2	5.66	44	16.59
60	261	2	3	1.9	3	3	5	4	5	7.66	5	3	4	4.59	4	2	2	3	3	4	3	8.04	58	22.20
80	250	3	4	2.8	4	4	6	5	7	10.4	6	4	6	6.40	5	3	3	4	4	5	5	11.60	78	31.20
100	245	4	5	3.6	5	6	8	6	8	13.46	7	4	7	7.34	6	3	4	5	5	6	5	13.87	94	38.34
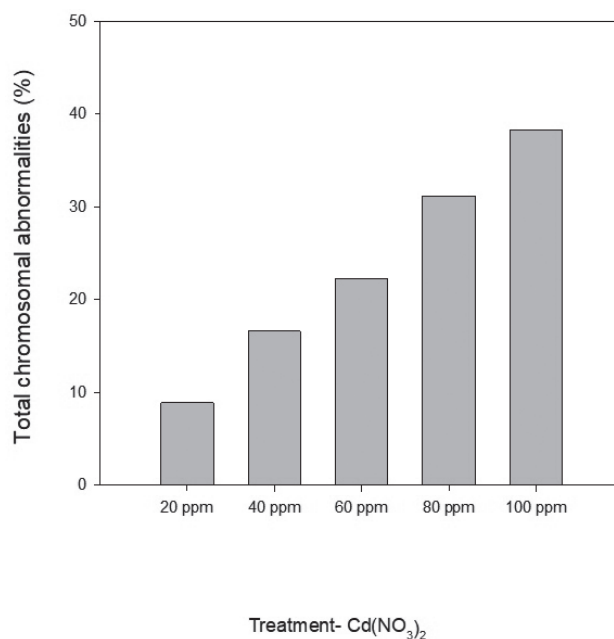
Figure 7. Effect of Cd(NO₃)₂ on percentage of total chromosomal aberrations in *Lens culinaris* Medik.

somal anomalies in pollen mother cells of treated populations were observed, such as precocious movement of two univalents at metaphase I (Fig. 6b), unequal division with two laggards at anaphase I (Fig. 6c), stickiness at telophase I (Fig. 6d), stray chromosomes at metaphase II (Fig. 6e), disturb polarity with multi bridge formation at anaphase II (Fig. 6f), disturbed polarity at anaphase II (Fig. 6g), laggards at telophase II (Fig. 6h), two micronuclei at telophase II (Fig. 6i). In the present investigation, chromosomal aberrations and frequency of meiotic abnormalities at each concentration were calculated in percentage (Table 2). Maximum frequencies of chromosomal aberrations were observed at 100 ppm. The total percentage of abnormal PMCs ranged from 8.88 to 38.34% (Table 2, Fig. 7)

4. DISCUSSION

As reported earlier by many researchers, Cd is a non-essential element that is readily taken by plants and inhibits plant physiological processes such as water absorption, photosynthesis, stunted foliage, withering of leaf and alters normal meiotic division (Patra *et al.* 2004).The present study showed that exposure of lentil genotypes to different doses of heavy metal (Cd) exhibited substantial alterations in the phenotypic and genotypic makeup of the plant. During growth and develop-

mental stages, morpho-physiological parameters were examined as well as biochemical parameters, antioxidant enzymes activity, DNA damage, SEM and EDX analysis of leaf were also performed to evaluate the overall effect of Cd on plant ecology.

4.1. Growth and morphology

4.1.1 Seed Germination, Survival and pollen fertility

Germination percentage, survival and pollen fertility were found to decrease as cadmium doses increased in the present investigation. Similar observations were reported by (Choudhary*et al.* 2012) in *Trigonella*, (Shahwar *et al.* 2016) in *Vicia faba* and (Shahwar *et al.* 2018, Sharma *et al.* 2022) lentil, (Petrescu *et al.* 2020) in *Ocimum*. Inhibition in germination and root development was due to Cd (Pandit and Prasannakumar 1999) low water uptake, reduction in cell division and metabolic activity and enlargement of the embryo. It was reported by (Moreno *et al.* 1999) Cd disrupts the uptake of water and nutrients in plants and suppresses cell division (Liu *et al.* 2003). Kabir *et al.* (2008) and Farooqi *et al.* (2009) suggested that inhibition in germination percentage, seedling length, tolerance index and dry mass of root and shoot is due to heavy metal. The reason behind reduction in germination percentage under Cd stress might be due to escalated breakdown of reserved food material in seed embryo. Depletion in survival may be due to different cytological and physiological disturbances (Girija *et al.* 2013) and inability to maintain balance between growth regulators and promoters (Meherchandani 1975). The descending fertility is an outcome of chromosomal breakages and anomalies which affect microsporogenesis leading to generation of non-viable gametes and decreasing plant fertility (Kumar and Singh, 2020).

4.1.2 Root and shoot length

In the present investigation, root and shoot lengths minimized linearly as Cd doses increased. Similar result was also reported by Choudhary *et al.* (2012). Decrease in seedling length following metal treatment might be due to reduction in meristematic cells and also due to alteration in hydrolytic enzymes; sufficient food does not reach the developing radical and plumule, resulting in stunting of seedlings (Shafiq *et al.* 2008). According to Elloumi *et al.* (2007), effect of Cd exposure on root growth was more compared to shoot growth since roots are the first organ to contact the heavy metal and carry out the process of absorption (Guilherme *et al.* 2015)

4.1.3 Plant height and yield attributing traits

In the present work, metal treated plants exhibited linearly declined plant height in comparison to the control plants and this depletion was due to chromosomal damage. Reason behind the yield depletion was meiotic turbulences which affected the production of normal microspores and megaspores resulting in low fruit set. Higher concentration of Cd causes growth inhibition which ascribes to cell division or various desecrations in the plant genome. Thilagavathi and Mullainathan (2011) reported that a decrease in quantitative traits have been ascribed to the physiological perturbation or due to chromosomal breakage. Yield is considered an important agronomical parameter in breeding program. Data regarding yield and related traits, exhibited significant decrease in yield at higher concentration which might be due to metal induced genotoxicity resulting in alterations of physiological mechanisms, chromosomal aberrations and high pollen sterility.

Similar results were recorded in soyabean (Pavadi and Dhanavel, 2004), cotton (Sundaravadivelu *et al.* 2006) *Trigonella* (Choudhary *et al.* 2012), *Vicia faba* (Shahwar *et al* 2016) and *Capsicum annum* (Aslam *et al.* 2017).

4.2. Physio and biochemical aspects

4.2.1 Photosynthetic pigment

Photosynthetic pigment is an important parameter directly correlated with plant growth and biomass (Acosta-Motos *et al.* 2017). In our study, photosynthetic pigment was inversely proportional to cadmium doses, their content decreased with enhancing concentration of cadmium relative to the control. Zengin and Munzuroglu (2006) and Elloumi *et al.* (2007) demonstrated the same result in sunflower and almonds, respectively. The decline in the chlorophyll content in plants might be due to suppression of enzymes such as δ-aminolevulinic acid dehydratase and protochlorophyllide reductase (Van Assche and Clijsters 1990), which are necessary for chlorophyll biosynthesis. Lee*et al.* (2004) and Siler *et al.* (2007) while working on *Paspalum vaginatum* (L.) and *Centaurium erythraea* (L.) respectively reported that total chlorophyll diminished along with the enhanced metal concentration. Carotenoids are an important constituent of photosynthetic pigments which absorb light energy to make food for plant. Carotenoids also save chlorophyll from photo damage. In the present study, photosynthetic pigment, stomatal length and width reduce by cadmium treatment. This reduction is probably due to nutritional imbalance (Wong and Wong 1990).

4.2.2 Proline content

Proline, a non-enzymatic antioxidant, scavenger of ROS, which accumulates in plants when exposed to abiotic stress (Saradhi *et al.* 1993). Itis considered as stress signaling molecule having capability to act as an antioxidative defense molecule. (Maggaio *et al.* 2002). It was reported by researchers that proline accumulation might act as compatible osmolyte in cells, maintains the configuration of macromolecule and organelles and its enhanced production confirms the osmo-tolerance in plants (Nanjo *et al.* 1999; Junaid *et al.* 2008). Dhir *et al.* (2004) demonstrated that proline accumulates in shoots of higher plants such as *B. juncea, T. aestivum and Vigna radiata* in response to Cd toxicity.

4.2.3 Protein content

In present investigation, it was observed that cadmium treatments affected greatly protein synthesis. A significantnegative difference was seen between treated plants and control. Similar results were also found by Bavi *et al.* (2011) in pea plants and Choudhary *et al.* (2012) in *Trigonella*. Balestrasse *et al.* (2003) reported that decline in protein content might be due to inhibition in protein synthesis or an increase in the rate of protein degradation. Higher concentration of cadmium inhibits protease activity and total protein content. This shows toxic effect of cadmium concentration on mechanism of protein synthesis resulting in decreased protein content. Despite of these Chen *et al.* (2007) found that protein content decreased in *Vigna unguiculata* under the salt stress (sodium chloride).

4.2.4 Antioxidant and lipid peroxidation

Heavy metal stress may have detrimental effects on plant stress machinery. Andre *et al.* (2010) suggested that antioxidant enzymes are considered an essential defense element against stress and improve the activity of antioxidant system to overcome stress generated by ROS. ROS are known as the natural by-products of aerobic organisms and are generated during mitochondrial electron transport (Debnath *et al.* 2021). In the present investigation, dose-dependent enhancements in antioxidant enzyme activity were recorded, suggesting ROS production due to severity of Cd stress. Salama *et al.* (2009) and Shehab *et al.* (2010) observed that antioxidant activity elevates as concentration increases but decreases at higher concentrations, probably due to chronic stress exposure. SOD plays a crucial role to safeguard plants

against stressby converting O_2^- to H_2O_2 with the help of POX and subsequently reducing it into H_2O (Alscher *et al.* 2002). The results are supported by Arleta *et al.* (2001); Dixit *et al.* (2001); Choudhary *et al.* (2012). Elevated malondialdehyde (MDA) levels indicated enhanced lipid peroxidationincreasing concentration of Cd confirming metal induced oxidative stress in lentil plant. Similar results are recorded by Malecka *et al.* (2001); Unavyar *et al.* (2006).

4.3. DNA damage

Chromosomal anomalies are induced due to factors that affect DNA synthesis and replication or on nucleoproteins, resulting in chromosomal breakages or malfunctioning of spindle apparatus and abnormal chromosomal segregation (Sutan *et al.* 2018). In our investigation, adverse effect of cadmium on the frequency of chromosomal anomalies were observed, presumably due to mutagenic effect of subject heavy metal in inducing alterations in DNA. While we observed normal meiotic cells in control group, a spectrum of anomalies was observed in treated individuals. The frequency of chromosomal aberrations was directly proportional to the concentration of cadmium. The anomalies induced by cadmium nitrate were of broad spectrum and comparatively included a higher proportion of sticky chromosomes. Khan *et al.* (2012) suggested the occurrence of sticky chromosome as a result of improper folding of chromosome fibers and their intermingling. Jayabalan and Rao (1987) reported that stickiness was caused by the segregation of histone proteins and alterations in the pattern of cyto-chemically balanced reactions. Bhat *et al.* (2007) suggested that stray chromosomes may be due to spindle dysfunction and clustering of chromosomes. Anaphasic bridges originate due to unequal separation of dicentric chromosomes (Singh and Khanna, 1988) or presence of sticky chromosomes which remain connected by chromosome bridges during anaphase because of incomplete separation of the daughter chromosomes (Kabarity *et al.* 1974). Laggards were observed at anaphase and telophase in Cd treated plants, and it originates due to disruption of spindle. Das and Roy (1989) hold the view that spindle fibers fail to carry chromosomes to their respective poles due to mutagen reaction leaving the chromosome behind as a lagging chromosome or laggard. Stickiness of chromosomal end, delayed terminalization and failure of chromosomes to move at opposite poles were also possible reasons behind laggard production (Verma *et al.* 2012). Disturbed polarity at anaphase and telophase might be attributed to disturbances in the spindle fibers (Bhat *et al.* 2007).

Utsunomiya *et al.* (2002) had opinion that formation of micronuclei is because of non-oriented chromosomes which are unable to reach the pole. Ruan *et al.* (1992) suggested that micronuclei are kind of abnormality which culminates into loss of chromosomal material and is regarded as an indicator of mutagenicity.

Our result suggested a close colinearity between the treatments and percentage of chromosomal anomalies, higher the concentration, more the damage chromosome undergoes. Similar observations were also reported by treatment of different metals and chemicals by other workers such as Srivastava and Kapoor (2008); Khan *et al.* (2009b); Kumar and Yadav (2010);Tripathi and Kumar (2010); Jafri *et al.*(2011); Gulfishan *et al.* (2012); Shahwar *et al.* (2016, 2017, 2018, 2019, 2020); Aslam *et al.* (2017), Khan *et al.* (2019).

5. CONCLUSION

During the present investigation, it was concluded that cadmium induced morphological, physiological, biochemical variation and DNA damage over control in *Lens culinaris.* Genotypes of lentils were greatly affected due to the treatment of cadmium, recommending genetic variation in the subsequent generation. It was observed in this study that at their lower concentrations, cadmium was tolerable by the plant without losing viability, while higher concentrations were genotoxic and induce variation/mutation in the genotypes as well as phenotypes and causing more variation and developing variants/mutant of better quality and selected it. Therefore, plants with better characteristics should be isolated and selected for crop improvement programmes. Further molecular techniques or various genetic engineering techniques should be carried out to check the mutation at genic level as it will be acoherent tool to isolate the desired characters and produce a new variety of lentil through breeding program.

ACKNOWLEDGEMENT

REFERENCES

Acosta-Motos JR, Ortuño MF, Bernal-Vicente A, Diaz-Vivancos P, Sanchez-Blanco MJ, Hernandez JA (2017) Plant responses to salt stress: Adaptive mechanisms. Agronomy 7:18.

Akinci IE, Akinci S, Yilmaz K (2010) Response of tomato (*Solanum lycopersicum* L.) to lead toxicity: Growth, element uptake, chlorophyll and water content. Afr J Agric Res5:416-423.

Alscher RG, Erturk N, Heath LS (2002) Role of superoxide dismutases (SODs) in controlling oxidative stress in plants. J of Exp Bot53:1331-1341.

Andre CM, Larondelle Y, Evers D (2010) Dietary antioxidants and oxidative stress from a human and plant perspective: A review. Cur Nutri and Food Sci.62-12.

Arleta M, Wieslawa J, Barbara T (2001) Antioxidative defence to lead stress in subcellular compartment of pea root cells. Acta Bioch Polon 48:687–9.

Arnon, D. I. (1949) Copper enzymes in isolated chloroplasts. Polyphenol oxidase in *Beta vulgaris*. *Plant physiology*, *24*(1), 1.

Arumuganathan K, Earle ED (1991) Nuclear DNA content of some important plant species. Plant MolBiol9:208-218.

Aslam R, Bhat TM, Choudhary, Ansari MYK, Shahwar D (2017) Estimation of genetic variability, mutagenic effectiveness and efficiency in M2 flower mutant lines of *Capsicum annuum* L. treated with caffeine and their analysis through RAPD markers. J of King Saud Uni-Sci, 29:274-283

Balestrasse KB, Benavides MP, Gallego SM, Tomaro ML (2003) Effect of cadmium stress on nitrogen metabolism in nodules and roots of soybean plants Func. Plant Biol, 30:57-64.

Barulina H (1930) Lentils of the USSR and other countries. Bulle of App Bot, Gen and Plant Bree, 40:265–304.

Bates LS, Waldren RP, Teare ID (1973) Rapid determination of free proline for water stress studies. Plant and Soil 39:205–7.

Bavi K, Kholdebarin B, Moradshahi A (2011) Effect of cadmium on growth, protein content and peroxidase activity in pea plants. Pak. J. Bot, 43:1467-1470.

Bhat TA, Parveen S, Khan AH (2007) Meiotic studies in two varieties of *Vicia faba* L. (Fabaceae) after EMS treatment Asian J Plant Sci. 6:51–55.

Chaudhary J, Deshmukh R, Sonah H (2019) Mutagenesis Approaches and Their Role in Crop Improvement. Plants (Basel). Oct 31;8(11):467.

Chen C, Tao C, Peng H, Ding Y (2007) Genetic analysis of salt stress responses in asparagus bean (*Vigna unguiculata* L. ssp. *Sesquipedalis verdc.*) J. Hered. 98:655–665.

Choudhary S, Ansari MYK, Khan Z, Gupta H (2012) Cytotoxic action of lead nitrate on cytomorphology of *Trigonella foenum-graecum* L. Turkish J Biol. 36:267–273.

Das S, Roy SK, (1989) Radio cytogenetical studies on *Solanum* I. meiotic abnormalities. Cytologia 54:477–481.

Daud MK, Sun Y, Dawood M, Hayat Y, Variath MT, Wu YX, Zhu S (2009). Cadmium-induced functional and ultra structural alterations in roots of two transgenic cotton cultivars. J. Hazard. Mater. 161: 463-473.

Debnath S. Chandel RK. Devi K. Khan Z (2021) Mechanism and Molecular Response of Induced Genotoxicity and Oxidative Stress in Plants. In Induced Genotoxicity and Oxidative Stress in Plants; Khan, Z., Ansari, M.Y.K., Shahwar, D., Eds.; Springer: Singapore, 2021.

Dhir B, Sharmila P, Saradhi PP (2004) Hydrophytes lack potential to exhibit cadmium stress induced enhancement in lipid peroxidation and accumulation of proline. AquTox 66: 141–7

Dixit V, Pandy V, Shyam R (2001) Differential antioxidative responses to cadmium in roots and leaves of pea. J of Exp Bot 52:1101–9.

Duncan DB (1955) Multiple range and multiple 'F' tests. Biometrics.,11:1, 1-42.

Elloumi N, Ben F, Rhouma A, Ben B, Mezghani I, Boukhris M (2007) Cadmium induced growth inhibition and alteration of biochemical parameters in almond seedlings grown in solution culture. Acta Physio Plant 29:57–62.

Farooqi ZR, Iqbal ZM, Kabir M, NadShafiq M (2009) Toxic effect of lead and cadmium on germination and seedling growth of *Albizia lebbeck* (L.) Benth. Pakistan J Bot. 41:27–33.

Ferguson ME, Maxted N, Slageren MV, Robertson LD (2000) A reassessment of the taxonomy of Lens Mill (Leguminosae, Papilionoideae, Vicieae). Botanical J of the Linn Soc 133:41-59.

Kumar,G. Singh S. (2020) Induced cytomictic crosstalk behaviour among micro-meiocytes of *Cyamopsis tetragonoloba* (L.) Taub. (cluster bean): Reasons and repercussions. Caryologia 73(2): 111-119

Gallego, S. M., Benavides, M. P., & Tomaro, M. L. (1996). Effect of heavy metal ion excess on sunflower leaves: evidence for involvement of oxidative stress. *Plant Science*, *121*(2), 151-159.

Girija M, Gnanamurthy S, Dhanavel D (2013) Genetic diversity analysis of cowpea mutant (*Vigna unguiculata* (L.) Walp) as revealed by RAPD marker. Int J Adv Res 1:139–147.

Gulfishan M, Khan AH, Jafri IF, Bhat TA (2012) Assessment of mutagenicity induced by MMS and DES in *Capsicum annuum* L. Saudi j of bio sci 19:251-255

Haider FU, Liqun C, Coulter JA, Cheema SA, Wu J, Zhang R, Wenjun M, Farooq M (2021) Cadmium toxicity in plants: Impacts and remediation strategies. Ecotoxicol Environ Saf. 211:111887.

Hodges DM, Long JMD, Forney CF, Prange RK (1999) Improving the thiobarbituric acid-reactive-substances assay for estimating lipid peroxidation in plant tissues containing anthocyanin and other interfering compounds. Planta 207:604–11

Jafri IF, Khan AH, Gulfishan M (2011) Genotoxic effects of 5-bromouracil on cyto-morphological characters of *Cichorium intybus*L. African J. Biotech 10:10595-10599

Jayabalan N, Rao GR (1987). Gamma radiation induced cytological abnormalities in *Lycopersicon esculentum* Mill. var. Pusa Ruby. Cyto (Tokyo) 52:1–4

Jiang W, Liu D, Hou W (2001). Hyperaccumulation of cadmium by roots, bulbs and shoots of garlic (*Allium sativum* L.). Bioresou Techno 76:9–13.

Junaid A, Mujib A, Sharma MP (2008) Effect of growth regulators and ethyl methane sulphonate on growth, and chlorophyll, sugar and proline contents in *Dracaena sanderiana* cultured in vitro. Biol Plant 52:569–572.

Kabarity AA. El-Bayoumi, Habib A (1974) Effect of morphine sulphate on mitosis of *Allium cepa* L. root tips. Biol. Plant 16: 275-282.

Kabir M, Iqbal MZ, Shafigh M, Faroogi ZR (2008) Reduction in germination and seedling growth of *Thespesia populnea* L. caused by lead and cadmium treatments. Pakistan J Bot 40:2419–2426

Kar M, Mishra D (1976). Catalase, peroxidase and polyphenoloxidase activities during rice leaf senescence. Plant Physiol., 57, 315–319

Khan Z, Ansari MYK and Gupta H (2012). Induction of mutations by base analogue 6-AP (6-Amino Purine) and their detection with RAPD analysis. African Journal Of Biotechnology.11 (56):11901-11906

Khan Z, Gupta H, Ansari MYK, Chaudhary S (2009) Methyl methanesulphonate induced chromosomal variations in a medicinal plant Cichorium intybus L. during microsporogenesis Biology and Medicine, 1(2): 66-69, 2009.

Khan, Z, Shahwar, D, Ansari, M. K. Y, Chandel, R. (2019) Toxicity assessment of anatase (TiO$_2$) nanoparticles: A pilot study on stress response alterations and DNA damage studies in *Lens culinaris* Medik. Heliyon, 5(7), e02069.

Kumar G, Singh V (2003) Comparative analysis of meiotic abnormalities induced by gamma rays and EMS in Barley. J Indian Bot Soc. 82:19–22.

Kumar G, Srivastava S (2006) Buffering action of essential metals against heavy metal cytotoxicity in *Helianthus annus*. The Nucleus. 49:45-51

Kumar G, Tripathi R (2007) Lead-induced cytotoxicity

and mutagenicity in grass pea. Turk J of Bio, 3:73-78

Kumar G, Yadav RS (2010) EMS induced genomic disorders in sesame (*Sesamum indicum* L.) Rom. J. Biol. – Plant Biol. 55:97–104

Kumar S, Pandey G. (2020) Bio fortification of pulses and legumes to enhance nutrition. Heliyon 6 (3), e03682.

Lee G, Carrow RN, Duncan RR (2004) Photosynthetic responses to salinity stress of halophytic seashore paspalum ecotypes. Plant Sci. 166:1417–1425.

Liu D, Jiang W, Zhao FM, Lu C (1994) Effects of lead on root growth, cell division and nucleolus of *Allium cepa*. Env Poll 86:1-4

Liu JG, Li JK, Xu KQ, Zhang ZJ, Ma TB, Lu XL, Yang JH, Zhu QS (2003) Lead toxicity uptake and translocation in different rice cultivars. Plant Sci 165:793–802

Lowry OH, Rosebrough NJ, Farr AL, Randall RJ (1951) Protein measurement with the Folin phenol reagent J BiolChem 193:265–275

Maggaio A, Miyazaki S, Veronese P, Fujita T, Ibeas JI, Damsz B, Narasimhan ML, Hasegawa PM, Joly RJ, Bressan RA (2002) Does proline accumulation play an active role in stress induced growth reduction? Plant J.31:699-712

Malecka A, Jarmuszkiewicz W, Tomaszevska B (2001) Antioxidative defense of lead stress in subcellular compartments of pea root cells. Acta Biochim Polon 48:687–98.

Maria de Fátima de Souza Guilherme, Habyhabanne Maia de Oliveira and Edevaldo da Silva (2015) Cadmium toxicity on seed germination and seedling growth of wheat *Triticum aestivum*. Acta Scientiarum 37: 499-504

Meherchandani M (1975) Effect of gamma radiation on dormant seeds of *Avena sativa* L. Rad Bot 15:439–445.

Mishra RK, Singhal GS (1992) Function of photosynthetic apparatus in intact wheat leaves under highlight and heat stress and its relationship with peroxidation of thylakoid lipids. Plant Physio 98:1–6

Moreno JL, Hernandez T, Garcia C (1999) Effects of cadmium containing sewage sludgecompost on dynamics of organic matter and microbial activity in an arid soil. Biol and Fertility of Soils 2: 8230–7

Nanjo T, Kobayashi M, Yoshiba Y, Sanada Y, Wada K, Tsukaya H, Kakubari Y, Yamaguchi-Shinozaki K, Shinozaki K (1999) Biological functions of proline in morphogenesis and osmotolerance revealed in antisense transgenic *Arabidopsis thaliana*. Plant J. 18:185–192

Sharma N., Shahwar D. Choudhary S (2022). Induction of chromosomal and morphological amelioration in lentil (*Lens culinaris* Medik.) mutagenized population developed through chemical mutagenesis. *Vegetos*, 35:474–483.

Pandit BR, Prasannakumar PG (1999) Effect of metals on jowar (*Sorghum bicolor* L.) seedling growth, germination and absorption of elements. Pollu Res 18:307–15.

Patra M, Bhowmik N, Bandopadhyay B, Sharma A (2004) Comparison of mercury, lead andarsenic with respect to genotoxic effects on plant systems and the development of genetic tolerance. Env and Exp Bot 52:199–223

Pavadai P, Dhanavel D (2004) Effect of EMS, DES and colchicines treatment in soybean. Crop Res. 28:118–120

PetrescuI, Sarac I, Bonciu E, Madosa E, RosculeteCA, Butnariu M (2020). Study regarding the cytotoxic potential of cadmium and zinc in meristematic tissues of basil (*Ocimumbasilicum* L.). Caryologia 73(1): 75-81. doi: 10.13128/caryologia-138

Yu, Q., &Rengel, Z. (1999). Micronutrient deficiency influences plant growth and activities of superoxide dismutases in narrow-leafed lupins. *Annals of Botany*, *83*(2), 175-182.

Qian H, Li L, Sun W, Chen GD, Sheng W, Liu, Fu Z (2009) Combined effect of copper and cadmium on *Chlorella vulgaris* growth and photosynthesis-related gene transcription. Aqua Toxico 9:456–61

Rathore H, Punyasi R, Joshi P, Rathore D, Bhatnagar D (2007) Studies on the reversal of lead induced mitostatic effect in *Allium cepa* root tip cells with myrobalan (fruit of *Terminalia chebula*, Retz, Combretaceae). Internet J Altern Med 4(1)

Ruan C, Lian Y, Lium J (1992) Application of micronucleus test in *Vicia faba* root tips in the rapid detection of mutagenic environmental pollutants. Chinese J Environ Sci. 4:56–58

Ruley AT, Sharma NC, Sahi SV (2004) Antioxidant defense in a lead accumulating plant, *Sesbania drummondii*. Plant Physio and Biochem42:899-906

Salama ZA, El-Beltagi HS, El-Hariri DM (2009) Effect of Fe deficiency on antioxidant system in leaves of three flax cultivars. Notulae Botanicae Horti Agrobotanici Cluj-Napoca 37:122–8.

Saradhi PP, Alia V B, (1993). Inhibition of mitochondrial electron transport is the prime cause behind proline accumulation during mineral deficiency in *Oryza sativa*. Plant Soil 155/156: 465 8.

Shafiq M, Zafar MI, Athar M (2008) Effect of lead and cadmium on germination and seedling growth of *Leucaena leucocephala* . J. Appl. Sci. Environ. Manage 12:61–66.

Shahwar D, Ansari MYK, Bhat TM (2016) Assessment of genetic variability, morphology and productivity response of *Vicia faba* under the stress of lead nitrate, International J of Adv Life Sci9:58-64.

Shahwar D, Ansari MYK, Choudhary S (2018) Evaluation of Genotoxic Potential of Heavy Metal in a Proteina-

ceous Crop (*Lens culinaris* Medik) in Aspect to Cyto-morphological Parameters.J of Bio Sci 18:208-215.

Shahwar, D., Ansari, M. Y. K., Bhat, T. M., Choudhary, S., & Aslam, R. (2017). Evaluation of high yielding mutant of lentil developed through caffeine of an exotic germplasm. *Int. J. Plant Breed. Genet*, *11*, 55-62.

Shahwar, D., Ansari, M. Y. K., Choudhary, S. (2019). Induction of phenotypic diversity in mutagenized population of lentil (*Lens culinaris* Medik) by using heavy metal. *Heliyon*, *5*(5), e01722.

Shahwar, D., Ansari, M. Y. K., Choudhary, S., Aslam, R. (2017). Evaluation of yield attributing variants developed through ethyl methane sulphonate in an important proteinaceous crop-*Vicia faba. Asian J. Crop Sci*, *9*, 20-27.

Shahwar, D., Khan, Z., Ansari, M. Y. K. (2020). Evaluation of mutagenized lentil populations by caffeine and EMS for exploration of agronomic traits and mutant phenotyping. *Ecological Genetics and Genomics*, *14*, 100049

Shahwar, D., Ansari, M. Y. K., & Park, Y. (2022). Physio-biochemical analysis and molecular characterization of induced lentil mutant lines. *Plos one*, *17*(10), e0274937.

Shehab GG, Ahmed OK, El-Beltagi HS (2010) Effect of various chemical agents for alleviation of drought stress in rice plants (*Oryza sativa* L.) Notulae Botan Horti Agrobotanici Cluj-Napoca 38:139–48.

Siler B, Misic D, Filipovic B, Popovic Z, Cvetic T, Mijovic A (2007). Effects of salinity on in vitro growth and photosynthesis of common centaury (*Centaurium erythraea* Rafn.). Arch. Biol. Sci. 59:129–134.

Singh M, Khanna VK, (1988) Effect of gamma radiation on the crossability of wheat, triticale and rye on meiosis: pollen grains germination and pollen tube growth. Cyto 53:123–130.

Sinha R, Pal AK, Singh AK (2018) Physiological, biochemical and molecular responses of lentil (*Lens culinaris* Medik.) genotypes under drought stress, Ind J Plant Physiol. 23:772-784

Smith J H, Benitez A (1955) Chlorophylls: analysis in plant materials. In Modern Methods of Plant Analysis/Moderne Methoden der Pflanzenanalyse Springer Berlin Heidelberg, 142-196

Srivastava A, Kapoor K (2008) Seed yield is not impaired by chromosome stickiness in sodium azide treated *Trigonella foenum-graecum*. Cyto 73:115-121

Sundaravadivelu K, Ranjithselvi P, Reddy VRK (2006) Induced genetic variability in cotton *(Gossypium hirsutum* L.*)* for yield and its components. Crop Res 32: 442–446

Suprasanna P, Mirajkar SJ, Bhagwat SG (2015) Induced mutations and crop improvement. In Plant bio and biotech, vol I. plant diversity organization function

and improvement Springer, New Delhi, 593-617

Şuţan NA. Blănaru RG, Şuţan C (2018) Cytogenotoxic potential of surface water – a case study of Argeş River, Romania. Current Trends in Natural Sciences, 7(13):312-318.

Suzuki N (2005) Alleviation by calcium of cadmium-induced root growth inhibition in *Arabidopsis* seedlings. Plant Biotech 22:19–25

Tharanathan RN, Mahadevamma S (2003) Legumes – A boon to human nutrition. Trends in Food Science and Technology, 14:507–518

Thilagavathi C, Mullainathan L (2011) influence of physical and chemical mutagens on quantitative characters of *Vigna mungo* (L.Hepper) IRMJ-Agriculture,1/1:06-08.

TripathiR, Kumar G (2010) Genetic loss through heavy metal induced chromosomal stickiness in Grass pea, Caryologia, 63:3, 223-228.

Tripathy BC, Oelmüller R (2012) Reactive oxygen species generation and signaling in plants. Plant Signal Behav, 7(12):1621-33.

Unyayar S, Celik A, Cekic FO, Gozel A (2006) Cadmium-induced genotoxicity, cytotoxicity and lipid peroxidation in *Allium sativum* and *Vicia faba*. Mutagenesis 21:77–81.

Utsunomiya KS, Bione NCP, Pagliarini MS (2002) How many different kinds of abnormalities could be found in unique endogamous maize plant? Cyto 67:69-176

Van AF, Clijsters H (1990) Effects of metals on enzyme activity in plants. Plant Cell Environment 13:195–206

Van OSS H, Amn Y, Ladizinsky G (1997) Chloroplast DNA variation and evolution in the genus lens Mill. 'Theo and Applied Gen 94: 452-457.

Verma AK, Singh RR, Singh S (2012) Cytogenetic effect of EMS on root meristem cells of *Catharanthusroseus* (L.) G. Don var. Nirmal. Inter J Pharm BiolSci 2:20–24.

Wong JWC, Wong MH (1990) Effects of fly ash on yields and elemental composition of two vegetables, *Brassica parachinensis* and *B. chinensis*. Agric Ecosyst Environ 30:251–264

Xu BJ, Chang SKC (2010) Phenolic substance characterization and chemical and cell-based antioxidant activities of 11 lentils grown in the northern United States. J. Agric. Food Chem 58: 1509–1517

Yi H, Meng Z (2003) Genotoxicity of hydrated sulphur dioxide on root tips of *Allium sativum* and *Viciafaba*. Mutat Res 537: 109-114

Zengin FK, Munzuroglu O (2006) Toxic effects of cadmium (Cdþþ) on metabolism of sunflower (*Helianthus annuus* L.) seedlings. Acta Agricul Scand, Section B–Soil & Plant Science 56: 224–9.

Caryologia

International Journal of Cytology,
Cytosystematics and Cytogenetics

Biogenic synthesis of noble metal nanoparticles using *Melissa officinalis* L. and *Salvia officinalis* L. extracts and evaluation of their biosafety potential

Denisa Manolescu[1,2], Georgiana Uță[1,2,*], Anca Șuțan[3], Cătălin Ducu[1], Alin Din[1], Sorin Moga[1], Denis Negrea[1], Andrei Biță[4], Ludovic Bejenaru[4], Cornelia Bejenaru[5], Speranța Avram[2]

[1] *Regional Research and Development Center for Innovative Materials, Products and Processes from Automotive Industry, University of Pitesti, 11 Doaga Street, 110440 Pitesti, Arges, Romania*
[2] *Department of Anatomy, Animal Physiology and Biophysics, Faculty of Biology, University of Bucharest, 91-95th Independence Street, RO-050095 Bucharest, Romania*
[3] *Department of Natural Sciences, Faculty of Science, Physical Education and Informatics, University of Pitesti, Targu din Vale Street, 110040 Pitesti, Arges, Romania*
[4] *Department of Pharmacognosy & Phytotherapy, Faculty of Pharmacy, University of Medicine and Pharmacy of Craiova, 2 Petru Rareș Street, 200349 Craiova, Dolj County, Romania*
[5] *Department of Pharmaceutical Botany, Faculty of Pharmacy, University of Medicine and Pharmacy of Craiova, 2 Petru Rareș Street, 200349 Craiova, Dolj County, Romania*
* Corresponding author. E-mail: georgiana.uta@drd.unibuc.ro

Abstract. In this study we targeted the noble metal nanoparticles (MNPs) biogenic synthesis capacity of two medicinal species with therapeutic potential, namely *Melissa officinalis* L. (lemon balm) and *Salvia officinalis* L. (sage), cultivated in Romania. Plant material was extracted by maceration, microwave assisted extraction (MAE) and ultrasound assisted extraction (UAE). Bright field scanning transmission electron microscopy and energy dispersive X-ray spectroscopy (BFSTEM-EDS) techniques were used in order to investigate particles shape, dispersion and chemical elemental analysis. The total polyphenol content for both simple extracts and nanostructured mixtures was determined using the Folin-Ciocalteu method and antioxidant activity using the 2,2-diphenyl-1-picrylhydrazyl (DPPH) method. Identification and quantification of secondary metabolites of *M. officinalis* and *S. officinalis* were performed by ultra-high performance liquid chromatography (UHPLC). The *Allium* assay was used to evaluate the potential cytogenotoxic activity, for both simple and nanostructured phytochemical complexes, in the case of *S. officinalis* L. species being performed for the first time. Spherical shaped MNPs with diameters of about 20 nm were biosynthesised in lemon balm extracts. Larger AuNPs were phytosynthesized in sage extract obtained by UAE. Compared to the simple extracts, the antioxidant capacity as well as the amount of total polyphenols in the nanostructured extracts decreased, substantiating the involvement of bioorganic material in the reduction of metal ions. Low frequency of chromosomal aberrations corresponding to crude extracts and extracts supplemented with MNPs, suggest the cytoprotective, antigenotoxic, and safe use of these plant species as potential therapeutic forms in various diseases.

Keywords: lemon balm, sage, metal nanoparticles, antioxidant, cytotoxicity.

INTRODUCTION

Melissa officinalis L. (lemon balm) and *Salvia officinalis* L. (sage) are representatives medicinal plant species family Lamiaceae, whose remarkable therapeutic effects have been attested since ancient times (Shakeri et al. 2016; Ghorbani and Esmaeilizadeh 2017).

The bioactivity of natural compounds of *M. officinalis* has been noted especially for the treatment of neuropsychiatric disorders such as Alzheimer's and Parkinson's diseases, epilepsy, psychosis, depression or anxiety (Gomes et al. 2009; Shakeri et al. 2016; Avram et al. 2017; Udrea et al. 2018). As for *S. officinalis*, this plant species has been cultivated both as a medicinal plant, used therapeutically by humans for the treatment of various diseases such as gout, hyperglycemia, paralysis, rheumatism, cancer, bronchitis, and not least in the relief of symptoms of neurodegenerative diseases (Garcia et al. 2016; Šulniūtė et al. 2016), for decorative purposes (Kintzios 2000) and food or spice (Longaray Delamare et al. 2007).

However, the use of plant extracts in medicine is quite limited, mainly due to the inability of therapeutic plant compounds to penetrate the target, affected structures of organisms. This phenomenon occurs because of the large size of phytochemicals compared to the size of the target structures. It is now well known that due to the nanometric size of noble metal nanoparticles (MNPs), biocompounds embedded in such "capsules" or attached to their surface show both higher bioavailability and stability (Pandey et al. 2003).

At present, the literature abounds with information on the advantages of using different types of metal nanoparticles synthesised using plant extracts in therapy, making phytosynthesis a promising and sustainable alternative to conventional chemical or physical methods (Azeez et al. 2020; Naikoo et al. 2021; Shelembe et al. 2022). These nanostructured phytocomplexes are also only toxic at extremely high concentrations, doses which are not currently used for therapeutic purposes (Badmus et al. 2022).

The biosynthesis of MNPs aims, along with the fragmentation of phytochemicals, to embed various therapeutic plant compounds, or even certain drugs, in nanosized "metal envelopes" that allow their penetration and release into all structures of the target organism (Sun et al. 2008; Kumari et al. 2010; Parveen et al. 2012).

In addition, in recent decades several technologies have emerged to deliver along with NPs conventional drugs, recombinant proteins or even vaccines or nucleotides needed to treat cancer or other diseases (Parveen et al. 2012).

Since the antibacterial and anti-inflammatory action of silver nanoparticles (AgNPs) due to Ag ions is well known worldwide (Kirsner et al. 2001; Tripathy et al. 2008; Yilmaz Öztürk 2019), recently, the attention of researchers has been directed towards obtaining silver chloride nanoparticles (AgClNPs) which have been shown to exhibit identical or even improved properties compared to AgNPs (Eugenio et al. 2018). Moreover, AgClNPs have attracted considerable attention because they are easier to synthesize and also exhibit strong antimicrobial activity (Hu et al. 2009).

Gold (Au) nanorods have become some of the most important and commonly used materials in drug delivery and nanomedicine. The main reason for the use of AuNPs is to facilitate targeted drug transport, particularly in cancer therapy. To this end, a system using AuNPs conjugated with tumour necrosis factor (TNF) molecules has been designed, that has the effect of efficiently destroying only tumour cells while having low cytotoxicity to healthy cells (Mocellin and Nitti 2008; Das et al. 2011).

In addition, the pharmacological properties of lemon balm and sage are due to the content in secondary metabolites, such as polyphenols, alkaloids, triterpenes or sterols (Jaimez Ordaz et al. 2018; Uță et al. 2021) which are usually found in quite low concentrations, their recovery in a higher concentration being a challenge. One of the most important factors affecting the quality of bioactive compounds obtained from plant sources is the extraction method, also considered as a sample preparation technique, playing a vital role on the overall yield and final result. The conventional extraction methods, e.g. maceration, Soxhlet extraction, have been intensively used in recent decades (Zhang et al. 2018), but they have a number of drawbacks like time-consuming and use of a large amount of solvent. The latter not only increases process costs but is also associated with a negative environmental impact (Sasidharan et al. 2011). Therefore, numerous studies have aimed at developing efficient and environmentally friendly extraction techniques. Among the extraction techniques that have been successfully applied in obtaining active phytocompounds are microwave-assisted extraction (MAE) and ultrasound-assisted extraction (UAE) (Wang and Weller 2006; Grosso et al. 2015). Studies in the literature highlight that the amount of polyphenols extracted from this medicinal plant varies depending on certain factors such as: extraction method, solvent range, solvent:plant ratio, temperature, extraction time (Hernández et al. 2009; Zhang et al. 2018), stages of its primary processing (drying, grinding), harvesting area of plant material (Dent et al. 2017), and harvesting period (Francik et al. 2020).

Phytotherapy based on plant extracts has gained worldwide popularity because it is not addictive, it does not have harmful side effects and a high risk of toxicity like synthetic medicines, and last but not least it is cheap (Avram et al. 2005; Andrade et al. 2019; Lin et al. 2019).

Thus, based on this information, this study was focused on the biogenic synthesis of noble metal nanoparticles, namely AgClNPs and AuNPs, using the medicinal species *M. officinalis* and *S. officinalis*, correlated with the determination of the optimal method for extracting the highest possible concentrations of phytocompounds from the plant species, the analysis of the antioxidant capacity of simple extracts and extracts supplemented with MNPs, as well as *in vivo* testing of the cytotoxic activity of the extracts obtained and of nanostructured phytochemical complexes, in order to highlight the safety of these systems as potential therapeutic forms.

MATERIALS AND METHODS

Reagents and chemicals

The 96.9% pharmaceutical ethyl alcohol used for the extraction processes was purchased from SC. Coman Product S.A.; 2,2-diphenyl-1-picrylhydrazyl (DPPH), Folin-Ciocalteu reagent, 99.5% absolute ethyl alcohol, distilled water, Na_2CO_3 powder, gallic acid, Trolox, glacial acetic acid, absolute ethyl alcohol, 1N HCl and orcein were purchased from Carlo Erba Reagents S.A.S; acetonitrile, methanol and water were purchased from Merck. Reference compounds such as protocatechuic acid, ferulic acid, p-coumaric acid, caffeic acid were obtained from Merck, while quercetin, rutin and rosmarinic acid were purchased from Sigma-Aldrich and chlorogenic acid was purchased from Alfa Aesar.

The plant material

Aerial parts of *M. officinalis*, *S. officinalis* leaves and *Allium cepa* L. bulbs, were collected from a local producer, Arges county, in September 2020. The authentication of the plant material was performed by Assoc. Prof. Ph.D. Anca Sutan, and kept in paper bags, protected from moisture and sunlight, until primary processing. Primary processing of lemon balm and sage consisted of drying the plants in an oven at 40°C, a temperature designed not to denature the phenolic compounds of interest, and grinding the plant material in a Retsch Grindomix laboratory mill at the following parameters: 3 min pulse grinding at 4,000 RPM and 30 sec continuous grinding at 10,000 RPM (Manolescu et al. 2022).

Extraction procedures

The extraction of secondary metabolites was performed by maceration as classical method and two non-conventional methods, MAE and UAE, respectively. Two different ratios of pharmaceutical ethyl alcohol and distilled water were used as solvent mixtures: 70:30 v/v and 50:50 v/v.

For plant maceration, 1 g of dry sample, ground and weighed on an analytical balance to 4 decimal places, was immersed in 10 ml solvent (pharmaceutical ethyl alcohol:distilled water). Maceration was carried out at room temperature, shielded from sunlight, for 7 days; the first 4 days with continuous stirring for 6 hours at 30 RPM on the Biosan mini-rotator, and the next 3 days without stirring (Dent 2015).

The same binary solvents and the same 1:10 plant to solvent ratio were used for MAE. Initially the plant material was hydrated in the solvent for 1 hour and then subjected to microwave irradiation for 3, 5 and 10 minutes at a maximum power of 250 W. Microwave-assisted extraction was performed using the NEOS-GR equipment, Milestone. The final temperature range of the samples was between 54-78°C (Dent 2015).

UAE was carried out using a Hielscher UP200St ultrasonic extraction system under a working amplitude equal to 80% of the maximum rated output power of the device. In order to avoid overheating of the experimental samples and possible destruction of phytocompounds we used a cooling system, extracts were obtained at temperatures below 45°C (Dent 2015; Žlabur et al. 2016).

All experimental variants (Table 1) were then centrifuged twice (10 min total time) at 6,000 RPM. The supernatants obtained were subjected to vacuum filtration through Pall Flex Membrane Filters QRY:100; MM: 47 filter paper on a Rocker model filtration system: VF6. Pending analysis of total polyphenol content, antioxidant activity, HPLC analysis, MNPs synthesis and evaluation of cytogenotoxicity, samples were kept in glass vials at -18°C.

Determination of the total polyphenol content of the obtained plant extracts and nanostructured phytochemical complexes

Quantitative determination of polyphenolic structure compounds in the obtained extracts was carried out by the Folin-Ciocalteu spectrophotometric method (Sutan et al. 2018). From each experimental variant, diluted beforehand until a dilution factor of 600 was reached, a volume of 500 µL extract was taken over which 2.5 ml Folin-Ciocalteu reagent 10% (aqueous mixture of phosphomolybdate and phosphotungstate) was

Table 1. Experimental variants used in this study.

No	Sample code	Plant species	Extraction procedure	Pharmaceutical ethyl alcohol:distilled water ratio (v/v)	Extraction parameters
1	M_M_50		Maceration	50:50	7 days; room temperature; in the dark
2	M_M_70		Maceration	70:30	7 days; room temperature; in the dark
3	M_MAE_3_50		MAE	50:50	3 min; 250 W
4	M_MAE_5_50		MAE	50:50	5 min; 250 W
5	M_MAE_10_50		MAE	50:50	10 min; 250 W
6	M_MAE_3_70		MAE	70:30	3 min; 250 W
7	M_MAE_5_70	*M. officinalis*	MAE	70:30	5 min; 250 W
8	M_MAE_10_70		MAE	70:30	10 min; 250 W
9	M_UAE_3_50		UAE	50:50	3 min; 80% Amp
10	M_UAE_5_50		UAE	50:50	5 min; 80% Amp
11	M_UAE_10_50		UAE	50:50	10 min; 80% Amp
12	M_UAE_3_70		UAE	70:30	3 min; 80% Amp
13	M_UAE_5_70		UAE	70:30	5 min; 80% Amp
14	M_UAE_10_70		UAE	70:30	10 min; 80% Amp
15	S_M_50		Maceration	50:50	7 days; room temperature; in the dark
16	S_M_70		Maceration	70:30	7 days; room temperature; in the dark
17	S_MAE_3_50		MAE	50:50	3 min; 250 W
18	S_MAE_5_50		MAE	50:50	5 min; 250 W
19	S_MAE_10_50		MAE	50:50	10 min; 250 W
20	S_MAE_3_70		MAE	70:30	3 min; 250 W
21	S_MAE_5_70	*S. officinalis*	MAE	70:30	5 min; 250 W
22	S_MAE_10_70		MAE	70:30	10 min; 250 W
23	S_UAE_3_50		UAE	50:50	3 min; 80% Amp
24	S_UAE_5_50		UAE	50:50	5 min; 80% Amp
25	S_UAE_10_50		UAE	50:50	10 min; 80% Amp
26	S_UAE_3_70		UAE	70:30	3 min; 80% Amp
27	S_UAE_5_70		UAE	70:30	5 min; 80% Amp
28	S_UAE_10_70		UAE	70:30	10 min; 80% Amp

added. The tubes were kept at room temperature for 5 minutes and then 2 mL sodium carbonate solution (7.5%) was added. The tubes were shaken vigorously and kept in the dark at room temperature for 1 hour. Total polyphenol content (TPC) analysis was performed on the Ocean Optics HR2000+ UV-VIS spectrophotometer at 765 nm wavelength. Distilled water was used as blank instead of extract. Polyphenol concentration was expressed as mg gallic acid equivalent/g plant (mg GAE/g) based on the calibration curve constructed for different concentrations of the etalon, i.e. for 7 points of concentrations from 10 to 70 µg/mL gallic acid (y = 0.0115x + 0.0094; R^2 = 0.9995). TPC values, expressed in mg gallic acid equivalent/g plant were obtained according to the formula (Phuyal et al. 2020):

$$TPC = \frac{\left(\frac{C}{M} \times DF\right)}{1000} \quad (1)$$

Where C is the concentration measured from the calibration curve, M is the dry plant mass and DF is the dilution factor.

The quantitative determination of compounds with polyphenolic structure in all phytochemical complexes supplemented with MNPs was also carried out by the Folin-Ciocalteu spectrophotometric method, also used for simple extracts (Sutan et al. 2018).

Determination of the Trolox Equivalent Antioxidant Capacity (TEAC) of simple extracts and nanostructured phytochemical complexes using the DPPH method

The free radical scavenging activity of the extracts and nanostructured mixtures was measured using the 2,2-diphenyl-1-picrylhydrazyl (DPPH) method. The analysis was determined according to Shimamura et al. (2014), but with some modifications.

For the preparation of the standard, 2.50 mg Trolox was weighed on a microbalance and placed in a 10 mL volumetric flask. 5 mL of 99.5% ethanol was added and sonicated for complete dissolution, after which the solvent was made up to 10 mL. This was the stock solution from which the dilution range of 10-70 µg/mL was prepared, which was necessary to carry out the calibration curve (y = 1.4028x + 2.4888; R^2 = 0.9991).

The DPPH reagent used for both the standard and all experimental variants was prepared as follows: 3.2 mg of 2,2-diphenyl-1-picrylhydrazyl was placed in a 100 mL volumetric flask to which 50 mL of 99.5% ethanol was added; it was then sonicated and made up to 100 mL with solvent. The DPPH solution was prepared fresh and stored at room temperature, protected from light.

From all 28 experimental variants of simple extracts, only those samples with the highest polyphenol content for each extraction procedure were chosen to show DPPH free radical scavenging activity and to assess the biogenic synthesis capacity of noble MNPs. Simple extracts were diluted to obtain 6 different concentrations (250 µg/mL; 500 µg/mL; 1,000 µg/mL; 5,000 µg/mL; 10,000 µg/mL; 100,000 µg/mL), and those supplemented with MNPs were diluted to obtain 3 different concentrations (500 µg/mL; 1,000 µg/mL; 5,000 µg/mL). From each sample of different concentration, 250 µL simple extract/nanostructured mixture was taken over which 1,750 µL DPPH was added. The systems were kept in the dark at room temperature for 30 minutes and then for each sample, the absorbance at 517 nm wavelength was read after 5 minutes of stabilization under UV influence.

The inhibition percentage of DPPH (%IP) was calculated according to the formula (Adebiyi et al. 2017):

$$\%IP = \frac{A0 - A1}{A0} \times 100 \qquad (2)$$

Where A0 is the control sample absorbance and A1 is the sample absorbance.

To determine the half maximum inhibitory concentration (IC50), two concentration points of each sample were selected for which the inhibition ratio had a value around 50% (one < 50% and one > 50%) and the regression curve (Y = AX + B) was drawn. The IC50 value (sample concentration - X) was calculated by replacing Y by 50 (Shimamura et al. 2014).

The half maximum inhibitory concentration values are required for the determination of the antioxidant activity calculated in Trolox equivalent according to the formula:

$$TEAC = \frac{IC50 Trolox}{IC50 Sample} \qquad (3)$$

UHPLC Analysis. Sample preparation

A stock solution of 0.1 mg/mL from all standard compounds was prepared by dissolving 10 mg of each reference in 100 mL methanol. This stock solution was kept refrigerated at 4°C and used when needed. To obtain the solutions for the calibration curve the stock solution was diluted with a mixture of the first gradient line of the mobile phase. The dilution factors were 2000, 1000, 500, 250 and 100, respectively.

UHPLC-PDA-MS analysis

Separation of polyphenols was carried out on a Waters Arc System coupled with a Waters 2998 PDA detector and a Waters QDa mass detector. The column used was a Waters Cortecs C18 (4.6 × 50 mm, 2.7 µm) eluting with solvent A (0.1% formic acid in water), solvent B (0.1% formic acid in methanol) and solvent C (0.1% formic acid in acetonitrile). Solvent B was set at 1% during the entire separation. The gradient was as follows: 0–4 min 3%-14% C, 4–7.5 min 14% to 29% C, 7.5–13 min 29% to 89% C, 13–15 min 89% to 3% C. The flow rate of the mobile phase was set at 1.0 mL/ min. The column temperature was equilibrated to 35°C. The injection volume was 5 µL. All samples were kept at 20°C during the entire analysis (Velamuri et al. 2020).

Eluted compounds were analysed using a Waters PDA 2998 and a QDa mass detector equipped with electrospray ionization (ESI) source. Capillary voltage was maintained at 0.8 kV, cone voltage was kept at 20 V and the mass spectra spectra were recorded in negative ion mode in the range 100–800 m/z. Quantification was established in selected ion recording (SIR) mode for each compound (as shown in Table 2) using external calibration curves prepared for each standard. Also, the retention times for all reference compounds are presented in Table 3.

Biogenic synthesis of noble metal nanoparticles mediated by plant extracts

For the biosynthesis of MNPs using extracts of lemon balm and sage, the experimental variant that was found to contain the highest content of polyphenols was used from each extraction procedure, since literature data show that phytochemicals, especially polyphenols, present in plant extracts have the strongest reducing properties of silver and gold ions and also confer the highest stability of the nanoparticles (Swilam and Nematallah 2020). For the synthesis of AgClNPs, a 1mM

Table 2. Calibration curve statistics of reference compounds.

Calibration curve standard	Fit Type	Equation	R^2
Protocatechuic acid		$Y = -3.98e{+}003\ X^2 + 1.41e{+}005\ X + 5.19e{+}003$	0.998221
Chlorogenic acid		$Y = -9.88e{+}003\ X^2 + 1.40e{+}005\ X + 1.83e{+}004$	0.994078
Caffeic acid		$Y = -1.98e{+}004\ X^2 + 3.63e{+}005\ X + 2.73e{+}004$	0.997099
p-Coumaric acid	Quadratic (2nd Order)	$Y = -3.79e{+}003\ X^2 + 1.01e{+}005\ X + 2.14e{+}003$	0.997983
Ferulic acid		$Y = -4.99e{+}002\ X^2 + 2.01e{+}004\ X - 2.72e{+}002$	0.998986
Rutin		$Y = -1.52e{+}003\ X^2 + 7.64e{+}004\ X + 4.40e{+}003$	0.998255
Rosmarinic acid		$Y = -5.96e{+}001\ X^2 + 5.35e{+}004\ X + 3.51e{+}005$	0.994586
Quercetin		$Y = -2.50e{+}004\ X^2 + 7.79e{+}005\ X - 5.95e{+}001$	0.999115

Table 3. Retention times for all reference compounds.

Peak no.	Compound name	Coding	m/z	Retention time [min]
1	Protocatechuic acid	PRO	153	1.667
2	Chlorogenic acid	CHL	353	3.082
3	Caffeic acid	CAF	179	3.332
4	p-Coumaric acid	COU	163	4.459
5	Ferulic acid	FER	193	5.152
6	Rutin	RUT	609	5.580
7	Rosmarinic acid	ROS	359	6.715
8	Quercetin	QUE	301	7.757

silver nitrate ($AgNO_3$) solution obtained by weighing 16.98 mg $AgNO_3$ salt was used as a precursor and made up to 100 mL volume with distilled water.

Tetrachloroauric acid ($HAuCl_4$) solution of 1mM concentration, obtained by adding 35.80 mg $HAuCl_4$ to 100 mL of distilled water, was the precursor for the phytosynthesis of gold nanoparticles. The simple extracts were then mixed with the specific precursors in volume ratios of 1:1 and incubated for 24 h at room temperature (25°C). The colour change of the extracts after the addition of the 2 types of precursor solutions was noticeable within the first 2 min, which was a first confirmation of the formation of noble MNPs (Sutan et al. 2019).

BFSTEM-EDS analysis of nanostructured phytochemical complexes

Bright field scanning transmission electron microscopy (BFSTEM) and energy dispersive X-ray spectroscopy (EDS) were used to investigate particles size, shape and dispersion and perform chemical elemental analysis. These analyses were carried out using the FESEM-HITACHI SU8230 microscope. Prior to these analyses, samples were homogenized for 1 minute in an ultrasonic bath (Kerry Guyson) for a better dispersion. Then, one drop of each sample was spread on a copper grid with formvar and the grid was kept for 24 hours in the exicator to evaporate the solvent.

Coating Cu grids with formvar film

Cu grids with thin formvar films are primarily used for transmission electron microscopy for sampling and analysis of ultra-thin sections (Shields 1999).

The formvar film also acts as a support for various suspensions or powders to be analysed by SEM/BFSTEM.

To obtain Cu grids with formvar film, the ~1% formvar solution in 1,2-dyclorethane was poured into a tall covered container. A glass microscope slide was cleaned with distilled water, but not insistently. The glass slide was inserted into the container with the formvar solution and left for 2-3 minutes. The glass slide was then removed from the formvar solution and drained, after which the slide was left at room temperature for a further 2-3 minutes after which the excess solution was removed. After drying the film, it was cut on the edge of the glass blade using a razor blade. A container was filled with clean distilled water and the glass blade was inserted at an angle of 45° to loosen the formvar film. The Cu grids were placed face down over the formvar film on the surface of the water. The formvar grids were collected using another pre-cleaned glass slide, after which the grids were left at room temperature covered with the lid of a petri dish to dry and adhere the film to the Cu grid (Sherman 2014).

In vivo testing of the cytogenotoxic activity of simple extracts and nanostructured phytochemical complexes

Root tip cells were obtained by placing bulbs of *Allium cepa* L. with discoidal stem in contact with distilled water for 48 h, in the dark. The bulbs were transferred to
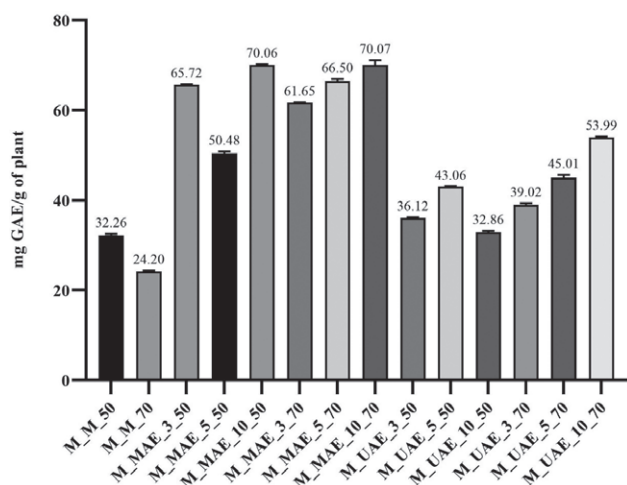
simple extracts and nanostructured mixtures (24 h).

After 24 h the root tip meristematic cells were removed and subjected to fixation using Farmer's reagent (glacial acetic acid:absolute ethyl alcohol, 1:3 v/v) overnight and then transferred to 70° ethyl alcohol for long-term preservation. For each experimental variant a number of 5 roots were subjected to attenuated hydrolysis with 1N HCl for 18 minutes at 60°C. The fixed and macerated roots were stained with 2% aceto-orcein solution for 15 minutes at 60°C. From the stained meristematic tips, microscopic preparations were made by the squash technique.

Microscopic slides were analysed under the Mshot Trinocular ML 11-II biological microscope at 400× magnification. Microscopic analysis consisted of determining the number of cells at different stages of mitosis, the frequency of chromosomal and nuclear aberrations, based on approximately 3,000 cells per experimental sample. The mitotic index (MI) was determined as the percentage ratio of the number of cells in mitosis to the total number of cells analysed (Tedesco and Laughinghouse 2012). Based on the total number of cells in mitosis, the percentage ratio of cells in prophase, metaphase, anaphase or telophase was determined. The frequency of chromosomal aberrations and nuclear abnormalities was determined by relating them to the appropriate stage of the cell cycle, i.e. mitosis.

Statistical interpretation of the results

The results of the experimental analyses were expressed as mean values ± standard deviation (SD). One-way analysis of variance (ANOVA) followed by Šídák's multiple comparisons test was used to analyse differences between mean values. A probability of p<0.0001 was considered highly significant. Statistical analysis was performed using GraphPad Prism 9.0.0.0 software.

For cytogenetic analysis, statistical processing of data was performed using IBM SPSS Statistics 20 software. Statistical significance and significant differences between variables were determined using analysis of variance (one way ANOVA) and Duncan's test for multiple comparisons, respectively. Values of p ≤ 0.05 were considered statistically significant. Graphs and tables were compiled based on mean values ± standard error of several independent experiments.
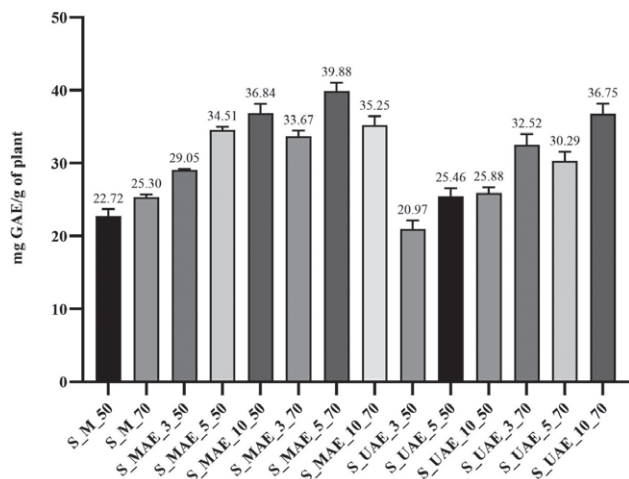
RESULTS AND DISCUSSIONS

Determination of the total polyphenol content of the obtained plant extracts and nanostructured phytochemical complexes

As can be seen in Figure 1, the highest amount of polyphenols, i.e. 70.07±1.07 mg GAE/g plant, was recorded for the lemon balm extracts obtained by microwave-assisted extraction technique, in solvent with a volume ratio of pharmaceutical ethyl alcohol and distilled water of 70:30, and after 10 minutes of microwave action on the extraction mixture. For macerates, the highest amount of total polyphenols (32.26±0.26 mg GAE/g plant) was recorded for those obtained in the solvent with equal ratio of water and solvent. For the ultrasound-assisted extraction of aerial parts from lemon balm plants with solvent with a volume ratio of pharmaceutical ethyl alcohol and distilled water of 70:30, there is a directly proportional increase in the amount of total polyphenols with the time of ultrasound action, with the highest amount of these compounds (53.98±0.16 mg GAE/g plant) obtained after 10 minutes of extraction.

A variation from 2.816 to 7.796 mg/mL of phenolic compounds was reported by Papoti et al. (2019) in aqueous preparations, respectively: infusion, decoction, maceration, ultrasound-assisted extraction. Total polyphenols ranging from 18.17±0.04 to 64.17±0.52 mg GAE/g dry plant was obtained by Petkova et al. (2017) when infusions made from lemon balm plants cultivated in Bulgaria were analysed.

Of the two sage extracts obtained by maceration, the highest polyphenol content was determined for the one with a ratio of 70:30 pharmaceutical ethyl alcohol:distilled water (v/v) (25.30±0.96 mg GAE/g plant), data illustrated in Figure 2.

Figure 1. Total polyphenol content of *M. officinalis* extracts (Data are expressed as mean ±SD values from independent triplicate experiments).
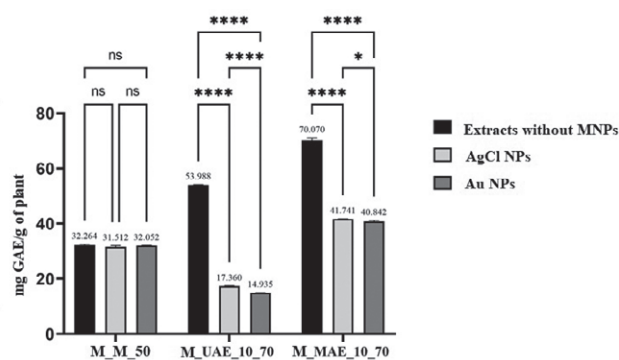
Figure 2. Total polyphenol content of *S. officinalis* extracts (Data are expressed as mean ±SD values from independent triplicate experiments).

Figure 3. Total polyphenols content of simple extracts and nanostructured phytochemical complexes of *M. officinalis* (Data are expressed as mean ± SD values from independent triplicate experiments and p values were calculated by one-way ANOVA followed by Šídák's multiple comparisons test; ****p < 0.0001; *p = 0.0472; ns p =0.1058; 0.8170; 0.2920).

In contrast, Pop et al. (2015) doubling the extraction time by maceration and using 80% EtOH obtained lower TPC values, 19.49 mg GAE/g dry plant, which shows that a prolonged extraction time may not always lead to a higher phytocompound concentration. This is also confirmed by the results obtained by Osmić et al. (2019), who using a 40% aqueous ethanol solution and the same plant:solvent ratio used by us, obtained from the leaves of *S. officinalis* L. a polyphenol content of 137.11 mg GAE/g in only 60 minutes of maceration at room temperature. However, there are experimental studies in which maceration resulted in much lower TPC values than the present study, namely 13.6±0.4 mg GAE/g (Proestos et al. 2005); 4.25 mg-5.95 mg GAE/g (Roby et al. 2013). Moreover Gîrd et al. (2014) using the same solvent, ethanol 70% managed to extract from one gram of sage leaves only a minimum TPC of 3.26 mg GAE/g and a maximum of 6.32 mg GAE/g.

The extracts obtained using MAE showed a total amount of polyphenolic compounds between 29.05±0.16-39.88±1.19 mg GAE/g plant, the maximum of 39.88±1.19 mg GAE/g plant being obtained after irradiating the plant material with electromagnetic waves for 5 minutes, also at a higher concentration of alcohol, at a temperature of 75°C and a power of 250W. Similar values were also recorded in the experimental study conducted by Dragović-Uzelac et al. (2012), where the range of TPC values obtained was between 31.7-47.0 mg RAE/g, the maximum being determined in the sample irradiated for 9 minutes at a power of 500W.

For the samples subjected to sonication, in order to reach a maximum TPC of 36.75±1.41 mg GAE/ g plant,

it was necessary to prolong the acoustic cavitation phenomenon to a maximum of 10 minutes, an alcohol concentration of 70% and a temperature of 45°C. This polyphenol content is much higher compared to Pop et al. (2015) 19.06 mg GAE/g plant and Brindisi et al. (2021), 18.7-35.3 mg CA/g. In contrast, there are studies attesting the recovery of higher concentrations of polyphenolic compounds from sage, such as 67.75 mg GAE/g (Dent 2015); 99.03 mg GAE/g (Zeković et al. 2017); 61.3-143.6 mg GAE/g (Veličković et al. 2011).

A possible explanation for the differences between the TPC values in the literature, and those obtained by us, except for the extraction technique and parameters, would be the time at which the plant material was harvested, Farhat et al. (2014), demonstrating that the highest polyphenol content was recorded for sage plants harvested at the fruiting stage. The results could also be attributed to the drying protocol of the plants (Hamrouni-Sellami et al. 2012) as well as the geographic area of cultivation (Farhat et al. 2014; Dent et al. 2017).

As can be seen in Figure 3, the highest amount of phenolic compounds for lemon balm extracts supplemented with MNPs was recorded for those obtained by MAE technique, i.e. 41.741±0.052 mg GAE/g plant for M_MAE_10_70_AgCl and 40.842±0.343 mg GAE/g plant for M_MAE_10_70_Au.

For the macerates, it can be seen that there are statistically insignificant differences between the TPC values of extracts and mixtures with AgClNPs and AuNPs.

Strongly statistically significant higher values were observed for extracts obtained by using UAE without MNPs comparing with the extracts supplemented with MNPs, the TPC content ranging from 53.988±0.166 mg
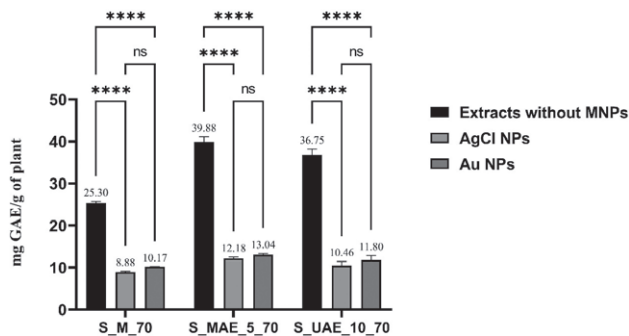
Figure 4. Total polyphenols content of simple extracts and nanostructured phytochemical complexes of *S. officinalis* (Data are expressed as mean ± SD values from independent triplicate experiments and p values were calculated by one-way ANOVA followed by Šídák's multiple comparisons test; ****p < 0.0001; ns p = 0.1310; 0.1497; 0.4079).
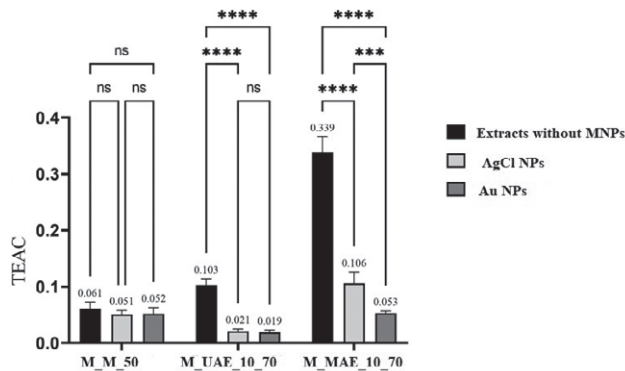

Figure 5. Trolox equivalent antioxidant capacity of simple extract and nanostructured phytochemical complexes of *M. officinalis* (Data are expressed as mean ± SD values from independent triplicate experiments and p values were calculated by one-way ANOVA followed by Šídák's multiple comparisons test; ****p < 0.0001; ***p = 0.0003; ns p = 0.6144; 0.6707; 0.9953; 0.9814).

GAE/g plant to 17.360±0.069 mg GAE/g plant for M_UAE_10_70_AgCl and 14.932±0.044 mg GAE/g plant for M_UAE_10_70_Au.

A statistically significant decrease was also observed for extracts obtained by MAE technique with AgClNPs (41.741±0.052 mg GAE/g) and AuNPs(40.842±0.343 mg GAE/g) compared to extracts without MNPs (70.070±1.070 mg GAE/g plant).

It is important to highlight unlike lemon balm extracts enriched with MNPs where the highest amount of polyphenols was obtained for extracts with AgClNPs, for sage, extracts with AuNPs were found to exhibit this characteristic (Figure 4). Moreover, in the case of nanostructured phytochemical complexes of sage, the maximum total amount of polyphenols was also recorded for the experimental variant using the extract obtained after microwave irradiation of the plant material, i.e. 13.04±0.26 mg/g GAE for sample S_MAE_5_70_70_Au.

However, there are no significant differences between the amount of polyphenols obtained for sage extracts with AgClNPs versus those with AuNPs, for these extracts enriched with MNPs the amount of total polyphenols remained relatively constant regardless of the extraction technique used, with TPC values varying only from 8.88±0.2 mg GAE/g plant for the AgClNPs macerate and 13.04±0.26 mg GAE/g plant for the extract obtained by MAE and with AuNPs.

Making a comparison between the TPC values of simple extracts and phytochemical complexes, in the case of both medicinal species it can be observed that following the phytosynthesis of MNPs, the amount of polyphenols was decreased. An explanation for this is provided by the experimental study conducted by Dzimitrowicz et al. (2016), which highlights that following

the reduction reaction of metal ions by a plant extract, a large part of the compounds of polyphenolic nature are oxidized.

Determination of the Trolox Equivalent Antioxidant Capacity (TEAC) of simple extracts and nanostructured phytochemical complexes using the DPPH method

From Figure 5 it can be seen that the best ability of the lemon balm extracts with MNPs to behave as hydrogen atom or electron donors for the conversion of the purple free radical DPPH- to its reduced yellow form DPPH-H was for extracts obtained by the MAE technique, the TEAC values were 0.106±0.019 for M_MAE_10_70_AgCl and 0.053±0.003 for M_MAE_10_70_Au. Also, for these types of extracts a highly significant statistical difference is observed compared to extracts without metal nanoparticles whose TEAC values were 0.339±0.027.

Similar to the TPC values, the statistical differences of TEAC values are insignificant between macerates without MNPs and those supplemented with MNPs. A highly significant statistical difference can also be observed for the TEAC values of the extract obtained by ultrasound action on plant material without MNPs (0.103±0.011) compared to extracts with AgClNPs (0.021±0.004) and AuNPs (0.019±0.004).

For both simple extracts and systems consisting of sage extracts and MNPs, the highest antioxidant activity was recorded for the experimental variant S_MAE_5_70 (Figure 6).

At the opposite pole, the lowest antioxidant activities were recorded for the samples subjected to macera-
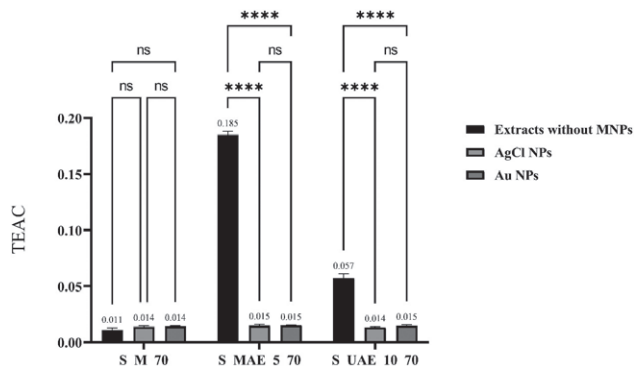
Figure 6. Trolox equivalent antioxidant capacity of simple extract and nanostructured phytochemical complexes of *S. officinalis* (Data are expressed as mean ± SD values from independent triplicate experiments and p values were calculated by one-way ANOVA followed by Šidák's multiple comparisons test; ****p < 0.0001; ns p = 0.1727; 0.1231; 0.6421; 0.9794; 0.9908).

tion and sonication processes. In contrast Zeković et al. (2017), using other extraction parameters, demonstrate that their simple extracts obtained by the cavitating phenomenon show a slight improvement in antioxidant activity as opposed to those subjected to microwaving, but the difference is not a noticeable one.

Comparing the antioxidant activity of simple extracts with that of nanostructured phytochemical complexes, both *M. officinalis* L. and *S. officinalis* L. simple extracts have the highest free radical scavenging capacity, as they also have the highest concentrations of polyphenols.

The results of the evaluation of the antioxidant capacity as well as the amount of total polyphenols in the nanostructured extracts obtained are in agreement with the existing data in the literature, data which show that the reduction in the amount of total polyphenols correlated with a decrease in the antioxidant activity of extracts with MNPs compared to simple extracts is attributed to the fact that the bioorganic material, especially the polyphenols, participates in the reduction of metallic ions as well as in the formation of the coating

halo that stabilizes the nanoparticles (Csakvari et al, 2021; Nayeri et al., 2021; Siakavella et al., 2020).

UHPLC Analysis

To identify the compounds obtained by the 3 different extraction methods, 6 experimental variants were subjected to UHPLC-PDA-MS analysis (M_M_50; M_MAE_10_70; M_UAE_10_70; S_M_70; S_MAE_5_70; S_UAE_10_70), namely those variants with the highest TPC.

Thus, according to the data presented in Table 4, maceration of the aerial parts of lemon balm resulted in significant amounts of rosmarinic acid (227,120 µg/mL), the most abundant compound in this medicinal species (Kim et al. 2010). However, modern extraction methods have allowed the recovery of much higher concentrations of it. Thus, UAE revealed a quantity of 263.805 µg/mL of rosmarinic acid, and the MAE method yielded the highest amount of rosmarinic acid, i.e. 1,266.89 µg/mL. Similar value (17.03 mg/g) indicating a significant amounts of rosmarinic acid was obtained by Caniova and Brandsteterova (2001) using the liquid extraction technique (methanol and water in a volume ratio of 60:40) of *M. officinalis* L. plants grown in Slovakia.

The highest concentrations of protocatechuic acid and rutin were obtained from maceration of sage leaves. However, MAE proved to be the optimal method to obtain the highest amounts of all other compounds. As mentioned above, the final temperature range of the samples subjected to sonication and microwaves, was in the case of UAE between 37-45°C, and in MAE between 54-75°C, the final temperature of 75°C being reached in sample S_MAE_5_70. Based on this result, we can also see that at higher temperatures, the solvent's solubilizing power of dissolved substances increases due to the decrease in viscosity and surface tension, thus facilitating wetting and matrix penetration (Paré et al. 1991; Chen et al. 2006; Hayat

Table 4. The amount of natural compounds (µg/mL) obtained from *M. officinalis* and *S. officinalis* by the three extraction techniques.

| Sample/Compound name	PRO	CHL	CAF	COU	FER	RUT	ROS	QUE
M_M_50	25.640	15.960	131.650	5.280	2.805	27.735	227.120	0.450
M_MAE_10_70	34.675	49.190	77.585	3.530	1.400	31.645	1266.890	0.230
M_UAE_10_70	24.245	39.795	40.010	2.245	1.000	28.265	263.805	0.190
S_M_70	35.930	12.125	27.845	3.465	6.895	30.295	502.540	0.000
S_MAE_5_70	35.845	16.140	48.935	3.790	12.520	10.240	593.715	0.000
S_UAE_10_70	9.560	11.610	44.045	3.035	6.450	26.195	687.260	0.225
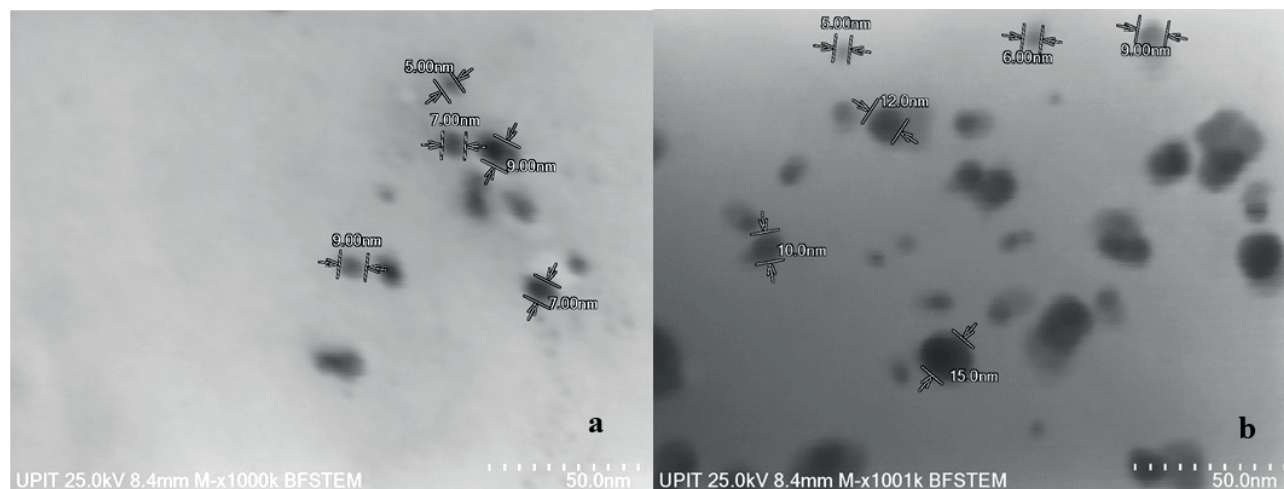
Figure 7. Dispersion dimensional analysis of AgClNPs for M_UAE_10_70_AgCl (a) and for S_M_70_AgCl (b) in BFSTEM at 1,000,000 (x1000k) magnification.

et al. 2009). Consistent with the results in Table 4, it can be seen that depending on the compound targeted for extraction, one extraction technique may be more advantageous than another. Thus, if in order to extract a maximum concentration of rosmarinic acid of 687.26 µg/mL from sage leaves, the phenomenon of acoustic cavitations is the most beneficial, the same cannot be said in the case of protocatechuic acid where the exposure of plant material to sound waves allowed the recovery of the lowest amounts of this phenolic acid compared to the other extraction techniques. Similar results regarding the discrepancy between the values of recovered compounds from this medicinal species were also recorded in the study conducted by Zeković et al. (2017).

BFSTEM-EDS analysis of nanostructured phytochemical complexes

From the dimensional analysis on AgClNPs dispersion in BFSTEM at 1,000,000 magnifications for the lemon balm extracts, it is observed that all these extracts showed the ability to phytosynthesize spherical shaped MNPs with diameters of about 20 nm, most of them having sizes just below 10 nm (5 nm, 6 nm, 7 nm and 9 nm). AgClNPs phytosynthesized in sage extracts are also spherical in shape, ranging in size from 5 mm to 20 mm. These aspects illustrated in Figure 7.

For the AuNPs phytosynthesized in all three types of extracts, a reduced dispersion was observed, being found as agglomerates, in which, AuNPs show sizes of about 10 nm. However, larger AuNPs were phytosynthe-
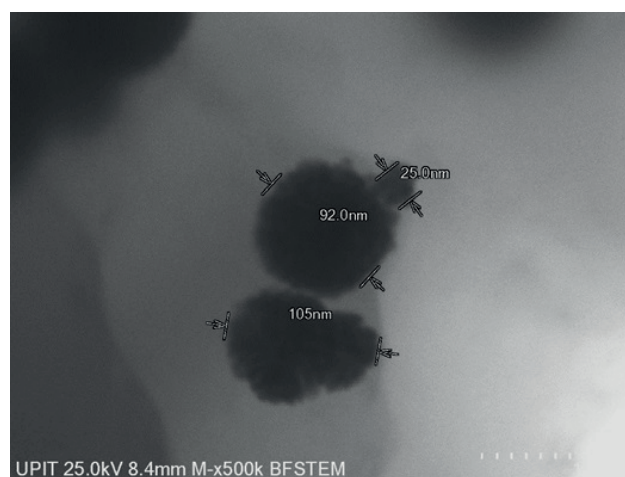
Figure 8. Dimensional analysis of AuNPs aggregates obtained in sage ethanolic extracts.

sized in sage extract obtained by UAE, Figure 8 showing 3 agglomerates of AuNPs with sizes of 105 nm, 92 nm and 25 nm.

The aggregation phenomenon of AuNPs may be due to the low concentration of the precursor salt (i.e. HAuCl$_4$), but also to the pH of the solution or even the age of the plants (Teimouri et al. 2018; Boruah et al. 2021).

EDS analysis allowed us to superimpose the spectra generated for the formvar film-coated copper grids and those with nanostructured phytochemical complexes. In Figure 9 it can be seen that AgClNPs and AuNPs are present only in these phytocomplexes.
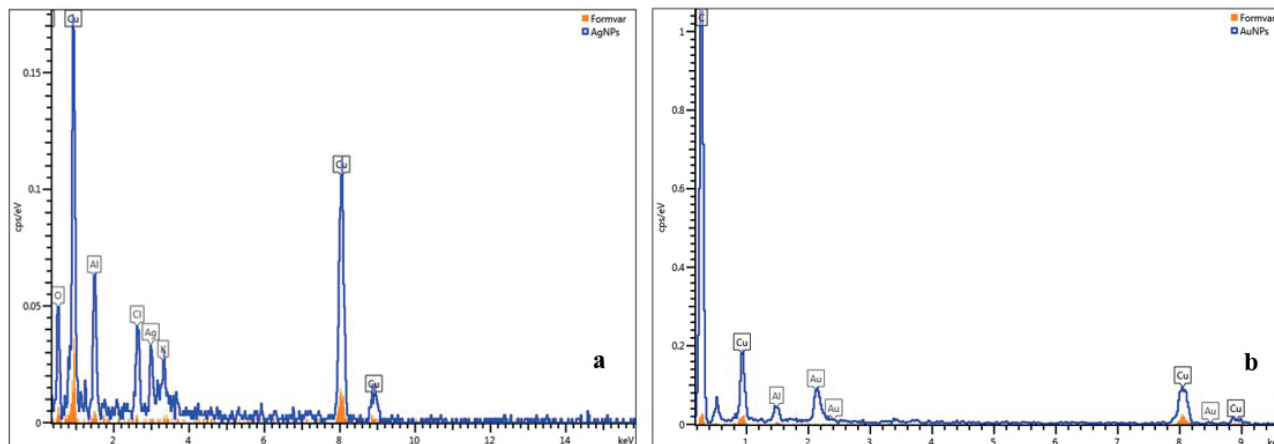
Figure 9. Superimposed EDS spectra obtained for Cu grid with formvar and M_MAE_10_70_AgCl with AgClNPs on Cu grid with formvar (a) and Cu grid with formvar and S_MAE_5_70_Au with AuNPs on Cu grid with formvar (b).

In vivo testing of the cytogenotoxic activity of simple extracts and nanostructured phytochemical complexes

The *Allium cepa* L. test is widely used to determine the benefits and especially the adverse effects of medicinal plants, which are increasingly used nowadays. This is because the test is a very good indicator of toxicity and mutagenicity (Tedesco and Laughinghouse 2012). In our study, the *Allium* assay was used to evaluate the possible cytogenotoxicity of crude or supplemented extracts with MNPs. While for *M. officinalis* L. there is some data on the use of this test, in the case of *S. officinalis* L. it is performed for the first time.

The variation of the MI in onion root tip meristematic cells subjected to treatment with ethanolic extracts of *Melissa officinalis* L. before and after MNPs phytosynthesis is shown in Figure 10.

These results revealed that for *M. officinalis* L. extracts, the highest percentage value of the MI (11.126%) corresponded to the sample M_M_50. Likewise, for the control, the highest MI was recorded for roots incubated in solvent with a ratio of 96% pharmaceutical ethyl alcohol and 50:50 distilled water (8.643%).

Phytosynthesis of AgClNPs and AuNPs inhibited the mitostimulatory action of ethanolic extracts. Thus, there was a statistically significant reduction in the percentage of dividing cells. The sample defined by the extracts supplemented with MNPs, showed a MI values close to those determined for the corresponding concentrations of alcohols, except for the sample M_MAE_10_70_Au for which the frequency of dividing cells was significantly higher (9.613%).

The inhibition of mitotic activity, in the experimental variant M_MAE_10_70_AgCl compared to con-
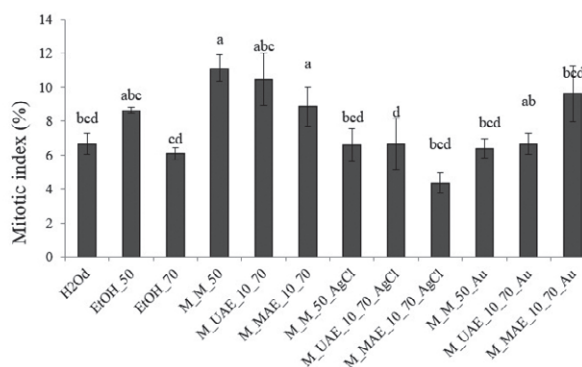
Figure 10. MI (%) of simple extracts of *M. officinalis* and nanostructured phytochemical complexes (a–d: interpretation of the significance of the differences, by means of the Duncan test, p < 0,05).

trols, may be correlated with the ion imbalance that can be induced at the cellular level by the extracts tested (Chakraborty et al., 2009).

Hsin et al. (2008) showed that AgNPs stimulate intracellular production of reactive oxygen species (ROS), which stimulates cell cycle progression while causing oxidative stress at the DNA level (Carlson et al., 2008).

Statistical analysis of the results on the distribution of mitosis phases (Figure 11) indicates a significant increase of prophase index that the decrease in for sample M_M_50_Au compared to the control. However, a distribution of mitosis phases similar to the control variants was noted for sample M_MAE_10_70_AgCl. Moreover, a significantly higher frecvency of metaphases were defining for thesamples M_UAE_10_70_AgCl and M_M_50_AgCl, suggesting the interference ofAgClNP-

Figure 11. Frequency of mitosis phases (%) in simple extracts of *M. officinalis* and nanostructured phytochemical complexes (a–c: interpretation of the significance of the differences, by means of the Duncan test, p < 0,05).

Figure 13. Frequency of mitosis phases (%) in simple extracts of *S. officinalis* and nanostructured phytochemical complexes (a–e: interpretation of the significance of the differences, by means of the Duncan test, p < 0,05).
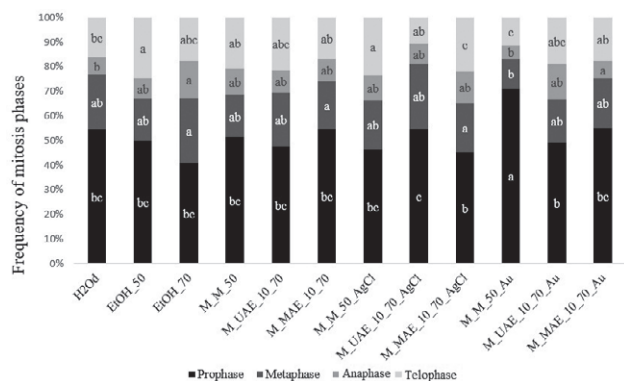

Figure 12. MI (%) of simple extracts of *S. officinalis* and nanostructured phytochemical complexes (a–d: interpretation of the significance of the differences, by means of the Duncan test, p < 0,05).
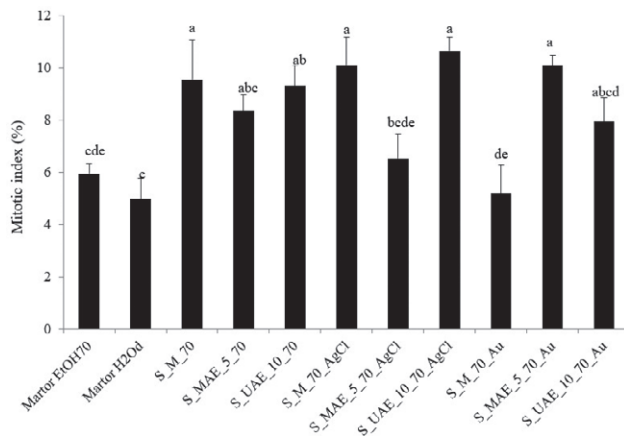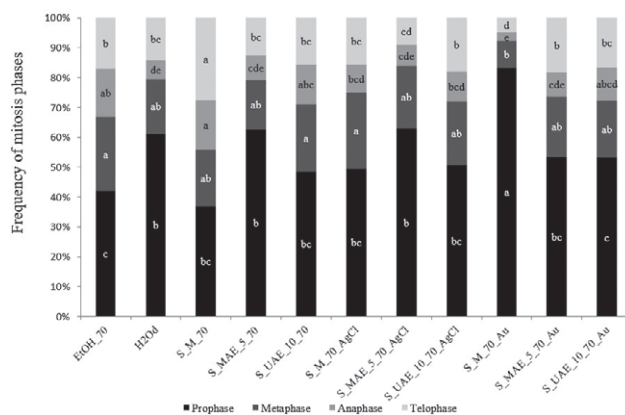
son the formation and/or functioning of the mitotic spindle.

Results of cytogenotoxicity analysis show that extracts of *S. officinalis* and those enriched with MNPs induced statistically significant variation of MI compared to distilled water, and to the control with the equivalent concentration of pharmaceutical ethyl alcohol (Figure 12).

Thus, treatment of onion root meristems with these samples resulted in a statistically significant increase of MI, with a maximum value of 10.01% for the experimental variant S_M_70_AgCl, in contrast to control samples, which showed mitoinhibitory effects.

The distribution of mitosis phases has been investigated and is shown in Figure 13. The highest prophase frequency was observed in the S_M_70_Au variant,

which was associated with the lowest anaphase and telophase indices.

The *Allium* test allows the assessment of the toxic potential of substances both by significant variation of MI and by analysing the type and frequency of chromosomal aberrations. Statistical interpretations of the results on the frequency of chromosomal aberrations (Figure 14) such as vagrant chromosomes, laggard chromosomes, sticky chromosomes, metaphase chromosomes (C-mitosis), fragmented chromosomes, pole-to-pole metaphases, bridge cells or multipolar anaphases are presented in Table 5 and Table 6, as well as nuclear aberrations (Figure 15) such as binucleated cells, budded nuclei, irregularly shaped nuclei, ghost cells and giant cells found in the *Allium cepa* L. root tip meristematic cells exposed to the action of controls, ethanolic extracts of lemon balm and sage and mixtures with MNPs for 24 hours.

Vagrant chromosomes represent the chromosomal aberrations found with a high frequency in all control samples but also in all experimental variants with the exception of those defined by *S. officinalis* macerate and ethanolic extracts of *M. officinalis* obtained by MAE technique supplemented with AgClNPs and AuNPs. These types of chromosomal aberrations occur as a result of "weak spindle formations" (Onwuamah et al. 2014).

Laggard chromosomes were observed in all samples defined by the ethanolic extracts of lemon balm and sage extracts obtained by using UAE and in those with MNPs, with the exception of sage extracts with AuNPs. It is believed that the formation of lagging chromosomes is the result of the disruption of the division spindle for-
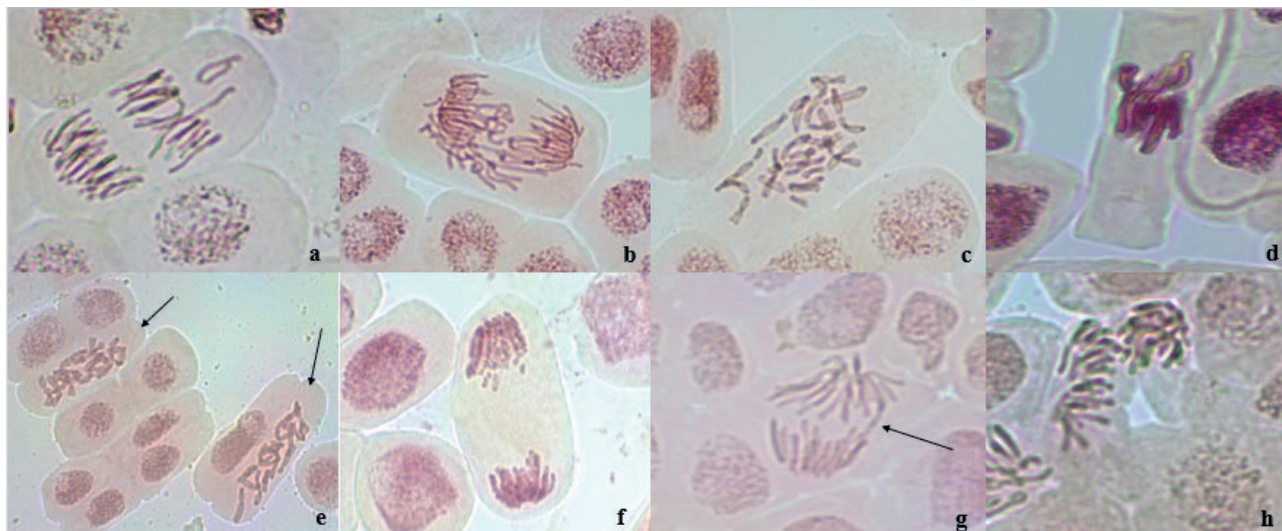
Figure 14. Chromosomal aberrations found in *A. cepa* root tip meristematic cells following treatments with simple extracts and with extracts supplemented with MNPs (a – Vagrant in EtOH_50; b – Laggards in M_UAE_10_70_AgCl; c – C-mitosis in M_UAE_10_70_AgCl; d – Sticky chromosomes in M_MAE_10_70_AgCl; e – Pole-to-pole metaphase in S_UAE_10_70_Au; f – Cell with fragmented chromosomes in S_MAE_5_70; g – Bridges in S_MAE_5_70_Au; h – Multi-polar anaphase cell in M_M_50).
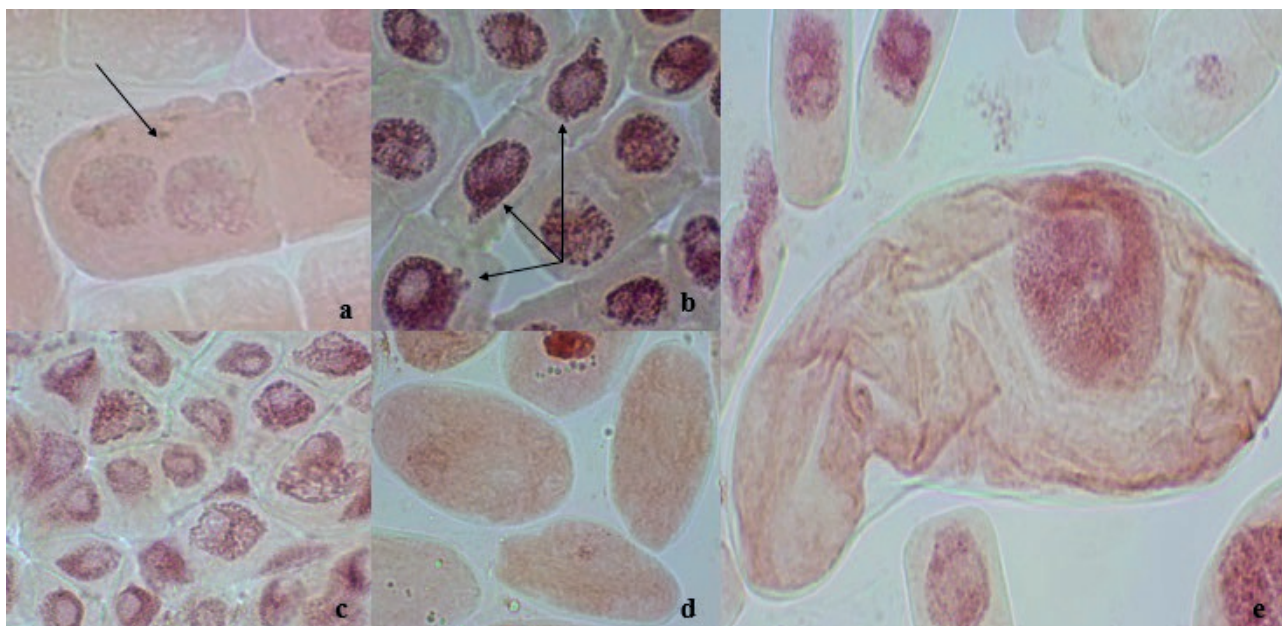
Figure 15. Nuclear aberrations found in *A. cepa* root tip meristematic cells following treatments with simple extracts and with extracts supplemented with MNPs (a – Binucleate cells in M_MAE_10_70; b – Nuclei buds in M_M_50_AgCl; c – Irregularly shaped nuclei in H2Od; d – Ghost cells in M_M_50_AgCl; e – Giant cell in EtOH_70).

mation process under the action of toxic agents (Haliem, 1990).

The frequency of sticky chromosomes significantly decreased in cells treated with lemon balm ethanolic extracts supplemented with AgClNPs and AuNPs regard-less of the extraction technique used. Stickies may be the consequence of subchromatid bonds between chromosomes (Liman et al., 2010). Although present at a moderate frequency in the control variants, but also in some experimental variants, the frequency of cells with nucleic buds

Table 5. Chromosomal and nuclear aberrations observed in *A. cepa* root tip meristematic cells treated with ethanolic extracts and nanostructured phytochemical complexes of *M. officinalis*.

SAMPLE	Cells with vagrant chromosomes	Laggard chromosomes	C-mitosis	Sticky chromosomes	Pole-to-pole metaphase	Cells with fragmented chromosomes	Bridges	Multi-polar anaphase cells	Binucleate cells	Nuclei buds	Irregularly shaped nuclei	Ghost cells	Giant cells	TOTAL
H2Od	3.51±1.76 ab	0.00±0.00 c	0.00±0.00 b	12.83±6.43 ab	0.00±0.00 b	1.85±1.00 a	0.00±0.00 b	0.00±0.00 b	0.00±0.00 b	0.00±0.00 b	33.69±6.06 a	0.00±0.00 b	0.06±0.06 a	32.71±5.52 a
EtOH_50	36.47±19.57 a	0.00±0.00 c	0.00±0.00 b	9.44±3.88 bc	0.00±0.00 b	0.00±0.00 b	1.11±1.11 b	0.00±0.00 b	0.00±0.00 b	0.03±0.03 b	0.4±0.30 b	0.00±0.00 b	0.00±0.00 a	0.98±0.29 b
EtOH_70	14.16±3.81 ab	0.00±0.00 c	0.00±0.00 b	4.16±4.00 b	0.00±0.00 b	0.00±0.00 b	0.00±0.00 b	0.00±0.00 b	0.00±0.00 b	0.00±0.00 b	33.82±16.59 a	0.00±0.00 b	0.33±0.33 a	32.85±15.58 a
M_M_50	10.92±1.44 ab	0.00±0.00 c	0.00±0.00 b	13.42±4.63 ab	0.00±0.00 b	0.00±0.00 b	2.75±1.42 ab	8.51±5.96 a	0.00±0.00 b	0.00±0.00 b	4.46±2.84 b	0.00±0.00 b	0.07±0.07 a	4.87±2.69 b
M_MAE_10_70	27.62±19.52 ab	0.00±0.00 c	0.00±0.00 b	12.40±8.58 ab	0.00±0.00 b	0.00±0.00 b	0.61±0.60 b	1.38±1.30 b	0.23±0.15 a	0.00±0.00 b	0.00±0.00 b	0.00±0.00 b	0.36±0.30 a	1.26±0.67 b
M_UAE_10_70	15.07±8.15 ab	3.05±1.54 c	0.00±0.00 b	24.30±9.30 ab	0.23±0.19 a	0.00±0.00 b	3.72±2.93 ab	0.00±0.00 b	0.00±0.00 b	0.09±0.06 b	0.00±0.00 b	0.00±0.00 b	0.00±0.00 a	1.28±0.15 b
M_M_50_AgCl	6.66±5.00 ab	0.00±0.00 c	0.00±0.00 b	9.44±3.88 ab	0.23±0.00 ab	0.00±0.00 b	0.00±0.00 b	0.00±0.00 b	0.00±0.00 b	2.08±0.63 a	0.00±0.00 b	1.83±1.83 b	0.09±0.09 a	3.86±2.15 b
M_MAE_10_70_AgCl	0.00±0.00 a	0.00±0.00 c	0.00±0.00 b	33.88±9.64 a	0.00±0.00 b	0.00±0.00 b	0.00±0.00 b	0.00±0.00 b	0.00±0.00 b	0.25±0.12 b	0.00±0.00 b	0.25±0.20 b	0.34±0.21 a	1.17±1.15 b
M_UAE_10_70_AgCl	16.66±9.62 ab	12.29±7.84 ab	47.66±12.46 a	1.33±1.33 b	0.00±0.00 b	0.00±0.00 b	1.66±1.50 ab	0.00±0.00 b	0.00±0.00 b	0.08±0.08 b	0.20±0.20 b	0.00±0.00 b	0.12±0.12 a	1.90±0.20 b
M_M_50_Au	5.00±2.88 ab	0.74±0.5 c	0.00±0.00 b	3.88±3.00 b	0.00±0.00 b	0.00±0.00 b	0.00±0.00 b	0.00±0.00 b	0.00±0.00 b	0.00±0.00 b	2.52±0.90 b	0.00±0.00 b	0.00±0.00 a	2.56±0.89 b
M_MAE_10_70_Au	11.11±7.34 ab	1.11±1.11 c	0.00±0.00 b	11.57±8.93 ab	0.00±0.00 b	0.00±0.00 b	9.24±5.79 a	0.00±0.00 b	0.00±0.00 b	0.00±0.00 b	1.06±0.36 b	0.00±0.00 b	0.00±0.00 a	1.32±0.42 b
M_UAE_10_70_Au	0.00±0.00 a	0.00±0.00 c	0.00±0.00 b	19.23±12.42 ab	0.00±0.00 b	0.00±0.00 b	6.33±4.66 ab	0.00±0.00 b	0.00±0.00 b	0.00±0.00 b	0.75±0.51 b	0.00±0.00 b	0.02±0.02 a	1.36±0.42 b

Table 6. Chromosomal and nuclear aberrations observed in meristematic root cells of *A. cepa* treated with ethanolic extracts and nanostructured phytochemical complexes of *S. officinalis*.

SAMPLE	Metaphase with vagrant chromosomes	Anaphase with vagrant chromosomes	Laggard chromosomes	Sticky chromosomes	Pole-to-pole metaphase	Cells with fragmented chromosomes	Bridges	Multi-polar anaphase cells	Binucleated cells	Irregularly shaped nuclei	Giant cells	Elongated nucleus cells	Other aberrations	TOTAL
EtOH70	6.50±3.71 ab	10.83±6.51 a	0.00	1.67±1.67 cd	0.00	0.00	0.00	0.00	0.00	29.69±12.39 b	0.38±0.38 a	0.00	0.00	28.95±11.82 a
H2Od	2.78±2.78 b	6.67±6.67 a	1.33±1.33 b	6.67±3.33 bcd	0.00	0.00	0.00	0.00	0.00	28.66±4.04 b	0.06±0.06 a	0.00	0.00	27.75±3.64 a
S_M_70	0.00	3.24±1.67 a	0.00	0.00	0.00	0.00	2.72±1.36 c	0.00	0.00	0.00	0.00	0.00	0.06±0.06 a	0.21±0.10 b
S_MAE_5_70	14.94±5.76 a	4.76±4.76 a	0.00	3.70±3.70 cd	0.00	20.63±9.15 a	1.85±1.85 c	2.38±2.38 a	0.09±0.09 a	0.00	0.00	0.00	0.08±0.04 a	1.27±0.25 b
S_UAE_10_70	7.10±5.16 ab	0.00	1.04±1.04 b	10.95±3.43 abc	0.00	6.94±4.22 b	17.65±5.71 abc	2.78±2.78 a	0.04±0.04 a	0.00	0.00	1.37±0.73 a	0.15±0.10 a	2.51±1.21 b
S_M_70_AgCl	0.00	0.00	0.00	0.00	6.25±3.68 ab	3.89±3.89 b	7.5±3.82 a	10.78±3.01 abc	0.00	16.27±12.34 abc	2.38±2.38 a	0.00	0.12±0.09 a	0.98±0.21 b
S_MAE_5_70_AgCl	0.00	0.00	0.00	4.3±2.08 c	0.00	0.00	10.48±5.79 a	0.00	0.00	10.00±5.77 abc	0.00	0.00	0.06±0.03 a	4.34±2.04 b
S_UAE_10_70_AgCl	0.00	0.00	0.00	49.00±16.44 a	0.33±0.33 b	0.67±0.67 b	0.00	3.67±0.88 cd	0.33±0.33 a	6.00±0.58 bc	0.00	0.00	0.00	5.59±1.67 b
S_M_70_Au	0.43±0.43 b	0.00	0.00	19.47±3.88 a	0.00	0.00	21.74±3.55 abc	0.00	0.06±0.06 a	0.00	0.00	0.00	0.00	2.62±1.51 b
S_MAE_5_70_Au	4.44±2.42 ab	0.00	0.00	14.93±4.90 ab	0.00	0.00	31.11±7.47 a	0.00	0.00	0.04±0.04 a	0.00	0.00	0.04±0.04 a	1.44±0.26 b
S_UAE_10_70_Au	6.35±6.35 ab	0.00	4.52±2.43 a	6.77±4.01 bcd	1.19±1.19 b	0.00	24.86±13.15 ab	0.00	0.00	0.00	0.00	0.00	0.05±0.05 a	2.94±0.85 abc

was null in all sage extracts and in lemon balm extracts supplemented with AuNPs, regardless of the extraction method used, suggesting the protective action of these MNPs on the organization and function of nuclei in onion root cells. Giant cells and cells with irregularly shaped nuclei characterized the control variants, being encountered with much decreased frequency in the experimental variants, including those with AgClNPs and AuNPs.

CONCLUSIONS

Our experimental study demonstrated that the two species of medicinal plants, namely *M. officinalis* L. and *S. officinalis* L., can be considered valuable sources of bioactive compounds, being likely to design novel functional products with different therapeutic properties. According to BFSTEM analysis the biogenic synthesis process of noble metal nanoparticles, was successfully carried out. The AgClNPs particle sizes under 10 nm were obtained in both lemon balm and sage extracts. Irrespective of the species tested, a direct proportionality between the total content of polyphenols of the extracts and nanostructured mixtures and their antioxidant activities was noticed. The most efficient method for obtaining polyphenols with the highest antioxidant activity was found to be microwave-assisted extraction, both for extracts and nanostructured mixtures. Mitosis was slightly inhibited in nanostructured phytochemical complexes of lemon balm compared to those of sage. The controls showed the highest frequency of chromosomal aberrations compared both to samples of simple extracts and extracts supplemented with MNPs, suggesting the cytogenoprotective, antigenotoxic, and the safety of using these bioformulations as therapeutic alternatives.

ACKNOWLEDGEMENTS

REFERENCES

Adebiyi OE, Olayemi FO, Ning-Hua T, Guang-Zhi Z. 2017. *In vitro* antioxidant activity, total phenolic and flavonoid contents of ethanol extract of stem and leaf of *Grewia carpinifolia*. Beni-Seuf Univ J Appl. 6:10-14.

Andrade S, Ramalho MJ, Loureiro JA, Pereira M do C. 2019. Natural compounds for Alzheimer's Disease therapy: A systematic review of preclinical and clinical studies. Int J Mol Sci. 20:2313-2313.

Avram S, Bologa C, Flonta ML. 2005. Quantitative structure-activity relationship by CoMFA for cyclic urea and nonpeptide-cyclic cyanoguanidine derivatives on wild type and mutant HIV-1 protease. J Mol Model. 11:105-115.

Avram S, Mernea M, Bagci E, Hritcu L, Borcan LC, Mihailescu DF. 2017. Advanced structure-activity relationships applied to *Mentha spicata* L. *subsp. spicata* essential oil compounds as AChE and NMDA ligands, in comparison with donepezil, galantamine and memantine – new approach in brain disorders pharmacology. CNS Neurol Disord - Drug Targets. 16:800-811.

Azeez MA, Durodola FA, Lateef A, Yekeen TA, Adubi AO, Oladipo IC, Adebayo EA, Badmus JA, Abawulem AO. 2020. Green synthesized novel silver nanoparticles and their application as anticoagulant and thrombolytic agents: A perspective. IOP Conference Series: Materials Science and Engineering 805: 012043.

Badmus JA, Oyemomi SA, Fatoki JO, Yekeen TA, Adedosu OT, Adegbola PI, Azeez MA, Adebayo EA, Lateef A. 2022. Anti-haemolytic and cytogenotoxic potential of aqueous leaf extract of *Annona muricata* (L.) and its bio-fabricated silver nanoparticles. Caryologia. 75(1):3-13.

Bonciu E, Firbas P, Fontanetti CS, Wusheng J, Karaismailoğlu MC, Liu D, Menicucci F, Pesnya DS, Popescu A, Romanovsky AV, et al. 2018. An evaluation for the standardization of the *Allium cepa* test as cytotoxicity and genotoxicity assay. Caryologia. 71:191-209.

Boruah JS, Devi C, Hazarika U, Bhaskar Reddy PV, Chowdhury D, Barthakur M, Kalita P. 2021. Green synthesis of gold nanoparticles using an antiepileptic plant extract: *in vitro* biological and photo-catalytic activities. RSC Adv. 11:28029-28041.

Brindisi M, Bouzidi C, Frattaruolo L, Loizzo MR, Cappello MS, Dugay A, Deguin B, Lauria G, Cappello AR, Tundis R. 2021. New insights into the antioxidant and anti-Inflammatory effects of italian *Salvia officinalis* leaf and flower extracts in lipopolysaccharide and tumor-mediated inflammation models. ANTIGE. 10:311.

Caniova A, Brandsteterova E. 2001. HPLC Analysis of phenolic acids in *Melissa officinalis*. J Liq Chromatogr Relat Technol. 24:2647-2659.

Carlson C, Hussain SM, Schrand AM, Braydich-Stolle LK, Hess KL, Jones RL, Schlager JJ. 2008. Unique cellular interaction of silver nanoparticles: size-dependent generation of reactive oxygen species. J. Phys. Chem. A. 112:13608-13619.

Chakraborty R, Mukherjee AK, Mukherjee A. 2009. Evaluation of genotoxicity of coal fly ash in *Allium cepa* root cells by combining comet assay with the Allium test. Environ. Monit. Assess. 153:351-357.

Chen L, Ding L, Zhang H, Li J, Wang Y, Wang X, Qu C, Zhang H. 2006. Dynamic microwave-assisted extraction coupled with on-line spectrophotometeric determination of safflower yellow in *Flos Carthami*. Anal Chim Acta. 580:75-82.

Csakvari AC, Moisa C, Radu DG, Olariu LM, Lupitu AI, Panda AO, Pop G, Chambre D, Socoliuc V, Copolovici L, et al. 2021. Green synthesis, characterization, and antibacterial properties of silver nanoparticles obtained by using diverse varieties of *Cannabis sativa* leaf extracts. Molecules. 26(13):4041.

Das M, Shim KH, An SSA, Yi KD. 2011. Review on gold nanoparticles and their applications. Toxicol Environ Health Sci. 3:193-205.

Dent M, Bursać Kovačević D, Bosiljkov T, Dragović-Uzelac V. 2017. Polyphenolic composition and antioxidant capacity of indigenous wild dalmatian sage (*Salvia officinalis* L.). Croat Chem Acta. 90(3):451-459.

Dent M. 2015. Comparison of conventional and ultrasound-assisted extraction techniques on mass fraction of phenolic compounds from sage (*Salvia officinalis* L.). Chem Biochem Eng Q. 29:475-484.

Dragović-Uzelac V, Elez Garofulić I, Jukić M, Penić M, Dent M. 2012. The influence of microwave-assisted extraction on the isolation of sage (*Salvia officinalis* L.) polyphenols. Food Technol Biotechnol. 50:377-383.

Dzimitrowicz A, Jamróz P, diCenzo GC, Sergiel I, Kozlecki T, Pohl P. 2016. Preparation and characterization of gold nanoparticles prepared with aqueous extracts of *Lamiaceae* plants and the effect of follow-up treatment with atmospheric pressure glow microdischarge. Arab J Chem. 12:4118-4130.

Eugenio M, Campanati L, Müller N, Romão LF, de Souza J, Alves-Leon S, de Souza W, Sant'Anna C. 2018. Silver/silver chloride nanoparticles inhibit the proliferation of human glioblastoma cells. Cytotechnology. 70(6):1607-1618.

Farhat MB, Chaouch-Hamada R, Sotomayor JA, Landoulsi A, Jordán MJ. 2014. Antioxidant potential of *Salvia officinalis* L. residues as affected by the harvesting time. Ind Crops Prod. 54:78-85.

Fernandes TCC, Mazzeo DEC, Marin-Morales MA. 2007. Mechanism of micronuclei formation in polyploidizated cells of *Allium cepa* exposed to trifluralin herbicide. Pestic Biochem Phys. 88:252-259.

Francik S, Francik R, Sadowska U, Bystrowska B, Zawiślak A, Knapczyk A, Nzeyimana A. 2020. Identification of phenolic compounds and determination of antioxidant activity in etracts and infusions of Salvia leaves. Mater. 13:5811.

Garcia CS, Menti C, Lambert AP, Barcellos T, Moura S, Calloni C, Branco CS, Salvador M, Roesch-Ely M, Henriques JA. 2016. Pharmacological perspectives from Brazilian *Salvia officinalis* (*Lamiaceae*): antioxidant, and antitumor in mammalian cells. AABC. 88:281-292.

Ghorbani A, Esmaeilizadeh M. 2017. Pharmacological properties of *Salvia officinalis* and its components. J Tradit Complement Med. 7:433-440.

Gȋrd CE, Nencu I, Costea T, Duţu LE, Popescu ML, Ciupitu N. 2014. Quantitative analysis of phenolic compounds from *Salvia officinalis* L. leaves. Farmacia. 62:649-657.

Gomes NGM, Campos MG, Órfão JMC, Ribeiro CAF. 2009. Plants with neurobiological activity as potential targets for drug discovery. Prog Neuropsychopharmacol Biol Psychiatry. 33:1372-1389.

Grosso C, Valentão P, Ferreres F, Andrade PB. 2015. Alternative and efficient extraction methods for marine-derived compounds. Mar Drugs. 13:3182-3230.

Haliem AS. 1990. Cytological effect of the herbicide sencorer on mitosis of *A. cepa*. Egypt. J. Bot. 33:93-104.

Hamrouni-Sellami I, Rebey IB, Sriti J, Rahali FZ, Limam F, Marzouk B. 2012. Drying sage (*Salvia officinalis* L.) plants and its effects on content, chemical composition, and radical scavenging activity of the essential oil. Food Bioproc Tech. 5:2978-2989.

Hayat K, Hussain S, Abbas S, Farooq U, Ding B, Xia S, Jia C, Zhang X, Xia W. 2009. Optimized microwave-assisted extraction of phenolic acids from citrus mandarin peels and evaluation of antioxidant activity *in vitro*. Sep Purif Technol. 70:63-70.

Hernández Y, Lobo MG, González M. 2009. Factors affecting sample extraction in the liquid chromatographic determination of organic acids in papaya and pineapple. Food Chem. 114:734–741.

Hsin YH, Chen CF, Huang S, Shih TS, Lai PS, Chueh PJ. 2008. The apoptotic effect of nanosilver is mediated by a ROS- and JNK-dependent mechanism involving the mitochondrial pathway in NIH3T3 cells. Toxicol. Lett. 179:130-139.

Hu W, Chen S, Li X, Shi S, Shen W, Zhang X, Wang H. 2009. In situ synthesis of silver chloride nanoparticles

into bacterial cellulose membranes. Mater. Sci. Eng. C. 29(4):1216-1219.

Jaimez Ordaz J, Martínez Hernández J, Ramírez Godínez J, Castañeda Ovando A, González Olivares LG, Contreras López E. 2018. Bioactive compounds in aqueous extracts of lemon balm (*Melissa officinalis*) cultivated in Mexico. Arch Latinoam Nutr. 68:268-279.

Kim S, Yun EJ, Bak JS, Lee H, Lee SJ, Kim CT, Lee JH, Kim KH. 2010. Response surface optimised extraction and chromatographic purification of rosmarinic acid from *Melissa officinalis* leaves. Food Chem. 121:521-526.

Kintzios SE. 2000. Sage: The Genus Salvia. In: Kintzios SE, editor. Botany. Amsterdam: CRC Press, p. 10-11.

Kirsner R, Orsted H, Wright B. 2001. Matrix metalloproteinases in normal and impaired wound healing: a potential role of nanocrystalline silver. Wounds. 13:5-10.

Kumari A, Yadav SK, Yadav SC. 2010. Biodegradable polymeric nanoparticles based drug delivery systems. Colloids Surf B. 75:1-18.

Liman R, Akyil D, Eren Y, Konuk M. 2010. Testing of the mutagenicity and genotoxicity of metolcarb by using both Ames/Salmonella and Allium test. Chemosphere. 80(9):1056-1061.

Lin SR, Chang CH, Hsu CF, Tsai MJ, Cheng H, Leong MK, Sung PJ, Chen JC, Weng CF. 2019. Natural compounds as potential adjuvants to cancer therapy: preclinical evidence. Br J Pharmacol. 177:1409-1423.

Longaray Delamare AP, Moschen-Pistorello IT, Artico L, AttiSerafini L, Echeverrigaray S. 2007. Antibacterial activity of the essential oils of *Salvia officinalis* L. and *Salvia triloba* L. cultivated in South Brazil. Food Chem. 100:603–608.

Manolescu DŞ, Uţă G, Din A, Avram S. 2022. The particle size influence of *Melissa officinalis* L. powder on TEAC and TPC correlated with the *in silico* study of one of the antioxidants: caffeic acid. Rom J Biophys. 32:1-16.

Mocellin S, Nitti D. 2008 TNF and cancer: the two sides of the coin. Front Biosci. 13:2774-2783.

Naikoo GA, Mustaqeem M, Hassan IU, Awan T, Arshad F, Salim H, Qurashi A. 2021. Bioinspired and green synthesis of nanoparticles from plant extracts with antiviral and antimicrobial properties: A critical review. J. Saudi Chem. Soc. 25(9): 101304.

Nayeri FD, Mafakheri S, Mirhosseini M, Sayyed R. 2021. Phyto-mediated silver nanoparticles via *Melissa officinalis* aqueous and methanolic extracts: synthesis, characterization and biological properties against infectious bacterial strains. Int. J. Adv. Biol. Biomed. Res. 9(3):270-285.

Onwuamah CK, Ekama SO, Audu RA, Ezechi OC, Poirier MC, Odeigah PGC. 2014. Exposure of *Allium cepa* root cells to zidovudine or nevirapine induces cytogenotoxic changes. PLoS ONE. 9:e90296.

Osmić S, Begić S, Mićić V, Petrović Z, Avdić G. 2019. Effect of solvent and extraction conditions on antioxidative activityof sage (*Salvia officinalis* L.) extracts obtained by maceration. Technologica Acta. 11:1-8.

Pandey R, Zahoor A, Sharma S, Khuller GK. 2003. Nanoparticle encapsulated antitubercular drugs as a potential oral drug delivery system against murine tuberculosis. Tuberculosis (Edinb). 83:373-378.

Papoti V, Totomis N, Atmatzidou A, Zinoviadou K, Androulaki A, Petridis D, Ritzoulis C. 2019. Phytochemical content of *Melissa officinalis* L. herbal preparations appropriate for consumption. Processes. 7:8-88.

Paré JRJ, Sigouin M, Lapointe J. 1991. Microwave-assisted natural product extraction. US Patent 5 002:784.

Parveen S, Misra R, Sahoo SK. 2012. Nanoparticles: a boon to drug delivery, therapeutics, diagnostics and imaging. Nanomed: Nanotechnol Biol Med. 8:147-166.

Petkova N, Ivanov I, Mihaylova D, Krastanov A. 2017. Phenolic acids content and antioxidant capacity of commercially available *Melissa officinalis* L. teas in Bulgaria. Bulg Chem Commun. 49:69-74.

Phuyal N, Jha PK, Raturi PP, Rajbhandary S. 2020. Total phenolic, flavonoid contents, and antioxidant activities of fruit, seed, and bark extracts of *Zanthoxylum armatum* DC. Sci World J .16:1-7.

Pop AV, Tofană M, Socaci SA, Vârban D, Nagy M, Borş MD, Sfechiş S. 2015. Evaluation of antioxidant activity and phenolic content in different *Salvia officinalis* L. extract. Bulletin UASVM Food Science and Technology. 72:210-214.

Proestos C, Chorianopoulos N, Nychas GJE, Komaitis M. 2005. RP-HPLC analysis of the phenolic compounds of plant extracts. Investigation of their antioxidant capacity and antimicrobial activity. J Agric Food Chem. 53:1190-1195.

Roby MHH, Sarhan MA, Selim KAH, Khalel KI. 2013. Evaluation of antioxidant activity, total phenols and phenolic compounds in thyme (*Thymus vulgaris* L.), sage (*Salvia officinalis* L.), and marjoram (*Origanum majorana* L.) extracts. Ind Crops Prod. 43:827-831.

Sasidharan S, Chen Y, Saravanan D, Sundram KM, Latha YL. 2011. Extraction, isolation and characterization of bioactive compounds from plants' extracts. Afr J Tradit Complement Altern Med. 8:1-10.

Shakeri A, Sahebkar A, Javadi B. 2016. *Melissa officinalis* L. – A review of its traditional uses, phytochemistry and pharmacology. J Ethnopharmacol. 188:204-228.

Shelembe B, Mahlangeni N, Moodley R. 2022. Biosynthesis and bioactivities of metal nanoparticles mediated by *Helichrysum aureonitens*. J Anal Sci Technol. 13:8.

Sherman D. 2014. Preparation of formvar film-coated grids, DS Imaging, LLC. https://www.emsdiasum.com/microscopy/technical/techtips/formvar_film-coated_grids.aspx. [Accessed 10 January 2022].

Shields JP. 1999. Using a formvar-coated bridge to apply formvar support film to TEM grids. MTO. 7:18-19.

Shimamura T, Sumikura Y, Yamazaki T, Tada A, Kashiwagi T, Ishikawa H, Matsui T, Sugimoto N, Akiyama H, Ukeda H. 2014. Applicability of the DPPH assay for evaluating the antioxidant capacity of food additives – inter-laboratory evaluation study. Anal Sci. 30:717-721.

Siakavella IK, Lamari F, Papoulis D, Orkoula M, Gkolfi P, Lykouras M, Avgoustakis K, Hatziantoniou S. 2020. Effect of plant extracts on the characteristics of silver nanoparticles for topical application. Pharmaceutics. 12(12):1244.

Šulniūtė V, Ragažinskienė O, Venskutonis PR. 2016. Comprehensive evaluation of antioxidant potential of 10 Salvia species using high pressure methods for the isolation of lipophilic and hydrophilic plant fractions. Plant Foods Hum Nutr. 71:64-71.

Sun C, Lee JSH, Zhang M. 2008. Magnetic nanoparticles in MR imaging and drug delivery. Adv Drug Deliv Rev. 60:1252-1265.

Sutan NA, Manolescu DS, Fierascu I, Neblea AM, Sutan C, Ducu C, Soare LC, Negrea D, Avramescu SM, Fierascu RC. 2018. Phytosynthesis of gold and silver nanoparticles enhance *in vitro* antioxidant and mito-stimulatory activity of *Aconitum toxicum* Reichenb. Rhizomes alcoholic extracts. Mater. Sci. Eng. C. 93:746–758.

Sutan NA, Vilcoci DŞ, Fierascu I, Neblea AM, Sutan C, Ducu C, Soare LC, Negrea D, Avramescu SM, Fierascu RC. 2019. Influence of the phytosynthesis of noble metal nanoparticles on the cytotoxic and genotoxic effects of *Aconitum toxicum* Reichenb. leaves alcoholic extract. J Clust Sci. 30:647-660.

Swilam N, Nematallah KA. 2020. Polyphenols profile of pomegranate leaves and their role in green synthesis of silver nanoparticles. Sci Rep. 10:14851.

Tedesco SB, Laughinghouse HD. 2012. Bioindicator of genotoxicity: the *Allium cepa* test. In: Srivastava JK, editor. Environmental Contamination. Rijeka: InTech Publisher; p. 137-156.

Teimouri M, Khosravinejad F, Attar F, Saboury AA, Kostova I, Benelli G, Falahati M. 2018. Gold nanoparticles fabrication by plant extracts: synthesis, characterization, degradation of 4-nitrophenol from industrial wastewater, and insecticidal activity – A review. J. Clean. Prod. S0959652618306000.

Tripathy A, Chandrasekran N, Raichur AM, Mukherjee A. 2008. Antibacterial applications of silver nanoparticles synthesized by aqueous extract of *Azadirachta indica* (Neem) leaves. J Biomed Nanotechnol. 4:1-6.

Udrea AM, Puia A, Shaposhnikov S, Avram S. 2018. Computational approaches of new perspectives in the treatment of depression during pregnancy. Farmacia. 66:680-687.

Uţă G, Manolescu DŞ, Avram S. 2021. Therapeutic properties of several chemical compounds of *Salvia officinalis* L. in Alzheimer's Disease. Mini Rev Med Chem. 21:1421-1430.

Velamuri R, Sharma Y, Fagan J, Schaefer J. 2020. Application of UHPLC-ESI-QTOF-MS in phytochemical profiling of sage (*Salvia officinalis*) and rosemary (*Rosmarinus officinalis*). Planta Med. 7:133-144.

Veličković DT, Karabegović IT, Stojičević SS, Lazić ML, Marinković VD, Veljković VD. 2011. Comparison of antioxidant and antimicrobial activities of extracts obtained from *Salvia glutinosa* L. and *Salvia officinalis* L. Hem Ind. 65:599-605.

Wang L, Weller CL. 2006. Recent advances in extraction of nutraceuticals from plants. Trends Food Sci Technol. 17:300-312.

Yilmaz Öztürk B,2019. Intracellular and extracellular green synthesis of silver nanoparticles using *Desmodesmus* sp.: their Antibacterial and antifungal effects. Caryologia. 72(1): 29-43.

Zeković Z, Pintać D, Majkić T, Vidović S, Mimica-Dukić N, Teslić N, Pavlić B. 2017. Utilization of sage by-products as raw material for antioxidants recovery—Ultrasound versus microwave-assisted extraction. Ind Crops Prod. 99:49-59.

Zhang QW, Lin LG, Ye WC. 2018. Techniques for extraction and isolation of natural products: a comprehensive review. Chin. Med. 13:20.

Žlabur JŠ, Voća S, Dobričević N, Pliestić S, Galić A, Boričević A, Borić N. 2016. Ultrasound-assisted extraction of bioactive compounds from lemon balm and peppermint leaves. Int Agrophys. 30:95-104.

Polyploid cytotypes and formation of unreduced male gametes in wild and cultivated fennel (*Foeniculum vulgare* Mill.)

Egizia Falistocco

Department of Agricultural, Food and Environmental Sciences, University of Perugia, Perugia, Italy
Email: egizia.falistocco@unipg.it

Abstract. *Foeniculum vulgare* Mill. (2n=22) is an herbaceous species native to the Mediterranean region and naturalized in many temperate areas around the world. It includes subsp. *piperitum* and subsp. *vulgare* which are, respectively, the wild and cultivated forms. Fennel is of economic importance both as a vegetable crop and for its wide use in the food and pharmaceutical industries. In recent years, the therapeutic and pharmacological potential of this species has been widely analyzed, its cytogenetic traits have aroused less interest. Therefore, the intention of this study was to reduce this gap by investigating some aspects, such as the variations in its chromosome number and the occurrence of polyploidization events, so far neglected. By means of extensive chromosome counting, the presence of tetraploid cytotypes has been discovered both in the wild and cultivated fennel. Moreover, the analysis of pollen and PMCs at the tetrad stage provided evidence for spontaneous sexual polyploidization as the most probable origin of the tetraploid cytotypes discovered. The results of this study provide the first evidence of the occurrence of polyploidization events in *F. vulgare* and suggest that the use of 2*n* gametes could be a useful approach to genetic improvement of this crop.

Keywords: *Foeniculum vulgare* Mill., fennel, polyploid cytotypes, polyploidization, unreduced gametes.

INTRODUCTION

Foeniculum vulgare Mill., of the Apiaceae (syn. Umbelliferae) family, is a biennial-perennial herb native to the Southern Mediterranean region from where it was brought for cultivation throughout the temperate regions of Asia, North America and Europe. Fennel is described as a diploid species (2n=22) characterized by erect, cylindrical, bright green and smooth stems growing up to 2 m in height. Its leaves are finely dissected with terminal filiform segments. Its bright yellow flowers are contained in terminal compound umbels with a variable number of rays (Subramanian 1986; Badgujar 2014).

Two subspecies of *F. vulgare* are generally recognized: subsp. *piperitum* and subsp. *vulgare* which represent the wild and cultivated forms, respec-

tively. The wild fennel (subsp. *piperitum*) is abundantly present in the Mediterranean flora and commonly found in limey soil near the sea and on river banks. Subsp. *vulgare* includes var. *azoricum* which is cultivated as a vegetable for its enlarged leaf base and var. *dulce* which is grown prevalently for its seeds containing essential oil (Pignatti 1982).

F. vulgare is commonly called fennel and it is denoted locally by more than 100 vernacular names. It is a traditional and popular species with a long history having been appreciated and utilized as a medicinal, aromatic and edible plant at least since Roman times up to the present day. In some countries, for example, fennel is currently used to stimulate lactation and to improve the taste of some medicines, while the seeds are widely used as a spice (Simon et al. 1984; Sheidai et al. 2007; Faudale et al. 2008; Badgujar et al. 2014; Rather et al. 2012).

F. vulgare is at present a species of considerable economic interest not only for its wide diffusion as a vegetable crop but also for its pharmaceutical properties which, in recent years, have been re-evaluated and extensively investigated. The species possesses antioxidant, antispasmodic, carminative, diuretic and laxative properties and is useful in the treatment of numerous infectious disorders of bacterial, fungal, viral and protozoal origin (Agarwal et al. 2017). Fennel is also widely used in the food industry as a flavor additive to meats, salad dressing, breads, pastries, teas and alcoholic beverages (Badgujar et al. 2014).

Despite its economic importance and wide diffusion in the wild, only limited attention has been dedicated to it by cytologists mainly interested in its karyological aspects (Garde and Garde 1949; Das and Mallick 1988; Lentini et al. 1988; Paul and Datta 2003¸ Subramanian 1986; Jovine et al. 2008; Ozkan et al. 2017). Most of these studies were carried out on only few samples. Extensive cytogenetic investigations have been to date very limited. The purpose of this study was to expand the study of *F. vulgare* and explore areas of cytogenetics so far overlooked, such as the existence of chromosome variants and events of polyploidization. To realize this, investigations on wild and cultivated populations of *F. vulgare* were carried out by attempting, as first step, an extensive chromosome count. Then, because tetraploid cytotypes were identified during this survey, the successive objective was to clarify the contribution of 2n gametes to the origin of the polyploid plants discovered. For this purpose the size of pollen grains and the constitution of sporads were analyzed to verify the occurrence of unreduced gametes and to estimate the frequency of their formation. It has been widely demonstrated that pollen grains and PMCs (Pollen Mother Cells) at the tetrad stage provide essential data on the tendency of plants to produce 2n male gametes and offer information on the origin of polyploids (Orjeda et al., 1990; Ramsey and Schemske 1998; Garcia et al. 2020). Large pollen is normally 2n pollen because there is a positive correlation between DNA content and cell volume, which in turn influences the size of the pollen grain. Thus, 2n pollen grains are larger than reduced grains. On the other hand, microsporogenesis offers irrefutable indications of the occurrence of 2n gametes because the presence of dyads and triads in the sporad stage constitutes strong evidence for the formation of unreduced pollen (Garcia et al. 2020). This study is the first to document the occurrence of polyploidization events in *F. vulgare*. It also provides data supporting sexual polyploidization as the possible origin of the polyploid cytotypes discovered.

MATERIALS AND METHODS

Plant material

Seeds and plants of *F. vulgare* subsp. *piperitum* and subsp. *vulgare* were used for this study.

Seeds of wild fennel (subsp. *piperitum*) were collected by the author in two different localities of Italy: the countryside surrounding the Trasimeno Lake in Central Italy (population1), and the North-East coast of Sardinia (population 2). Seeds of the cultivated varieties *azoricum* and *dulce* (subsp. *vulgare*) were provided by specialized nurseries (Table 1).

The seeds were germinated at 20-22 °C in Petri dishes on filter paper moistened with distilled water. A part of the seedlings was transplanted to obtain plants for the production of flowers and roots. A total of 400 seeds and 10 plants for each accession were checked for their chromosome numbers. The same plants were also used for the analysis of microsporogenesis and pollen size.

Chromosome counts

Roots 5-10 mm long were collected from seedlings and adult plants and immersed in ice-cold water for about 16 h to accumulate metaphases. Then they were pre-treated in a 1‰ aqueous solution of a stock solution consisting of 1 ml of a-bromonaphthalene dissolved in 100 ml of absolute ethanol (Linde-Laursen 1978) for 3 h, fixed in ethanol-glacial acetic acid (3:1) at room temperature overnight and then stored at -20 °C until required. Mitotic chromosome preparations were realized according to the protocol described in detail in Falistocco (2018).

Table 1. List of accessions of *F. vulgare* subspp. *piperitum* and *vulgare* examined and number of tetraploid (2n=44) plants discovered.

Subspecies	Accessions	Origin	n. of tetraploid (2n=44) plants
piperitum	population 1	Central Italy	3
	population 2	Sardinia	4
vulgare	cv. *azoricum*	commercial source	5
	cv. *dulce*	commercial source	7

The excised roots were washed in distilled water for 10 min and transferred to the enzyme buffer (10mM citric acid/sodium citrate, pH 4.6) for 20 min. Root tips were then excised and digested in the enzyme solution (4% cellulase Onozuka R10 and 1% pectolyase Sigma-Aldrich in distilled water) for 45-60 min at 37°C. The cell suspension was pelleted and resuspended in enzyme buffer. After pelleting, the material was washed twice with the fixative and resuspended in the fixative. Finally, 20-30 ml of cell suspension was applied to a slide. The slides were air-dried and stained with 2mg/ml DAPI (4', 6-diamidino-2-phenylindole) for the determination of the chromosome numbers.

Detection of unreduced male gametes

Pollen analysis

Pollen from five flowers per plant was spread over five slides and stained with a solution of acetocarmine and glycerol (1:1). The dark colored and regular shaped pollen grains were considered as viable. The pollen size was determined by measuring the major diameter of the grains by using an ocular micrometer. Measurements revealed two types of pollen grains which can be considered normal pollen and large pollen. The size of the normal pollen was determined by measuring the grains present in three light vision fields of the microscope for each slide. About 600 grains for each plant were measured. All large pollen grains present in the slides were measured.

Analysis of PMCs at the tetrad stage

Inflorescences were collected and immersed in the fixative ethanol-glacial acetic acid (3:1) for 24 hours and then they were transferred to 70% ethanol and stored at 4°C until analysis. For cytological preparations anthers of a single flower were squashed on a glass slide with some drops of 0.5% acetocarmine (Merk Life Science, Italy), intensified by ferric oxide. In order to select only

anthers containing PMCs at the tetrad stage, preliminary observations were made to assess the meiotic stage of the flowers. One single anther was removed from the floral bud, squashed on a slide as described above and examined. When the anther contained sporads the other anthers of the same flower were used for cytological preparations. Five flowers per plant were analyzed. The number of dyads, triads and tetrads detected in four light vision fields for each slide were counted. About 1500 sporads for each plant were examined. Estimation of the theoretical frequency of 2n pollen grains was made from the number of observed dyads, triads, and tetrads at the end of microsporogenesis. Considering that a dyad evolves into two unreduced pollen grains, a triad produces one unreduced pollen grain and two reduced pollen grains, and each tetrad gives origin to four reduced pollen grains, the frequency of 2n pollen grains was calculated by applying the equation F2n (%) = (2xDy + Tr) / (2xDy+ 3x Tr + 4x Te) x 100, for which Dy, Tr and Te, are the number of dyads, triads and tetrads, respectively (Kumar and Singhal 2012).

Chromosome preparations and slides containing pollen and sporads were observed under UV and light illumination, respectively, with a Microphot Nikon microscope. Images were recorded with a digital photocamera SONY ICX282AQ and then processed using Adobe Photoshop 5.0.

RESULTS

Chromosome counts

All plants examined resulted diploid having the chromosome number 2n=22 (Figure 1a), but polyploid seedlings were detected in each accession of subspp. *piperitum* and *vulgare* (Figure 1b). Three seeds from population 1 (Central Italy) and four seeds from population 2 (Sardinia) were found to be tetraploid with 2n=2x=44 (Figure 1b). The frequency of tetraploids discovered in cultivated fennel was greater: five in the cv. *azoricum* and seven in the cv. *dulce* (Table 1). The tetraploid condition was always clearly distinguishable in all metaphases analyzed. No other ploidy levels were detected.

Estimation of the occurrence of unreduced male gametes

To detect the formation of unreduced male gametes pollen size was measured and the constitution of the sporads analyzed.

Full pollen viability was generally observed, with very sporadic cases of shriveled and unstained grains present.
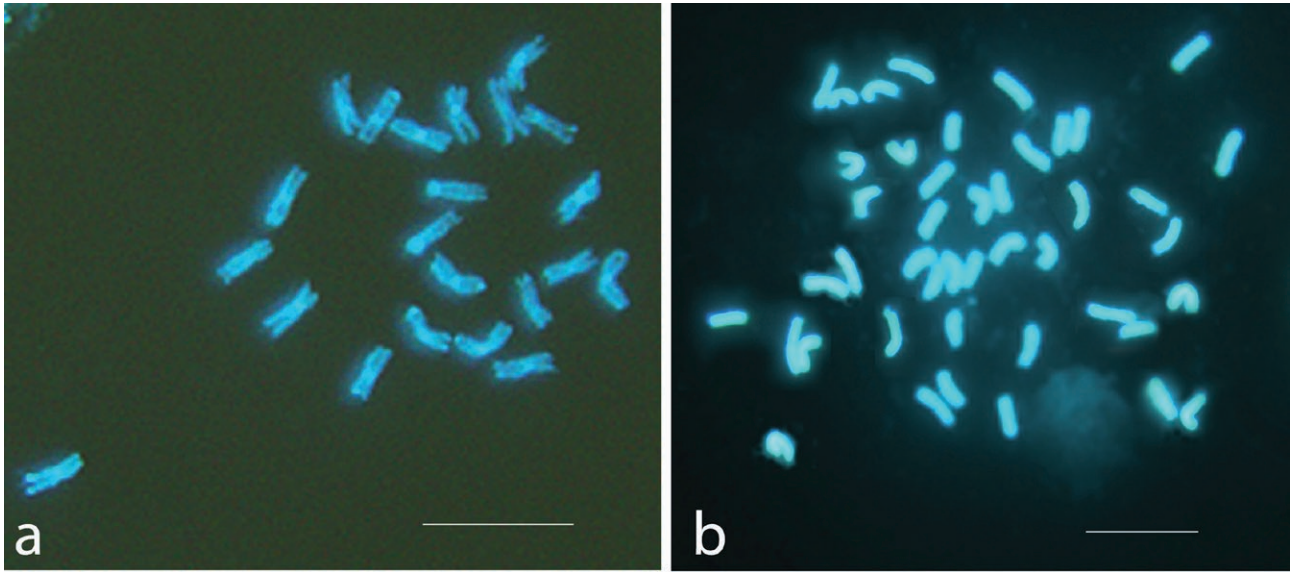
Figure 1. Mitotic metaphases of *F. vulgare*. Chromosome complements of diploid (a) and tetraploid (b) cytotypes. The bar represents 5μm.

Figure 2. Example of pollen grains and PMCs at the sporad stage observed in plants producing large pollen. Pollen sample showing normal and large pollen grains (a); group of 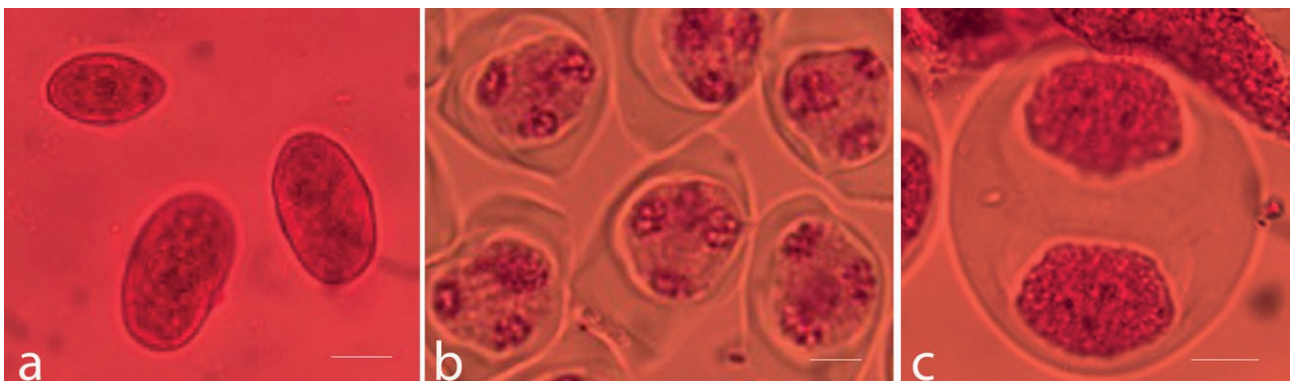tetrads with four *n* (reduced) microspores (b); dyad containing two 2*n* (unreduced) microspores (c). The bar represents 10 μm.

Most of plants examined produced pollen of uniform size, but few plants produced also noticeably larger grains (Figure 2a). Diameter measurements confirmed the results of visual observation. According to their size, pollen grains were categorized as *n*, that is normal reduced pollen, with its diameter ranging from 33.0 to 35.0 μm; and 2*n*, unreduced pollen, measuring from 42.0 to 44.0 μm. Large pollen was identified as unreduced 2n pollen according to Darlington (1937) who defines as 2n pollen the grains with a size 1,25x larger than the average size of normal pollen. Pollen grains of intermediate size were not observed. Large pollen grains were detected in two plants of population 1, three plants of population 2, one plant of cv. *azoricum* and three plants of cv. *dulce* (Table

2). The sporad constitution was analyzed to confirm that large pollen grains effectively represent 2*n* pollen production. This analysis revealed, in addition to the expected normal tetrads, the presence of dyads in all plants producing large pollen grains (Figure 2b,c). The frequency of dyads produced was 2.26 and 4.0% in plants of population 1; 2.44, 3.0 and 4.0% in plants of population 2; 5.0% in the plant of var. *azoricum*; and 5.00, 7.00 and 8.00% in plants of var. *dulce* (Table 2). Dyads or triads were not observed in the remaining plants examined. Additionally, abnormal tetrads (that is containing microspores of different sizes, collapsed or with micronuclei) or polyads were not found in any of the plants object of this analysis. By the rule that each tetrad can form four *n* micro-

Table 2. Frequencies of dyads and 2n pollen recorded in plants of of subspp. *piperitum* and *vulgare* producing large pollen.

Subspecies	Accessions	Plants * producing large pollen	Dyad %	2n pollen %
piperitum	population 1	3	2.26	1.14
		7	4.00	2.00
	population 2	1	2.44	1.23
		4	3.00	1.50
		9	4.00	2.00
vulgare	cv. *azoricum*	2	5.00	2.50
	cv.*dulce*	3	5.00	2.50
		5	7.00	3.60
		7	8.00	4.10

*Plants examined were numbered from 1 to 10.

spores and each dyad can form two 2n microspores, the frequency of 2n pollen grains could be estimated for each plant according to the abovementioned formula. The results are reported in Table 2.

DISCUSSION

The discovery of tetraploid cytotypes deriving from this study provided the first evidence of polyploidy in *F. vulgare*. Furthermore, the pollen and sporad analyzed indicate spontaneous sexual polyploidization as the most probable origin of such cytotypes. Various methods exist to reveal the formation of 2n pollen and one of these is based on the size of the pollen grains. Due to the relatively close correlation between large pollen and the 2n status, the presence of large pollen has been frequently used as an indicator for 2n pollen (Ghaffari 2006; Kumar and Singhal 2012). The analysis of pollen size carried out during this study revealed two types of pollen grains which according to the criterion of Darlington (1937) were classified as n (normal reduced) and 2n (unreduced) pollen. Further evidence that large pollen effectively indicates unreduced pollen formation was provided by the sporad analysis demonstrating that fennel plants producing dyads also produce large pollen grains. The large 2n pollen grains examined were well filled, stained, and apparently fertile; therefore, it is very possible that fertilization by these 2n gametes led to the formation of polyploid cytotypes. The tetraploid constitution of these cytotypes suggests that in fennel unreduced 2n gametes are generated also during the macrosporogenesis process.

The formation of 2n pollen grains in *F. vulgare* has been previously observed in natural populations from Iran (Sheidai et al. 2007); but they have never been sought in cultivated fennel. The production of 2n gametes in plants is a common phenomenon which may result from a variety of different meiotic irregularities (Dewitte et al. 2012). The microsporogenesis analysis carried out during this study was focused on meiocytes at the tetrad stage, so that the meiotic events occurring in the phases preceding the tetrad stage still remain unknown. Therefore, no definitive conclusion on the meiotic aberrations responsible for the formation of 2n pollen is possible. The absence of abnormal sporads and the irrelevant number of non viable pollen grains observed would exclude the occurrence of meiotic abnormalities affecting chromosome segregation with the consequent formation of aneuploid gametes. Rather, the regularity of microspores would suggest that the origin of unreduced pollen is principally due to the meiotic events connected to a process of nuclear restitution during the first or second division.

Another interesting point is the higher incidence of tetraploids detected in the cultivars with respect to wild populations. The greater tendency of cultivated plants to produce unreduced gametes could be connected to this phenomenon. However, it may be assumed that the tetraploid condition generates characteristics in plants favoring their selection during the breeding activities.

Clarification of this and the other hypotheses inherent in this study will come from further investigations. The fact that tetraploid plants were found in all accessions examined suggests that polyploidy in *F. vulgare* is a rather widespread phenomenon and not a sporadic event. The demonstrated characteristic of fennel plants to produce 2n gametes should be exploited to generate polyploid genotypes. The induction of polyploidy could be a useful method for improving specific traits in crop varieties, such as quality, yield and environmental adaptation. In fennel, this practice has been attempted by colchicine treatments but with scarce results (Solanki et al. 2017). Polyploid plants obtained by sexual polyploidization may turn out to be a promising approach to breeding programs of this species.

FUNDING

REFERENCES

Agarwal D, Sharma LK, Saxena SN. 2017. Anti-microbial properties of fennel *(Foeniculum vulgare* Mill.) seed

extract. *J Pharmacogn Phytochem*. 2017; 6(4): 479-482. www.phytojournal.com.

Badgujar SB, Patel VV, AH Bandivdekar, 2014. *Foeniculum vulgare* Mill: A Review of Its Botany, Phytochemistry, Pharmacology, Contemporary Application, and Toxicology. Hindawi Publishing Corporation *BioMed Research International*. Article ID 842674, Vol. 14. https://doi.org/10.1155/2014/842674.

Darlington, C. D. (1937). Recent advances in cytology (2nd ed.). London: J. and A. Churchill.

Das AB, Mallick R. 1989. Variation in karyotype and nuclear DNA content in different varieties of *Foeniculum vulgare* Mill. *Cytologia*. 54: 129-134. DOI: 10.1508/cytologia.54.129.

Dewitte A, Eeckhaut T, Huylenbroeck JV, Bockstaele EV. 2010. Meiotic aberrations during 2n pollen formation in *Begonia*. *Heredity*. 104: 215–223. https://doi.org/10.1038/hdy.2009.111.

Falistocco E. 2018. Cytogenetics and chromosome number evolution of annual *Medicago* species (Fabaceae) with emphasis on the origin of the polyploid *Medicago rugosa* and *M. scutellata*. *Plant Biosyst*. 153, 1-7. DOI: 10.1080/11263504.2018.1462864.

Faudale M, Viladomat F, Bastida J, Poli F, Codina C. 2008. Antioxidant activity and phenolic composition of wild, edible, and medicinal fennel from different Mediterranean countries. *J. Agric. Food Chem*. 56 (6): 1912–1920. DOI: 10.1021/jf073083c.

García AV, Ortiz AM, Silvestri MC, Custodio AR, Moretzsohn MC, Lavia GI. 2020. Occurrence of 2n microspore production in diploid interspecific hybrids between the wild parental species of peanut (Arachis hypogaea L., Leguminosae) and its relevance in the genetic origin of the cultigen. Crop Sci. 60: 2420–2436. DOI: 10.1002/csc2.20233..

Garde A, Garde N. 1949. Contribuisao para o estudo cariologico da familia Umbelliferae I. *Agron. Lusit*. 11: 91-140.

Ghaffari, S.M. and Tajik, F. (2007). Chromosome counts of some angiosperm species from Iran (III). *Rostaniha*, 8(2): 74-83.

Jovine M, Grzebelus E, Carputo D, Jiang J, Simon PW. 2008. Major cytogenetic landmarks and karyotype analysis in *Daucus carota* and other Apiaceae. *Am. J. Bot*. 95 (7): 793-804. DOI: 10.3732/ajb.0700007.

Kumar P, Singhal VK. 2012. Erratic male meiosis resulting in 2*n* pollen grain formation in a 4x cytotype (2*n* = 28) of *Ranunculus laetus* Wall. ex Royle. *Sci. World J*. Vol. 12 article ID 691545. DOI:10.1100/2012/691545.

Lentini F, Romano S, Raimondo FM. 1988. Numeri cromosomici per la flora Italiana: 1185-1196. *Informatore Botanico Italiano*. 20: 637-646.

Linde-Laursen I. 1978. Giemsa C-banding of the chromosomes of 'Emir' barley. *Hereditas*. 81(2): 285-289. doi:10.1111/j.1601-5223.1978.tb01603.x.

Orjeda G, Freyre R, Iwanaga M. 1990. Production of 2n pollen in diploid *Ipomoea trifida*, a putative wild ancestor of sweet potato. *J. Hered*. 81: 462–467. doi.org/10.1093/oxfordjournals.jhered.a111026.

Ozkan U, Benlioglu B, Ozgen Y. 2017. Karyotype analysis of fennel (*Foeniculum vulgare* Mill.) from Ankara province. *Res. J. Agric. Sci*. E-ISSN: 1308-027X, 10(2): 01-03.

Paul R, Datta AK. 2003. Chromosomal studies in four seed spices of Umbelliferae. *Indian J Genet Plant Breed*. 63(4): 361- 362.

Pignatti S. 1982. *Flora d'Italia*. Edagricole Bologna.

Ramsey, J., Schemske, D. W. (1998). Pathways, mechanisms, and rates of polyploid formation in flowering plants. *Annu. Rev. Ecol. Evol. Syst*. 29: 467–501. https://doi.org/10.1146/annurev.ecolsys.29.1.467.

Rather MA, Dar BA, Sofi SN, Bhat BA, Qurishi MA. 2012. *Foeniculum vulgare*: a comprehensive review of its traditional use, phytochemistry, pharmacology, and safety. *Arab. J. Chem*. 9: 1514-1583. https://doi.org/10.1016/j.arabjc.2012.04.011.

Sheidai M, Kalhor-Home N, Poorneydanei A, 2007. Cytogenetic study of some populations of *Foeniculum vulgare* (Umbelliferae). *Caryologia* 60 (3): 257-261. https://doi.org/10.1080/00087114.2007.10797945.

Simon JE, Chadwick AF, Craker LE. 1984. *Herbs: An Indexed Bibliography*. 1971-1980. The Scientific Literature on Selected Herbs, and Aromatic and Medicinal Plants of the Temperate Zone. Archon Books. Hamden, CT. https://wellcomecollection.org/works/kat5wpf8.

Solanki RK, Verma P, Meena RS, Meena NK, Singh B. 2017. FENNEL. In: *Breeding of Horticultural Crops* Vol. 1 -Part A: *Spices* (2017): 409-424. Editors: Parthasarathy VA, Aswath C, Nirmal Babu K & Senthil Kumar R Today & Tomorrow's Printes and Publishers, New Delhi - 110 002, India.

Subramanian D. 1986. Cytotaxonomical studies in South Indian Apiaceae. *Cytologia* 51: 479-488.

ORCID
SS: 0000-0001-5448-7617

Methomyl has clastogenic and aneugenic effects and alters the mitotic kinetics in *Pisum sativum* L.

Sazada Siddiqui*, Sulaiman A. Alrumman

Department of Biology, College of Science, King Khalid University, Abha 61413, Saudi Arabia
*Corresponding author. E-mail: sasdeky@kku.edu.sa; kalasaz@yahoo.co.in

Abstract. Methomyl is a carbamate pesticide that is frequently applied to crops all over the world. This research aims to evaluate the *Pisum sativum* L mitotic process and potential genotoxicity. The Cell Proliferation Kinetics (CPK) frequencies demonstrated changes in kinetics of mitotic process, and study of Mitotic Index (MI) demonstrated that methomyl had cytotoxic properties. In fact, the telophases ratio dropped at 0.1% to 0.5% methomyl treatment, while there was an increase in prophases, metaphases, and anaphases from 0.1% to 0.5% in a dose dependent manner. In terms of genotoxicity, methomyl cause an increase in the frequency of clastogenic and aneugenic chromosomal abnormalities at metaphase-anaphase at 0.1% to 0.5%. The effects on the mitotic spindle were further confirmed by an increase in the frequencies of c-mitosis from 0.1 to 0.5% methomyl treatment. The outcome of the current analysis indicates that regularly used insecticides methomyl has a considerable cytotoxic effect on mitotic cells of *Pisum sativum* L.

Keywords: methomyl, mitotic index, clastogenic, aneugenic, C- mitosis *Pisum sativum* L.

INTRODUCTION

In public areas, agricultural lands and gardens, pesticides are extensively used to eradicate weeds, undesirable pests, and diseases transmitted by vectors. Nevertheless, the prolonged usage of pesticides may leave behind toxic remains that, through surface drains, spray drift, runoff, spray leftovers, and leaching may pollute nearby surface water and ground natural water bodies (Mojiri et al. 2020; Chandra et al. 2021). The accumulation of residual pesticides in aquatic and marine organisms food chains can pose a risk to human health and have a detrimental effect on ecological systems (Lukaszewicz et al. 2019; Jing et al. 2022a; Abdel-Wahab et al. 2021).

From many decades, pesticides have been a crucial component in reducing crop loss and increasing output. Due to these advantages, farmers are spraying pesticides on crops more frequently and using modern techniques like drones (Nie et al. 2020). However, the propensity of pesticides to bio accumulate in edible goods may have an undesirable impact on human

health (Yu et al. 2016; Ramadan et al. 2020). Beyond their maximum residue limits (MRLs), pesticides in water and agricultural products have the potential to cause both acute and chronic illnesses in people (Li and Jennings 2018; Amaç and Liman 2021).

Carbamates are a diverse group of chemicals that are used as insecticides. The acetylcholinesterase (AChE) enzyme is selectively affected by carbamates, which results in a buildup of acetylcholine and overstimulation of the nervous system in both target and non-target species, including human beings (Eddleston et al. 2004). In the areas where onions, cucumbers, cabbage, and chili peppers are grown, methomyl, a carbamate insecticide, is frequently used (Ramadan et al. 2020). Acute poisoning may result from methomyl consumption by using contaminated agrifoods and water via occupational or non-occupational ways (Jing et al. 2022 b).

Due to its highly effective biological action in controlling pests and safeguarding the crops, methomyl (C5H10N2O2S), S-methyl-1-N- [(methyl carbamoyl)-oxy]-thioacetimidate, belongs to carbamate pesticide group that is commonly applied in various countries (Laicher et al. 2022; Pietrini et al. 2022). Several pesticides are designed to strike a particular group of targets, although their noxious constituents will affect the whole organism, both target and non-target (Castellanos et al. 2022). According to a study, methomyl causes genotoxic effects in fish (Afaf et al. 2022). Fish and aquatic creatures including Danio rerio, coastal aquatic system and water spinach have also shown toxicity to methomyl (Jablonski et al. 2022; Camilo-Cotrim et al. 2022).

DNA damage is a preliminary biotic phenomenon which could disrupt biological developments and structures and produce genotoxic disorders associated with carcinogenic complications (Acar et al. 2022; Siddiqui and Sulaiman 2022 a and b; El-Houseiny et al. 2022). As per a recent report, numerous species undergo carcinogenic progressions due to various causes, such as DNA damage instigated by chemical contaminants (Pesavento et al. 2018; Velázquez et al. 2022; Liman et al. 2022). This study aims to analyze the potential adverse effects of methomyl on mitotic processes and DNA integrity in the terrestrial plant *Pisum sativum* L.

MATERIAL AND METHODS

Purchasing of chemicals and seeds

Methomyl insecticide were bought from Sigma Chemicals Ltd., United States (CAS No. 16752-77-5). *Pisum sativum* L (Pea) seeds were procured from a licensed trader at a community market in Abha, Saudi Arabia.

Exposure conditions

Even sized *P. sativum* L seeds were chosen, pre-soaked for 12 hours in distilled water and then divided into various groups of 30 seeds each. After that, the seeds were exposed to various methomyl concentrations (0.1, 0.2, 0.3, 0.4, and 0.5%) for 1 h by soaking in 250 mL solutions of methomyl. Double-distilled water was used to soak the seeds in the control group. Throughout the treatment time, the containers were shaken repeatedly to make available ample aeration to the seeds. Following treatment, seeds were extensively rinsed with double distilled water (DDW) to eliminate any remaining traces of adhering methomyl and were placed in Petri dishes on moisturized Whatman Filter Paper. For the following 72 hours, the Petri dishes were kept in dark in a plant growth cabinet at 25±2°C. The experiment was conducted on newly emerging roots that were 1-2 cm long. The complete experiment was conducted thrice in identical conditions.

Evaluation of mitotic kinetics and genotoxicity

One to two cm long roots were collected between 8 to 10 am, soaked for 24 h in a fixation solution (ethanol: glacial acetic acid, 3:1), then transferred to 70% ethanol, maintained at 5°C till microscopic examination. For each sample, 10 roots were hydrolyzed in 1N HCl for 10 minutes, and with 2% acetocarmine solution, root tips were dyed for 10 minutes for preparing each slide. Chromosome preparation was done from root tips as stated by Qian et al. 1998 with minor modifications (Siddiqui and Suleiman 2022b). To calculate the MI, which is a proportion of dividing cells, 1000 cells from each sample were evaluated. The no. of cells in each division phase to all mitotic cells was used to compute CPK frequencies. All mitotic cells were studied in a light microscope under oil immersion (100 x). All slides were examined blind and coded.

Ratio of aberrant cells over 500 metaphase/anaphase cells per root tips were used to calculate the frequency of chromosomal aberrations. Chromosomal aberrations were categorized as per their origin in clastogenic (resulting in chromosomal breakage) or aneugenic (disrupting spindle function and leading to asynchronic chromosomal migration). Laggards and vagrants chromosomes have been scored with regards to aneugenic abnormalities. Single bridges, fragments, double bridges, and sticky chromosomes were taken into considera-

tion in clastogenic aberrations. C-mitosis as defined by Grant (1978) is an inactivation of spindle ensued by a haphazard scattering of chromosomes over the cell and is quantified and scored by assessing the frequency over 100 metaphases per root tips. All the aberrant and c-mitosis cells were studied in a light microscope under oil immersion (100x). All slides were examined blind and coded.

Statistical analysis

A one-way ANOVA test using GPIS 1.13 software (GRAPHPAD, California, USA) was applied to find significance of differences in variables. All results were articulated as mean ± standard error.

RESULTS

It is clear from the results that methomyl is toxic to MI, CPK, c- mitosis, aneugenic and clastogeneic aberrations. The observed MI, CPK, c-mitosis, aneugenic and clastogeneic aberrations are well represented in (Fig. 1, Table 1, Fig. 2, Fig. 3 and Fig. 4). The clastogenic abnormalities observed were single bridges, fragments, double bridges, sticky chromosome and aneugenic abnormalities were laggards and vagrants.

Effect of methomyl treatment on mitotic index of P. sativum L.

Fig**.** 1 shows how methomyl affected the MI of root tip cells in *P. sativum*. In control group, seeds treated with DDW for 1 hour had a MI of 9.3%. From 0.1 to 0.2% methomyl treated seeds, a non-significant decline (p>0.05) in MI was observed and at 0.3% concentration, there was a significant decrease (p< 0.05) in MI and at 0.4 to 0.5%, a very significant decrease (p< 0.01) in MI was reported in comparison to control for 1 hour. Overall, MI decreases dose dependently in all concentrations from 0.1 to 0.5%.

Effect of methomyl in Cell Proliferation Kinetics (CPK) of P. sativum L

Cell proliferation kinetics (CPK), assessed as the ratio of prophases, metaphases, anaphases and telophases revealed a rise in prophase, metaphase and anaphase from (0.1 to 0.5%) and a decrease in telophase at 0.1 to 0.5% of methomyl treated root tips in comparison to control (Table 1).
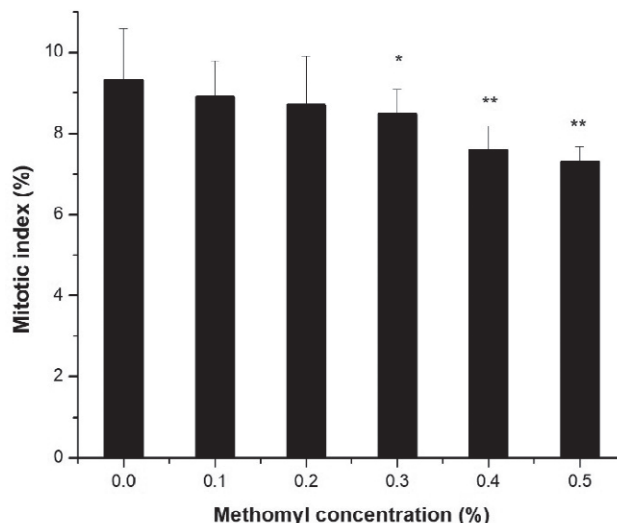
Figure 1. Effect of methomyl on mitotic index of *P. sativum* for 1 h. *p<0.05; compared to control group. Data are mean of three replicates ±SE, 0.0 = Control group.

Table 1. Effect of methomyl on cell proliferation kinetics in *P. sativum* L.

Concentration (%)	Prophases	Metaphases	Anaphases	Telophases
0.0	52.5±4.8	21.7± 2.7	18.5±3.4	23.12.8±2.3
0.1	50.7±4.6	23.5±1.7	20.4±2.4	21.5.6±3.0
0.2	50.4±2.4	27.4±3.5*	21.3±1.9*	20.9±1.30
0.3	55.7± 2.2	27.3.3±3.8**	23.1±1.7 **	19.12±3.6*
0.4	58.34±1.2*	28.45±3.6**	24.5±1.9 **	17.6±2.5**
0.5	60.12±2.6 **	29.40±1.2**	25.5± 1.6 **	16.80±3.6**

*p<0.05; **p<0.01 compared to control group. Data are mean of three replicates ±SE, 0.0 = Control group.

A significant increase (p<0.05) was reported in prophase at 0.4 % (58.34±1.2); metaphase at 0.2% (27.3±3.8), and anaphase at 0.2% (21.3±1.9) but a significant decrease (p<0.05) was observed in telophase at 0.3% (19.12 ±3.6) in comparison to control. Prophase at 0.5% (60.12±2.6); metaphase from 0.3 to 0.5% (27.4±3.5; 28.45±3.6; 29.40±1.2 respectively) and anaphase from 0.3 to 0.5% (23.1±1.7; 24.5±1.9; 25.5±1.6 respectively) resulted in a very significant increase (p<0.01) and telophase from 0.4 to 0.5% (17.6±2.5; 16.80±3.6) showed a very significant decrease (p<0.01) in comparison to control.

Effect of methomyl treatment on C-mitosis of P. sativum L

Fig. 2 demonstrates how methomyl affects c-mitosis in *P. sativum* root tips cells. Seedlings treated for 1h with
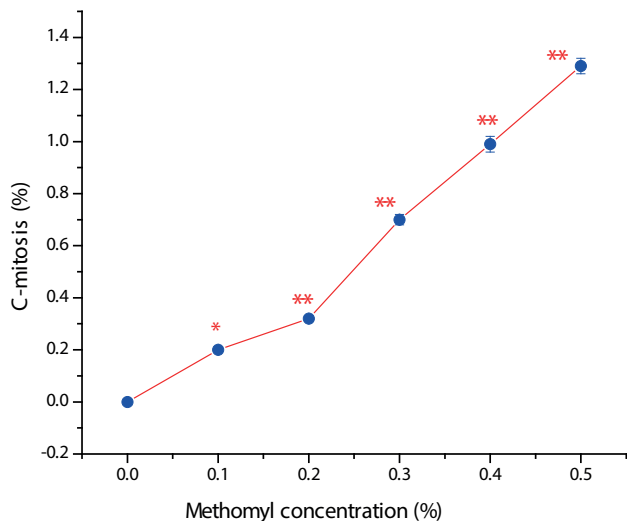
Figure 2. Effect of methomyl on c-mitosis in *P. sativum* for 1 h. *p<0.05; **p<0.01 compared to control group. Data are mean of three replicates ±SE, 0.0 = Control group.
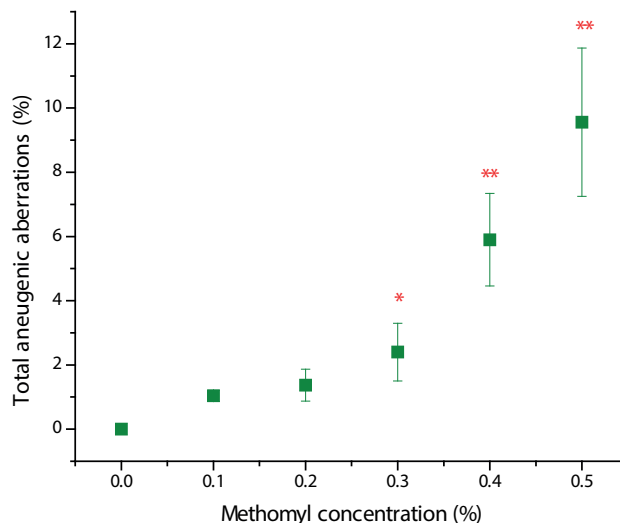
Figure 3. Effect of methomyl on total aneugenic aberrations in *P. sativum* for 1 h. *p<0.05; **p<0.01 compared to control group. Data are mean of three replicates ±SE, 0.0 = Control group.

DDW in the control group exhibited 0% c-mitosis. A significant increase (p<0.05) in the number of c-mitosis cells were seen in seeds treated with 0.1% methomyl for 1 hour and from 0.2 to 0.5%, there was a very significant increase (p<0.01) in c-mitosis cells in comparison to control for 1 hour. Overall, c-mitosis increases dose dependently in all concentrations ranging from 0.1 to 0.5%.

Effect of methomyl on aneugenic and clastogeneic aberration cells in P. sativum L

The incidence of aneugenic aberrations (laggards and vagrants) in metaphase-anaphase plates in the control group was zero. Percentage of aneugenic aberrations (laggards and vagrants) in the metaphase-anaphase plate dose dependently increased with methomyl treatment (Fig. 3 and Fig. 5). Seeds treatment with 0.1% methomyl resulted in a 1-fold increase and 0.2% treatment resulted in a 1.37-fold increase which was not significant and 0.3% methomyl treated seeds resulted in a 2.4-fold increase which was significant (p<0.05) in comparison to control. Further increase in concentration from 0.4 to 0.5% methomyl treated seeds resulted in a rise in incidence of aneugenic aberrations, 5.9-fold, and 9.56-fold respectively, which was very significant (p<0.01) in comparison to control.

The incidence of clastogeneic aberrations (single bridges, fragments, double bridges and sticky chromosome) at metaphase-anaphase plates in control group was zero (Fig. 4, and Fig. 5). Percentage of root tip cells with clastogeneic aberrations (single bridges, fragments,

Figure 4. Effect of methomyl on total clastogenic aberrations in *P. sativum* for 1 h. *p<0.05; **p<0.01 compared to control group. Data are mean of three replicates ±SE, 0.0 = Control group.

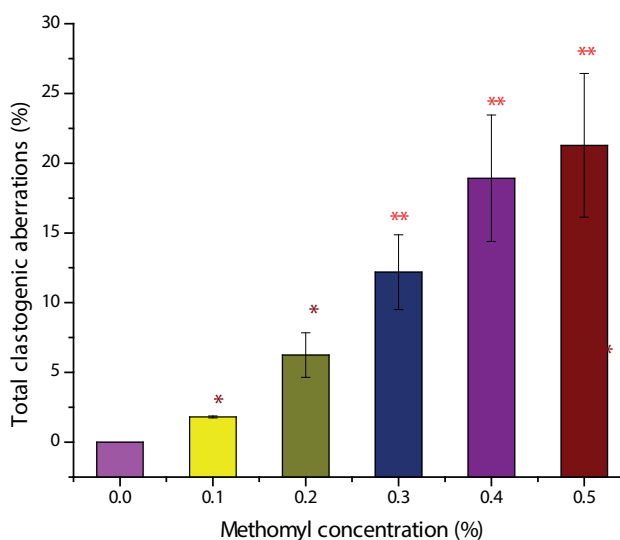double bridges and sticky chromosomes) at metaphase-anaphase plate increased dose dependently with methomyl treatment (Fig. 4). Treatment of seeds with 0.1% methomyl resulted in 1.81-fold increase which was non-significant as compared to control. However, from 0.2 to 0.5 % methomyl treated seeds resulted in 6.25-fold, 12.19-fold, 18.92-fold and 21.28-fold increase in clastogeneic aberrations respectively which was very significant (p<0.01) in comparison to control.
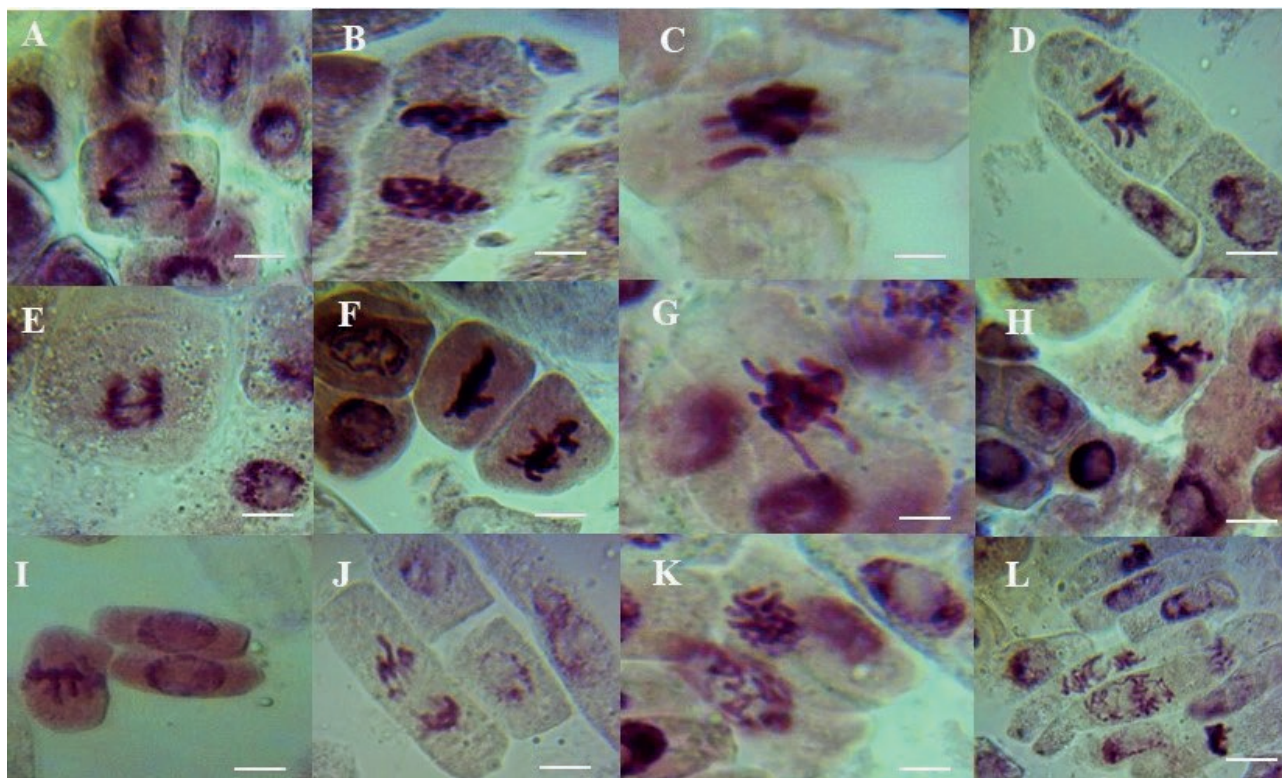
Figure 5. Clastogenic and aneugenic aberrations in methomyl treated *P. sativum* L root tip cells. Clastogenic aberrations A to F: A) Bridge in anaphase; B) Single bridge in telophase; C-D) Chromosome fragment in metaphase; E) Double bridge at anaphase; F) Sticky chromosome at metaphase. Aneugenic aberrations G to J: G-H-I) Chromosome vagrant at metaphase; J) Vagrant chromosome at anaphase; K –L) C-mitosis in metaphase; Bar - 10 μm.

DISCUSSION

This study shows that reduction in cell division indicates that tested methomyl have a mitodepressive potential. When mitotic activity is reduced, the amount of DNA also declines. This could be due to the blockage of cell cycle in the G2 phase or DNA synthesis inhibition or stopping the cell from starting mitosis (Siddiqui et al. 2007; Siddiqui et al. 2012; Siddiqui and Alrumman 2020 a and b). The significant decrease in mitotic index observed in this study might be the effect of methomyl interfering with the cell cycle by blocking G2 phase of cell cycle or DNA synthesis inhibition, or it could be the outcome of a rise in the frequency of chromosomal anomalies with analogous increase in methomyl concentration. These findings are also consistent with the outcomes of several research teams which have stated the cytotoxic effects of ethephon (Ayşe and Kılıç 2017; Bonciu et al. 2022), various synthetic plant growth regulators (Singh et al. 2022; Asif et al. 2022), and various pesticides (Lukaszewicz et al. 2019; Siddiqui and Alrumman 2022 a and b; Omeiri et al. 2022; Hafez et al. 2022; Bandopadhyay et al. 2022).

In this study, Methomyl raised the percentage of metaphase, prophase and anaphase and reduced the percentage of telophase in all concentrations in a dose dependent manner, as per the outcomes of proportions of distribution of specific mitotic stages. There is an increase at all concentrations of metaphase, prophase and anaphase phases. The outcomes are consistent with the findings of Liman et al. (2010), Priya et al. (2014), and Ozkul et al. 2016). Furthermore, the percentage of telophase stage decreased in comparison to control. These findings suggest that decline in telophase stages and henceforth MI might be due to arrest of one or more mitotic stages or due to a slowdown in the rate of cell development during mitosis (Ping et al. 2012).

C-mitosis was found in the present study. C-mitosis was created by unstable microtubules (Odeigah et al. 1997) or disruptions in the development of spindle fibers (Shimoi et al. 2019; Haliem 1990). The incidence of c-mitosis in root tip cells of Pisum sativum shows that spindle formation was harmfully affected (El-Ghamery et al. 2000). Considerable numbers of c-mitosis detected in this study implies that methomyl is a strong spindle

inhibitor. C-mitosis is also an indication of spindle poisoning, as per Rank (2003). The cause of the generation of c-mitosis might be due to disruptions in spindle formation, affected by methomyl.

In relation to genotoxicity, methomyl enhanced the incidence of clastogenic as well as aneugenic anomalies at the metaphase-anaphase plate. Single bridges, fragments, double bridges and stickiness, were the clastogenic anomalies whereas vagrants and laggards were the aneugenic anomalies observed in the present study. In treated seeds, a number of bridges were created in anaphases I and II plate. Bridges were most likely formed by breakage and combining of chromosomal bridges, which got enhanced with methomyl treatment. Chromosome stickiness and subsequent failure of free anaphase division or irregular translocation or inversion of chromosomal fragments can all lead to the creation of chromosomal bridges (Jing et al. 2022ª; Honles et al. 2022). The fusion of broken chromosomes was the primary cause of the formation of bridges as per Rosculet et al (2019; Honles et al. 2022).

Increases in methomyl concentrations were associated with stickiness. Stickiness may result from partial detachment of nuclear proteins and alterations in their association design or from partial detachment of nucleoproteins and alterations in their association design or due to nucleic acid depolymerization activated by methomyl treatment. Disruptions in cytochemical balance reaction may lead to stickness (Dewitte et al. 2010; Rosculet et al. 2019). Nucleic acid depolymerization because of herbicidal treatment or by partial detachment of nucleoproteins (Kaufman et al. 1955) or by incomplete separation of nucleoprotein variation in their organization design (Evans 1962) might cause stickness.

The fragments formed from chromatid and chromosomal break imply its mutagenic events within the cell. In a previous study, Siddiqui et al. (2020 a,b) had reported that pesticides cause various chromosomal anomalies. Generation of giant cells having diverse chromosomal anomalies had been reported in a previous study by food colorants (Prajitha and Thoppil 2016).

The laggards observed during the current study may result from failure of chromosome movement or from deferred ending of stickiness of ends of chromosomes. At metaphase I, chromosome lagging could result from disturbances in bivalents motion to equatorial plate. Single univalent lagging was the most common incidence (Zeyad et al. 2019). Laggards and bridges could be created due to deferred ending of stickiness of ends of chromosomes (Kaur and Grover 1985). Laggards are responsible for the formation of micronuclei at telophase I. Acentric fragments or laggards are liable for micro-

nuclei generation at telophase II and hence it leads to the changes in size and number of pollen grains arising from mother cells.

The other frequent aneugenic form of anomaly observed in dividing cells was vagrant chromosomes. As per Rank (2003), vagrant chromosomes are pointers of spindle poisoning. These aberrations might have developed as a result of the disruption in spindle formation, which was affected by methomyl treatment.

Genotoxic stress or genomic instability caused by DNA damage may result in illnesses, senescence, alterations in gene expression or cellular aging (Bonciu et al. 2018; Iturburu et al. 2018; Shabbir et al. 2021; Omeiri et al. 2022; Castellanos et al. 2022). In both plants and animals, a rise in genomic instability has been advocated as a basis for the decline in population fitness. Genotoxicity biomarkers must be taken into consideration when assessing potential noxious effects in aquatic organisms since genotoxic substances have the potential to cause damage that extends beyond the individual and can be seen over several generations (Frenzilli et al. 2009; Fioresi et al. 2020; Ergin et al. 2020 Amac and Liman 2021; Menzyanova et al. 2022).

CONCLUSION

According to the findings of the current study, methomyl can alter kinetics of mitotic cell process in root tip cells and can have genotoxic effects on *P. sativum* L through aneugenic and clastogenic processes. These findings raise concern about noxious effects of pesticides on non-target organisms. For the benefit of human welfare, additional genotoxicological and risk assessment studies needs to be conducted on various eukaryotic test systems.

sity, Saudi Arabia for providing administrative and technical support.

REFERENCES

Abdel-Wahab SI, Aioub AA, Salem RE, El-Sobki AE. 2021. Do the herbicides pinoxaden, tribenuron-methyl, and pyroxsulam influence wheat (*Triticum aestivum* L.) physiological parameters? Environmental Science and Pollution Research, 28:51961–51970. https://doi.org/10.1007/s11356-021-14390-8

Acar A. 2021. In vivo toxicological assessment of diquat dibromide: cytotoxic, genotoxic, and biochemical approach. Environ Sci and Pollut Res. 28(34): 47550-61.

Afaf N, Abdel R, Amany AR, Mohamed ND, Mohamed FM, Farag LS, Alqahtani MA, Nassan Saed AAl Thobaiti, Nesma IEl-Naseery. 2022. Appraisal of sub-chronic exposure to lambada-cyhalothrin and/or methomyl on the behavior and hepato-renal functioning in *Oreochromis niloticus*: Supportive role of taurine-supplemented feed. Aquat. Toxicol. 250:106257.

Amac E, Liman R. 2021. Cytotoxic and genotoxic effects of clopyralid herbicide on *Allium cepa* roots. Environmental Science and Pollution Research, 28(35):48450–48458. https://doi.org/10.1007/s11356-021-13994-4

Asif R, Yasmin R, Mustafa M, Ambreen A, Mazhar M, Rehman A, Umbreen S, Ahmad M. 2022. Phytohormones as plant growth regulators and safe protectors against biotic and abiotic stress. Plant Hormones: Recent Advances, New Perspectives and Applications. p.115.

Ayse YK, Eriş K. 2017. Evaluation of the genotoxicity of commercial formulations of ethephon and ethephon+cyclanilide on *Allium cepa* L. root meristematic cells, Caryologia, 70:(3) 229-237. DOI: 10.1080/00087114.2017.1329960

Bandopadhyay A, Roy T, Alam S, Majumdar S, Das N. 2022. Influence of pesticide-tolerant soil bacteria for disease control caused by *Macrophomina phaseolina* (Tassi.) Goid and plant growth promotion in *Vigna unguiculata* (L.) Walp. Environ. Dev. Sustain. pp.1-21.

Bonciu E, Firbas P, Fontanetti CS, Wusheng J, Karaismailoglu MC, Donghua Liu, Menicucci F, Pesnya DS, Popescu A, Romanovsky AV, Schiff S, Ślusarczyk J, de Souza CP, Srivastava A, Sutan A, Papini A. 2018. An evaluation for the standardization of the *Allium cepa* test as cytotoxicity and genotoxicity assay. Caryologia, 71(3): 191-209.

Bonciu E, Para-schivu M, Şuţan NA, Olaru AL. 2022. Cytotoxicity of Sunset Yellow and Brilliant Blue food dyes in a plant test system. Caryologia, 75(2):143-149.

Camilo-Cotrim CF, Bailao EFLC, Ondei LS, Carneiro MF, Almeida LM. 2022. What can the *Allium cepa* test say about pesticide safety? A review. Environmental Science and Pollution Research, 29: 48088–48104. https://doi.org/10.1007/s11356-022-20695-z

Castellanos NL, Smagghe G, Taning CNT, Oliveira EE and Christiaens O. 2022. Risk assessment of RNAi-based pesticides to non-target organisms: Evaluating the effects of sequence similarity in the parasitoid wasp *Telenomus podisi*. Sci. Total Environ. 832:154746.

Chandra R, Sharpanabharathi N, Prusty BAK. et al. 2021. Organochlorine pesticide residues in plants and their possible ecotoxicological and agri food impacts. Sci Rep. 11:17841. https://doi.org/10.1038/s41598-021-97286-4

Dewitte A, Eeckhaut T, Van Huylenbroeck J, Van Bockstaele E. 2010. Meiotic aberrations during 2n pollen formation in Begonia. Heredity. 104:215–23.

Eddleston M, Dawson A, Karalliedde L, Dissanayake W, Hittarage A, Azher S, Buckley NA. (2004). Early management after selfpoisoning with an organophosphorus or carbamate pesticide—A treatment protocol for junior doctors. Crit Care. 8(6): R391–R397.

El-Ghamery AA, El-Nahas AI, Mansour MM. 2000. The action of atrazine herbicide as an inhibitor of cell division on chromosomes and nucleic acids content in root meristems of *Allium cepa* and *Vicia faba*. Cytologia. 65(3):277–287.

El-Houseiny, Algharib W, Mohamed SA, Metwally EA, Mahmoud MM, Alghamdi YK, Soliman YS, Abd-Elhakim MM, El-Murr AE. 2022. Dietary parsley seed mitigates methomyl-induced impaired growth performance, hemato-immune suppression, oxidative stress, hepato-renal damage, and pseudomonas aeruginosa susceptibility in Oreochromis niloticus. Antioxidants. 11(6);1185.

Ergin T, Inceer H, Ergin B. 2020. Investigation of anti-mutagenic effect of *Rosa canina* L. against linuron induced DNA damage on root meristematic cells of *Allium cepa* L. Cytologia 85:233–237. https://doi.org/10.1508/cytologia.85.233

Evans HJ. 1962. Chromosome aberrations induced by ionizing radiations. Int Rev Cytol. 13:221– 232

Fioresi VS, de Vieira BCR, de Campos JMS, da Souza TS. 2020. Cytogenotoxic activity of the pesticides imidacloprid and iprodione on *Allium cepa* root meristem. Environmental Science and Pollution Research,

27:28066–28076. https://doi.org/10.1007/s11356-020-09201-5

Frenzilli G, Nidro M, Lyons BP. 2009. The comet assay for the evaluation of genotoxic impact in aquatic environments. Mutat Res Rev Mutat Res. 681:80–92.

Grant WF. 1978. Chromosome aberrations in plants as a monitoring system. Environ Health Perspect. 27:37–43.

Hafez ZM, Sobieha AK, Asran AA, Emam HM. 2022. Toxicity of Lambada Cyhalothrin, and Methomyl on terrestrial snails, *Eobania Vermiculata*, and *Helicella Vestalis*, under laboratory conditions. Res J Environ Sci. 51(4):93-108.

Haliem AS. 1990. Cytological effects of the herbicide sencorer on mitosis of *A.cepa*. Egypt J Bot. 33:93–104.

Honles J, Clisson C, Monge C, Vásquez-Ocmin P, Cerapio JP, Palamy S, Casavilca-Zambrano S, Herrera J, Pineau P, Deharo E, Peynet V. 2022. Exposure assessment of 170 pesticide ingredients and derivative metabolites in people from the central andes of Peru. Sci. Rep. 12(1):1-15. https://doi.org/10.1186/cc2953

Iturburu FG, Simoniello MF, Medici S, Panzeri AM, Menone ML. 2018. Imidacloprid causes DNA damage in fish: clastogenesis as a mechanism of genotoxicity. Bull Environ Contam Toxicol. 100 (6):760–764.

Jablonski CA, Pereira TCB, Teodoro LDS, Altenhofen S, Rübensam G, Bonan CD, Bogo MR. 2022. Acute toxicity of methomyl commercial formulation induces morphological and behavioral changes in larval zebrafish (*Danio rerio*). Neurotoxicol Teratol. 89:107058.

Jing X, Liu T, Fateh B, Chen J, Zheng Y, Xu G. 2022[a]. Effect of methomyl on water quality, growth performance and antioxidant system in liver of GIFT (Oreochromis niloticus) in the presence of peppermint (Mentha haplocalyx Briq.) as a floating bed. Sci Prog. 105(3): p.00368504221124047

Jing X, Zheng Y, Mulbah JP, Chen J, Xu G. 2022[b]. Effect of methomyl on growth, antioxidant system of gift (oreochromis niloticus), and residue in the presence of water spinach (Ipomoea aquatica Forsk). J Environ Anal Chem.7434426. doi: 10.1155/2022/7434426.

Kaufman BP, McDonald MR, Bernstein MH. 1955. Cytochemical studies of changes induced in cellular materials by ionizing radiations. Ann N Y Acad Sci. 59:553–566.

Kaur P, Grover IS. 1985. Cytological effects of some organophosphorus pesticides. II. Meiotic effects. Cytologia. 50:199–211.

Laicher D, Benkendorff K, White S, Conrad S, Woodrow, RL, Butcherine P, Sanders CJ. 2022. Pesticide occurrence in an agriculturally intensive and ecologically important coastal aquatic system in Australia. Mar. Pollut. Bull.180:113675.

Li Z, Jennings A. 2018. Global variations in pesticide regulations and health risk assessment of maximum concentration levels in drinking water. J Environ Manage. 212:384–394. https:// doi.org/10.1016/j.jenvman.2017.12.083

Liman R, Akyıl D, Eren Y, Konuk M. 2010. Testing of the mutagenicity and genotoxicity of metolcarb by using both Ames/Salmonella and *Allium* test. Chemosphere. 80(9):1056–1061.

Liman R, Ali MM, Istifli ES, Cigerci IH, Bonciu E. 2022. Genotoxic and cytotoxic effects of pethoxamid herbicide on Allium cepa cells and its molecular docking studies to unravel genotoxicity mechanism. Environmental Science and Pollution Research, 29: 63127–63140.

Lukaszewicz G, Iturburu FG, Garanzini DS, Menone ML, Pflugmacher S. 2019. Imidacloprid modifies the mitotic kinetics and causes both aneugenic and clastogenic effects in the macrophyte *Bidens laevis* L. Heliyon. 5(7):e02118. doi: 10.1016/j.heliyon.2019.e02118.

Menzyanova NG, Shishatskaya EI, Pyatina SA, Volova TG. 2022. Cytogenotoxic activity of herbicidal and fungicidal pesticides on *Triticum aestivum* root meristem. Environmental Science and Pollution Research, 29: 87602–87612.

Mojiri A, Zhou JL, Robinson B, Ohashi A, Ozaki N, Kindaichi T, Farraji H, Vakili M. 2020. Pesticides in aquatic environments and their removal by adsorption methods. Chemosphere. 253: 126646.

Nie J, Sun Y, Zhou Y, Kuma M, Usman M, Li J, Tsang DCW. (2020). Bioremediation of water containing pesticides by microalgae: Mechanisms, methods, and prospects for future research. Sci. Total Environ. 707:136080. https://doi.org/10.1016/j. scitotenv.2019.136080

Odeigah PGC, Nurudeen O, Amund OO. 1997. Genotoxicity of oil field wastewater in Nigeria. Hereditas. 126(2):161–167.

Omeiri M, Khnayzer R, Yusef H, Tokajian S, Salloum T, Mokh S. 2022. Bacillus spp. isolated from soil in Lebanon can simultaneously degrade methomyl in contaminated soils and enhance plant growth. Biocatal. Agric. Biotechnol. 39:102280.

Ozkul M, Ozel CA, Yuzbaşıoglu D, Unal F. 2016. Does 2,4-dichlorophenoxyacetic acid (2,4-D) induce genotoxic effects in tissue cultured *Allium* roots? Cytotechnology. 68(6):2395–2405

Pesavento PA, Agnew D, Keel MK, Woolard KD. 2018. Cancer in wildlife: patterns of emergence. Nat Rev Cancer. 18: 646–661.

Pietrini F, Iannilli V, Passatore L, Carloni S, Sciacca G, Cerasa M, Zacchini M. 2022. Ecotoxicological and genotoxic effects of dimethyl phthalate (DMP) on *Lemna minor* L. and *Spirodela polyrhiza* (L.) Schleid. plants under a short-term laboratory assay. Science of The Total Environment, 806 (4):150972. https://doi.org/10.1016/j.scitotenv.2021.150972.

Ping KY, Darah I, Yusuf UK, Yeng C, Sasidharan S. 2012. Genotoxicity of *Euphorbia hirta*: an *Allium cepa* assay. Molecules.17(7):7782–7791.

Prajitha V, Thoppil JE. 2016. Genotoxic and antigenotoxic potential of aqueous leaf extracts of *Amaranthus spinosus* Linn. Using *Allium cepa* assay. S Afr J Bot. 102:18–25.

Priya JS, Purushothaman P, Hannah C, Matthew S, Thomas S. 2014. Genotoxic effect of ethephon on the root meristems of *Allium cepa* L. Commun Plant Sci. 4:19–22.

Qian XW. 1998. Improvement on experiment method of micronucleus in root tip cell of *Vicia faba*. J Wenzhou Norm Coll. 19: 64–65.

Ramadan MF, Abdel-Hamid M, Altorgoman MM, AlGaramah HA, Alawi MA, Shati, AA, Awwad NS. 2020. Evaluation of pesticide residues in vegetables from the Asir Region, Saudi Arabia. Molecules. 25(1):205. https://doi.org/10.3390/molecules 25010205

Rank J. 2003. The method of *Allium* anaphase-telophase chromosome aberration assay. Ekologija (Vilnius). 1: 38–42.

Rosculete CA, Bonciu E, Rosculete E, Olaru LA. 2019. Article determination of the environmental pollution potential of some herbicides by the assessment of cytotoxic and genotoxic effects on *Allium cepa*. Int J Environ Res Public Health.16: 75.

Shabbir MD, Mukesh S, Swati M, Samar KS. 2021. Organophosphate pesticide (Chlorpyrifos): Environmental menace; study reveals genotoxicity on plant and animal cells. Environmental Challenges. 5:100313.

Shimoi G, Tomita M, Kataoka M, Kameyama Y. 2019. Destabilization of spindle assembly checkpoint causes aneuploidy during meiosis II in murine post-ovulatory aged oocytes. J Reprod Dev. 65(1):57-66. doi: 10.1262/jrd.2018-056.

Siddiqui S, Al-Rumman S. 2020[a]. Cytological changes induced by clethodim in *Pisum sativum* plant. Bangladesh J. Bot. 49(2):367–374.

Siddiqui S, Al-Rumman S. 2020[b]. Clethodim induced pollen sterility and meiotic abnormalities in vegetable crop *Pisum sativum* L. Caryologia. 73(1):37–44.

Siddiqui S, Al-Rumman S. 2022[a]. Methomyl, imbraclaobrid and clethodim induced cytomixis and syncytes

behaviors in PMCs of *Pisum sativum* L: Causes and outcomes. Saudi J Biol Sci. 29(9):103390. doi: 10.1016/j.sjbs.2022.103390.

Siddiqui S, Al-Rumman S. 2022[b]. Exposure of *Pisum sativum* L. seeds to methomyl and imidacloprid cause genotoxic effects in pollen-mother cells. biology. 11: 1549. https://doi.org/10.3390/ biology11111549

Siddiqui S, Meghvansi MK, Hasan Z. 2007. Cytogenetics changes induced by sodium azide on *Trigonella foenum-greacum* L. seeds. S Afr J Bot. 73: 632–635.

Siddiqui S, Meghvansi MK, Khan SS. 2012. Glyphosate, alachor and maleic hydrazide have genotoxic effect on *Trigonella foenum-graecum* L. Bull Environ Contam Toxicol. 88(5): 659-65. doi: 10.1007/s00128-012-0570-6.

Singh D, Sahu TL, Netam N, Nishad D, Banjare B. 2022. Effect of plant growth regulators on growth and flowering of China aster (*Callistephus chinensis* L.) cv. Phule Ganesh pink. J. Pharm. Innov. 11 (2): 297–949.

Velazquez G, Pérez B, Rodríguez V, Handal A. 2022. Genotoxicity and cytotoxicity of Sambucus canadensis ethanol extract in meristem cells of *Allium sativum*. Caryologia.75(1): 99-107.

Yu R, Liu Q, Liu J, Wang Q, Wang Y. 2016. Concentrations of organophosphorus pesticides in fresh vegetables and related human health risk assessment in Changchun, Northeast China. Food Control. 60: 353–360. https://doi.org/10.1016/j.foodcont.2015.08.013

Zeyad MT, Kumarb M, Malika A. 2019. Mutagenicity, genotoxicity and oxidative stress induced by pesticide industry wastewater using bacterial and plant bioassays. Biotech Reports. 24: e00389.

Caryologia

International Journal of Cytology,
Cytosystematics and Cytogenetics

Comparative study and genetic diversity in *Malva* using srap molecular markers

Syamand Ahmed Qadir[1], Chnar Hama Noori Meerza[2], Aryan Mahmood Faraj[3], Kawa Khwarahm Hamafaraj[4], Sherzad Rasul Abdalla Tobakari[5], Sahar Hussein Hamarashid[6,*]

[1] Medical laboratory techniques department/Halabja Technical Institute, Research center/ Sulaimani Polytechnic University, Sulaymaniyah, Iraq
[2] Food Science and Quality Control Department, Bakrajo Technical Institute, Sulaimani Polytechnic University, Sulaymaniyah, Iraq
[3] Medical Laboratory Science Department/ Technical College of Applied Science/Sulaimani Polytechnic University, Sulaymaniyah, Iraq
[4] Nursing department/Halabja Technical Institute/ Sulaimani Polytechnic University, Sulaymaniyah, Iraq
[5] Medical laboratory techniques department/Halabja Technical Institute, Research center/ Sulaimani Polytechnic University, Sulaymaniyah, Iraq
[6] Agricultural Project Management Department/ Technical College of Applied Science/ Sulaimani Polytechnic University, Sulaymaniyah, Iraq
*Corresponding author. E-mail: sahar.rashid@spu.edu.iq

Abstract. The *Malva* genus has 25-40 species and it can be considered as an annual and/or biannual herb. *Malva* species are indicated with potential therapeutic as cicatrizing and analgesic by the Ministry of Health. The aim of this study was to analyze SRAP (Sequence-related amplified polymorphism) markers in a total of 70 accessions of *Malva* species, which included five species *Malva neglecta* Wallr., *Malva pusilla* Sm., *Malva sylvestris* L., *Malva verticillata* L., *Malva nicaeensis* All.. A total of 89 (Number of total loci) (NTL) DNA bands were produced through polymerase chain reaction amplifications (PCR) amplification of five *Malva* species. These bands were produced with the combinations of 5 selective primers. The total number of amplified fragments ranged from 10 to 27. The predicted unbiased gene diversity (UHe) varied between 0.077 (*Malva sylvestris*) and 0.382 (*Malva pusilla*). The genetic similarities between three species are estimated from 0.70 to 0.91. Neighbor-Joining tree results showed two major clusters. According to the SRAP (Sequence-related amplified polymorphism) markers analysis, *Malva pusilla* and *Malva aegyptia* had the lowest similarity. Our results provided great molecular identification of all assayed genotypes, which have shown that there is large quantity of genetic diversity among the *Malva* accessions. Objectives of the study were; a) to estimate genetic diversity; b) to evaluate population relationships using NJ approaches. Current results have implications in breeding and conservation programs.

Keywords: Sequence-related amplified polymorphism, Genetic Diversity, Medicinal Plants *Malva,* Taxonomy.

INTRODUCTION

The use of medicinal plants can be influenced by the economic condition, the high cost of medicines and the difficult access to public consultations. In addition to that, there is difficulty of access by residents in rural areas to health care units located in urban areas. Moreover, the increase the trend for considering traditional knowledge that supports using natural resources as an alternative to synthetic drugs (Battisti et al., 2013). Given the significance of genetic diversity in conservation strategies, it is of utmost importance to disentangle genetic diversity in plant species, particularly threatened and rare species (Esfandani-Bozchaloyi et al. 2018a, 2018b, 2018c, 2018d).

The indiscriminate use of plants due to the lack of phytochemical, pharmacological and mainly toxicological knowledge is of great concern for public health. The correct identification of medicinal plant species is necessary, especially when they are processed in order to avoid misuse of medicinal plants (Romitelli & Martins, 2013). The *Malva* genus presents different species with therapeutic potential and inadequate consumption can occur due to the incorrect identification of the plant in the market.

Malvaceae or the mallow family is the family of flowering plants containing over 200 genera with close to 2300 species (la Duke and Dobley 1995). Many researches have been published on the ecology, taxonomy, genetic, cytology, chemotaxonomy, physiology, seed germination and economic uses of family Malvaceae such as (El-Rjoob and Omari 2009) in ecology; in taxonomy in chemotaxonomy (Blunden et al., 2001) and in genetic researches (Baum et al., 2004) studied the pollen.

Malva L. (mallow) is the genus within the Malvaceae Juss. family, which includes 25–40 species and several hybrids (Ray 1995). This genus contains herbaceous annual, biennial, and perennial species that are native to regions of Africa, Asia, and Europe (Shaheen et al., 2009). In medicine, mallow species are used in the treatment of respiratory, urinary, and digestive problems as they have high bactericidal, antiulcerogenic, anti-inflammatory, hepatoprotective, and antidiabetic activities (Pandey et al, 2012). The *Malva* genus is morphologically very diverse, but some species are hardly distinguishable based on morphological features (Escobar et al., 2009). Several studies have been conducted to clarify the taxonomic affiliation of *Malva* species using different features, such as molecular data (nuclear ribosomal DNA (rDNA), internal transcribed spacer (ITS) region, intron–exon splice junction (ISJ), and inter simple sequence repeat polymerase chain reaction (ISSR) mark-

ers), differentiation of seed and seed coat structure (El Naggar, 2001), morphology of pollen grains (El Naggar, 2004), epidermal structures and stem hairs (Akçin and Özbucak, 2006), and plant morphological traits (Michael et al., 2009).

The variability in mallow species is due, at least in part, to hybridization. Natural crossings between *M. pusilla* Sm. and *M. neglecta*, *M. alcea* L., and *M. moschata* L. as well as *M. sylvestris* and *M. neglecta* were found in Europe. Ray (1995) stated that hybridization or polyploidy is probably a factor in the evolution of these species, but this aspect has not been investigated so far. The taxonomy and systematics of the *Malva* genus are still unclear and very complicated. Taxonomic doubts have appeared because of the high level of homoplasty in morphological traits that are usually used as diagnostic features (Chen et al. 2021 ; BI et al. 2021). Sequence-related amplified polymorphism (SRAP) is PCR –based marker system. It is one of the efficient and simple marker systems to study gene mapping and gene tagging in plant species (Li and Quiros 2001), and SRAP are potential markers to assess plant systematics and genetic diversity studies (Robarts and Wolfe 2014). Previously, Wu et al. (2010) assessed genetic diversity and population structure in *Pogostemon cablin* with the aid of SRAP markers. SRAP markers were successfully implemented in Lamiaceae, Geraniacea, Caryophyllacea and Rosaceae family to study natural populations and variations within the family (Peng et al., 2021; Ma et al.,2021). Objectives of the study were; a) to estimate genetic diversity; b) to evaluate population relationships using NJ approaches. Current results have implications in breeding and conservation programs. The present study is the first report on genetic diversity and phylogenetic relationships between and within *Malva* species in Iraq using SRAP markers.

MATERIALS AND METHODS

Plants collection

Five wild *Malva* species (*Malva neglecta* Wallr., *Malva pusilla* Sm., *Malva sylvestris* L., *Malva vericillata* L., *Malva nicaeensis* All..) in Halabja, Sulaimanieh, Kalar, Chamchamal and Basreh Provinces of Iraq were selected and sampled during July-August 2015-2020. Morphometric and SRAP analyses on 70 plant accessions were carried out. Five to twelve samples from each population belonging to three different species were selected based on other eco-geographic characteristics. Detailed information about locations of samples and geographical distribution of species are mentioned.

Morphological studies

Five to twelve samples from each species were used for Morphometry. In total 36 morphological (13 qualitative, 23 quantitative) characters were studied. Data obtained were standardized (Mean= 0, variance = 1) and used to estimate Euclidean distance for clustering and ordination analyses (Podani 2000). Morphological characters studied are: corolla shape, bract shape, calyx shape, calyx length, calyx width, calyx apex, calyx margins, bract length, corolla length, corolla width, corolla apex, leaf length and leaf width, leaf apex, leaf margins, leaf shape, leaf gland and bract margins.

Sequence-related amplified polymorphism method

Fresh leaves were used randomly from one to twelve plants. These were dried with silica gel powder. Genomic DNA was extracted while following previous protocol. SRAP assay was performed as described previously (Li and Quiros 2001). Five SRAP in different primer combinations were used (Table 1). The overall reaction volume consisted of 25 μl. This PCR reaction was carried out in Techne thermocycler (Germany). The following cycles and programs were observed. The initial denaturation step was performed for 5 minutes at 94°C. The initial denaturation step was followed by 40 cycles for 1 minute at 94°C; 1 minute at 52-57°C, and 2 minutes at 72°C. The reaction was completed by a final extension step of 7-10 min at 72°C. Staining was performed with the aid of ethidium bromide. DNA bands/fragments were compared against a 100 bp molecular size ladder (Fermentas, Germany).

Data analyses

ANOVA (Analysis of variance) was conducted to assess morphological differences among species. Principal component analysis (PCA) was implemented to identify variable morphological characters in *Malva* species. Multivariate statistical analyses i.e., PC analysis, were performed in PAST software version 2.17 (Hammer et al. 2001).

Molecular analyses

Sequence-related amplified polymorphism (SRAP) bands were recorded. Presence and absence of bands were scored present (1) and absent (0), respectively. Total loci (NTL) and the number of polymorphism loci (NPL) for each primer were calculated. Furthermore, the polymorphic ratio was assessed based on NPL/NTL values. Polymorphism information content was calculated as previously suggested by Roldan-Ruiz et al. (2000). Parameter like Nei's gene diversity (H), Shannon information index (I), number of effective alleles, and percentage of polymorphism (P% =number of polymorphic loci/number of total loci) were determined. Nei's genetic distance among populations was used for Neighbor Joining (NJ) clustering and Neighbor-Net networking. Mantel test checked the correlation between geographical and genetic distances of the studied populations (Podani 2000). These analyses were done by PAST ver. 2.17 (Hammer *et al.* 2012), DARwin ver. 5 (2012) and SplitsTree4 V4.13.1 (2013) software. To assess the population structure of the pistachio genotypes, a heuristic method based on Bayesian clustering algorithms were utilized. The clustering method based on the Bayesian-model implemented in the software program STRUCTURE () was used on the same data set to better detect population substructures. This clustering method is based on an algorithm that assigns genotypes to homogeneous groups, given a number of clusters (K) and assuming Hardy-Weinberg and linkage equilibrium within clusters, the software estimates allele frequencies in each cluster and population memberships for every individual (Pritchard et al. 2000). The number of potential subpopulations varied from two to ten, and their contribution to the genotypes of the accessions was calculated based on 50,000 iteration burn-ins and 100,000 iteration sampling periods. The most probable number (K) of subpopulations was identified following Evanno et al. (2005). In K-Means clustering, two summary statistics, pseudo-F, and Bayesian Information Criterion (BIC), provide the best fit for k. Pairwise genetic similarity between species was evaluated to reveal genetic affinity between species (Jaccard, 1908). Unbiased expected heterozygosity and Shannon information index were calculated in GenAlEx 6.4 software (Peakall and Smouse, 2006).

Table 1. SRAP primer information and results.

Primer name	NTL[a]	NPL[b]	P[c]	PIC[d]	RP[e]
Em3-Me4	**27**	27	100.00%	0.55	33.24
Em3-Me1	16	10	75.00%	0.11	55.55
Em4-Me1	17	17	100.00%	0.39	11.23
Em5-Me1	10	10	100.00%	0.50	38.55
Em5-Me2	19	13	66.00%	0.32	44.65
Mean	19	15	83.10%	0.44	39.23
Total	89	80			

RESULTS

Morphometry

The ANOVA findings showed substantial differences ($p<0.01$) between the species in terms of quantitative morphological characteristics. Principal component analysis results explained 60% cumulative variation. The first PCA axis explained 40% of the total variation. The highest correlation (> 0.7) was shown by morphological characters such as corolla apex, seed length; number of segment stem leaves; calyx length, calyx width; bract length and leaf shape. The morphological characters of five *Malva* species are shown in PCA plot (Figure 1). Each species formed separate groups based on morphological characters. The morphometric analysis showed clear difference among *Malva* species and separated each groups.

Species identification and genetic diversity

Five (5) suitable primer combinations (PCs), out of 25 PCs were screened in this research. Figure 2 illustrates the banding pattern of Em2-Me4 and Em4-Me1 primer by the SRAP marker profile. Eighty (80) amplified polymorphic bands (number of polymorphic loci) were produced. These bands (fragments) had different range i.e. 100bp to 3000 bp. Maximum and minimum numbers of polymorphic bands were 27 and 10

Table 2. Genetic diversity parameters in the different *Malva* populations, species, and cultivars; Abbreviations.

Population	%P	N	Na	Ne	I	He	UHe
Malva pusilla Sm.	53.00%	15.000	1.500	1.432	0.388	0.310	0.382
Malva sylvestris L.	22.11%	10.000	1.333	1.177	0.130	0.033	0.077
Malva vericillata L.	33.33%	12.000	1.300	1.388	0.271	0.167	0.288
Malva nicaeensis All.	49.00%	17.000	1.580	1.077	0.395	0.156	0.277
Malva aegyptia L.	30.33%	13.000	1.110	1.366	0.299	0.238	0.144

for Em3-Me4 and Em5-Me1, respectively. Each primer produced 15 polymorphic bands on average. The PIC ranged from 0.11 (Em3-Me1) to 0.55 (Em1-Me4) for the 5 SRAP primers, with an average of 0.44 per primer. RP of the primers ranged from 11.23 (Em4-Me1) to 55.55 (Em3-Me1) with an average of 39.23 per primer (Table 2). The calculated genetic parameters of *Malva* species are shown (Table 2). The unbiased heterozygosity (H) varied between 0.077 (*Malva sylvestris*) and 0.382 (*Malva pusilla*) with a mean of 0.23. Shannon's information index (I) was maximum in *Malva nicaeensis* (0.395), where as we recorded minimum Shannon's information index in *Malva sylvestris* (0.13). The observed number of alleles (Na) ranged from 1.11 in *Malva aegyptia* to 1.580 in *Malva nicaeensis*. The significant number of alleles (Ne) ranged from 1.077 (*Malva nicaeensis*) to 1.432 (*Malva pusilla*).
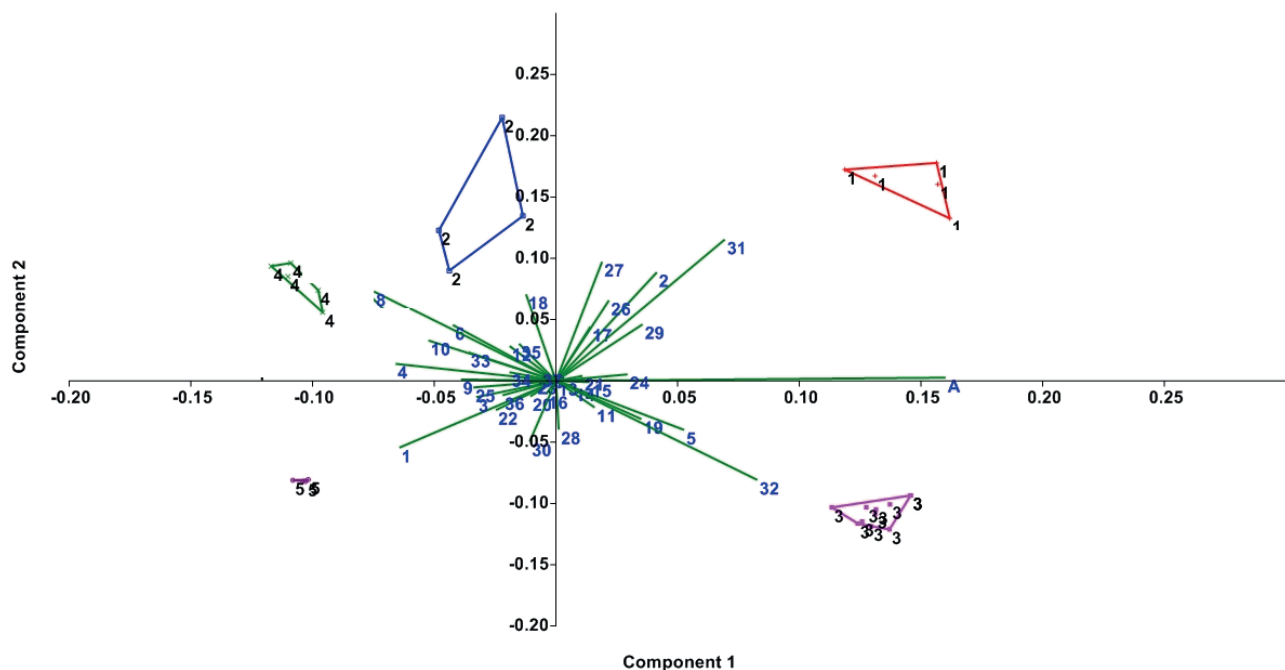
Figure 1. Morphological characters analysis of the *Malva* species by PCoA plot.

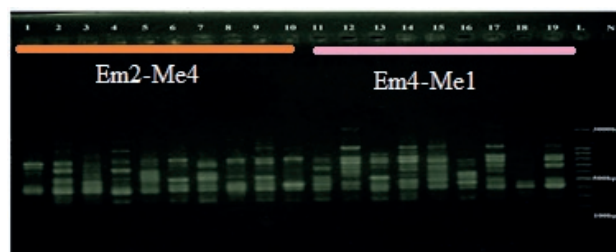**Table 3.** Analysis of molecular variance (AMOVA) of the studied species.

Source	df	SS	MS	Est. Var.	%	*ΦPT*
Among Pops	70	2701.394	77.782	10.166	66%	66%
Within Pops	10	111.449	390.19	27.833	34%	
Total	80	2875.807		37.060	100%	

df: degree of freedom; SS: sum of squared observations; MS: mean of squared observations; EV: estimated variance; *Φ*PT: proportion of the total genetic variance among individuals within an accession, (*P* < 0.001).

Figure 2. Electrophoresis gel of studied ecotypes from DNA fragments produced by SRAP profile; 1, 7: *Malva neglecta* 2,8: *Malva parviflora* 3,9: *Malva pusilla*. 4,10: *Malva sylvestris* 5,11: *Malva vericillata* 6,12: *Malva nicaeensis* = Ladder 100 bp.

Analysis of Molecular Variance results in significant genetic difference (*p* = 0.01) among *Malva* species. The majority of genetic variation occurred among species. AMOVA findings revealed that 66% of the total variation was between species and comparatively less genetic variation was recorded at the species level (Table 3). Genetic difference between *Malva* species was highlighted by genetic statistics (Nei's G_{ST}), as evident by significant *p* values i.e. Nei's G_{ST} (0.578, *p* = 0.01) and D_est values (0.829, *p* = 0.01) .

NJ tree and UPGMA clustering produced similar results therefore only NJ tree is presented and discussed (Figure 3). This result show that molecular characters studied can delimit *Malva* species in two different major clusters or groups. In general, two major clusters were formed in NJ tree (Fig. 3), 20 individual of *Malva nicaeensis* and *Malva aegyptia* formed a single cluster. Cluster II contained two sub-clusters, and most of individual *Malva pusilla*; *Malva sylvestris* and *Malva vericillata* formed cluster II. There were 50 individuals in this cluster.

We detected strong correlation between geographical and genetic distances (r = 0.45, *p*=0.0002) and gene flow ($N_{m)}$ score of 0.48 was reported among species.

Detailed information about genetic distances and genetic identity (Nei's) are described (Table not included). The findings suggested that there was the highest degree of genetic similarity (0.91) between *Malva vericillata* and *Malva nicaeensis*. On the contrary to this, *Malva pusilla* and *Malva aegyptia* (0.70) had lowest genetic resemblance.

The Evanno test ΔK =5 (Figure not included), showed the genetic details of the *Malva* species. According to STRUCTURE analysis, the *Malva* species are genetically differentiated due to different allelic structures (Figure not included). Limited gene flow results were supported by K-Means and STRUCTURE analyses too. We could not identify substantial gene flow among the *Malva* species. This result is in agreement with grouping we obtained with NJ tree (Figure 3), as these populations were placed close to each other. As evidenced by STRUCTURE plot based on admixture model, these shared alleles comprise very limited part of the genomes in these populations and all these results are in agreement in showing high degree of genetic stratification within *Malva* populations.
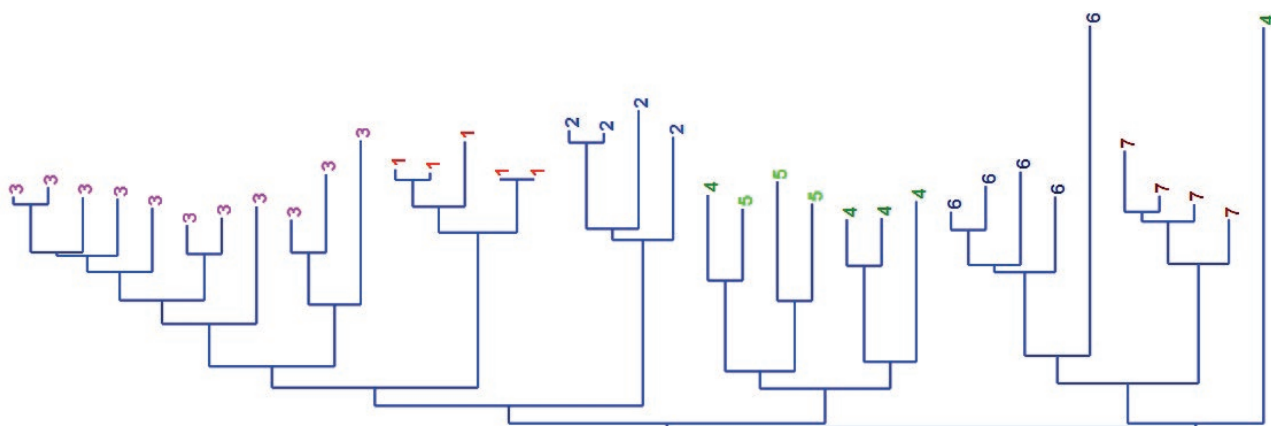
Figure 3. Neighbor-Joining tree of populations in *Malva* species based on SRAP molecular markers.

DISCUSSION

In the present study, we used morphological and molecular (SRAP) data to evaluate species relationships in *Malva*. Morphological analyses of *Malva* species showed that quantitative indicators (ANOVA test results) and qualitative characteristics are well differentiated from each other. PCA analysis suggests that morphological characters such as corolla shape, bract shape, calyx shape, calyx length, calyx width, calyx apex, calyx margins, bract length have the potentials to identify and delimitate *Malva* species. Principal component analysis results suggests the utilization of morphological characters to identify and delimitate *Malva* species. Morphological characters including corolla length, corolla width, corolla apex, leaf length and leaf width, leaf apex, leaf margins, leaf shape, leaf gland and bract margins play key role in plant systematics and taxonomy. Our work also highlighted the significance of morphological characters and molecular data to identify and study species genetic diversity. In general, genetic relationships obtained from SRAP data coincides with morphometric results. This is in accordance with the parameters of AMOVA and genetic diversity results. SRAP molecular markers detected clear genetic difference among species. These results indicate that SRAP have potentials to study plant systematics and taxonomy in *Malva* members.

Given the negative impact of biodiversity threats and overexploitation of *Malva* plant species in Iran, it is necessary to conduct genetic diversity studies on *Malva* species. Genetic diversity based studies pave our understanding to develop conservation strategies (Jia *et al.* 2020; Shi *et al.*, 2021; Zheng *et al.*, 2021; Zhu *et al.*, 2021). Genetic diversity studies are conducted through appropriate selection of primers and indexes including Polymorphic information content (PIC) and marker index (MI) are important indexes to fathom genetic variation in species (Wang *et al.*, 2021; Yin *et al.*, 2021; Zhao *et al.*, 2021). Common logic suggests that different makers have different abilities to assess genetic diversity, and usually, genetic diversity is linked with polymorphism (Sivaprakash et al. 2004).

In the present work, 5 *Malva* species were characterized with 5 SRAP markers. The results confirm the efficiency of microsatellite markers for fingerprinting purposes. Our results demonstrated that the PIC ranged from 0.11 (Em3-Me1) to 0.55 (Em3-Me4) for the 5 SRAP primers, with an average of 0.44 per primer. RP of the primers ranged from 11.23 (Em4-Me1) to 55.55 (Em3-Me1) with an average of 39.23 per primer.

Diversity study in Malva species

Malvaceous germplasm has been variously investigated by different molecular marker techniques but the earlier studies either focused on the comparison of the Malvaceae with other families in the order Malvales or to explore the genetic relationships and diversity within and among population and limited number of species in the same genus. Very little attention has been given to the analysis at interspecific and intergeneric levels. La Duke and Dobley (1995) has the only worth mentioning work in this regard. Their results showed that, the genetic relationships and diversity within and between 12 malvaceous species belonging to five genera are investigated by using the Amplified fragment length polymorphism (AFLP).

Shaheen et al., (2009) with used AFLP (Amplified fragment length polymorphism) marker to explore phenetic relationships and diversity within and between 13 Malvaceae species belonging to 5 different genera. Their primary objective of the study was to evaluate the taxonomic potential, usefulness and applicability of AFLP marker system to reconstruct genetic relationships at interspecific and intergeneric level in Malvaceae. Two primer pairs produced a total of 73 bands, of which 70 were polymorphic.

According to Celka et al (2010) two categories of DNA markers were used to determine genetic relationships among eight *Malva* taxa. A maximum parsimony analysis validated the division of the genus *Malva* into the sections *Bismalva* and *Malva*. The species classified into those sections formed separate clusters. *M. moschata* was a distinctive species in the section *Bismalva*, as confirmed by previous genetic research based on ITS and cpDNA sequence analyses. The applied markers revealed a very high level of genetic identity between *M. alcea* and *M. excisa* and enabled molecular identification of *M. alcea* var. *fastigiata*.

Jedrzejczyk and Rewers (2020) applied flow cytometry and inter simple sequence repeat polymerase chain reaction (ISSR-PCR) for fast and accurate species identification. Genome size estimation by flow cytometry was proposed as the first-choice method for quick accession screening. Out of the 12 tested accessions, it was possible to identify six genotypes based on genome size estimation, whereas all species and varieties were identified using ISSR markers. Flow cytometric analyses revealed that *Malva* species possessed very small (1.45–2.77 pg/2C), small (2.81–3.80 pg/2C), and intermediate (11.06 pg/2C) genomes, but the majority of accessions possessed very small genomes. The relationships between the investigated accessions showed the presence of two clus-

ters representing malvoid and lavateroid group of species. Their results showed that Flow cytometry and ISSR molecular markers can be effectively used in the identification and genetic characterization of *Malva* species.

CONCLUSIONS

The present study investigated the molecular variation of five species. Molecular and morphometric analysis confirmed morphological and genetical difference between *Malva* species. This was first attempt to assess genetic diversity through Sequence-related amplified polymorphism and morphometrics analysis in Iraq. Current study reported two major clusters. These two major groups were separated on the basis of genetic and morphological characters. The genetic similarities between three species was estimated from 0.70 to 0.91. Current study also reported correlation between genetic and geographical distances. This clearly indicated isolation mechanism envloved in the ecology of *Malva* species . Present results indicated the potential of sequence-related amplified polymorphism to assess genetic diversity and genetic affinitiy among *Malva* species. Current results have implications in biodiversity and conservation programs. Besides this, present results could pave the way for selecting suitable ecotypes for forage and pasture purposes in Iraq.

REFERENCES

Akçin, Ö.E.; Özbucak, T.B. (2006). Morphological, anatomical and ecological studies on medicinal and edible plant Malva neglectaWallr. (Malvaceae). Pak. J. Biol. Sci. 9, 2716–2719.

Blunden G, Patel AV, Armstrong NJ, Gorham J. (2001). Betaine distribution in the Malvaceae. Phytochemistry. 58:451e4.

Bi, D., C. Dan, M. Khayatnezhad, Z. Sayyah Hashjin, Z. Y. Ma (2021). Molecular Identification And Genetic Diversity In Hypericum L.: A High Value Medicinal Plant Using Rapd Markers Markers. Genetika *53*(1): 393-405.

Chen, Weimiao; Khayatnezhad, Majid; Sarhadi, Nima (2021). PROTOK GENA I STRUKTURA POPU-LACIJE KOD ALLOCHRUSA (CARYOPHYL-LOIDEAE, CARYOPHYLLACEAE) POMOCU MOLEKULARNIH MARKERA. Genetika ; *53*(2): 799-812.

El-Rjoob AO, Omari MN.(2009). Heavy metal contamination in Malva parviflora, (Malvaceae) grown in

soils near the Irbid-Amman high way. J Bot Environ Appl Sci. 4(4):433e41.

Evanno, G, S., Regnaut, J., Goudet (2005): Detecting the number of clusters of individuals using the software STRUCTURE: a simulation study. Mol. Ecol., *14*:2611-2620.

Frankham R (2005) Stress and adaptation in conservation genetics. J Evol Biol. 18(4):750-755.

Jia, Y., M. Khayatnezhad, s. mehri (2020). Population differentiation and gene flow in Rrodium cicutarium: A potential medicinal plant. Genetika 52(3): 1127-1144.

Jaccard P (1908) Nouvelles Recherches Sur la Distribution Florale. Bulletin de la Societe Vaudoise des Sciences Naturelles 44(163):223-270. https://doi.org/10.5169/seals-268384

Li, A. Mu, X. Zhao, X. Xu, J. Khayatnezhad, M. Lalehzari, R. 2021. Developing the non-dimensional framework for water distribution formulation to evaluate sprinkler irrigation; Irrigation And Drainage; 70,4; 659-667

Liu, S., Wang, Y., Song, Y., Khayatnezhad, M., & Minaeifar, A. A. 2021. Genetic variations and interspecific relationships in Salvia (Lamiaceae) using SCoT molecular markers. Caryologia, 74(3), 77-89.

Michael, P.J.; Steadman, K.J.; Plummer, J.A.(2009). The biology of Australian weeds 52. Malva parviflora L. Plant Prot. Q. 24, 2–9.

Ma, S., M. Khayatnezhad, A. A. Minaeifar. 2021. Genetic diversity and relationships among Hypericum L. species by ISSR Markers: A high value medicinal plant from Northern of Iran. Caryologia, 74(1): 97-107.

Peng, X., M. Khayatnezhad, L. Ghezeljehmeidan. 2021. Rapd profiling in detecting genetic variation in stellaria l. (caryophyllaceae). Genetika-Belgrade, *53*(1): 349-362.

Pandey A, Tomer AK, Bhandari D, Pareek S. 2008. Towards collection of wild relatives of crop plants in India. Genet Resour Crop Evol 55(2):187–202

Pritchard JK, Stephens M, Donnelly P. 2000. Inference of population structure using multilocus enotype Data. Genetics. 155:945–959.

Podani J (2000) Introduction to the exploration of multivariate data. Backhuyes, Leide, Netherlands.

Prevost A, Wilkinson MJ (1999) A new system of comparing PCR primers applied to ISSR fingerprinting of potato cultivars. Theoretical and Applied Genetics 98(1):107-112. https://doi.org/10.1007/s001220051046

Peakall R, Smouse PE (2006) GENALEX 6: Genetic Analysis in Excel. Population genetic software for teaching and research. Molecular Ecology Notes 6(1):288-295. https://doi.org/10.1111/j.1471-8286.2005.01155.x

Robarts DWH, Wolfe AD (2014) Sequence-related amplified polymorphism (SRAP) markers: A potential resource for studies in plant molecular biology. Applications in Plant Sciences 2(7):apps.1400017. https://doi.org/10.3732/apps.1400017

Roldán-Ruiz I, Dendauw J, Van Bockstaele E, Depicker A, De Loose M (2000) AFLP markers reveal high polymorphic rates in ryegrasses (Lolium spp.). Molecular Breeding 6(2): 125-134. https://doi.org/10.1023/A:1009680614564

Ray, M.F. (1995).Systematics of Lavatera and Malva (Malvaceae, Malveae) – A new perspective. Plant Syst. Evol. 198, 29–53. [CrossRef]

Si, X., L., Gao, Y. Song, M, Khayatnezhad, A.A. Minaeifar 2020. Understanding population differentiation using geographical, morphological and genetic characterization in *Erodium cicunium*. Indian J. Genet., 80(4): 459-467.

Shi, B., Khayatnezhad, M., Shakoor, A. 2021. The interacting effects of genetic variation in Geranium subg. Geranium (Geraniaceae) using scot molecular markers. Caryologia, 74(3), 141-150.

Wang, C., Y. Shang, M. Khayatnezhad 2021. Fuzzy Stress-based Modeling for Probabilistic Irrigation Planning Using Copula-NSPSO. Water Resources Management. 35, 4943–4959

Wang, J., Ye, Q., Zhang, T., Shi, X., Khayatnezhad, M., Shakoor, A. 2021. Palynological analysis of genus Geranium (Geraniaceae) and its systematic implications using scanning electron microscopy. Caryologia, 74(3), 31-43.

Wu Y-G, Guo Q-S, He J-C, Lin Y-F, Luo L-J, Liu G-D (2010) Genetic diversity analysis among and within populations of Pogostemon cablin from China with ISSR and SRAP markers. Biochemical Systematics and Ecology 38(1):63-72. https://doi.org/10.1016/j.bse.2009.12.006

Yeh FC, Yang R, Boyle T (1999). POPGENE. Microsoft Windows-based freeware for population genetic analysis. Release 1.31. University of Alberta, 1-31.

Yin, J., M. Khayatnezhad, A. Shakoor 2020. Evaluation of genetic diversity in Geranium (*Geraniaceae*) using rapd marker. Genetika, 53(1): 363-378.

Zheng, R., S. Zhao, M. Khayatnezhad, S, Afzal Shah 2021. Comparative study and genetic diversity in Salvia (Lamiaceae) using RAPD Molecular Markers. Caryologia, 74(2): 45-56.

Zhu, P., H. Saadati, M. Khayatnezhad. 2021. Application of probability decision system and particle swarm optimization for improving soil moisture content. Water Supply.

Zhao Y, Wang H, Liang W, Khayatnezhad, M, Faisal. 2021. Genetic Diversity And Relationships Among Salvia Species By Issr Markers; Genetika-Belgrade, 53(2): 559-574

Zhu, K., L. Liu, S. Li, B. Li, M. Khayatnezhad and A. Shakoor. 2021. "Morphological method and molecular marker determine genetic diversity and population structure in *Allochrusa*." Caryologia 74(2): 121-130.

Caryologia

International Journal of Cytology,
Cytosystematics and Cytogenetics

ORCID
IS: 0000-0001-6548-8535
HC: 0000-0002-8059-2397
HO: 0000-0002-4673-0696
MS: 0000-0001-8060-2842
PS: 0000-0002-9253-5381

Nuclear DNA 2C-values for 16 species from Timor-Leste increases taxonomical representation in tropical ferns and lycophytes

Inês da Fonseca Simão[1], Hermenegildo Ribeiro da Costa[1,2,3], Helena Cristina Correia de Oliveira[1,2], Maria Helena Abreu Silva[1,2], Paulo Cardoso da Silveira[1,2,*]

[1] *Department of Biology, University of Aveiro, 3810-193 Aveiro, Portugal*
[2] *CESAM-Centre for Environmental and Marine Studies, Department of Biology, University of Aveiro, 3810-193 Aveiro, Portugal*
[3] *Faculty of Education, Arts and Humanities, National University Timor Lorosa'e (UNTL), Avenida Cidade de Lisboa, Dili, East Timor*
* Corresponding author. E-mail: psilveira@ua.pt

Abstract. Knowledge regarding genome size allows us to infer relationships between taxa, address questions related to systematics and contribute to biodiversity studies. However, currently, less than 3% of the described Pteridophyta species have genome size estimates reported in databases, and only around one third of these are tropical species, although the tropics are home of 86% of fern diversity. The region of Timor-Leste, included in one of the 25 hotspots of biodiversity, is considered one of the richest areas of the world in terms of pteridophyte species. Nonetheless, biodiversity-driven research focused on this territory's biodiversity is scarce. This study presents novel 2C-values for 15 species of ferns collected in Timor-Leste, using flow cytometry. Furthermore, one species of the lycophyte *Palhinhaea cernua* (L.) Vasc. & Franco, was also studied and its estimated genome size compared to a previous report. Estimates ranged from 10.45 pg in *Selliguea feei* Bory to 29.7 pg in *Microsorum punctatum* (L.) Copel, and are considered medium-size genomes. The data was compared with previous reports for closely related species. These are the first 2C-values for two families and seven genera of ferns, increasing the number of pteridophytes with reported C-values from 292 to 307.

Keywords: genome size, chromosome, cytogenetics, DNA amount, nuclear DNA content, Malesia, geographical distribution.

INTRODUCTION

Information regarding genome size plays a fundamental role in understanding a species' evolutionary history and is a tool that allows us to infer relationships between taxa, address questions related to cellular and developmental biology and systematics, among others, and contributes to biodiversity studies (Leitch 2005; Kumar et al. 2011). The considerable differences

in nuclear DNA content across species can be related to adaptive features, which shows that genome size can be under selective pressure and its variations may be related to the evolutionary history of a given group (Ohri 1998). Currently, flow cytometry is the main technique used to obtain information related to species DNA C-value (Dolezel 2005). However, despite the importance of these studies, and the recent efforts concerning information about genome size in plants, there is still a substantial gap in knowledge, with only a very small portion of species studied, and more research is required.

The majority of values reported in the Plant DNA C-value database (Release 7.1, April 2019:https://cvalues.science.kew.org/) (Leitch et al. 2019) belong to angiosperms. The 2C-value for 10.770 species of angiosperms is known, corresponding to 3.3% of their global diversity (Antonelli et al. 2020). Pteridophytes are even more under-represented, with only 292 species reported in the database. These numbers account for 2.45% of the 11,916 species of pteridophytes described (PPG 2016). In 2001, Bennet & Leitch set the goal of obtaining the C-value for 200 pteridophytes species by 2005, with a special focus on those that maximize systematic and geographic representation (Bennet and Leitch 2001). Although this goal was met, further studies regarding this group are fundamental, since the pteridophytes represent an important evolutionary transition between bryophytes and spermatophytes and, as such, are critical to our understanding of how DNA content has evolved across land plants (Bainard et al. 2011). Furthermore, since the laboratories adequately equipped to make 2C-values estimation are mostly located in temperate climate areas, with more difficult access to tropical fern species, we suspected such species would be underrepresented in the Plant DNA C-value database. Yet, pteridophyte diversity in the tropics is significantly higher than in any other region of the globe. Estimates point to the existence of 4500 species of ferns and lycophytes in Southeast Asia, more than twice the number of species of the entire Holarctic Kingdom (Moran 2008). At the same time, the region of Timor-Leste, located in Southeast Asia, is included in the biogeographic region of Malesia, which is considered one of the richest areas of the world in terms of tropical pteridophyte species diversity (Ebihara and Kuo 2012). Additionally, Timor-Leste is included in Wallacea, an area classified as one of the 25 hotspots of biodiversity identified by Myers et al. (2000) as a priority of conservation at a global scale. Despite the rich biological patrimony of Timor-Leste, research focused on the country's biodiversity and genetic resources is lacking, mainly due to the military occupation of the territory that took place between 1975 and 1999 (Bouma and Kobryn 2004). In this sense, better coverage of pteridophytes nuclear DNA values data in this territory is crucial to understand the mechanisms behind genome size evolution and their relationship with geographic and ecological factors (Dagher-Kharrat et al. 2013).

Therefore, the aims of this paper are: 1. to check what percentage of genome size data from tropical pteridophytes has been estimated, comparing with other biogeographic regions; and 2. to expand knowledge about genome sizes of tropical fern species occurring in Timor-Leste.

MATERIALS AND METHODS

Plant material

Prior to the field work, a search was conducted in the Plant DNA C-value database to establish which pteridophytes species, known to occur in Timor-Leste, had already 2C-values estimations published, and which had not. From the latter list, those species with populations that could more easily be sampled were selected as target species for this study (Table 1). Leaves of 15 ferns and one lycophyte were collected from several field locations in Timor-Leste (Table 1). These samples were kept fresh (at 0-5ºC) for a period no longer than a week and used for flow cytometry analysis. Voucher specimens were prepared and kept in the herbaria of the University of Aveiro (AVE) and Naturalis Biodiversity Center (L). Duplicates were also kept at the National University of East Timor (UNTL, Díli, Timor-Leste).

Nuclear DNA content estimation

The nuclear DNA content of fresh leaf samples was assessed using flow cytometry, currently the most used technique to estimate C/2C-value in plants for its simplicity, accuracy, convenience, and speed (Galbraith et al. 1983, 2009). The methodology used followed Loureiro et al. (2007), which included the preparation of nuclear suspensions by chopping 50 mg of leaf sample tissue and 50 mg of internal standard leaves, *Vicia faba* "Inovec" (2C= 26.90 pg; Dolezel, Sgorbati and Lucretii 1992) or *Pisum sativum* "Ctirad" (2C= 9.09 pg; Dolezel et al. 1992), with a razor blade in a glass Petri dish containing 1 mL of WPB isolation buffer (200 mM Tris.HCl, 4mM $MgCl_2.6H_2O$, 2 mM EDTA $Na_2.2H_2O$, 86 mM NaCl, 10 mM sodium metabisulfite, 1% PVP-10, 1% (v/v) Triton X-100, pH 7.5; Loureiro et al. 2007). The nuclear solution was then filtered through a nylon net of 50 μm, and 50 μg.mL^{-1} of propidium iodide (PI, Sigma-Aldrich, St. Lou-

Table 1. Scientific names and localities of samples collected for this study. Voucher specimens are kept in the Herbarium of the University of Aveiro (AVE) and of the Naturalis Biodiversity Center (L). Family circumscription according with PPG (2016).

Taxon	Family	Localities in Timor-Leste
Lycopodiophyta		
Palhinhaea cernua (L.) Vasc. & Franco	Lycopodiaceae	Ainaro, roadside between Maubisse and Turiscai, [8°49'33" S, 125°38'10" E], *Costa et al.* 254 (AVE)
Pteridophyta		
Calochlaena javanica (Blume) M.D.Turner & R.A.White	Dicksoniaceae	Ainaro, roadside from Maubisse to Turiscai, [8°49'22" S, 125°37'01" E], *Costa et al.* 245 (AVE, L.3959675)
Pityrogramma calomelanos (L.) Link	Pteridaceae	Ainaro, roadside between Maubisse and Turiscai, [8°49'33" S, 125°38'10" E], *Costa et al.* 253 (AVE)
Adiantum philippense L.	Pteridaceae	Liquiçá, roadside between Tibar and Faiten, [8°36'59" S, 125°29'09" E], *Costa et al.* 8 (AVE, L.3959700)
Pteris ensiformis Burm.	Pteridaceae	Manufahi, roadside of Laclo, [8°51'28" S, 125°41'36" E], *Costa et al.* 320 (AVE)
Blechnopsis orientalis (L.) C.Presl	Blechnaceae	Ainaro, roadside from Maubisse to Turiscai, [8°49'22" S, 125°37'01" E], *Costa et al.* 244 (AVE)
Diplazium esculentum (Retz.) Sw.	Athyriaceae	Aileu, from Díli to Aileu, after the crossroad to Remexio and Remexio, [8°37'05" S, 125°38'25" E], *Costa et al.* 195 (AVE, L.3959688)
Tectaria melanocaulos (Blume) Copel.	Tectariaceae	Aileu, Asumau, [8°37'19" S, 125°38'37"], *Costa et al.* 200 (AVE, L.3959765)
Oleandra musifolia (Blume) C.Presl	Oleandraceae	Ainaro, roadside between Maubisse and Turiscai, [8°48'57" S, 125°38'39" E], *Costa et al.* 258 (AVE)
Goniophlebium subauriculatum (Blume) C.Presl	Polypodiaceae	Viqueque, on the Waibua forest at foothills of Mundo Perdido mountain, [8°43'59" S, 126°22'10" E], *Costa et al.* 303 (AVE)
Microsorum punctatum (L.) Copel.	Polypodiaceae	Viqueque, on the Waibua forest at the foothills of Mundo Perdido mountain, [8°43'59" S, 126°22'10" E], *Costa et al.* 307 (AVE)
Microsorum scolopendria (Burm.f.) Copel.	Polypodiaceae	Viqueque, on the Waibua forest at the foothills of Mundo Perdido mountain, [8°43'59" S, 126°22'10" E], *Costa et al.* 301 (AVE)
Platycerium bifurcatum subsp. *willinckii* (T.Moore) Hennipman & M.C.Roos	Polypodiaceae	Díli, Dare, [8°35'38" S, 125°34'07" E], *Costa et al.* 84 (AVE, L.3959789)
Pyrrosia lanceolata (Wall.) Farw.	Polypodiaceae	Aileu, roadside between Aileu and Maubisse, [8°48'16" S, 125°35'31" E], *Costa et al.* 238 (AVE)
Pyrrosia longifolia (Burm.f.) C.V.Morton	Polypodiaceae	Viqueque, roadside of Urulita, [8°46'21" S, 126°22'11" E], *Costa et al.* 290 (AVE)
Selliguea feei Bory	Polypodiaceae	Ainaro, Maubisse - Turiscai, at Rita-Uruho, [8°49'22" S, 125°37'01" E], *Costa et al.* 243 (AVE)

is, MO, USA) and 50 µg.mL^{-1} of RNAse (Sigma-Aldrich, St. Louis, MO, USA) were added to the sample, to stain nuclear DNA and prevent staining of double stranded RNA, respectively. Samples were analyzed within a 10 min period on an Attune® Acoustic Focusing Cytometer (TermoFisher Scientific) equipped with a 488 nm laser.

For each sample, at least 5,000 nuclei were analyzed. As a quality control, nuclear DNA content estimates were only considered when the coefficient of variation of G_0/G_1 peaks (CV_{peak}) were below 5%. Samples with higher CV_{peak} values were discarded and a new sample was prepared.

For most of the taxa, three to five individuals were analyzed, but for *Selliguea feei* and *Tectaria melanocau-*

los, only one individual for each of the species survived the time between sampling in Timor and analysis in Aveiro. The number of individuals measured for each population is provided in Table 1.

Statistical analysis

Descriptive statistics were calculated for each taxa studied namely, mean, standard deviation (SD), coefficient of variation (CV), and minimum and maximum values of the holoploid genome size (2C, pg).

Chromosome number

The median of the chromosome numbers for 14 taxa was obtained from the online Chromosome Counts Database (CCDB) (Rice et al. 2015).

Floristic kingdoms versus *2C values analysis*

The floristic kingdom's classification by Takhtajan (1986) was applied to the Pteridophyta taxa whose DNA C-values are available in the Plant DNA C-value database. For that, Global Biodiversity Information Facility (GBIF, at https://www.gbif.org/, January 2022) was consulted to establish each species' main occurrence. Finally, the distribution of species listed in the Plant DNA C-value database by each floristic kingdom was compared with the equivalent distribution of the total World number of Pteridophyte species given by Moran (2008). For this comparison, the Paleotropical and the Cape floristic kingdoms had to be included in the same group, because Moran (2008) gives a single total number for Africa, without segregating the Cape floristic kingdom. The same was not adopted for the Holantarctic kingdom, because Moran (2008), provides separate figures for New Zealand, which allows some separation from other kingdoms. In South America no separation was possible between the Holantarctic and the Neotropical kingdoms, but since the number of Neotropical species should be much greater than the Holantarctic species present in the region, we assumed that the error would not be critical.

RESULTS

DNA content estimates were obtained for the 16 samples, 15 of them representing taxa with no previous 2C-value reported. These estimates, as well as the chromosome median *2n* value that are described in literature, are presented in Table 2. The 2C DNA content ranged from 10.45 pg in *Selliguea feei* Bory, with the *Vicia faba* standard, to 29.7 pg in *Microsorum punctatum* (L.) Copel. with the *Pisum sativum* standard. The average 2C-value for Polypodiopsida was 20.62 pg, and for Lycopodiophyta, represented only by one taxon, the 2C-value was 25.65 pg.

The coefficients of variation (CVs) for the samples varied between 3.7% and 6.7%.

The list of Pteridophyte taxa for which nuclear DNA 2C-values have been published in the Plant DNA C-value database (Leitch 2019) is presented in the Supplementary Material 1, alongside with the Takhtajan's floristic kingdoms (Takhtajan 1986) embraced by

their geographical distributions ranges. This information is summarized in Table 3, alongside with the total world estimated number, and percentage, of Pteridophyte species for each floristic kingdom, according with Moran (2008). We can see in this table, that the Paleotropical+Cape kingdoms, together with the Neotropical floristic kingdoms, with 45% and 42%, respectively, include the vast majority of the world's pteridophyte diversity (87%). Contrariwise, the most diverse group of pteridophytes whose nuclear DNA 2C-values are known is the Holarctic, with 44%, followed by the Paleotropical+Cape, with only 23% and the Neotropical with 18%. With this study, the percentages of Holarctic species is reduced to 42%, and the percentage of species from Paleotropical+Cape area increases to 25%.

DISCUSSION

In spite of the long journey between the field in Timor-Leste and the cytometry laboratory in Aveiro, where the analysis was done, we succeed to analyze, at least, three individuals for 14 of the 16 species, and five/six, for nine of the 16 species.

The higher intraspecific variations detected are, most likely, related to difficulties associated to the flow cytometry technique, since the easiness of obtaining data differs between the taxa, as mentioned by Obermayer, et al. (2002).

Following Leitch, Chase & Bennet (1998) genome size classification, all taxa have "intermediate" genomes ($7 < 2C \leq 28$ pg). The median value established for genome size in ferns is 22.8 pg/2C and it has been related, partially, to variation in post-polyploidization processes- such as additional chromosomes and DNA arising from whole genome duplications-, since diploidization is not linked with genome downsizing in ferns in opposition to angiosperms, a group with smaller genomes (median= 3.4 pg/2C) (Liu et al. 2019). Regarding the lycophytes, the median 2C-value for the group is 0.26 pg (Liu et al. 2019), corresponding to a very small genome (≤ 2.8 pg) (Leitch et al. 1998). Despite the 2C-value previously reported in the literature of 2.75 pg for *Palhinhaea cernua* (L.) Vasc. & Franco (Kuo et al. 2016), the 2C-value estimated for this species is 25.65 pg, corresponding to the "intermediate" category and to the highest genome size in the Lycopodiaceae family reported until present, more than twice that of *Huperzia lucidula* (Michx.) Trevis., which has 11.28 pg (Bainard et al. 2011) and was the previous highest value reported. Considering that the coefficient of variation for this estimate is 5.5%, it doesn't seem likely that the 2C-value for *P. cernua* was

Table 2. Mean 2C-value estimates (pg) for 15 fern species and 1 lycophyte collected in East-Timor, with standard deviation (SD), minimum and maximum values, average coefficient of variation (CV %) for each taxon. Family circumscription according with PPG (2016). Estimates obtained using the *Vicia faba* standard (2C= 26.90) are identified with "*". The remaining measurements were obtained using the *Pisum sativum* standard (2C= 9.09 pg). Reported chromosome number (median n value) for the taxa available is also presented, according to the CCDB database (release 1.58, http://ccdb.tau.ac.il/).

Taxon	Family	Median 2n value	Genome size (2C, pg)				Average CV (%)	n. samples
			Mean ± SD	Min.	Max.			
Lycopodiophyta								
Palhinhaea cernua (L.) Vasc. & Franco	Lycopodiaceae	208, 220, 272, 312, 330, 340, 416	25.65 ± 0.43	25.32	26.32		5.52	5
Pteridophyta								
Calochlaena javanica (Blume) M.D.Turner & R.A.White	Dicksoniaceae	?	11.41 ± 0.11	11.32	11.43		4.78	5
Pityrogramma calomelanos (L.) Link	Pteridaceae	232, 240	26.41 ± 0.36	26.12	26.85		6.72	4
Adiantum philippense L.		60, 90	21.92* ± 2.3	18.48	23.29		4.03	4
Pteris ensiformis Burm.		58, 87-88, 116, 168, 185	19.15* ± 0.55	18.71	19.81		4.71	5
Blechnopsis orientalis (L.) C.Presl	Blechnaceae	?	13.57* ± 0.11	13.43	13.61		5.91	5
Diplazium esculentum (Retz.) Sw.	Athyriaceae	82	22.68 ± 0.70	22	23.57		5.88	4
Tectaria melanocaulos (Blume) Copel.	Tectariaceae	?	24.68	-	-		3.69	1
Oleandra musifolia (Blume) C.Presl	Oleandraceae	80	13.65* ± 0.08	13.57	13.75		6.11	5
Goniophlebium subauriculatum (Blume) C.Presl		72	21.06* ± 0.38	20.59	21.52		4.98	5
Microsorum punctatum (L.) Copel.		72	29.72 ± 0.44	29.43	30.23		4.56	3
Microsorum scolopendria (Burm.f.) Copel.	Polypodiaceae	36**	24.55 ± 1.92	21.14	25.76		4.53	5
Platycerium bifurcatum subsp. *willinckii* (T.Moore) Hennipman & M.C.Roos		74	28.47 ± 2.88	23.74	30.8		3.93	5
Pyrrosia lanceolata (Wall.) Farw.		74	23.73 ± 0.31	23.47	24.16		5.34	4
Pyrrosia longifolia (Burm.f.) C.V.Morton		74	28.79 ± 3.58	26.06	35.7		4.96	6
Selliguea feei Bory		74	10.45*	-	-		5.44	1

** n value presented, no 2n value reported.

negatively influenced by artefacts such as the presence of interfering secondary metabolites (Hanusová et al. 2014). This novel result shows that genome size within the Lycopodiaceae family may be more variable than what was thought until now In fact, the chromosome numbers reported for this species varies from n=34 to 2n=208-416 (Rice et al. 2015).

Comparing the 2C-value of *Diplazium esculentum* (Retz.) Sw. (22.68 pg) with *Diplazium pycnocarpon* (Sprengel) M. Broun (12.63 pg), the only other species of the same genus that has been screened for its genome size by Bainard et al. (2011), the 2C-value differs by approx. 10 pg. This variation shows that even within the same genus, genome size may vary greatly, regardless of the two species' chromosome number being very similar, with *D. esculentum* (2n=82) and *D. pycnocarpon* (2n=80). The same conclusion can be drawn when comparing our estimate for *Adiantum philippense* L., (2C= 21.9 pg) with previous work on the genus: 2C-value estimates reported for *Adiantum pedantum* L. are 10.16 pg (Bainard et al. 2011) and for *Adiantum aleuticum* (Rupr.) C. A. Paris are 11.42 pg (an approx. difference of 10.5 pg) (Clark et al. 2016). The 2C-value discrepancy between *Adiantum* species may be related, most probably, to differences in chromosome numbers between taxa, since both 2n=60 and 2n=90 have been reported for *A. philippense* in literature. Although 2n=60 is similar to chromosome number for *A. pedantum* and *A. aleuticum* (2n=58), a 2n=90 could be a reason to explain this variation.

The 2C-value discrepancy between *Adiantum* species may also be related, in part, to the different geographical origin of the material. Some evidence points towards the prevalence of smaller genomes in plant species that exist in harsher, drier, environments, with shorter growing seasons (Knight, Molinari and Petrov 2005). But checking this would require investigations out of the scope of this paper.

What we could contribute was towards improving the representation of the most diverse phytogeographical kingdoms for this group (Table 3), following Moran's (2008) suggestion that this group of organisms shows a dominant pattern called "the latitudinal diversity gradient", which means that species diversity in ferns increases from the pole towards the equator (Moran 2008). Despite this pattern, almost half of the studied species found in the Plant DNA C-value database (Leitch et al. 2019) belong to the Holarctic kingdom. Therefore, an already understudied group of plants in terms of genome size lacks, to a great extent, estimates from species of the most representative phytogeographical kingdoms for this group, which we tried to counteract with the new data presented in this study (Table 3).

CONCLUSIONS

The present work includes novel data that contributes to the knowledge regarding genome size of 15 species of ferns and 1 species of lycophytes. Our data increases the taxonomic representation of DNA content in pteridophytes databases by two families- Blechnaceae and Oleandraceae-, as well as seven genera (*Blechnopsis*, *Goniophlebium, Microsorum, Palhinhaea*, *Pityrogramma*, *Pyrrosia* and *Selliguea*). Furthermore, the representation of Paleotropical fern species has increased by 2%. However, with almost 12.000 species of pteridophytes described to date, further work focused on the DNA content of more lycophyte and fern species, especially from tropical regions, is crucial to expand taxonomic representation and fill in the phylogenetic gaps within the group.

Although we could not perform chromosome counts alongside with the 2C value estimations, this should be a future target, allowing to draw more complete conclu-

Table 3. Distribution of the number and percentage of species of Pteridophytes recognized by each of Takhtajan's floristic kingdoms comparing with the same distribution in terms of species with published DNA C-values including the contribution of this study.

Takhtajan's floristic kingdoms	No. (%) of species estimated*	No. (%) of species with known DNA C-values	No. of species added in this study**	Current No. (%) of species with known DNA C-values
Holartic	1470 (9.4)	190 (44)		188 (42)
Neotropical	6500 ((41.7)	76 (18)	4	80 (18)
Paleotropical + Cape	6980 (44.7)	94 (23)	16	110 (25)
Australian	456 (2.9)	37 (8)	5	42 (9)
Holantarctic	193 (1.2)	29 (7)		29 (6)
Total	15599 (100)	429 (100)	25	454 (100)

* Numbers of species estimated to occur taken from Moran (2008: 369); ** the numbers presented exceed the 16 species analyzed, because several of them are distributed among more than one floristic kingdom, as it was also adopted by Moran (2008).

sions about the genome of the studied species, namely, concerning ploidy levels.

Bearing this in mind, in spite of the relatively modest contribution in terms of species numbers (not so modest when we consider the number of new families and genera), this paper increases the representation of tropical Pteridophyte diversity whose nuclear 2C-values are known, and highlights that further studies on genome size in ferns are crucial, especially in species from areas that are considered hotspots of tropical fern biodiversity, such as Timor-Leste. The lack of studies on the country's biodiversity coupled with the human impact in the region, makes the execution of these studies even more important, since genome size data is basic information for an appropriate management and conservation of the plant genetic resources of the area.

ACKNOWLEDGEMENTS

REFERENCES

Antonelli A, Fry C, Smith RJ, Simmonds MSJ, Kersey PJ, Pritchard HW, Abbo MS, Acedo C, Adams J, Ainsworth AM, Allkin B, et al. 2020. State of the world's plants and fungi 2020. Royal Botanic Gardens, Kew. DOI: https://doi.org/10.34885/172

Bainard J, Henry, TA, Bainard LD, Newmaster SG. 2011. DNA content variation in monilophytes and lycophytes: large genomes that are not endopolyploid. Chromosome Res. 19(6): 763-775. DOI: https://doi.org/10.1007/s10577-011-9228-1

Bennett M, Leitch IJ. 1995. Nuclear DNA Amounts in angiosperms. Ann Bot. 76(2), 113–176. DOI: https://doi.org/10.1006/anbo.1995.1085

Bennett M, Leitch IJ. 2001. Nuclear DNA amounts in pteridophytes. Ann Bot. 87(3): 335-345. DOI : https://doi.org/10.1006/anbo.2000.1339

Bouma GA, Kobryn HT. 2004. Change in vegetation cover in East Timor, 1989-1999. Nat Resour Forum. 28(1): 1-12. DOI: https://doi.org/10.1111/j.0165-0203.2004.00067.x

Clark J, Hidalgo O, Pellicer J, Liu H, Marquardt J, Robert Y, Christenhusz M, Zhang S, Gibby M, Leitch IJ, Schneider H. 2016. Genome evolution of ferns: evidence for relative stasis of genome size across the fern phylogeny. New Phytol. 210(3): 1072-1082. DOI: https://doi.org/10.1111/nph.13833Dagher-Kharrat MB, Abdel-Samad N, Douaihy B, Bourge M, Fridlender A, Siljak-Yakovlev S, Brown SC. 2013. Nuclear DNA C-values for biodiversity screening: Case of the Lebanese flora. Plant Biosyst. 147(4): 1228-1237. DOI: https://doi.org/10.1080/11263504.2013.861530

Dolezel J. 2005. Plant DNA flow cytometry and estimation of nuclear genome size. Ann Bot. 95(1): 99–110. DOI: https://doi.org/10.1093/aob/mci005

Dolezel J, Sgorbati S, Lucretii S. 1992. Comparison of three DNA fluorochromes for flow cytometric estimation of nuclear DNA content in plants. Physiol Plant. 85(4): 625-631. DOI: https://doi.org/10.1111/j.1399-3054.1992.tb04764.x

Ebihara A, Kuo LY. 2012. East and Southeast Asian pteridophyte flora and DNA barcoding. In: Nakano S., Yahara T., Nakashizuka T. (eds) The Biodiversity Observation Network in the Asia-Pacific Region. Ecological Research Monographs. Tokyo (TK): Springer. DOI: https://doi.org/10.1007/978-4-431-54032-8_2

Galbraith DW. 2009. Simultaneous flow cytometry quantification of plant nuclear DNA contents over the full range of described angiosperm 2C values. Cytometry A. 75A(8): 692-698. DOI: https://doi.org/10.1002/cyto.a.20760

Galbraith DW, Harkins KR, Maddox JM, Ayres NM, Sharma DP, Firoozabady E. 1983. Rapid flow cytometric analysis of the cell cycle in intact plant tissues. Science. 220(4601): 1049–1051. DOI: https://doi.org/10.1126/science.220.4601.1049

Hanusová K, Ekrt L, Vít P, Kolár F, Urfus T. 2014. Continuous morphological variation correlated with genome size indicates frequent introgressive hybridization among *Diphasiastrum* species (lycopodiaceae) in central Europe. Plos One. 9(6): e99552 DOI: https://doi.org/10.1371/journal.pone.0099552

Knight CA, Molinari NA, Petrov DA. 2005. The large genome constraint hypothesis: evolution, ecology and phenotype. Ann Bot. 95(1): 177-190. DOI: https://doi.org/10.1093/aob/mci011

Kuo LY, Huang YJ, Chang JY, Chiou WL, Huang YM. 2017. Evaluating the spore genome sizes of ferns and lycophytes: a flow cytometry approach. New Phytologist. 213: 1974-1983. DOI: 10.1111/nph.14291

Kumar PP, Turner IM, Nagaraja R, Arumuganathan K. 2011. Estimation of nuclear DNA content of various

bamboo and rattan species. Plant Biotechnol Rep. 5(3): 317–322. https://doi.org/10.1007/s11816-011-0185-0

Leitch IJ. 2005. Evolution of DNA amounts across land plants (Embryophyta). Ann Bot. 95(1): 207–217. DOI: https://doi.org/10.1093/aob/mci014

Leitch IJ, Chase MW, Bennet MD. 1998. Phylogenetic analysis of DNA C-values provides evidence for a small ancestral genome size in flowering plants. Ann Bot. 82(Supplement A): 85-94. DOI: https://doi.org/10.1006/anbo.1998.0783

Leitch IJ, Johnston E, Pellicer J, Hidalgo O, Bennett MD. 2019. Pteridophyte DNA C-values database (release 7.1, Apr 2019) https://cvalues.science.kew.org/

Liu H, Ekrt L, Koutecky P, Pellicer J, Hidalgo O, Marquardt J, Pustahija F, Ebihara A, Siljak-Yakovlev S, Gibby M, Leitch I, Schneider H. 2019. Polyploidy does not control all: Lineage-specific average chromosome length constraints genome size evolution in ferns. J Syst Evol. 57(4): 418-430. DOI: https://doi.org/doi.org/10.1111/jse.12525

Loureiro J, Rodriguez E, Dolezel J, Santos C. 2007. Two new nuclear isolation buffers for plant DNA flow cytometry – a test with 37 species. Ann Bot. 100:875–888.

Moran RC. 2008. Diversity, biogeography, and floristics. In T. A. Ranker & C. H. Haufler (Eds.) Biology and Evolution of Ferns and Lycophytes. New York (NY): Cambridge, 367-394.

Myers N, Mittermeier R, Mittermeier C, da Fonseca GAB, Kent J. 2002. Biodiversity hotspots for conservation priorities. Nature. 403(6772): 853–858. DOI: https://doi.org/doi.org/10.1038/35002501

Obermayer R, Leitch IJ, Hanson L, Bennet MD. 2002. Nuclear DNA C-values in 30 species double the familial representation in pteridophytes. Ann Bot. 90(2): 209-217. DOI: https://doi.org/10.1093/aob/mcf167

Ohri D. 1998. Genome size variation and plant systematics. Ann Bot. 82(Supplement 1), 75–83. DOI:10.1006/anbo.1998.0765

Pellicer J, Leitch IJ. 2013. The application of flow cytometry for estimating genome size and ploidy level in plants. Molecular Plant Taxonomy. 1115: 279–307. DOI: https://doi.org/10.1007/978-1-62703-767-9_14

Plant DNA C-value database. 2001-. Release 7.1. Royal Botanic Gardens, Kew (UK): [updated 2019 April; accessed 2021 Oct] https://cvalues.science.kew.org/)

[PPG] Pteridophyte Phylogeny Group. 2016. A community-derived classification for extant lycophytes and ferns. J Syst Evol. 54(6): 563–603. DOI: https://doi.org/10.1111/jse.12229.

Rice A, Glick L, Abad S, Einhorn M, Kopelman NM, Salman-Minkov A, Mayzel J, Chay O, Mayrose I. 2015. The Chromosome Counts Database (CCDB) – a community resource of plant chromosome numbers. New Phytol. 206(1): 19-26.

Takhtajan A. 1986. Floristic regions of the world. Berkley and Los Angeles: University of California Press (CA)

Wagner FS. 1992. Cytological problems in *Lycopodium* Sens. Lat. Ann Mo Bot Gard. 79(3): 718-729. DOI: https://doi.org/10.2307/2399761

Supplementary Material 1. Distribution of Pteridophyta taxa with studied DNA C-value (from https://cvalues.science.kew.org/) among Takhtajan's Floristic Kingdoms (1986).

Genus	Species	Subspecies/Variety	Phytogeographical region(s)
Acrostichum	*aureum*		Neotropical, Palaeotropical, Australian
Adiantum	*aleuticum*		Holarctic
Adiantum	*capillus-veneris*		Holarctic, Neotropical, Palaeotropical, Australian, Holantarctic
Adiantum	*pedatum*		Holarctic
Adiantum	*venustum*		Holarctic
Alsophila	*spinulosa*		Holarctic, Palaeotropical
Amauropelta	*bergiana*	var. *bergiana*	Palaeotropical
Anemia	*collina*		Neotropical
Anemia	*phyllitidis*		Neotropical
Anemia	*rotundifolia*		Neotropical
Anemia	*tomentosa*		Neotropical
Angiopteris	*latipinna*		Holarctic
Angiopteris	*lygodiifolia*		Holarctic
Angiopteris	*pruinosa*		Palaeotropical
Arthropteris	*orientalis*		Palaeotropical
Asplenium	*achilleifolium*		Neotropical
Asplenium	*adiantum-nigrum*	var. *adiantum-nigrum*	Holarctic, Palaeotropical
Asplenium	*adulterinum*		Holarctic
Asplenium	*aethiopicum*	subsp. *tripinnatum*	Palaeotropical
Asplenium	*Aethiopicum*	subsp. *dodecaploideum*	Palaeotropical
Asplenium	*billotii*		Holarctic
Asplenium	*boreale*		Holarctic
Asplenium	*caucasicum*		Holarctic
Asplenium	*ceterach*		Holarctic
Asplenium	*cristatum*		Neotropical
Asplenium	*cuneifolium*		Holarctic
Asplenium	*dalhousiae*		Holarctic
Asplenium	*daucifolium*		Palaeotropical
Asplenium	*flabellifolium*		Australian, Holantarctic
Asplenium	*griffithianum*		Holarctic, Palaeotropical
Asplenium	*hallbergii*		Neotropical
Asplenium	*hemionitis*		Holarctic
Asplenium	*javorkeanum*		Holarctic
Asplenium	*lividum*		Palaeotropical
Asplenium	*marinum*		Holarctic
Asplenium	*mauritiensis*		Palaeotropical
Asplenium	*myriophyllum*		Neotropical
Asplenium	*neolaserpitifolium*		Palaeotropical
Asplenium	*nidus*		Holarctic, Neotropical, Palaeotropical, Australian
Asplenium	*obtusatum*		Neotropical, Palaeotropical, Australian, Holantarctic
Asplenium	*onopteris*		Holarctic
Asplenium	*quadrivalens*		Holarctic
Asplenium	*rhizophyllum*		Holarctic
Asplenium	*richardii*		Holantarctic
Asplenium	*ruta-muraria*		Holarctic
Asplenium	*scolopendrium*		Holarctic, Holantarctic
Asplenium	*septentrionale*		Holarctic
Asplenium	*subglandulosum*		Australian, Holantarctic
Asplenium	*tenerum compl*		Palaeotropical

Genus	Species	Subspecies/Variety	Phytogeographical region(s)
Asplenium	*trichomanes*		Holarctic, Neotropical, Palaeotropical, Australian, Holantarctic
Asplenium	*trichomanes*	subsp. *quadrivalens*	Holarctic, Palaeotropical
Asplenium	*varians*		Holarctic, Palaeotropical
Asplenium	*Víride*		Holarctic
Asplenium	*viviparum*		Palaeotropical
Asplenium	*x- lolegnamense*		Holarctic
Asplenium	*x-lucrosum*		Holantarctic
Asplenium	*x-poscharskyanum*		Holarctic
Athyrium	*filix-femina*	var. *angustum*	Holarctic
Azolla	*microphylla*		Holarctic, Neotropical
Blechnum	*microphyllum*		Neotropical
Blechnum	*nudum*		Australian, Holantarctic
Blechnum	*spicant*		Holarctic
Bolbitis	*heudelotii*		Palaeotropical
Bolbitis	*singaporensis*		Palaeotropical
Botrychium	*neolunaria*		Holarctic
Botrychium	*alaskense*		Holarctic
Botrychium	*boreale*		Holarctic
Botrychium	*echo*		Holarctic
Botrychium	*hesperium*		Holarctic
Botrychium	*lanceolatum*		Holarctic
Botrychium	*lunaria*		Holarctic, Australian
Botrychium	*matricariifolium*		Holarctic
Botrychium	*michiganense*		Holarctic
Botrychium	*minganense*		Holarctic
Botrychium	*montanum*		Holarctic
Botrychium	*pallidum*		Holarctic
Botrychium	*pinnatum*		Holarctic
Botrychium	*simplex*		Holarctic
Botrychium	*spathulatum*		Holarctic
Botrychium	*virginianum*		Holarctic
Botrypus	*cf. virginianus*		Holarctic, Neotropical
Brainea	*insignis*		Palaeotropical
Calochlaena	*dubia*		Australian
Ceratopteris	*thalictroides*		Holarctic, Neotropical, Palaeotropical, Australian
Ceterach	*officinarum*	subsp. *officinarum*	Holarctic
Cheilanthes	*marantae*		Holarctic
Cibotium	*barometz*		Palaeotropical
Cibotium	*hawaiense*		Palaeotropical
Cryptogramma	*crispa*		Holarctic
Ctenitis	*sinii*		Holarctic
Culcita	*macrocarpa*		Holarctic
Cyathea	*crinita*		Palaeotropical
Cyclosorus	*arbusculus*		Palaeotropical
Cyclosorus	*asperum*		Palaeotropical
Cyclosorus	*dentatus*		Holarctic, Palaeotropical
Cystopteris	*bulbifera*		Holarctic
Cystopteris	*dickieana*		Holarctic
Cystopteris	*fragilis*	agg.	Holarctic, Neotropical, Cape, Holantarctic
Cystopteris	*tenuis*		Holarctic
Danaea	*antillensis*		Neotropical

Genus	Species	Subspecies/Variety	Phytogeographical region(s)
Danaea	*kalevala*		Neotropical
Danaea	*mazeana*		Neotropical
Davallia	*denticulata*	var. *denticulata*	Palaeotropical, Australian
Davallia	*tyermanii*		Holarctic
Dendrolycopodium	*dendroideum*		Holarctic
Dendrolycopodium	*obscurum*		Holarctic
Dennstaedtia	*globulifera*		Neotropical
Dennstaedtia	*wilfordii*		Holarctic
Deparia	*acrostichoides*		Holarctic
Deparia	*boryana*		Holarctic, Palaeotropical
Deparia	*japonica*		Holarctic, Palaeotropical
Dicksonia	*antarctica*		Holarctic, Australian
Dicranopteris	*linearis*		Holarctic, Neotropical, Palaeotropical, Australian, Holantarctic
Diphasiastrum	*alpinum*		Holarctic
Diphasiastrum	*digitatum*		Holarctic
Diphasiastrum	*complanatum*		Holarctic, Neotropical, Palaeotropical
Diphasiastrum	*tristachyum*		Holarctic
Diplazium	*arborescens*		Palaeotropical
Diplazium	*australe*		Palaeotropical, Australian, Holantarctic
Diplazium	*proliferum*		Palaeotropical, Australian
Diplazium	*pycnocarpon*		Holarctic
Diplopterygium	*bancroftii*		Neotropical
Dipteris	*chinensis*		Holarctic
Dracoglossum	*plantagineum*		Neotropical
Drynaria	*heraclea*		Palaeotropical
Dryopteris	*bernieri*		Palaeotropical
Dryopteris	*carthusiana*		Holarctic
Dryopteris	*clintoniana*		Holarctic
Dryopteris	*cristata*		Holarctic
Dryopteris	*cycadina*		Holarctic, Holantarctic
Dryopteris	*dilatata*		Holarctic, Holantarctic
Dryopteris	*filix-mas*		Holarctic, Neotropical, Holantarctic
Dryopteris	*goldiana*		Holarctic
Dryopteris	*intermedia*		Holarctic
Dryopteris	*marginalis*		Holarctic
Elaphoglossum	*aubertii*		Palaeotropical
Elaphoglossum	*crinitum*		Neotropical
Elaphoglossum	*hybridum*		Neotropical, Palaeotropical
Elaphoglossum	*lepervanchii*		Palaeotropical
Equisetum	*arvense*		Holarctic, Holantarctic
Equisetum	*bogotense*		Neotropical
Equisetum	*moorei*		Holarctic
Equisetum	*fluviatile*		Holarctic
Equisetum	*giganteum*		Neotropical
Equisetum	*hyemale*		Holarctic, Neotropical, Australian, Holantarctic
Equisetum	*laevigatum*		Holarctic, Neotropical
Equisetum	*myriochaetum*		Neotropical
Equisetum	*palustre*		Holarctic
Equisetum	*pratense*		Holarctic
Equisetum	*ramosissimum*	subsp. *ramosissimum*	Holarctic, Palaeotropical
Equisetum	*scirpoides*		Holarctic

Genus	Species	Subspecies/Variety	Phytogeographical region(s)
Equisetum	*sylvaticum*		Holarctic
Equisetum	*variegatum*		Holarctic
Gymnocarpium	*dryopteris*		Holarctic
Gymnocarpium	*fedtschenkoanum*		Holarctic
Gymnocarpium	*robertianum*		Holarctic
Gymnosphaera	*podophylla*		Holarctic, Palaeotropical
Huperzia	*lucidula*		holarctic
Hymenophyllum	*badium cf*		Holarctic, Palaeotropical
Hymenophyllum	*sibthorpioides*		Palaeotropical
Isoetes	*engelmannii*		Holarctic
Isoetes	*lacustris*		Holarctic
Lepisorus	*excavatus*		Palaeotropical
Lindsaea	*ensifolia*		Palaeotropical, Australian
Llavea	*cordifolia*		Neotropical
Lonchitis	*occidentalis*		Palaeotropical
Loxsoma	*cunninghami*		Holantarctic
Lycopodium	*annotinum*		Holarctic
Lycopodium	*clavatum*		Holarctic, Neotropical, Palaeotropical
Lycopodium	*dendroideum*		Holarctic
Lycopodium	*obscurum*		Holarctic
Lygodium	*japonicum*		Holarctic, Neotropical, Palaeotropical, Australian
Lygodium	*microphyllum*		Holarctic, Palaeotropical, Australian
Lygodium	*volubile*		Neotropical
Marattia	*purpurascens*		Holarctic
Marsilea	*quadrifolia*		Holarctic, Neotropical, Palaeotropical
Matteuccia	*struthiopteris*	var. *pensylvanica*	Holarctic
Megalastrum	*macrotheca*		Neotropical
Mickelia	*nicotianifolia*		Neotropical, Palaeotropical
Microgramma	*percussa*		Neotropical, Palaeotropical
Microlepia	*speluncae*		Neotropical, Palaeotropical, Australian
Microlepia	*strigosa*		Holarctic, Palaeotropical
Nephrolepis	*biserrata*		Neotropical, Palaeotropical, Australian
Nephrolepis	*cordifolia*	'Duffi'	Holarctic, Neotropical, Palaeotropical, Australian, Holantarctic
Nephrolepis	*exaltata*		Holarctic, Neotropical, Palaeotropical, Australian
Oleandra	*neriiformis*		Palaeotropical, Australian
Onoclea	*orientalis*		Holarctic
Onoclea	*sensibilis*		Holarctic
Onychium	*lucidum*		Holarctic, Palaeotropical
Ophioglossum	*gramineum*		Palaetropical, Australian
Ophioglossum	*pendulum*		Palaeotropical, Australian
Ophioglossum	*petiolatum*		Holarctic, Palaetropical, Holantarctic
Osmunda	*cinnamomea*		Holarctic, Neotropical
Osmunda	*claytoniana*		Holarctic
Osmunda	*regalis*	var. *spectabilis*	Holarctic, Neotropical
Paragymnopteris	*marantae*		Holarctic
Paragymnopteris	*vestita*		Holarctic
Pellaea	*atropurpurea*		Holarctic, Neotropical
Pellaea	*glabella*	subsp. *glabella*	Holarctic
Phegopteris	*connectilis*		Holarctic
Phyllitis	*scolopendrium*	subsp. *scolopendrium*	Holarctic
Plagiogyria	*matsumureana*		Holarctic

Genus	Species	Subspecies/Variety	Phytogeographical region(s)
Platycerium	*coronarium*		Palaeotropical
Pleopeltis	*macrocarpa*		Neotropical, Palaeotropical
Polyphlebium	*capillaceum*		Neotropical
Polypodium	*australe*		Holarctic
Polypodium	*cambricum*		Holarctic
Polypodium	*glycyrrhiza*		Holarctic
Polypodium	*interjectum*		Holarctic
Polypodium	*scouleri*		Holarctic
Polypodium	*virginianum*		Holarctic
Polypodium	*vulgare*		Holarctic, Neotropical, Cape, Holantarctic
Polypodium	*Vulgare x interjectum*		Not defined
Polypodium	*x-font-queri*		Holarctic
Polypodium	*x-mantoniae*		Holarctic
Polypodium	*x-shivasiae*		Holarctic
Polystichum	*acrostichoides*		Holarctic
Psilotum	*nudum*		Holarctic, Palaeotropical, Neotropical, Australian, Holantarctic
Pteridium	*aquilinum*		Holarctic, Neotropical, Palaeotropical, Australian
Pteridium	*revolutum*		Palaeotropical
Pteridium	*subsp. caudatum*	*var. arachnoideum*	Neotropical
Pteridrys	*cnemidaria*		Palaeotropical
Pteris	*croesus*		Palaeotropical
Pteris	*linearis*		Palaeotropical, Neotropical
Pteris	*pseudolonchitis*		Palaeotropical
Pteris	*vittata*		Holarctic, Neotropical, Palaeotropical, Holantarctic, Australian
Ptisana	*salicina*		Holantarctic, Palaeotropical
Pyrrosia	*lingua*		Holarctic, Palaeotropical
Saccoloma	*domingense*		Neotropical
Sadleria	*cyatheoides*		Palaeotropical
Salvinia	*molesta*		Holarctic, Neotropical, Palaeotropical, Holantarctic, Australian
Selaginella	*apoda*		Holarctic, Neotropical
Selaginella	*arenicola*		Holarctic
Selaginella	*arizonica*		Holarctic
Selaginella	*asprella*		Holarctic
Selaginella	*bigelovii*		Holarctic
Selaginella	*braunii*		Holarctic
Selaginella	*cinerascens*		Holarctic
Selaginella	*densa*		Holarctic
Selaginella	*eremophila*		Holarctic
Selaginella	*exaltata*		Neotropical
Selaginella	*extensa*		Neotropical
Selaginella	*flabellata*		Neotropical
Selaginella	*hansenii*		Holarctic
Selaginella	*helvetica*		Holarctic
Selaginella	*involvens*		Holarctic, Palaeotropical
Selaginella	*kraussiana*	*var. poulteri*	Holarctic
Selaginella	*kraussiana*		Holarctic, Neotropical, Holantarctic, Palaeotropical, Australian
Selaginella	*landii*		Neotropical
Selaginella	*lepidophylla*		Holarctic, Neotropical
Selaginella	*leucobryoides*		Holarctic
Selaginella	*martensii*		Neotropical
Selaginella	*moellendorffii*		Holarctic, Holantarctic, Palaeotropical

Genus	Species	Subspecies/Variety	Phytogeographical region(s)
Selaginella	*mutica*		Holarctic
Selaginella	*oregana*		Holarctic
Selaginella	*pallescens*		Holarctic, Neotropical
Selaginella	*peruviana*		Neotropical
Selaginella	*pilifera*		Neotropical
Selaginella	*pulcherrima*		Neotropical
Selaginella	*rupestris*		Holarctic
Selaginella	*rupincola*		Holarctic
Selaginella	*selaginoides*		Holarctic
Selaginella	*sellowii*		Neotropical, Holarctic
Selaginella	*tortipila*		Holarctic
Selaginella	*uncinata*		Holarctic, Palaeotropical
Selaginella	*underwoodii*		Holarctic
Selaginella	*vogelii*		Palaeotropical
Selaginella	*wallacei*		Holarctic
Selaginella	*watsonii*		Holarctic
Selaginella	*weatherbiana*		Holarctic
Selaginella	*willdenowii*		Holarctic, Neotropical, Palaeotropical, Australian
Selaginella	*wrightii*		Holarctic, Neotropical
Serpocaulon	*triseriale*		Neotropical
Sphaeropteris	*lepifera*		Neotropical, Palaeotropical
Spinulum	*annotinum*		Holarctic
Stenochlaena	*tenuifolia*		Palaeotropical
Tectaria	*zeilanica*		Palaeotropical
Thelypteris	*noveboracensis*		Holarctic
Thelypteris	*palustris*	var. *pubescens*	Holarctic
Thyrsopteris	*elegans*		Neotropical
Tmesipteris	*obliqua*		Australian
Tmesipteris	*tannensis*		Holantarctic
Todea	*barbara*		Palaeotropical, Australian, Holantarctic
Trichomanes	*speciosum*		Holarctic
Vandenboschia	*auriculata*		Holarctic, Palaeotropical
Vandenboschia	*davallioides*		Palaeotropical
Vittaria	*lineata*		Neotropical, Palaeotropical
Woodsia	*alpina*		Holartic
Woodsia	*ilvensis*		Holartic
Woodsia	*pulchella*		Holartic
Woodwardia	*fimbriata*		Holartic
Woodwardia	*unigemata*		Holarctic, Palaeotropical

Nuclear DNA content and comparative FISH mapping of the 5s and 45s rDNA in wild and cultivated populations of *Physalis peruviana* L.

Marlon Garcia Paitan*, Maricielo Postillos-Flores, Luis Rojas Vasquez, Maria Siles Vallejos, Alberto López Sotomayor

Research Group on Genetic Resources (RecGen), Faculty of Biological Sciences, Universidad Nacional Mayor de San Marcos, Lima, Peru
*Corresponding author. E-mail: marlon.garcia@unmsm.edu.pe

Abstract. *Physalis peruviana* L. often known as goldenberry, has increased its commercial growth in the international market in recent years due to its nutritional value and antioxidant potential. This situation has enabled countries such as Peru to increase their production in order to meet the global demand. However, investigations about the genetic diversity of cultivated and wild populations of goldenberry are still in their early stages. FISH mapping of 5s and 45s rDNA loci and flow cytometry estimation of nuclear DNA content were used to assess genetic differences between wild and cultivated goldenberry populations from Ayacucho and Cajamarca. The majority of metaphases had six 5s rDNA sites for all populations and two and four 45s rDNA sites for the cultivated and wild populations, respectively. We were able to characterize nine different types of chromosomes based on their morphology, fluorescence, rDNA location, and conservation across populations by analyzing the chromosomes that contained rDNA. Furthermore, cultivated populations had more nuclear DNA (13.262±0.087 pg) than wild populations (12.955±0.086 pg). The results show genetic differences between wild and cultivated populations of goldenberry at molecular cytogenetic level as well as in genome size. These findings establish a precedent for future cytogenetic and genomic studies in goldenberry populations, enabling future breeding programs.

Keywords: Goldenberry, FISH, rDNA, chromosomes, flow cytometry.

1. INTRODUCTION

Physalis peruviana L., also known in Latin America as "aguaymanto," "uchuva," or "uvilla," is a plant in the Solanaceae family that originated as well as diversified in the Andes Mountains. It produces orange-yellow berry-shaped fruits covered by a calyx. These fruits are high in vitamin C, carotenoids, phenolic compounds with antioxidant precursors, and withanolides, which have anticancer and antitumor properties (Singh et al. 2019). Because of these characteristics and the increased international demand for organic food, the production of *Physalis peruviana* L. in Peru has quickly grown in recent years, establishing it as the second-largest producer of goldenberry

in Latin America. However, the amount of goldenberry production compared to Colombia, the leading producer in Latin America, and other countries outside the American continent remains limited (Sierra y Selva Exportadora 2021). To increase commercial competitiveness, genetic improvement programs that increase fruit quality and production must be implemented, and our understanding of the genetic diversity of *Physalis peruviana* L. in cultivated and wild populations will determine the success of these programs. Cytogenetic studies provide a foundation for the characterization of germplasm resources and offer guidance in selecting the parental cultivars for plant breeding programs (Herrera 2007). Furthermore, for future complex genomic projects such as cloning of genes of interest or genome sequencing, genome size data is essential to design effective projects (Doležel et al. 2007). Most cytogenetic studies in *Physalis peruviana* L. have used classical staining techniques to determine the chromosome number, where 2n=48 predominates (Rodríguez and Bueno 2006; Sánchez 2014; Liberato et al. 2014; Trevisani et al. 2018), while other studies report mixoploid plants (Sánchez 2014), and somatic aneuploidy (Carbajal et al. 2021). Karyotypic formulas of some populations have been previously reported (Azeez and Faluyi 2019; Carbajal et al. 2021). However, since goldenberry chromosomes are small, numerous, and have similar morphology, the karyotype determination and its analysis are considered limited when classical staining techniques are used.

FISH is a molecular cytogenetic technique for mapping specific sequences on chromosomes by hybridizing probes with their complementary sequences. 5s and 45s ribosomal DNA (rDNA) probes have been widely used to perform cytogenetic characterization and to understand intraspecific and interspecific evolutionary relationships at chromosomal level by determining the position and number of signals on metaphase chromosomes, even in species with numerous and small chromosomes (Herrera 2007). This is due to the nature of rDNA sequences, which are tandemly repeated DNA regions in the genome with high transcription rates and a predisposition for unequal recombination, which makes them inherently unstable and prone to variation in copy number and location in the genome (Salim and Gerton 2019). Previously, the number of 5s rDNA signals in two cultivated populations from the same region has been studied at the molecular cytogenetic level in *Physalis peruviana* L. (Siles et al. 2021). However, no studies have been conducted to analyze the number and position of the 5s and 45s rDNA sites to determine if there are any chromosomal differences between wild and cultivated populations as a consequence of the domestication of the species.

Plant genome size varies enormously and is considered a biodiversity trait that provides valuable information for systematic and evolutionary studies (Pellicer et al. 2018). It is also useful for determining the genetic characterization of germplasm and plant identification because of these characteristics (Jedrzejczyk and Rewers 2020). Flow cytometry is a quick and easy way to estimate nuclear DNA content, making it a powerful tool for accelerating selection processes in plant breeding and providing critical data for sequencing projects (Ciprian-Salcedo et al. 2020).

Given the foregoing, the goals of this study were to characterize and analyze the genetic differences between wild and cultivated populations of *Physalis peruviana* L. from the regions of Ayacucho and Cajamarca through the mapping of 5s and 45s rDNA by FISH, and to estimate the nuclear DNA content using flow cytometry. These two approaches will set a precedent as potential tools for programs to improve this genetic resource in Peru and, as a result, improve the international competitiveness of Peru against other producing countries.

2. METHODS AND MATERIALS

2.1 Plant material and preparation of metaphase chromosomes

Seeds were collected from wild and cultivated populations of ripe goldenberry fruits in the Cajamarca and Ayacucho regions (Figure 1). Plant material was transported to the Genetics Laboratory of the Universidad Nacional Mayor de San Marcos (UNMSM) and correctly identified as *Physalis peruviana* L. by the UNMSM Natural History Museum. (Certificates 224-USM-2015 and 001-USM-NHN -2022).

We modified the protocols described by Aguilera et al. (2016), Aliyeva-Schnorr et al. (2015), and Carbajal et al. (2021) in order to obtain mitotic metaphase chromosomes. Goldenberry seeds were germinated, and roots with an approximate size of 4 mm were treated with 0.03 percent colchicine for 80 minutes at room temperature before being submerged in distilled water for 60 minutes at 37 °C and fixed in an ethanol solution: acetic acid (3:1) at -20 °C for at least one day. Subsequently, the roots were washed in cold distilled water twice for 5 minutes, followed by two washes in cold citrate buffer (0.01 M at pH 4.6) for 5 minutes. They were then macerated in a 2% cellulase solution (from *Aspergillus niger*, Sigma) and a 10% liquid pectinase solution (from *Aspergillus niger*, Sigma) dissolved in 40% glycerol in 0.01M citrate buffer at pH 4.6, at 37 °C for 1 hour. Then, they were washed four times with cold citrate buffer for 5 minutes (0.01 M at pH
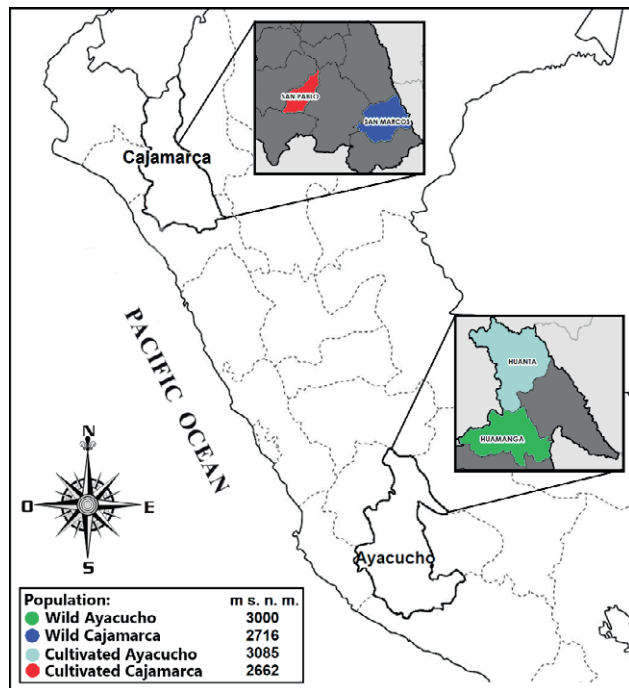
Figure 1. Map of Peru showing sampling locations for wild and cultivated populations of *Physalis peruviana* L.

4.6) and twice in ethanol 90° for 5 seconds. The apex of each root was then transferred to a slide, a drop of 45 percent acetic acid was placed on it, and the "squash" technique was performed. After that, the slide was frozen with dry ice to remove the coverslip slide, then air-dried and examined under a phase-contrast microscope to confirm the presence of cells with properly separated metaphase chromosomes. Finally, the selected slides were immersed in absolute ethanol at -20 °C until they were used.

2.2 Amplification of rDNA

Genomic DNA was extracted from seedlings grown from goldenberry seeds using the GF-1 Plant DNA extraction kit (Vivantis, Malaysia). To obtain the 5s rDNA probe, 5s rDNA amplification was performed using the primers pr5S14 (5'-GGCGAGTAGTACTAG-GATCCGTGAC-3') and pr5S15 (5'-GCTTAACTTCG-GAGTTCTGATGGGA-3') reported by Volkov et al. (2001). Because the 45s rDNA locus is too large to be completely amplified, it was decided to use the 18s rDNA gene as a probe. Since 18s rDNA is present within the gene structure of the 45s rDNA, mapping it would also show the location of the 45s rDNA locus. The following primers were used to achieve 18s rDNA amplification: primers F-566 (5'-CAGCAGCCGCGGTAATTCC-3') and

R-1200 (5'-CCCGTGTTGAGTCAAATTAAGC-3') which were previously reported by Hadziavdic et al. (2014). The PCR reaction mixture for both cases had a final volume of 20 μl containing 1X PCR buffer, 1.5 mM MgCl$_2$, 0.2 μM dNTPs, 0.2 μM of each primer, 1 U of Taq polymerase (abm, Canada), and 30 ng of genomic DNA. The PCR program for 5s rDNA began with an initial denaturation at 95 °C for 9 minutes, followed by 45 cycles of 95 °C for 30 seconds, 58 °C for 30 seconds and 72 °C for 45 seconds, and a final extension at 72 °C for 5 minutes. On the other hand, 18s rDNA involved an initial denaturation at 95 °C for 9 minutes, followed by 42 cycles of 95 °C for 30 seconds, 62 °C for 30 seconds and 72 °C for 60 seconds, and a final extension at 72 °C for 5 minutes. The amplicons were purified using the GeneJET PCR Purification kit (Thermo Scientific™) and quantified by spectrophotometry.

2.3 Labelling of DNA probes

The 5s rDNA amplicons were labeled with biotin-14-dATP for 90 minutes using the BioNick Labeling System commercial kit (Invitrogen, USA), and the 18s rDNA was labeled for 180 minutes with digoxigenin-11-dUTP using the DIG-Nick Translation Mix commercial kit (Roche, Switzerland).

2.4. FISH and signal detection

The FISH methodology used was slightly modified from that provided by Poggio et al. (2000). The slides with the chromosome preparation were treated with RNases and 4% (w/v) paraformaldehyde. The hybridization solution contained 15 μl of Formamide, 6 μl of 50% Dextran Sulfate, 3 μl of 20X SSC, 1 μl of Salmon DNA (10 mg/ml), 1μl of 10% SDS, and 50 ng of each 5s and 45s rDNA probe, with a final volume of 30 μl. This solution was applied to the chromosome preparations, and the hybridization program was as follows: 75 °C for 7 minutes, 55 °C for 6 minutes, 45 °C for 5 minutes, and 37 °C for 12 hours inside a hybridizer (Biobase, HS-500). After the hybridization, the following washes were performed to remove nonspecific binding: 2X SSC at 42 °C for 5 minutes, 20% formamide in 0.1X SSC at 42 °C for 10 minutes, 0.1X SSC at 42 °C for 5 minutes, 2X SSC for 5 minutes at 42 °C, and finally three washes with 0.2% (v/v) Tween 20 in 4X SSC for 5 minutes at room temperature. The 5s probe was detected with a Neutravidin-Oregon-Green 488 conjugate (Thermo Scientific™) while the 18s probe was detected with Anti-Digoxigenin-Rhodamine (Roche). The slides were mounted with Slow-

Fade™ Gold Antifade Mountant (Invitrogen™), which contained DAPI and an antifade solution.

The slides were observed and photographed under an epifluorescence microscope (ZEISS Axio Scope.A1). For DAPI fluorophore, BP 340/30 excitation and BP 510/90 emission filters were used; for Oregon Green 488, BP 470/40 excitation and BP 540/50 emission filters were used; and for Rhodamine, BP 560/40 excitation and BP 630/75 emission filters were used. We specifically worked with cells in metaphase that contained 48 recognizable chromosomes to avoid variation in the results attributable to any somatic aneuploidy present in the meristematic tissue of the root of the species, a phenomenon already observed in prior studies (Carbajal et al. 2021; Franco et al. 2021). The following programs were utilized: GIMP 2.10.14 was used for picture overlaying and chromosomal individualization; IdeoKar1.2 (Mirzaghaderi and Marzangi 2015) for morphological measurements of chromosomes and the production of ideograms; and ImageJ for fluorescence quantification of probe signals. The latter was achieved in accordance with Fitzpatrick (2021).

2.5 Determination of nuclear DNA content

Each wild and cultivated population had eight plants evaluated. These were obtained after a three-month seed culture in pots. Flow cytometry was used to determine the nuclear genome size of each plant in duplicate using *Pisum sativum* cv. 'Ctirad' (2C = 9.09 pg DNA) as an internal reference standard. The nuclear suspension preparation protocol and nuclear DNA content estimation were performed as described by Doležel et al. (2007). Young leaves of the standard and goldenberry were utilized as plant material in the streamlined two-step process for nuclei suspension preparation. Furthermore, propidium iodide was employed as a fluorochrome. The nuclear DNA content was estimated using an Attune NxT flow cytometer (Thermo Fisher Scientific) and the following formula:

$$\text{2C value of the sample (pg de ADN)} =$$

$$\frac{\text{Mean position of the 2C peak of the sample}}{\text{Mean position of the 2C peak of the reference standard}} \times 9.09\text{pg}$$

3. RESULTS

3.1 Number of 5s and 45s rDNA signals in wild and cultivated populations

FISH was used to identify the 5s and 45s rDNA probe signals in the metaphases of *Physalis peruvi-* *ana* L. populations (Figure 2). For each population, 25 metaphases with 48 chromosomes were analyzed. After studying the metaphases of all the populations, a total of five combinations of the number of 5s and 45s rDNA sites were identified; three of these combinations were detected in wild populations (Figure 2A, B, E, F, I, J) and four combinations in cultivated populations (Figure 2C, D, E, G, H, K, L). There were no significant variations in the number of 5s and 45s rDNA sites across wild populations (p=0.422), nor between cultivated populations (p=0.085), however, there were significant differences across populations from the same region (p<0.01). Furthermore, it was discovered that the predominant rDNA combination in wild populations was six 5s rDNA sites and four 45s rDNA sites, whereas in cultivated populations it was six 5s rDNA sites and two 45s rDNA sites (Figure 3). In general, a higher frequency of six 5s rDNA sites is observed in all goldenberry populations, while for 45s rDNA a number of two sites predominates for cultivated populations and 4 sites for wild populations.

3.2 Characterization of chromosomes with rDNA loci

The 12 best metaphases with clear and distinct rDNA signals in relation to their chromosomal arms and fluorescent signals were selected from the 25 metaphases per population, considering at least one metaphase that showed each combination of the number of 5s and 45s rDNA sites from each wild and cultivated population. The morphological characterization, individualization, and pairing with their homologous chromosomes that displayed rDNA signals were performed in each of the selected metaphases (Figure 4, Figure S1). Based on the study of the chromosomes that showed rDNA signals in all populations, nine types of chromosomes were identified according to their morphological features, the position of the 5s or 45s rDNA locus, the fluorescence intensity of the rDNA probe, and their presence in the populations (Figure 5 and Table 1). The *N* chromosomes are those that are found in all populations: *N1* has a metacentric morphology and the 5s rDNA in the p arm; *N2* is submetacentric and has the 45s rDNA in the p arm, and *N3* is acrocentric and has the 5s rDNA in the q arm. The *S* chromosomes, which stand for wild, are found specifically in wild populations: *S1* has a submetacentric morphology and 45s rDNA in the q arm; *S2* is metacentric and has 45s rDNA in the q arm; *S3* is metacentric and has 5s rDNA in the p arm. It should be noted that, while *N1* and *S3* are described in the same way, the difference between them is determined by the length of the chromosome (Table 1). *C* chromosomes are those found solely in cultivated populations: *C1* has a submetacentric
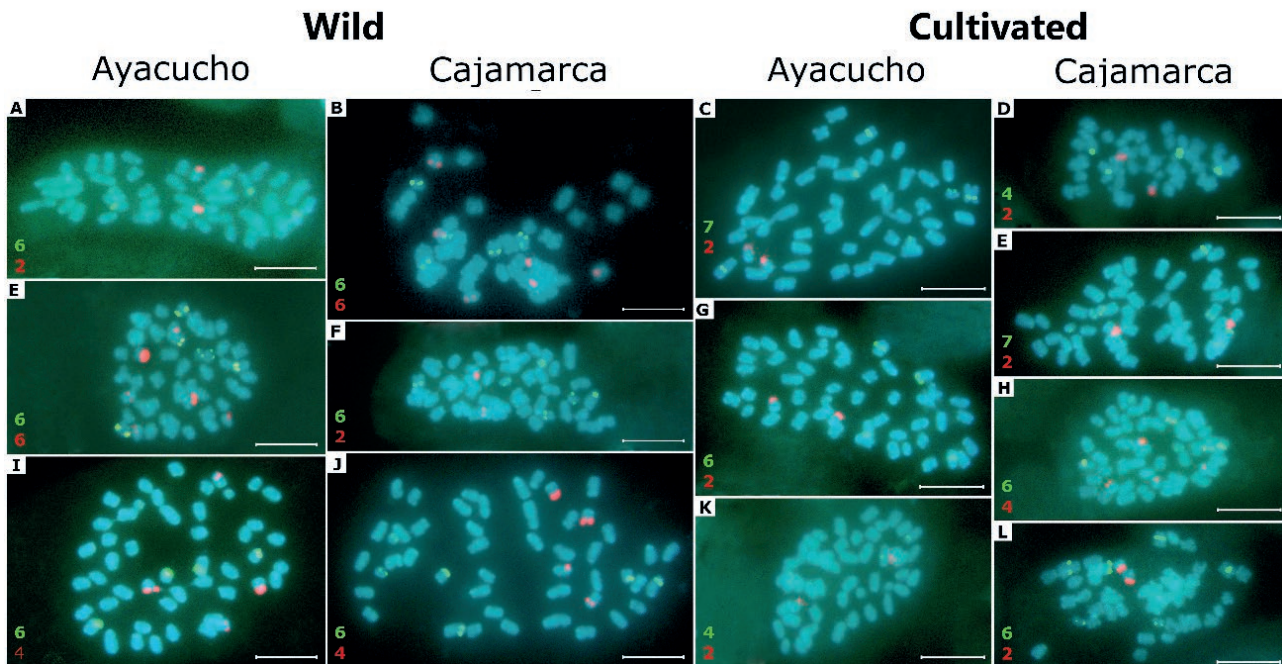
Figure 2 Fluorescent in situ hybridization signals of the 5s (green) and 45s (red) rDNA probes in *Physalis peruviana* L. metaphase chromosomes. The numbers at the bottom left of each image represent the number of 5s (green) and 45s (red) sites found in the metaphases. Combinations of the number of 5s and 45s rDNA sites identified in the population of wild Ayacucho are shown in A, E, and I; wild Cajamarca is shown in B, F, and J; cultivated Ayacucho is shown in C, G, and K; and Cultivated Cajamarca is shown in D, E, H, and L. The scale bar measures 10 μm.
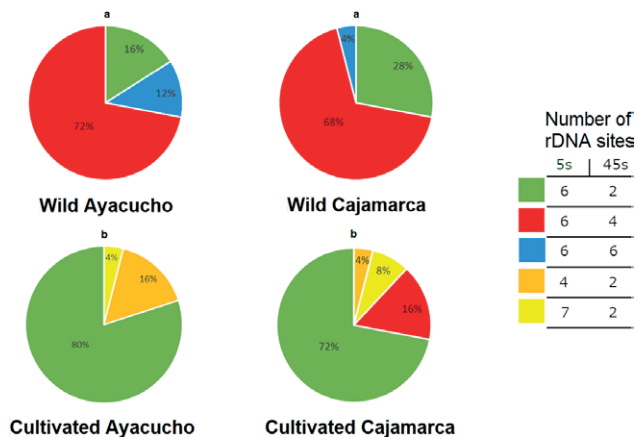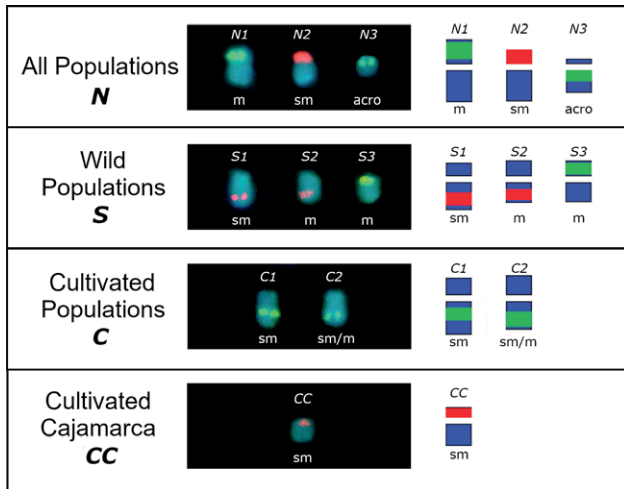

Figure 3 The frequency of 5s and 45s rDNA sites observed in the 25 metaphases of each goldenberry population. Different letters at the top of each frequency circle show significant differences (Fisher's Exact Test, p<0.05).

Figure 4 Chromosomes that showed hybridization of the 5s and 45s rDNA probes between the best 12 metaphases for each population, encompassing at least one metaphase for each of the combinations of the number of 5s and 45s rDNA sites reported for each population of goldenberry. m=metacentric, sm=submetacentric, acro=acrocentric.

morphology and has the 5s rDNA in the q arm, whereas *C2* has a metacentric/submetacentric morphology and has the 5s rDNA in the q arm, and a lower fluorescence intensity than *C1*. The morphology of the *C2* chromosome is attributable to the fact that only one *C2* chromo-

Figure 5 Characterization of the nine types of chromosomes that showed rDNA probe hybridization based on their existence in populations, morphology, size, presence of the 5s or 45s locus, position of the rDNA locus, and rDNA probe fluorescence intensity, m=metacentric, sm=submetacentric, and acro=acrocentric.

some was observed in each of the cultivated populations, resulting in a metacentric morphology in Ayacucho and a submetacentric morphology in Cajamarca (Figure 6). The *CC* chromosome, found only in the Cultivated

Cajamarca population, has a submetacentric morphology and the 45s rDNA in the p arm, similar to *N2*, although it differs in terms of chromosome length and rDNA probe fluorescence intensity (Table 1).

The types of chromosomes that contain rDNA are conserved among wild populations. However, there is a difference in the observed frequency of chromosomes *S1*, which is higher in Cajamarca, and *S2*, which is higher in Ayacucho (Figure 6). Additionally, in Ayacucho, the 45s rDNA locus of *S1* chromosome is found in the centromeric position, whereas in Cajamarca, it is found in the interstitial position. The *CC* chromosome was found only in Cajamarca among the cultivated populations, while the other chromosomes were found in both groups with no variations in frequency or position of the rDNA (Figure 6).

3.3 Size of the nuclear genome

All flow cytometric analyses showed high-resolution histograms with a coefficient of variation (CV) of the G0/G1 peaks between 1.63% and 2.85% (mean 2.04%). Representative histograms are shown with the peaks corresponding to the G0/G1 nuclei of *Physalis peruviana* L. and the internal standard *Pisum sati-*
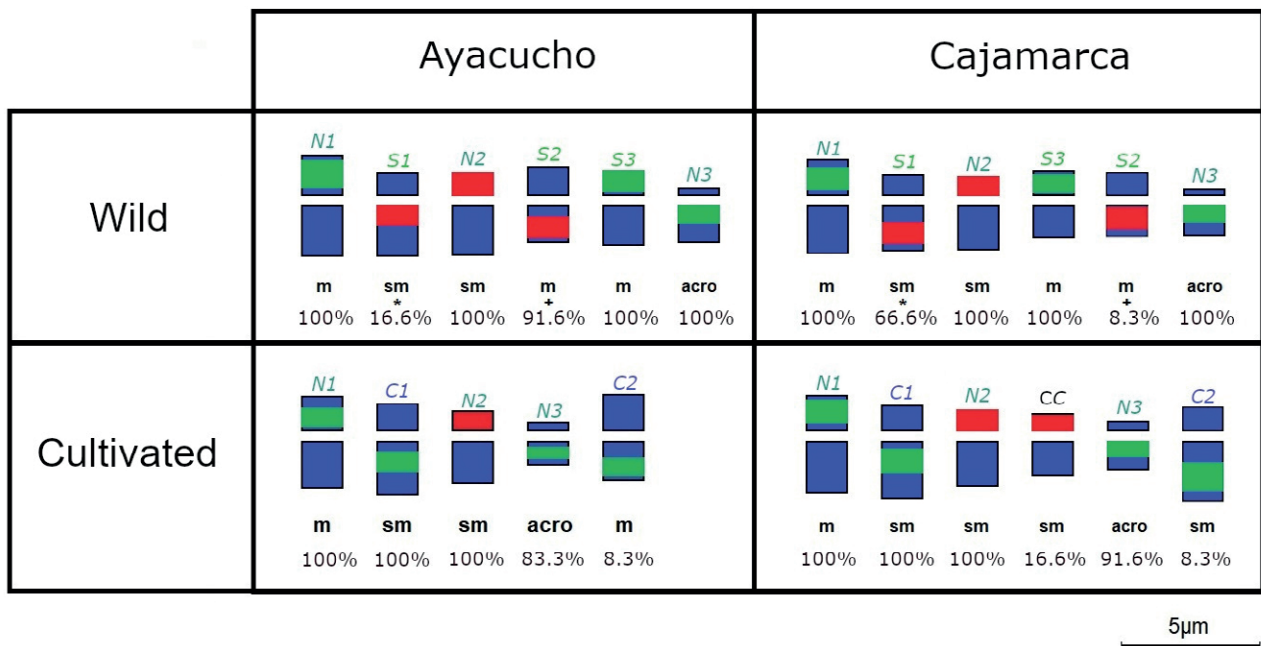
**Figure 6** The average ideogram of the types of chromosomes that included rDNA. The proportion observed in the total of the metaphases analyzed by each population is indicated beneath each chromosome. Equal symbols above the percentages indicate a significant difference between the observed frequencies of both populations (Fisher's Exact Test, p<0.05). m=metacentric, sm=submetacentric, and acro=acrocentric.

Table 1. Morphometric and fluorescence data of the nine types of chromosomes found in *Physalis peruviana* L. populations.

rDNA-bearing chromosome	n	Chromosome Length	Arm ratio	Log (DNA probe fluorescence intensity)	CM	Position of rDNA locus
N1	48	3.120 ± 0.416	1.363 ± 0.161	3.943 ± 0.265	m	5s -> p
N2	48	2.436 ± 0.332	2.191 ± 0.265	3.909 ± 0.404	sm	45s -> p
N3	45	1.499 ± 0.230	3.919 ± 0.641	3.078 ± 0.307	acro	5s -> q
S1	10	2.516 ± 0.341	2.189 ± 0.240	3.383 ± 0.318	sm	45s -> q
S2	12	2.417 ± 0.216	1.471 ± 0.112	3.371 ± 0.164	m	45s -> q
S3	24	2.241 ± 0.287	1.284 ± 0.167	3.995 ± 0.319	m	5s -> p
C1	24	3.002 ± 0.461	2.220 ± 0.292	3.930 ± 0.240	sm	5s -> q
C2	1	2.908 ± 0.106	1.951 ± 1.238	3.180 ± 0.001	m/sm	5s -> q
CC	2	1.922 ± 0.047	2.027 ± 0.366	3.212 ± 0.062	sm	45s -> p

The values are expressed as mean ± standard deviation. The "n" sample values are per chromosomal pair. CM = chromosome morphology; m = metacentric; sm = submetacentric; acro= acrocentric.
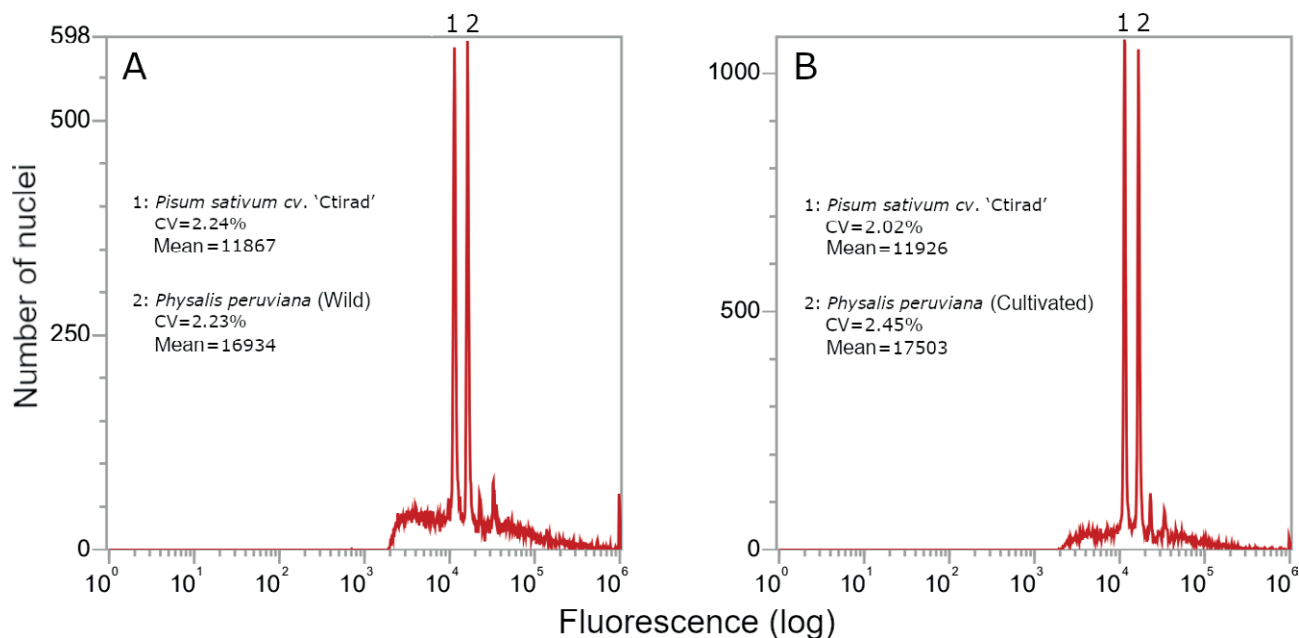
Figure 7 Fluorescence histograms of the nuclei of goldenberry and *Pisum sativum cv*. Ctirad populations (2C = 9.06 pg as internal reference standard) were analyzed simultaneously. Each peak denoted by the numbers 1 or 2 corresponds to the populations of nuclei in the G0/G1 phase of each species. Each histogram includes the percentage of the coefficient of variation (CV) and average absolute fluorescence for each of these peaks.

vum cv. Ctirad of the wild and cultivated populations in Figure 7. The nuclear DNA estimation content based on the amount of the 2C internal standard (9.09pg of DNA) displayed a substantial variation between both groups (Table 2).

4. DISCUSSION

The determination of the number of rDNA sites and their distribution on chromosomes by FISH has proven to be a reliable molecular cytogenetic marker when establishing genetic relationships of plant species that contain a significant number of small and homogenous chromosomes (Su et al. 2020). The current study

Table 2. Flow cytometry was used to quantify the nuclear DNA content and genome size of wild and cultivated populations of *Physalis peruviana* L. using *Pisum sativum cv.* Ctirad as the internal reference standard.

Population	n(R)	Average Values		CV (%)
		Nuclear DNA content 2C ± DE (pg)	Genome size 1C ± DE (x 10⁹ pb)**	
Wild	8(2)	12.955 ± 0.086*	6.335 ± 0.041*	2.124±0.360
Cultivated		13.262 ± 0.087*	6.485 ± 0.042*	1.960±0.216

The n represents the sample number, while the R represents the number of repetitions per sample, CV: The coefficient of variation of G0/G1 peaks in flow cytometry histograms.
* Indicates a significant difference between values of the same column p < 0.05.
** 1pg DNA equal to 0.978×10⁹ bp, according to Doležel et al. (2007).

found a substantial difference in the number of 5s and 45s rDNA sites between wild and cultivated populations of goldenberry (Figure 3). This is the first mapping of the 45s rDNA in *Physalis peruviana* L., where a number of two, four, and six sites have been reported for all the populations, prevailing a number of four sites in wild populations and two sites in cultivated populations. This intraspecific variation at the species level, as well as its variability among the populations analyzed, in terms of the number of 45s rDNA sites, can be explained by its nature as a fragile location within the plant genome (Huang et al. 2012). This trait increases the likelihood of chromosomal breakage in the rDNA region, resulting in a chromosomal rearrangement. Furthermore, because of its repetitive nature, it is an unstable genomic region that promotes homologous recombination (Rosato et al. 2016), resulting in increased variability in the amount of 45S rDNA sites within the genome. This variability has also been observed in other Solanaceae species, such as *Solanum* spp., which presents between 2 and 4 sites (Pendinen et al. 2008; Rego et al. 2009; Moyetta et al. 2017); *Capsicum* spp., which presents between 2, 4, 6, 8 up to 16, 24, 28, 36 sites (Youn-Kyu et al. 1999; Kwon and Kim 2009; Romero-da et al. 2017); *Nicotiana* spp. likewise shows considerable variety, reporting between 2, 4, 6, and, to a lesser extent, 8 and 10 sites (Lim et al. 2000; Nakamura et al. 2001; Kitamura et al. 2001; Matyasek et al. 2003; Kovarik et al. 2004). All of this suggests that the number of 45s rDNA sites of 2, 4, and 6 reported in the populations studied in this research is within the predicted range for the Solanaceae family. The variation between wild and cultivated populations was influenced by the unstable character of the 45s

rDNA region and was favored by the selective breeding process throughout the domestication of the species (Doebley et al. 2006).

In comparison to the number of 45s rDNA sites, the number of 5s rDNA sites has been found to remain reasonably consistent throughout most angiosperm and gymnosperm taxa (Garcia et al. 2017). This is consistent with the findings of the current study, which found a predominance of six 5s rDNA sites in all goldenberry populations, with a small fraction of four and seven sites in the cultivated populations (Figure 3). Similarly, Siles et al. (2021) discovered a prevalence of six 5s rDNA sites in goldenberry cultivated populations. However, other Solanaceae species have a lower number of 5s rDNA sites, such as *Solanum spp.*, which has a prevalence of two 5s rDNA sites and, to a lesser extent, four sites (Pendinen et al. 2008; Rego et al. 2009; Aguilera et al. 2016; Romero-da et al. 2017), *Capsicum spp.*, which typically presents two sites (Youn-Kyu et al. 1999; Park et al. 2000; Kwon and Kim 2009; Aguilera et al. 2016; Romero-da et al. 2017); *Nicotiana spp.*, which generally alternates between two and four sites (Nakamura et al. 2001; Kitamura et al. 2001; Fulneček et al. 2002; Matyasek et al. 2003; Kovarik et al. 2004), and *Cestrum spp.*, which has two 5s rDNA sites (Fregonezi et al. 2006; Fernandes et al. 2009; Urdampilleta et al. 2014). These data indicate that goldenberry populations have more 5s rDNA sites than other species in the family. However, not enough studies have been conducted on this clade or the *Physalis* genus to be conclusive. Furthermore, the presence of a considerable number of 5s rDNA sites may be due to ribosomal gene copy number amplification during crossing over or transposition events (Kapitonov and Jurka 2003; Su et al. 2020). In accordance to prior research (Garcia et al. 2017), the majority of angiosperm species have more 45s rDNA sites than 5s rDNA sites; this is also shown with molecular cytogenetic results in the Solanaceae family to a higher extent (Vitales et al. 2017). This contrasts with the findings in the goldenberry populations analyzed in this study, which revealed six 5s rDNA sites and two/four 45s rDNA sites (Figure 3). Therefore, these results will be helpful as precedents for the molecular cytogenetic characterization of the genus *Physalis* and the cytotaxonomic understanding of the Solanaceae family.

The nine types of chromosomes that contain rDNA (Figure 5) allowed cytogenetic distinction of wild and cultivated populations of goldenberries (Figure 6). These discrepancies are indistinguishable when only the chromosomal number (2n=48) is taken in consideration. Therefore, FISH significantly reduces the number of chromosomes that must be studied to determine cytoge-

netic differences, emphasizing its relevance in the study of plant species with multiple chromosomes (Su et al. 2020). The existence of different chromosomes in wild (*S1*, *S2*, and *S3*) and cultivated (*C1*, *C2*, and *CC*) populations could be attributed to multiple breeding events that happened throughout the domestication of the species, leading to chromosomal rearrangements (Bashir et al. 2018; Su et al. 2020). There is no variation in the presence of rDNA-containing chromosomes between the two wild populations, implying that there is no structure between these populations. However, discrepancies in the frequency of chromosomes *S1* and *S2* may imply a slight genetic distinction between the two wild populations as a result of their geographical separation (Figure 1). The presence of the *CC* chromosome in Cajamarca could be explained by the same trait found in cultivated populations (Figure 6). The 5s rDNA locus is present in three different chromosomal sites: telomeric (*N1* and *S3*), interstitial (*C1* and *C2*), and centromeric (*N3*) (Figure 5). The dispersed distribution of 5s rDNA has already been observed in numerous mappings of plant chromosomes (Vitales et al. 2017), which could be linked to the activity of mobile genetic elements such as transposons, which have been detected in association with ribosomal gene sequences (Kapitonov and Jurka 2003; Raskina et al. 2004). The 45s rDNA, on the other hand, has a more restricted position, with telomeric (*N2* and *CC*) and interstitial (*S1* and *S2*) sites reported (Figure 6). This more restricted variability is typical of angiosperms, and it has also been revealed that the 45s rDNA ancestral location is terminal (Garcia et al. 2017). The 45s rDNA locus is known to be involved in the creation of nucleoli during the cell cycle, especially if it is positioned in the satellite sections of the chromosomes since it correlates with the existence of nucleolar organizing areas (Long and Dawid 1980; Lopez et al. 2021). If the species has a large number of 45S sites, however, not all of them will be functional (Grabiele et al. 2018; Báez et al. 2020). In the current investigation, no satellites correlated with an active 45s rDNA locus were found in the analyzed chromosomes, however, the *N2* chromosome is likely to contain a functional locus because it is conserved in all goldenberry populations and is the only type of chromosome that has a 45s rDNA locus in the Ayacucho cultivated population. Garcia et al. (2017) propose that if a karyotype has a single 5s or 45s rDNA locus, that locus must be functional.

The fluorescence intensity of the rDNA probes that are highlighted in the differentiation of chromosome types *C1* and *C2*, as well as between *CC* and *N2*, could be related to the number of rDNA tandem repeats that they have between the loci, implying that low fluores-

cence would indicate a comparatively low number of repeats (Prado et al. 1996). Furthermore, events such as amplification, deletion, and unequal crossing over are known to change the number of repeats and result in variations in fluorescence signals (Su et al. 2020).

Differences in the amount of nuclear DNA between wild and cultivated populations of goldenberries may be due to the domestication process of the species, since artificial selection during domestication affects the evolution of its genome (Díez et al. 2013). The results reported in this study (Table 2) for the wild (12,955 pg) and cultivated (13,262 pg) populations are higher than those reported by Liberato et al. (2014) in Colombian accessions (between 5.77 pg and 8.12 pg). The values of the cultivated populations in this study are remarkably close to those published by Trevisani et al. (2018) in Colombian (13.29 pg), Brazilian (13.32 pg), and Peruvian populations (13 pg). It is important to note that all of these studies report a 2n=48 chromosome number. This could imply that they are related to the same population of goldenberries, however, more research into the molecular cytogenetics of these groups is needed to prove it. According to the plant genome size database (Pellicer and Leitch 2020), estimations of the amount of 2C DNA for the Solanaceae family are 5.68 ± 5.27 pg. This would place the *Physalis peruviana* L. populations studied here in the same family as the Solanaceae species with large genome sizes. Expansion of transposons, particularly retrotransposons with lengthy terminal repeats, has been identified as one of the main causes of genome size disparities in plants (Michael 2014), in addition to genome doubling events during speciation (Wendel et al. 2016). Based on the amount of nuclear DNA content in the goldenberry, all of our findings would be indicative of potential biodiversity and should be considered for future genomic investigations.

This is the first study in Peru to use molecular cytogenetics and genome size to compare wild and cultivated goldenberry populations. In conclusion, the molecular cytogenetic technique revealed a genetic variation in the number of 45s rDNA sites between wild and cultivated populations, as well as different types of chromosomes containing rDNA. This genetic difference was also detected when the amount of nuclear DNA in the populations was compared.

Finally, the findings show no difference between populations from different places, both for cultivated and wild, suggesting that they probably originated from the same population. This study also underlines the utility of these methodologies for analyzing and characterizing the genetic variability of *Physalis peruviana* L. populations, and it will be valuable for future genetic, genom-

ic, and phylogenetic research on this species, as well as the design of genetic improvement programs.

GEOLOCATION INFORMATION

The cultivated populations of goldenberry were collected from the province of Huanta (Department of Ayacucho) (GPS: 13°01'50.9"S, 74°10' 14.3"W) and the province of San Pablo (Department of Cajamarca) (GPS: 7°05'43.9"S, 78°49'13.9"W), the wild populations from the province of Huamanga (Department of Ayacucho) (GPS: 13°03'53.5"S, 74°09'13.1"W) and San Marcos (Department of Cajamarca) (GPS: 7°20'47.3"S, 78°06'0.3"W). The research procedure was developed in the Faculty of Biological Sciences of the UNMSM, Lima (GPS: 12°03'35.1"S, 77°04'55.6"W).

REFERENCES

Aguilera PM, Debat HJ, Scaldaferro MA, Martí DA, Grabiele M. 2016. FISH-mapping of the 5S rDNA locus in chili peppers (*Capsicum-Solanaceae*). Anais da Academia Brasileira de Ciências. 88(1): 117-125.

Aliyeva-Schnorr L, Ma L, Houben A. 2015. A fast air-dry dropping chromosome preparation method suit-able for FISH in plants. Journal of Visualized Experiments. 106: e53470.

Azeez S, Faluyi JO. 2019. Karyotypic studies of four *Physalis* species from Nigeria. Acta Botánica Hungarica. 61(1-2): 5-9.

Báez M, Souza G, Guerra M. 2020. Does the chromosomal position of 35S rDNA sites influence their transcription? A survey on *Nothoscordum* species (Amaryllidaceae). Genetics and molecular biology. 43(1): e20180194.

Bashir T, Chandra Mishra R, Hasan MM, Mohanta TK, Bae H. 2018. Effect of hybridization on somatic mutations and genomic rearrangements in plants. International journal of molecular sciences. 19(12): 3758.

Carbajal Y, Bonilla H, Siles-Vallejos M, López A. 2021. Comparative cytogenetics of *Physalis peruviana* in three cultivated populations from Cajamarca, Peru. Revista peruana de biología. 28(2):e20462.

Ciprian-Salcedo GC, Jimenez J, Zolla G. 2020. Flow cytometry applications in plant breeding. Revista Peruana De Biología. 27(1): 079-084.

Díez CM, Gaut BS, Meca E, Scheinvar E, Montes-Hernandez S, Eguiarte LE, Tenaillon MI. 2013. Genome size variation in wild and cultivated maize along altitudinal gradients. The new phytologist. 199(1): 264–276.

Doebley JF, Gaut BS, Smith BD. 2006. The molecular genetics of crop domestication. Cell. 127(7): 1309–1321.

Doležel J, Greilhuber J, Suda J. 2007. Estimation of nuclear DNA content in plants using flow cytometry. Nature Protocols. 2(9): 2233–2244

Fernandes T, de Almeida Rego L do NA, Nardy M, Yuyama PM, Vanzela ALL. 2009. Karyotype differentiation of four *Cestrum* species (Solanaceae) revealed by fluorescent chromosome banding and FISH. Genetics and molecular biology. 32(2): 320–327.

Fitzpatrick M. 2021. The Open Lab Book. Release 1.0. Readthedocs. p. 50-53;[accessed 2022 Apr 24]. https://buildmedia.readthedocs.org/media/pdf/theolb/latest/theolb.pdf

Franco CV, Liberato Guio SA, Sanchez Betancourt EP, García Arias FL, Nuñez Zarantes VM. 2021. Cytogenetic and cytological analysis of Colombian cape gooseberry genetic material for breeding purposes. Caryologia. 74(3): 21-30.

Fregonezi JN, Fernandes T, Torezan JMD, Vieira AOS, Vanzela ALL. 2006. Karyotype differentiation of four *Cestrum* species (Solanaceae) based on the physical mapping of repetitive DNA. Genetics and molecular biology. 29(1): 97–104.

Fulneček J, Lim KY, Leitch AR, Kovařík A, Matyášek R. 2002. Evolution and structure of 5S rDNA loci in allotetraploid *Nicotiana tabacum* and its putative parental species. Heredity. 88(1): 19-25.

Garcia S, Kovařík A, Leitch AR, Garnatje T. 2017. Cytogenetic features of rRNA genes across land plants: analysis of the Plant rDNA database. The Plant journal: for cell and molecular biology. 89(5): 1020–1030.

Grabiele M, Debat HJ, Scaldaferro MA, Aguilera PM, Moscone EA, Seijo JG, Ducasse DA. 2018. Highly GC-rich heterochromatin in chili peppers (*Capsicum*-Solanaceae): A cytogenetic and molecular characterization. Scientia Horticulturae. 238: 391–399.

Hadziavdic K, Lekang K, Lanzen A, Jonassen I, Thompson EM, Troedsson C. 2014. Characterization of the 18S rRNA gene for designing universal eukaryote specific primers. PLoS One. 9(2):e87624.

Herrera JC. 2007. La citogenética molecular y su aplicación en el estudio de los genomas vegetales. Agronomía colombiana. 25(1): 26–35.

Huang M, Li H, Zhang L, Gao F, Wang P, Hu Y, Yan S, Zhao L, Zhang Q, Tan J, Liu X, He S, Li L. 2012. Plant 45S rDNA clusters are fragile sites and their instability is associated with epigenetic alterations. PLoS One. 7(4): e35139.

Jedrzejczyk I, Rewers M. 2020. Identification and genetic diversity analysis of edible and medicinal Malva species using flow cytometry and ISSR molecular markers. Agronomy. 10(5): 650.

Kapitonov VV, Jurka J. 2003. A novel class of SINE elements derived from 5S rRNA. Molecular biology and evolution. 20(5): 694–702.

Kitamura S, Inoue M, Shikazono N, Tanaka A. 2001. Relationships among *Nicotiana* species revealed by the 5S rDNA spacer sequence and fluorescence in situ hybridization. Theoretical and applied genetics. 103(5): 678–686.

Kovarik A, Matyasek R, Lim KY, Skalická K, Koukalová B, Knapp S, Chase M, Leitch AR. 2004. Concerted evolution of 18-5.8-26S rDNA repeats in Nicotiana allotetraploids. Biological journal of the Linnean Society. Linnean Society. 82(4): 615–625.

Kwon J-K, Kim B-D. 2009. Localization of 5S and 25S rRNA genes on somatic and meiotic chromosomes in *Capsicum* species of chili pepper. Molecules and Cells. 27(2): 205–209.

Liberato S, Sánchez-Betancourt E, Argüelles JH, González C, Núñez VM, Barrero LS. 2014. Cytogenetics of *Physalis peruviana* L. and *Physalis floridana* Rydb. genotypes with differential response to Fusarium oxysporum. Corpoica Ciencia & Tecnología Agro-

pecuaria. 15(1): 51-61.

Lim KY, Matyások R, Lichtenstein CP, Leitch AR. 2000. Molecular cytogenetic analyses and phylogenetic studies in the *Nicotiana* section Tomentosae. Chromosoma. 109(4): 245–258.

Long EO, Dawid IB. 1980. Repeated genes in eukaryotes. Annual review of biochemistry. 49(1): 727–764.

Lopez FB, Fort A, Tadini L, Probst AV, McHale M, Friel J, Ryder P, Pontvianne FDR, Pesaresi P, Sulpice R, et al. 2021. Gene dosage compensation of rRNA transcript levels in *Arabidopsis thaliana* lines with reduced ribosomal gene copy number. The plant cell. 33(4): 1135–1150.

Matyasek R, Lim KY, Kovarik A, Leitch AR. 2003. Ribosomal DNA evolution and gene conversion in *Nicotiana rustica*. Heredity. 91(3): 268–275.

Michael TP. 2014. Plant genome size variation: bloating and purging DNA. Briefings in functional genomics. 13(4): 308–317.

Mirzaghaderi G, Marzangi K. 2015. IdeoKar: an ideogram constructing and karyotype analyzing software. Caryologia. 68(1)31-35.

Moyetta NR, Urdampilleta JD, Chiarini FE, Bernardello GL. 2017. Heterochromatin and rDNA patterns in *Solanum* species of the Morelloid and Dulcamaroid clades (Solanaceae). Plant biosystems. 151(3): 539–547.

Nakamura R, Kitamura S, Inoue M, Ohmido N, Fukui K. 2001. Karyotype analysis of *Nicotiana kawakamii* Y. Ohashi using DAPI banding and rDNA FISH. Theoretical and applied genetics. 102: 810–814.

Park YK, Park KC, Park CH, Kim NS. 2000. Chromosomal localization and sequence variation of 5S rRNA gene in five *Capsicum* species. Molecules and Cells. 10(1): 18–24.

Pellicer J, Hidalgo O, Dodsworth S, Leitch IJ. 2018. Genome size diversity and its impact on the evolution of land plants. Genes (Basel). 9(2): 88.

Pellicer J, Leitch IJ. 2020. The Plant DNA C-values database (release 7.1): an updated online repository of plant genome size data for comparative studies. New Phytologist. 226(2): 301-305.

Pendinen G, Gavrilenko T, Jiang J, Spooner DM. 2008. Allopolyploid speciation of the Mexican tetraploid potato species *Solanum stoloniferum* and *S. hjertingii* revealed by genomic in situ hybridization. Genome. 51(9): 714-20.

Poggio L, Confalonieri V, Comas C, Gonzalez G, Naranjo CA. 2000. Evolutionary relationships in the genus *Zea*: analysis of repetitive sequences used as cytological FISH and GISH markers. Genetics and Molecular Biology. 23(4):1021–1027.

Prado EA, Faivre-Rampant P, Schneider C, Darmency MA. 1996. Detection of a variable number of ribosomal DNA loci by fluorescent in situ hybridization in *Populus* species. Genome. 39(5): 1020–1026.

Raskina O, Belyayev A, Nevo E. 2004. Activity of the *En/Spm*-like transposons in meiosis as a base for chromosome repatterning in a small, isolated, peripheral population of *Aegilops speltoides* Tausch. Chromosome research: an international journal on the molecular, supramolecular and evolutionary aspects of chromosome biology. 12(2): 153–161.

Rego LN, da Silva CRM, Torezan JM, Gaeta ML, Vanzela AL. 2009. Cytotaxonomical study in Brazilian species of *Solanum, Lycianthes* and *Vassobia* (Solanaceae). Plant systematics and evolution. 279: 93–102.

Rodríguez NC, Bueno ML. 2006. Study of the cytogenetic diversity of *Physalis peruviana* L. (Solanaceae). Acta Biológica Colombiana, Bogotá. 11(2): 75-85.

Romero-da MV, Urdampilleta JD, Forni ER, Moscone EA. 2017. Cytogenetic markers for the characterization of *Capsicum annuum* L. cultivars. Plant Biosystems - An International Journal Dealing with all Aspects of Plant Biology. 151(1): 84-91.

Rosato M, Kovařík A, Garilleti R, Rosselló JA. 2016. Conserved organisation of 45S rDNA sites and rDNA gene copy number among major clades of early land plants. PloS one. 11(9): e0162544.

Salim D, Gerton JL. 2019. Ribosomal DNA instability and genome adaptability. Chromosome research: an international journal on the molecular, supramolecular and evolutionary aspects of chromosome biology. 27(1–2): 73–87.

Sánchez EP. 2014. Ploidy Level of Cape Gooseberry Plants from Anther Cultivation. [master's thesis]. Bogotá: Universidad Nacional de Colombia.

Sierra y Selva Exportadora. 2021. Analysis of the Goldenberry Market from 2015 to 2020. Peru: Unidad de Inteligencia Comercial; 9-18.

Siles M, Bracamonte O, García M, López A. 2021. The first report on the identification of the 5s rDNA locus in *Physalis peruviana* L. chromosomes. Scientia Agropecuaria. 12(2): 149-153.

Singh N, Singh S, Maurya P, Arya M, Khan F, Dwivedi DH, Saraf SA. 2019. An updated review on *Physalis peruviana* fruit: Cultivational, nutraceutical and pharmaceutical aspects. Indian Journal of Natural Products and Resources. 10(2): 97-110.

Su D, Chen L, Sun J, Zhang L, Gao R, Li Q, Han Y, Li Z. 2020. Comparative chromosomal localization of 45S and 5S rDNA sites in 76 purple-fleshed sweet potato cultivars. Plants. 9(7): 865.

Trevisani N, Melo, de Melo RC, Oliveira PM, Colli MP, Meirelles JL, Frederico A. 2018. Ploidy and DNA content of cape gooseberry populations grown in southern Brazil. Caryologia. 71(4): 414–419.

Urdampilleta J, Chiarini F, Stiefkens L, Bernardello G. 2014. Chromosomal differentiation of Tribe Cestreae (Solanaceae) by analyses of 18-5.8-26S and 5S rDNA distribution. Plant Systematics and Evolution. 301(5): 1325–1334.

Vitales D, D'Ambrosio U, Gálvez F, Kovařík A, Garcia S. 2017. Third release of the plant rDNA database with updated content and information on telomere composition and sequenced plant genomes. Plant Systematics and Evolution. 303(8): 1115–1121.

Volkov RA, Zanke C, Panchuk II, Hemleben V. 2001. Molecular evolution of 5S rDNA of *Solanum* species (sect. *Petota*): application for molecular phylogeny and breeding. Theoretical and Applied Genetics. 103: 1273–1282.

Wendel JF, Jackson SA, Meyers BC, Wing RA. 2016. Evolution of plant genome architecture. Genome biology. 17(1): 37.

Youn-Kyu P, Kim B-D, Kim B-S, Armstrong KC, Kim N-S. 1999. Karyotyping of the chromosomes and physical mapping of the 5S rRNA and 18S-26S rRNA gene families in five different species in *Capsicum*. Genes & genetic systems. 74(4): 149–157.

ONLINE SUPPLEMENTARY MATERIAL

Figure S1. Chromosomes from the 12 best metaphases among the populations of goldenberries studied.

https://drive.google.com/file/d/1FzgeeRgtUxS2GkD588N8m3cSwzF8Ss1_/view?usp=sharing

ORCID
ZN: 0000-0003-3890-9001

Identification of genetic regions associated with sex determination in date palm: A computational approach

Zahra Noormohammadi[1,*], Masoud Sheidai[2], Seyyed-Samih Marashi[3], Somayeh Saboori[1], Neda Moradi[1], Samaneh Naftchi[1], Faezeh Rostami[1]

[1] *Department of Biology, Science and Research Branch, Islamic Azad University, Tehran, Iran*
[2] *Faculty of Biological Sciences and Biotechnology, Shahid Beheshti University, Tehran, Iran*
[3] *Date Palm & Tropical Fruits Research Center, Horticultural Sciences Research Institute, Agricultural Research, Education and Extension Organization (AREEO), Ahwaz, Iran*
*Corresponding authors. E-mail: marjannm@yahoo.com, z-nouri@srbiau.ac.ir

Abstract. Sex determination of date palm seedlings is the challengeable effort for breeders. Different studies based on molecular markers and genome sequencing have provided some insight in to the genetic regions related to sex determination in date palms in general. But due to differences in cultivar population structure and also cost of whole genome sequencing, we may need a more suitable approach in developing countries for this task. Therefore, we suggest using a combination of different available molecular markers and a computational approach to identify the genetic regions involved in sex differentiation in date palm cultivars. In this study we used twenty-three cultivars including 7 male and 16 female cultivars that were examined by 30 different dominant and co-dominant molecular markers which deal with different genomic regions. Grouping of the tree samples based on 178 loci resulted in genetic differentiation of the studied male and female palm trees. Multiple correspondence analysis (MCA) bi-plot also showed genetic difference within male and female trees. Heatmap plot specified those markers which differentiate date palm trees. SSR (simple sequence repeats) and IRAP (inter retrotransposon amplified polymorphism) markers provided sex linked markers for male cultivars. In present study, we introduced sex specific alleles for Iranian male date palm cultivars as a fast track in seedlings. Different association studies performed identified the candidate genetic regions which are significantly associated with sex differentiation in date palm cultivars.

Keywords: DNA based markers, DAPC, LFMM, MCA, *Phoenix dactylifera*, sex determination.

1 INTRODUCTION

Date palm (*Phoenix dactylifera*, Arecaceae) is the one of the most important fruit products (more than 1.3 M tonnes, FAOSTAT, 2019) in

Iran. Date palm trees are propagated by both offshoots and seeds. Each female tree produces 0-3 offshoots per year. This kind of propagation is not in a way of classical breeding along with low diversity (Adawy et al. 2014). Seed germination is supposed to be easiest way for propagation with high heterozygousity while, it is a time consuming method and may take more than 5 years before flowering.

Date palm is dioecious and the only species of the Palmae with sex chromosomes with 2n =36. In fact, this phenomenon makes difficulty for identification of female trees at early stages of growth (Maryam et al. 2016). Using cytological and biochemical methods may not be used to discriminate date palm male trees from the female trees. However, recently, researchers reported the presence of the occurrence of sex-specific loci in date palm trees (Elmeer and Mattat 2012, Adawy et al. 2014, Al-Ameri et al. 2016, Hassanzadeh and Bagheri 2019). These authors used different molecular markers like random amplified polymorphic DNA (RAPD), inter simple sequence repeat (ISSR), simple sequence repeat (SSR), sequence characterized amplified region (SCAR) and start codon targeted polymorphism (SCoT).

Different genome sequencing approaches have been carried out on limited number of palm trees of different palm species (Torres et al. 2018) to date plan cultivars (Al-Dous et al. 2011, Hazzouri et. al. 2019). These studies have identified the genomic regions associated with sex determination and also a conserved two-locus system present in all palm species. However, due to possible interference of population genetic structure in different date palm cultivars cultivated throughout the world and the high expenses of whole genome sequencing, we suggest to use available molecular markers and analyze the results by using computational approaches to locate the genetic regions associated with dates palm sex determination.

Therefore, The present study was performed with following objectives:1-To identify sex-specific alleles for Iranian male date palm cultivars by using a combination of seven dominant and co-dominant molecular makers like, SSR, ISSR, SCoT, IRAP (inter retrotransposon amplified polymorphism), REMAP (retrotransposon microsatellite amplified polymorphismand SRAP (sequence related amplified polymorphism) for date palm sex determination and, 2- identify the candidate genetic regions involved in sex determination by applying different computational methods like, Fisher Exact test, DAPC (Discriminant analysis of principal components analysis), and LFMM (Latent factor mixed model, Collins and Jombbart 2015, Zhang et al. 2019).

2. MATERIALS AND METHODS

2.1. Plant materials and genetic analysis

In total we studied 23 date palm cultivars, of which 7 were male (including: Sabzparak, GhannamiSabz, Wardi, GhannamiSorkh 1, GhannamiSorkh 2, Foreign male 1 and Foreign male 2) and 16 female cultivars.

Two to three trees from each cultivar were randomly selected for molecular studies (totally 63 trees). Details of the cultivars with their accession numbers are provided in our previous study (Saboori et al. 2021). All cultivars are located Omol-tomair station of Date Palm & Tropical Fruits Research Center, Ahwaz, Iran.

For genetic analysis, genomic DNA was extracted based on Saboori et al. (2021). Seven different molecular markers as SSR (6 loci), EST-SSR (3 loci), SCoT (4 loci), ISSR (5 loci), SRAP (5 loci), IRAP (3 loci) and REMAP (4 loci) were examined for sexual determination (Table S1).

The touch-up PCR program was used for SSR markers; 94°C for 5 min, initial 10 cycles at 95°C for 30 sec, annealing step for 1 min at 51°C, 47.5 °C, 62 °C, 47.5°C, 46.9 °C and 45 °C for MPdCIR078, MPdCIR085, PdCUC3-ssr2, MPdCIR090, MPdCIR048 and MPd-CIR025 loci respectively, 72°C for 1 min and 30 sec. Then 30 cycles were set at 95°C for 30 sec, annealing step (MPdCIR078 52°C, MPdCIR085 49.9 °C, PdCUC3-ssr2 65 °C, MPdCIR090 49.9 °C, MPdCIR048 48.8 °C and MPdCIR025 48 °C) for 1 min. the extension segment was at 72°C for 1 min and 30 sec following final extension at 72 °C for 15 min.

For EST-SSR the following procedure was used; 5 min at 94 °C, 30 sec at 95 °C, 30 sec at 50 °C, 52 °C-and 60 °C for EST-PDG3119-rubisco, EST-GTE and EST-DPG0633- Laccase loci respectively and 1 min and 30 sec at 72 °C. These segments repeated for 35 cycles. Final extension was for 5 min at 72 °C.

The SCoT loci were amplified based on our previous study (Saboori et al. 2020) and its data used for sexual determination.

The PCR reaction for the ISSR markers were performed according to the following thermal program: 5 minutes at 94°C, 40 cycles of 30 seconds at 94°C, 60 seconds at 50-52.5°C (50°C for (GA)9T, (CA)7AT, and (GA)9A, 52/5°C for (GT)8YA and (AG) 8YT) and 90 seconds at 72°C and final extension for 7 minutes at 72°C. Molecular marker reactions were carried out in 25 μL volume with 20 ng genomic DNA and 5 U of *Taq* DNA polymerase (Bioron, Germany), 2X PCR buffer (50 mM KCl; 10 mM Tris-HCl, pH;8), 1.5-2 mM MgCl2; 0.2 mM of each dNTP (Bioron, Germany); 0.2 μM of each primer.

For IRAP and REMAP markers, we used thermal program: 3 min of initial denaturation at 94°C, followed

by 40 cycles of 94°C for 3 min and annealing temperature 51-54 °C for IRAPs and 51-56 °C for REMAPs for 30 s, 72°C for 3 min, and 10 min at 72°C for final extension. All reactions were set up at BIORAD Thermocycler, USA.

The band profile of each locus was visualized by using 2.5 % agarose gel electrophoresis. Staining of gels were performed by the sybergreen dye. We used the 100 base pair (bps) molecular size ladder for estimation of fragment size (Fermentas, Germany).

2.2. Data analysis

All obtained bands of 30 loci were scored as a binary data. Multiple correspondence analysis (MCA) of molecular data was performed to group the studied palm trees based on sex differentiation as performed in R-Package 4.1(Abdi and Williams 2010). AMOVA test was performed for differentiation of two male and female groups by using GenAlex ver. 6.5.

For Association studies, different statistical and bioinformatic approaches are available which have different assumptions. We used DAPC (Discriminant analysis of principal components), and Bayesian based method of LFMM (Latent factor mixed model), as suggested by Frichot et al (2013), and Collins and Jombbart (2015). These analyses were followed by Bonferroni correction as well

as false discovery rate (FDR) tests, to avoid both type I and type II errors of rejecting true association results. These were done in R package 4.1. Similarly, for accuracy of the model presented by. DAPC we used cross validation method as implemented in R. 4.1.

3. RESULTS

In total we obtained 178 loci/ bands by different molecular markers studied. Ward dendrogram (Fig. 1), differentiated between the studied male and female palm trees as the samples of either group were placed in a separate cluster. Therefore, it shows that the molecular markers used in present study can differentiate palm trees based on different sexes.

Multiple correspondence analysis (MCA) of molecular data obtained revealed that about 60% of total genetic variation of the studied samples may be explained by about 10 PCA axis (Fig. 2).

The grouping of the studied palm trees by MCA biplot by using the first two PCA axes (Fig. 3), not only separated male and female trees from each other but also revealed some degree of genetic difference within male and female samples studied.

In general, two different genetic groups can be seen in either of these sexes. A heat-map was constructed
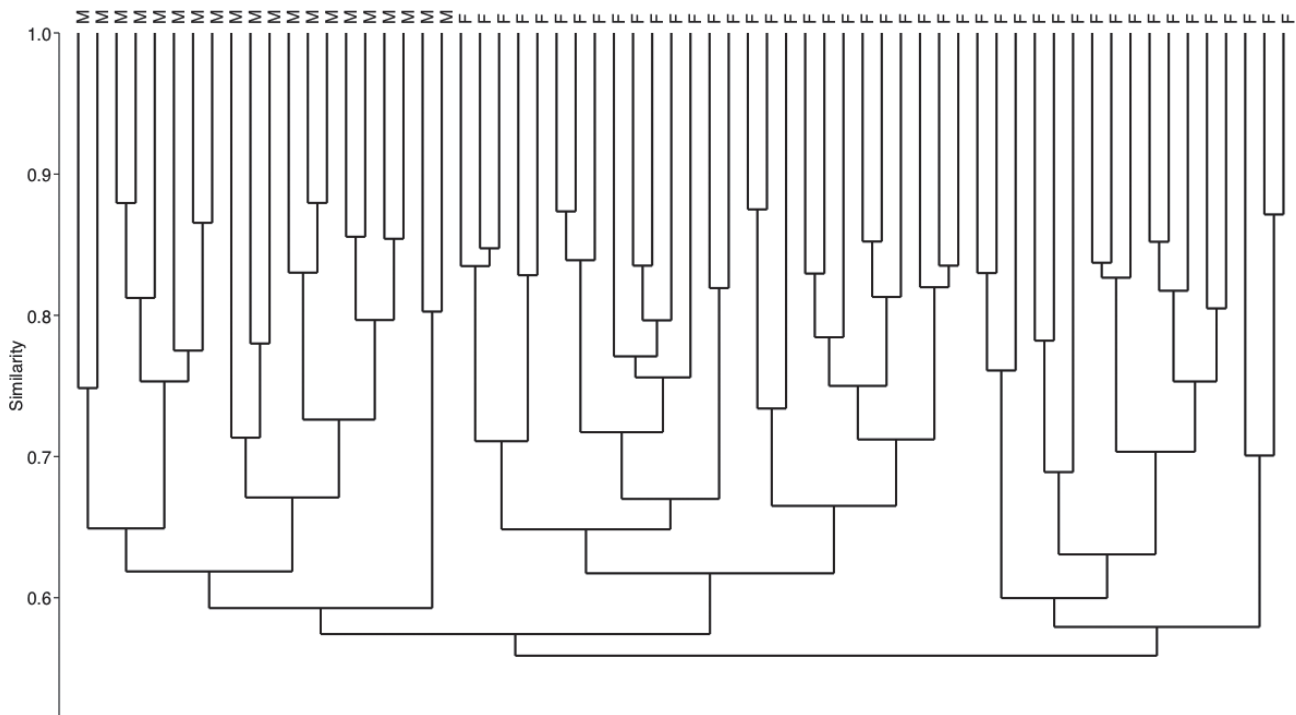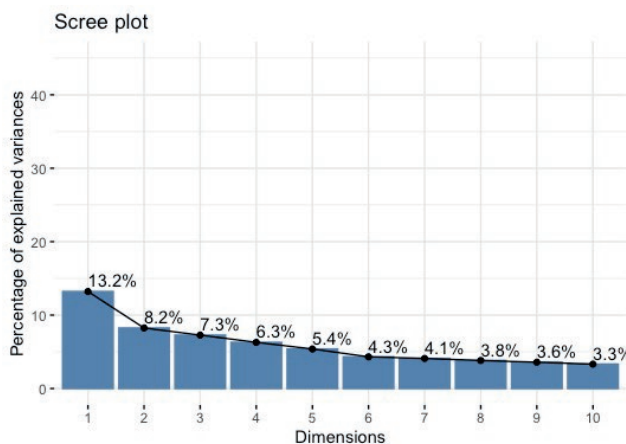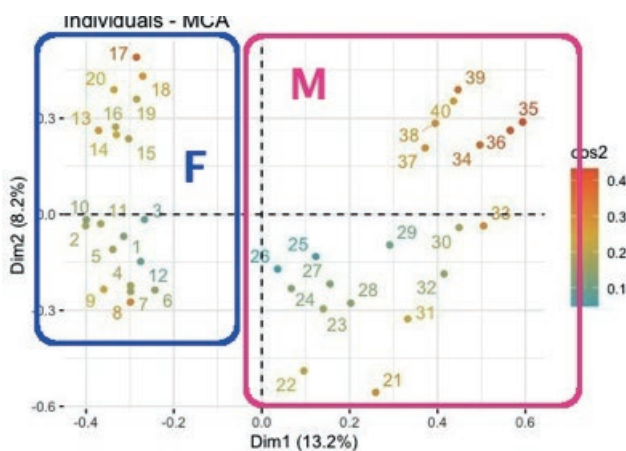

Figure 1. Ward dendrogram of male (M) and female (F) date palm trees based on combined molecular data.

Figure 2. Multiple correspondence analysis (MCA) based on 30 loci studied on date palm trees.
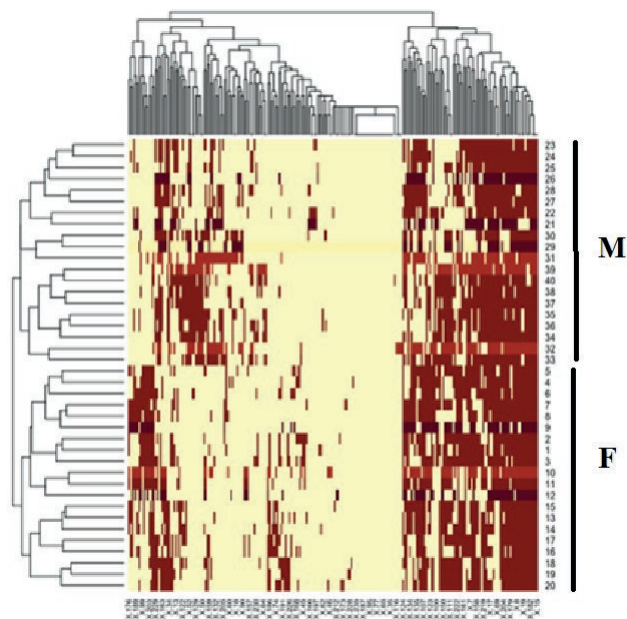

Figure 3. MCA biplot: Grouping date palm trees based on first two components. Numbers are individuals. Color gradient shows amount of variance based on MCAfrom high to low. M; male trees and F: female trees studied.

Figue 4. Heatmap cluster based on 30 molecular loci and male (M) and female (F) date palm trees studied.

(Fig. 4) to group those molecular markers which show similarity in differentiating palm tree samples.

AMOVA test also confirmed differentiation between two male and female groups ($r = 0.129$, $P = 0.001$, Table S2).

The primers with highest degree of contribution to genetic differentiation of male and female date palm trees have been shown in Fig. 5. Primer bands IRAP-Nikita_2000, 3'LTR_100, ISSR-(CA)7AT-400, SSR-MPd-CIR048-120, are among the most contributing primers of the first MCA axis. Similarly, primer bands IRAP-Nikita_200, SSR-MPdCIR048-200, Nikita+SSR2_100, are among the primers which highly contributed in MCA axis 2.

A much more detailed information can be obtained from MCA-biplot (Fig. 6), which shows the presence (Y), and absence (N), of the particular primer bands contributed in separating female (Numbers 1-20 in Fig. 5), and male (Numbers 21-40, in Fig. 5) palm trees. It is evident from this biplot that both presence and absence of different primer bands of the utilized molecular markers can together differentiate male palm trees from females.

We found some loci which are specific in male date palm cultivars (Table 1, Fig. S1). The MPdCIR048(GA)32-SSR locus, showed specific allele between 100-130 bps. The 110 bps band was unique for all male trees including SabzParak, GhannamiSabz, Wardi, GhannamiSorkh, GhannamiSorkh2, Foreign male1 and Foreign male2 cultivars. The 130 bps allele was observed only in GhannamiSorkh1, GhannamiSorkh2, Foreign male1 and Foreign male 2 while, allele in size of 120 bps was unique in two male cultivars (Sabzparak and Wardi). In EST-SSR data, one allele in EST-PDG3119-rubisco with 200 base pairs in size showed specificity in all male cultivars except SabzParak male cultivar.

Similarly, IRAP-3LTR locus produced alleles between 400 to 1600 bps which were specific at some of the male trees (Table 1). For instance, the band in 300 bps in length was amplified in all male trees except Sabzeparak male cultivar and were absent in all female date palm trees.
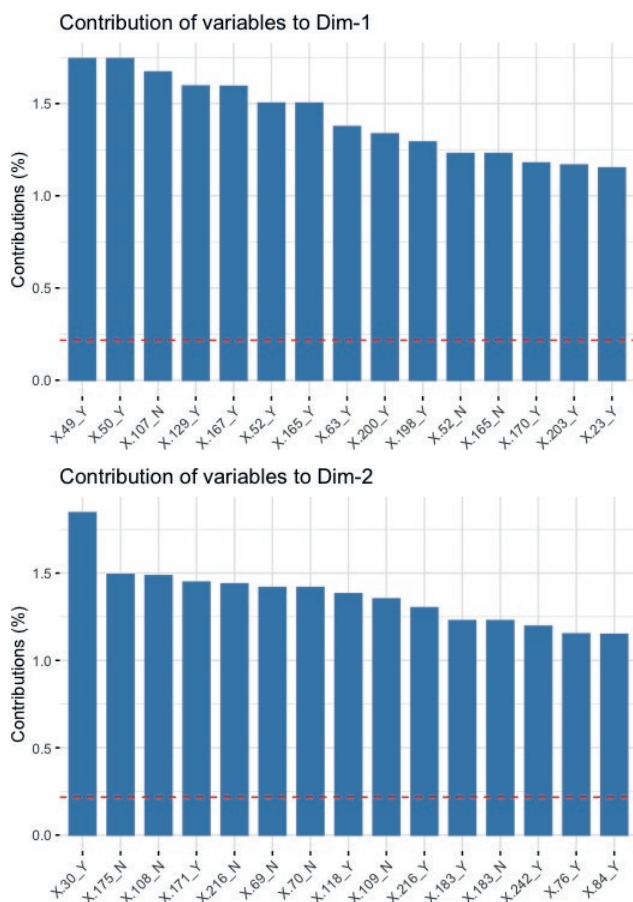
Figure 5. MCA axes. 1 and 2, showing primer bands with highest degree of contribution in date palm male and female differentiation.

3.1. Association studies molecular markers and sex differentiation

All association approaches produced almost similar results and identified the same loci as the genetic regions which are associated with sex differentiation. For example, Fisher exact test and DAPC identified three following marker loci after Bonferroni correction at p = 0.01: X18 (SRAP loci), X50 X51 X53 X64 (IRAP loci), X91 X98 X108 (REMAP loci), and X171 X174 X176 (SSR loci).

These loci can efficiently differentiate male versus female date palm trees studied (Fig. 7).

Similarly, LFMM analysis of both Lasso and Ridge methods produced almost similar results after Bonferroni correction and false discovery rate (FDR) test (Fig. 8). The loci which identified are in agreement with the results of Fisher exact test and DAPC presented before.

Therefore, a combination of molecular markers may be used in early-stages sex determination in date palm cultivars with focus on highly associated marker loci.

4. DISCUSSION

Sex determination is one of the main concerns of date palm breeders. Different studies have been reported to introduce proper biomarkers but they are restricted to few cultivars. Recent GWAS study revealed 112 SNPs related to sex determination in a region with ~6 Mb at LG 12 while other 43 SNPs dispersed on other date palm
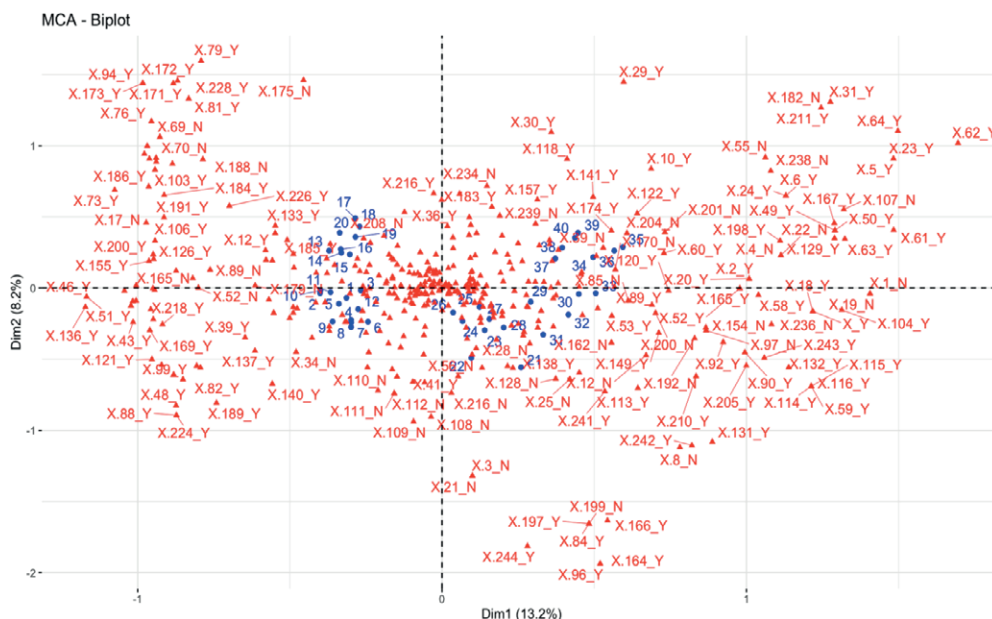
Figure 6. MCA-biplot based on alleles studied. Red numbers : alleles (Y=presence and N=absence), blue number: date palm trees numbers.
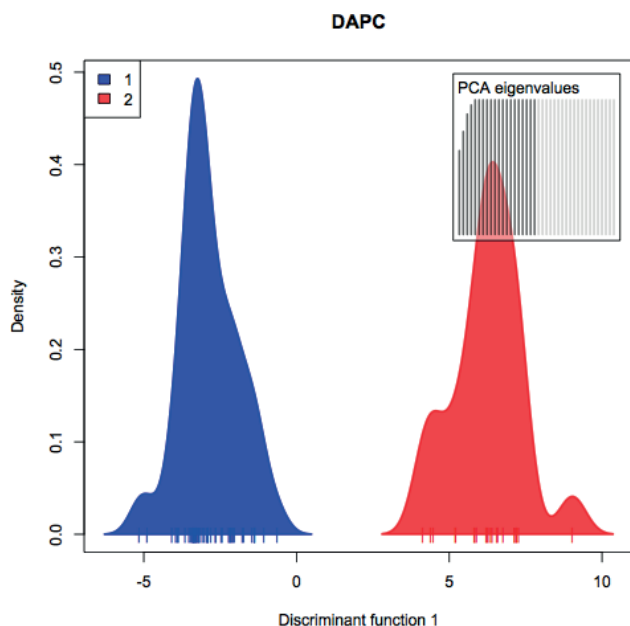
Figure 7. DAPC plot showing differentiation of female (1) versus male (2). date palm trees based on associated marker loci.

and therefore result in establishing male sex in palm tree (Torres et al. 2021). However, genetic variations have been observed in both sex linked and autosomal regions. It may call more effort to find proper sex biomarker for date palm cultivars.

In present study, we used 30 different loci may be located in different genome regions. Base on the allele data, 60% of alleles covered the most variable alleles. The first two MCA components showed the highest level of variation and ena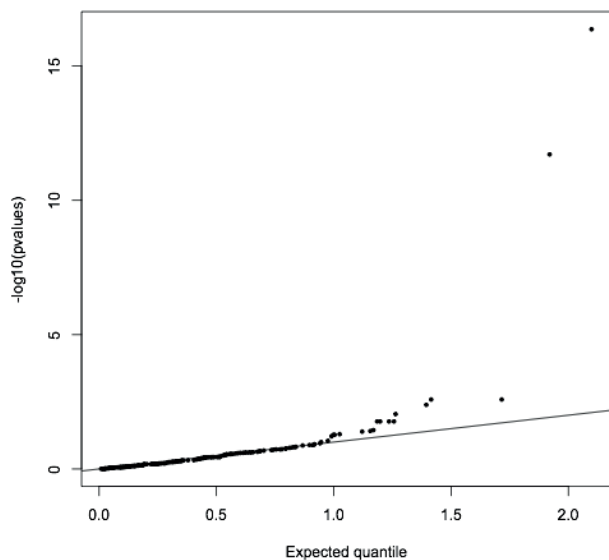bled to differentiate male and female trees. Most of the identified alleles in these two components belong to SSR and IRAP loci (Fig. 5).

We used multiple correspondence analysis (MCA) as a statistical precise method for categorical data (binary data, Abdi and Williams, 2010)

MCA bi-plot provides a picture which illustrates the variable that can discriminates the studied individual MCA bi-plots (Fig. 6) depicted all 250 alleles of 30 loci studied. It clearly shows the contribution of each allele to discrimination of male and female trees. Moreover, different association studies in present paper identified genomic regions which are associated with sex differentiation in date palm cultivars.

In details, we introduced male specific alleles for six important Iranian male date palm cultivars. The MPd-CIR048 SSR locus has two alleles (100, 130 bps) which could discriminate all male cultivars studied (Table 2). This SSR locus located in Cytosine-S-methyltransferase DRM2-like (DRM2). Jskani et al. (2016) also reported

chromosomes (Hazzouri et al. 2019). Torres et al. (2021) also reported four conserved genes in *Phoenix* males. Some mutations in putative genes involved in sex determination (CYP703 and GPAT3), is supposed to repress recombination in these regions, leading to gynodioecy
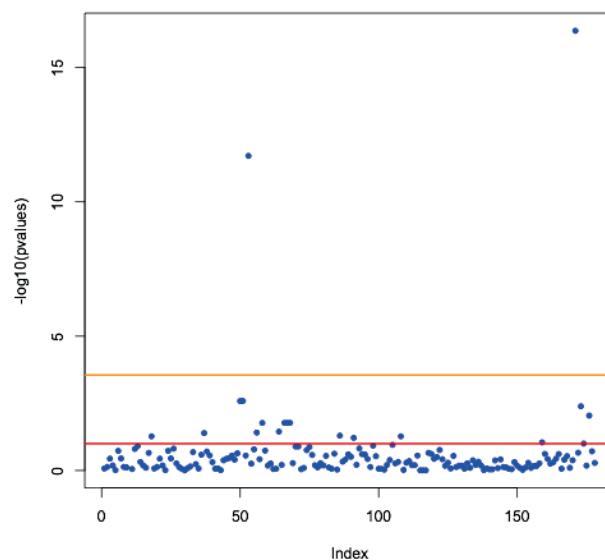
Figure 8. LFMM results showing associated marker loci with sex differentiation in date palm cultivars studied.

Table 1. Specific alleles in male date palm trees. M1 (SabzParak), M2 (GhannamiSabz), M3 (Wardi), M4 (GhannamiSorkh 1), M5 (GhannamiSorkh 2), M6 (Foreign male1), M7 (Foreign male 2)

Locus/Male	M1	M2	M3	M4	M5	M6	M7
SSR (bp)							
	110/120	110/110	110/110	110/130	110/130	110/130	110/130
MPdCIR048	100/120	110/110	110/110	110/110	110/130	110/130	110/130
	100/120	110/110	110/120	110/130	110/130	110/130	110/130
EST- PDG3119-rubisco	-	200	200	200	200	200	200
IRAP-3'LTR(bp)							
	400/500	300/500/600/	300/500/600/	100/200/300 400/500/600 700/800/900 1500	100/200/300 400/500/600 700/750/1500	100/200/300 400/600/700 900/1000/1500 1600	100/200/300 400/600/800 1500/1600

male specific alleles of this locus but in different size (250bps) while we detected that allele in both male and female trees. The 190/160 allele pattern for this SSR locus was reported by Elmeer and Mattat (2012) in Qatar male date palm trees. Maryam et al. (2016) also reported male specific alleles in this locus (250/250) for Pakestani cultivars. It clearly shows the pivotal role of this locus in sex determination although different allelic patterns may be obtained from different male cultivars due to genetic variations of the studied cultivars. On the other hand, Wang et al. 2020 reported that mPdIRDP52 was sex linked for cultivars collected from China.

ISSR markers as a dominant marker showed less discrimination power for sex discrimination. It is in agreement with the results of the study performed by Hassanzadeh Khankahdani and Bagheri (2019). In other plants like *Trichosantes dioica* Roxbi. and *Hippophae rhamnoides* ssp. *turkestanica* ISSR markers could show sex discrimination (Nanda et al. 2013, Adhikari et al. 2014,Das et al. 2017)

Retrotansposone based markers with their abundance, mode of amplification and insertion into the genome, have characteristics suitable for discriminate between species or genotypes (Biswas et al. 2010). About 21% of whole genome of *P.dactlylifera* defined for retrotransposons, mostly including Ty1/Copia and Ty3/gypsy (Al-Dous et al. 2011, Al-Mssallem et al. 2013, Nouroz and Mukaramin 2019). We used IRAP and REMAPs' profiles between male and female date palm trees. IRAP loci are among loci with the high degree of contribution to total variance in our MCA analysis. However, only one of IRAP loci (3´LTR) showed sex discrimination in 5 male cultivars. this a first report on male- link IRAP markers in date palm trees.

Adawy et al. (2014) introduced two SCoT alleles (850 bps and 1150 bps) in SCoT36 and SCoT4 in Egyptian female date palm trees as sex-linked markers while in present study we observed these alleles in both gender. cDNA-SCoT allele based on flowering stage was also used for development of SCAR maker by Al-Ameri et al. (2016) for determination of male trees of Saudi Arabia date palm cultivars. They believed that the different gene expression patterns in flowering stage in male and female trees may provide a simple and inexpensive tool for sex determination. However, our literature reviews revealed that sex linked markers in date pale cultivars are specified in local orchards and restricted to the countries. With regard to multilocus nature of SSR markers, it may make different size of alleles for one locus in different cultivars with different geographical locations probably due to newmutations and allele adaptation.

5. CONCLUSION

The urgent method for sex determination in date palm nursery orchards is pivotal for breeding industry. Our data could provide the highest variant alleles among 30 loci studied by MCA for sex determination. We also introduced sex specific alleles for male cultivars as a fast track in seedlings.

AUTHOR CONTRIBUTION STATEMENT

Z.N.: conceptualization of the project; M.Sh.: analyses of data; S.S, N.M., S.N., F.R.: data collection and lab

work; S.M.: providing samples; Z.N, M.Sh. S.M. and S.S. project design

DATA ARCHIVING STATEMENT

All tree samples used in this research are being archived in Herbarium of ShahidBeheshti University, Tehran, Iran. The accession numbers will be supplied once available.

REFERENCES

Abdi H, Williams LJ (2010) Principal component analysis Wiley interdisciplinary reviews: Comput Stat 2: 433-459.

Adawy SS, Jiang J, Atia MA (2014) Identification of novel sex-specific PCR-based markers to distinguish the genders in Egyptian date palm trees. Int J Agric Sci Res 4: 45-54.

Adhikari S, Saha S, Bandyopadhyay TK, Ghosh P (2014) Identification and validation of a new male sex-specific ISSR marker in pointed gourd (Trichosanthes dioica Roxb.). Sci World J;2014:216896. doi: 10.1155/2014/216896.

Al-Ameri AA, Al-Qurainy F, Gaafar ARZ, Khan S, Nadeem M (2016) Molecular identification of sex in *Phoenix dactylifera* using inter simple sequence repeat markers. BioMed Res Intl 2016: 1-5.

Al-Dous EK, George B, Al-Mahmoud M E, Al-Jaber MY, Wang H, Salameh YM, Malek J A (2011) De novo genome sequencing and comparative genomics of date palm (*Phoenix dactylifera*). Nature Biotechnol 29: 521.

Al-Mssallem I S, Hu S, Zhang X, Lin Q, Liu W, Tan J, Yu J (2013) Genome sequence of the date palm *Phoenix dactylifera* L. Nature Commun 4: 1-9.

Biswas MK, Xu Q, Deng XX (2010) Utility of RAPD, ISSR, IRAP and REMAP markers for the genetic analysis of *Citrus* spp. Sci Hort 124: 254-26.

Collins C, Jombbart T (2015) Genome-Wide association studies. Impeerial college London. MRC Center. For Outbreak Analysis and Modeling: 1-61.

Das K, Ganie SH, Mangla Y. et al. (2017) ISSR markers for gender identification and genetic diagnosis of Hippophae rhamnoides ssp. turkestanica growing at high altitudes in Ladakh region (Jammu and Kashmir). Protoplasma 254, 1063–1077. https://doi.org/10.1007/s00709-016-1013-8.

Elmeer K, Mattat I (2012) Marker-assisted sex differentiation in date palm using simple sequence repeats. 3 Biotech. 2: 241-247.

Frichot E, Schoville SD, Bouchard G, Francois O (2013) Testing for associations between loci and environmental gradients using latent factor mixed models. Mol Biol Evol 30:1687-1699.

Hassanzadeh Khankahdani H, Bagheri A (2016) Identification of genetic variation of male and female date palm (*Phoenix dactylifera* L.) cultivars using morphological and molecular markers. Intl J Hort Sci Technol 6: 63-76.

Hazzouri KM, Gros-Balthazard M, Flowers JM, Copetti D, Lemansour A, Lebrun M, Purugganan MD (2019) Genome-wide association mapping of date palm fruit traits. Nature Commun 10: 1-14. https://doi.org/10.1038/s41467-019-12604-9.

Jaskani MJ, Awan FS, Ahmad S, Khan IA (2016) Development of molecular method for sex identification in date palm (Phoenix dactylifera L.) plantlets using novel sex-linked microsatellite markers. 3 Biotech 6:22.

Maryam Jaskani MJ, Awan FS, Ahmad S, Khan IA (2016) Development of molecular method for sex identification in date palm (*Phoenix dactylifera* L.) plantlets using novel sex-linked microsatellite markers. 3 Biotech 6(22): 1-7.

Nanda S, Kar B, Nayak S, Jha S, Kumar Joshi R (2013) Development of an ISSR based STS marker for sex identification in pointed gourd (Trichosanthes dioica Roxb.). Sci Hort 150: 11-15.

Nouroz F, Mukaramin A (2019) Genomic and evolutionary diversity of LTR retrotransposons in date palm (*Phoenix dactylifera*) Pakistan J Bot 51: 1637-1644.

Saboori S, Noormohammadi Z, Sheidai M, Marashi S (2020) SCoT molecular markers and genetic fingerprinting of date palm (*Phoenix dactylifera* L.) cultivars. Genet Resour Crop Evol 67: 73-82.

Saboori S, Noormohammadi Z, Sheidai M, Marashi S (2021) Insight into date palm diversity: genetic and morphological investigations. Plant Mol Biol Rep 39: 137-145.

Torres MF, Mathew LS, Ahmed I, Al-Azwani IK, Krueger R, Rivera-Nuñez D, Malek JA (2018) Genus-wide sequencing supports a two-locus model for sex-determination in Phoenix. Nature Commun 9: 1-9. DOI: 10.1038/s41467-018-06375-y.

Zhang F, Chen W, Zhu Z *et al.* (2019) OSCA: a tool for omic-data-based complex trait analysis. Genome Biol 20: 107 . https://doi.org/10.1186/s13059-019-1718-z

Wang Y, Ihase LO, Htwe YM, Shi P, Zhang D, Li D, et al. (2020) Development of sex-linked SSR marker in the genus Phoenix and validation in *P. dactylifera*. Crop Sci 60: 2452-2466.

SUPPLEMENTARY DATA

Table S1. Molecular marker primers, their names and sequences used in this study.

Marker	Locus name	Sequence (5´-3´)
SSR (Bodian et al. 2014)		
	MPdCIR025(GA)22-F	GCACGAGAAGGCTTATAGT
	MPdCIR025(GA)22-R	CCCCTCATTAGGATTCTAC
	MPdCIR048(GA)32-F	CGAGACCTACCTTCAACAAA
	MPdCIR048(GA)32-R	CCACCAACCAAATCAAACAC
	MPdCIR078(GA)13-F	TGGATTTCCATTGTGAG
	MPdCIR078(GA)13-R	CCCGAAGAGACGCTATT
	mPdCIR085(GA)29-F	GAGAGAGGGTGGTGTTATT
	mPdCIR085(GA)29-R	TTCATCCAGAACCACAGTA
	MPdCIR090(GA)26-F	GCAGTCAGTCCCTCATA
	MPdCIR090(GA)26-R	TGCTTGTAGCCCTTCAG
	PdCUC3-ssr2(GA)22-F	ACATTGCTCTTTTGCCATGGGCT
	PdCUC3-ssr2(GA)22-R	CGAGCAGGTGGGGTTCGGGT
EST-SSR		
(Zhao et al. 2012)	EST-PDG3119-rubisco-F	CATACTGATTATTGGCACACC
	EST-PDG3119-rubisco-R	GTACCATACCGTACCAGTTCA
(Zhao et al. 2012)	EST-DPG0633- Laccase -F	AGACTGGTTAAGTTGGTGGAG
	EST-DPG0633-Laccase-R	CTACAAAACTGATGTGGTGGT
	EST-GTE-F	GCTTGGCCATCTATGAAAC
	EST-GTE-R	ACTCTGAGCATCCATATCG
SCoT (Collard and Mackill 2009)		
	SCoT1	CAACAATGGCTACCACCA
	SCoT2	CAACAATGGCTACCACCC
	SCoT36	GCAACAATGGCTACCACC
	SCoT41	CAATGGCTACCACTGACA
ISSR		
	(GA)9T	GAGAGAGAGAGAGAGAGAT
	(CA)7AT	CACACACACACACAAT
	UBC849	GTGTGTGTGTGTGTGTYA
	(GA)9A	GAGAGAGAGAGAGAGAGAA
	UBC834	AGAGAGAGAGAGAGAGYT
SRAP (Feng et al. 2014)		
	ME1	TGAGTCCAAACCGGATA
	ME4	TGAGTCCAAACCGGACC
	EM3	GACTGCGTACGAATTGAC
	EM4	GACTGCGTACGAATTTGA
IRAP		
	Nikita	CGCATTTGTTCAAGCCTAAACC
	3'LTR	TGTTTCCCATGCGACGTTCCCCAACA
	5'LTR1	TTGCCTCTAGGGCATATTTCCAACA
REMAP		
	SSR_PdCIR025_R + NIKITA	
	SSR_PdCIR025_R + 3'LTR	
	SSR_PdCIR048_R + NIKITA	
	SSR_PdCIR048_R + 5'LTR1	

Table S2. AMOVA test based on date palm trees in two groups: male and female trees. df; degree of freedom, SS: sum of square, MA: mean of square, Var: variance.

Source	df	SS	MS	Est. Var.	var%
Among Pops	1	135.730	135.730	3.491	13%
Within Pops	68	1598.284	23.504	23.504	87%
Total	69	1734.014		26.996	100%
Stat	Value	P value			
PhiPT	0.129	0.001			

Figure S1. Allele pattern of some femal and male date palm trees. Left to right: first 5 samples are female and 6-9 male trees.

Caryologia
International Journal of Cytology,
Cytosystematics and Cytogenetics

Comparative karyological analysis of some Turkish *Cuscuta* L. (Convolvulaceae)

Neslihan Taşar[1], İlhan Kaya Tekbudak[2], İbrahim Demir[3], Mikail Açar[1,*], Murat Kürşat[3]

[1] *Munzur University, Department of Plant and Animal Production, Tunceli Vocational School of Higher Education, Tunceli, 62000, Turkey*
[2] *Van Yüzüncü Yıl University, Faculty of Agriculture, Department of Plant Protection, Van, Turkey*
[3] *Bitlis Eren University, Faculty of Arts and Sciences, Department of Biology, Bitlis, Turkey*
*Corresponding author. E-mail: mikailacar@munzur.edu.tr

Abstract. This study investigated the somatic chromosome numbers and morphometric properties of 11 different taxa belonging to the genus *Cuscuta* L., which is one of the parasitic flowering plants and causes significant economic losses on agricultural products. For this purpose, the species were examined karyologically and compared statistically. Belonging to the genus *Cuscuta*, *C. campestris* Yunck., *C. hyalina* Roth, *C. kotschyana* Boiss., *C. babylonica* Aucher ex Choisy, *C. europaea* L., *C. kurdica* Engelm., *C. brevistyla* A.Braun ex A.Rich, *C. planiflora* Ten., *C. approximata* Bab., *C. lupuliformis* Krock. *C. palaestina* Boiss. the chromosome number and morphology of the species were investigated using karyological techniques. Chromosome numbers of the species; *C. kotschyana, C. babylonica, C. europaea, C. kurdica, C.planiflora* 2n=14; *C. campestris, C. hyalina, C. approximata, C. lupuliformis*, and *C. palaestina* 2n=28 and *C. brevistyla* 2n=42 is determined. Also, the species' chromosome number, total chromosome length, relative length, arm ratio, centromere index and centromere states, and karyotype asymmetry values were determined. Chromosome numbers of *C. kotschyana* and *C. kurdica* taxa were defined for the first time in this study. Thus, new data on the systematics of these species have been revealed.

Keywords: Convolvulaceae, *Cuscuta*, parasitic plant, Chromosome number, karyotype.

INTRODUCTION

Cuscuta (Dodder) is a member of the Convolvulaceae family, including about 200 different root parasite species. About 15-20 of these species cause severe problems in agricultural areas (Dawson et al., 1994). With this, most *Cuscuta* species are considered extinct in the wild, and some species even require conservation measures in nature (Costea and Stefanovic 2009a). *Cuscuta* species can be found in various habitats, including temperate, tropical, desert, riparian, coastal, high mountain, woodland, saltwater, and degraded environments (Costea et al., 2015). Like other parasitic plants, *Cuscuta* species play an essential role in ecosystems (Press et al. 1999).

Yunker (1932) divided the genus *Cuscuta* into three subgenera according to styles and stigma shapes. These; *Cuscuta* are Grammica (Lour.), Yunck, and Monogynella (Des Moul.). In the flora of Turkey, 15 species of these subgenera and two unknown species (*C. aratica* Butk. and *C. subuniflora* K. Koch), and one suspicious (*C. epilinum* Wiehe) species have been identified (Plitman, 1978). Since the vegetative parts of parasitic plants are generally reduced, flower characters are insufficient in taxonomy. This situation creates problems in diagnosis. For this reason, it is necessary to use some methods to identify species belonging to the genus *Cuscuta*. Studying chromosome numbers and structures can give valuable results in solving taxonomic problems (Taşar et al., 2018a; 2018b).

It has been determined that *Cuscuta* species generally have holocentric chromosomes and undergo inverted meiosis (Pazy and Putmann 1987; 1991; 1994).

Some morphological features are overlooked in plant determinations and classifications of classical taxonomy. Characteristics acquired according to environmental factors appear to be new features, confusing classification. For this reason, considering the characters in classical taxonomy, examining the chromosome numbers, structure and structures gives beneficial results in solving the problems (Taşar et al., 2018a; 2018b). In addition, statistical analyzes can be useful in morphological and anatomical studies recently (Genç et al. 2021; Arabacı et al. 2021; Dirmenci et al. 2019; Dirmenci et al. 2020; Açar and Satıl 2019; Açar and Taşar 2022). This study aims to reveal the karyological features of *Cuscuta* species distributed in Turkey, determine the relationships between them, and contribute to the genus's taxonomic classification.

MATERIAL AND METHODS

Material

Cuscuta samples, the study material, were obtained from the field. Localities of taxa are given in Table 1. Plant taxa were identified using the genus *Cuscuta* (Yuncker 1932) and Flora of Turkey. (Davis, 1978). The collected specimens have been turned into herbarium material and are kept in Van Yüzüncü Yıl University, Faculty of Agriculture, Plant Protection Department, and Bitlis Eren University, Biology Department.

Methods

Chromosome measurements

The seeds of the plant samples were sown in Petri dishes and germinated in an oven at 20-22 ºC. Roots reaching 1–2 cm in length from the germinated seeds were cut, kept in colchicine for 2 hours at room temperature, and subjected to pretreatment (Gedik et al., 2014). Then, the root tips were placed in Carnoy fixative (3:1) and fixed by keeping them in the refrigerator at +4 ºC for 24 hours. At the end of the period, root tips were hydrolyzed in 1N HCl in an oven at 60 ºC for 5-18 minutes. Root tips removed from hydrolysis were stained with Feulgen stain for 1 hour in a dark environment at room temperature. Then it was washed 2-3 times with tap water. For preparation, the growth meristem part was cut off with a sharp razor blade in a drop of 45% acetic acid on the slide, and the coverslip was closed. The best three somatic cells for each species were photographed using an Olympus BX53 microscope. The naming system of Levan (1964) was used to locate the centromere. The intra-chromosomal asymmetry index (A1) was calculated according to the formula proposed by Romero Zarco (1986). Interchromosomal asymmetry index (A2) and karyotype symmetry nomenclature were made according to Stebbins (1971).

Statistical analisyes

For analysis used, several formulas were established on chromosome characteristics. The measurements were built on haploid datasets. The calculations and abbreviations used in the analysis are as follows. TLC (total length of chromosomes), MTLC (mean of total length of chromosomes), MAX (maximum length of chromosome), MIN (minimum length of chromosomes), MLA (mean of long arms), MSA (mean of short arms), MrV (mean of r-value), MdV (mean of d value), MAR (mean of arm ratio), MCI (mean of chromosome index), MRLC (mean of the relative length of chromosomes), DRL (difference of range of relative length), TF% (total form percentage), S% (relative length of the shortest chromosome), A1 (intrachromosomal asymmetry index), A2 (interchromosomal asymmetry index), and A (Degree of asymmetry). Both arm ratios were assumed to be equally affected (Adhikary 1974). All karyotype formulas and asymmetry indexes were determined based on Huziwara (1962) (TF%), Levan et al. (1964) (r and d values), Zarco (1986) (A1 and A2), Watanabe (1999) (A), Peruzzi and Eroğlu (2013) (CI) as well. The abbreviations were taken from Rezeai et al. (2014) (RLC%, DRL, S%). The formulas are as follows.

Formulas

$$r\ value = \frac{Length\ of\ the\ long\ arm\ of\ chromosome}{Length\ of\ the\ short\ arm\ of\ chromosome}$$

d value=Length of the long arm of chromosome-Length of the short arm of chromosome

$$arm\ ratio = \frac{Length\ of\ the\ short\ arm\ of\ chromosome}{Length\ of\ the\ long\ arm\ of\ chromosome}$$

$$CI = \frac{Length\ of\ the\ short\ arm\ of\ chromosome}{Length\ of\ the\ long\ arm\ of\ chromosome + Length\ of\ the\ short\ arm\ of\ chromosome}$$

$$RLC\% = \frac{total\ length\ of\ each\ chromosome}{total\ length\ of\ chromosomes}\ x\ 100$$

DRL=(maximum relative length)- (minimum relative length)

$$TF\% = \frac{total\ length\ of\ short\ arms}{total\ length\ of\ chromosomes}\ x\ 100$$

$$S\% = \frac{length\ of\ shortest\ chromosome}{length\ of\ longest\ chromosome}\ x\ 100$$

$$A = \left(\frac{1}{n}\right)\sum Ai, \quad Ai = \frac{li-si}{li+si}$$

(li = lengths of a long arm, si = lengths of a short arm, n = haploid chromosome number).

$$A1 = 1 - \frac{\sum_{i=1}^{n}\frac{b_i}{B_i}}{n}$$

(n = number of homologous chromosome pairs, b_i = the average length of short arms in every homologous chromosome pair, B_i = the average length of long arms in every homologous chromosome pair).

$$A2 = \frac{s}{\bar{x}}$$

(S = standard deviation of chromosome lengths, = mean of chromosome lengths).

A data matrix was constructed according to 17 chromosomal traits in Table 1. The Principal Component Analysis (PCA) was used based on the data matrix. Next, the cluster analysis was made using the Gower similarity index to determine the relationships between *Cuscuta* taxa's chromosome traits. Also, the Pearson correlation coefficient (r) analysis was performed to see strong and weak relationships between chromosome traits. At the same time, Shapiro - Wilk normality test was performed. Then, the one-way analysis of variance (ANOVA) was performed to determine whether the difference between the data was statistically significant. All the analyses were carried out with PAleontoSTatistics (PAST) (Hammer et al. 2001).

RESULTS

In this study, the karyological characteristics of 11 different *Cuscuta* taxa were investigated, and their details are given below.

Cuscuta campestris: The chromosome number of *C. campestris*, native to the United States of America and spread to many countries from there, and can be found almost everywhere in Turkey, was found to be 2n=2x=28. The haploid karyotype formula of this species is 10 median regions (m), 2 submedian regions (cm), and 2 dotted median (M) regions. Metaphase chromosome length varies between 2.48-1.48 μm. Chromosome arm ratios vary between 1.43-1 μm. Its centromere index ranges from 50.00 to 29.44 μm, and its relative length is between 10.93 and 18.32 μm. The intra-chromosomal asymmetric index (A1) is 0.32, and the inter-chromosomal asymmetric index (A2) is 0.04 (Table 2, Figure 1).

Cuscuta hyalina: The chromosome number of *C. hyalina* species, distributed in Turkey's local area (Bitlis

Table 1. The localities of studied taxa.

Taxa	Localities	Voucher specimen
Cuscuta campestris Yunck.	Adana, İmamoğlu, Alaybey village	1752
Cuscuta hyalina Roth.	Bitlis, Hizan, Karbastı village	2101
Cuscuta kotschyana Boiss.	Bitlis, Süphan mountain	2098
Cuscuta babylonica Aucher ex Choisy.	Van, Çatak, Sırmalı village	2100
Cuscuta europaea L.	Bitlis, Hizan	1993
Cuscuta kurdica Engelm.	Hakkâri, Ördekli village	14935
Cuscuta brevistyla A.Braun ex A.Rich	Bitlis, Hizan	1786
Cuscuta planiflora Ten.	Van, Tuşba	1766
Cuscuta approximata Bab.	Denizli, Honaz mountain	1801
Cuscuta lupuliformis.	Hakkâri Centre	2099
Cuscuta palaestina Boiss.	Van, Gürpınar	2095

Table 2. Chromosomes measurements of *Cuscuta* taxa (Ch. No: Chromosome No, C: Total length of the chromosome, L: Length of the long arm, S: Length of the short arm, CP: Centromeric position).

Ch. No	C	L	S	L/S	CI	RL	CP
		Cuscuta campestris					
1	2,48	1,46	1,02	1,43	41,13	0,00	m
2	2,4	1,4	1	1,40	41,67	0,00	m
3	2,29	1,39	0,9	1,54	39,30	0,00	m
4	2,1	1,31	0,79	1,66	37,62	0,00	m
5	2,06	1,03	1,03	1,00	50,00	0,00	M
6	2,06	1,16	0,9	1,29	43,69	0,00	m
7	1,98	1,21	0,77	1,57	38,89	0,00	m
8	1,9	1,08	0,82	1,32	43,16	0,00	m
9	1,84	1,12	0,72	1,56	39,13	0,00	m
10	1,8	1,27	0,53	2,40	29,44	0,00	sm
11	1,67	1,03	0,64	1,61	38,32	0,00	m
12	1,54	0,84	0,7	1,20	45,45	0,00	m
13	1,51	1,03	0,48	2,15	31,79	0,00	sm
14	1,48	0,74	0,74	1,00	50,00	0,00	M
		Cuscuta kotschyana					
1	3,95	2,1	1,85	1,14	46,84	6,19	m
2	3,93	2,51	1,42	1,77	36,13	6,22	sm
3	3,51	1,89	1,62	1,17	46,15	6,96	m
4	3,47	1,93	1,54	1,25	44,38	7,04	m
5	3,36	1,68	1,68	1,00	50,00	7,27	M
6	3,18	1,61	1,57	1,03	49,37	7,69	m
7	3,04	1,52	1,52	1,00	50,00	8,04	M
		Cuscuta europaea					
1	6,48	3,60	2,88	1,25	44,44	5,25	m
2	5,58	3,42	2,16	1,58	38,71	6,10	m
3	4,72	3,00	1,72	1,74	36,44	7,21	sm
4	4,53	2,63	1,90	1,38	41,94	7,51	m
5	4,37	2,45	1,92	1,28	43,94	7,79	m
6	4,35	2,52	1,83	1,38	42,07	7,82	m
7	4,00	2,70	1,30	2,08	32,50	8,51	sm
		Cuscuta brevistyla					
1	3,95	2,10	1,85	1,14	46,84	6,19	m
2	3,93	2,51	1,42	1,77	36,13	6,22	sm
3	3,51	1,89	1,62	1,17	46,15	6,96	m
4	3,47	1,93	1,54	1,25	44,38	7,04	m
5	3,36	1,68	1,68	1,00	50,00	7,27	M
6	3,18	1,61	1,57	1,03	49,37	7,69	m
7	3,04	1,52	1,52	1,00	50,00	8,04	M
8	3,01	1,85	1,16	1,59	38,54	11,07	m
9	2,90	1,79	1,11	1,61	38,28	11,49	m
10	2,85	1,55	1,30	1,19	45,61	11,69	m
11	2,81	1,60	1,21	1,32	43,06	11,86	m
12	2,68	1,34	1,34	1,00	50,00	12,44	M
13	2,54	1,49	1,05	1,42	41,34	13,12	m
14	2,46	1,26	1,20	1,05	48,78	13,55	m
15	2,30	1,18	1,12	1,05	48,70	14,49	m
16	2,22	1,11	1,11	1,00	50,00	15,01	M

Ch. No	C	L	S	L/S	CI	RL	CP
17	2,03	1,10	0,93	1,18	45,81	16,42	m
18	1,94	1,16	0,78	1,49	40,21	17,18	m
19	1,92	1,00	0,92	1,09	47,92	17,36	m
20	1,89	1,05	0,84	1,25	44,44	17,63	m
21	1,78	0,92	0,86	1,07	48,31	18,72	m
		Cuscuta palaestina					
1	4,80	2,40	2,40	1,00	50,00	10,78	M
2	4,74	2,44	2,30	1,06	48,52	10,92	m
3	4,69	2,53	2,16	1,17	46,06	11,04	m
4	4,36	2,97	1,39	2,14	31,88	11,87	sm
5	4,28	2,93	1,35	2,17	31,54	12,09	sm
6	4,13	2,91	1,22	2,39	29,54	12,53	sm
7	3,93	2,37	1,56	1,52	39,69	13,17	m
8	3,72	2,34	1,38	1,70	37,10	13,91	sm
9	3,42	1,71	1,71	1,00	50,00	15,13	M
10	3,16	1,58	1,58	1,00	50,00	16,38	M
11	2,89	1,55	1,34	1,16	46,37	17,91	m
12	2,79	1,56	1,23	1,27	44,09	18,55	m
13	2,62	1,44	1,18	1,22	45,04	19,76	m
14	2,23	1,23	1,00	1,23	44,84	23,21	m
		Cuscuta hyalina					
1	5,18	2,63	2,55	1,03	49,23	11,08	m
2	5,05	2,58	2,47	1,04	48,91	11,36	m
3	4,93	2,50	2,43	1,03	49,29	11,64	m
4	4,80	2,40	2,40	1,00	50,00	11,95	M
5	4,50	2,35	2,15	1,09	47,78	12,75	m
6	4,40	2,20	2,20	1,00	50,00	13,04	M
7	4,25	2,15	2,10	1,02	49,41	13,50	m
8	4,18	2,30	1,88	1,22	44,98	13,72	m
9	4,00	2,00	2,00	1,00	50,00	14,34	M
10	3,58	1,85	1,73	1,07	48,32	16,03	m
11	3,42	1,71	1,71	1,00	50,00	16,77	M
12	3,19	1,61	1,58	1,02	49,53	17,98	m
13	3,09	1,57	1,52	1,03	49,19	18,57	m
14	2,80	1,50	1,30	1,15	46,43	20,49	m
		Cuscuta babylonica					
1	6,23	3,48	2,75	1,27	44,14	5,45	m
2	5,32	3,12	2,20	1,42	41,35	6,38	m
3	5,22	3,50	1,72	2,03	32,95	6,51	sm
4	4,69	3,24	1,45	2,23	30,92	7,24	sm
5	4,36	2,18	2,18	1,00	50,00	7,79	M
6	4,34	2,64	1,70	1,55	39,17	7,82	m
7	3,80	2,36	1,44	1,64	37,89	8,94	m
		Cuscuta kurdica					
1	4,80	2,40	2,40	1,00	50,00	6,46	M
2	4,67	2,45	2,22	1,10	47,54	6,64	m
3	4,66	2,50	2,16	1,16	46,35	6,65	m
4	4,40	3,00	1,40	2,14	31,82	7,05	sm

Ch. No	C	L	S	L/S	CI	RL	CP
5	4,36	2,97	1,39	2,14	31,88	7,11	sm
6	4,25	2,95	1,30	2,27	30,59	7,30	sm
7	3,87	2,36	1,51	1,56	39,02	8,01	m
			Cuscuta approximata				
1	3,68	1,84	1,84	1,00	50,00	8,87	M
2	3,36	1,68	1,68	1,00	50,00	9,72	M
3	3,08	1,82	1,26	1,44	40,91	10,60	m
4	2,48	1,28	1,20	1,07	48,39	13,17	m
5	2,42	1,50	0,92	1,63	38,02	13,49	m
6	2,36	1,36	1,00	1,36	42,37	13,83	m
7	2,28	1,40	0,88	1,59	38,60	14,32	m
8	2,12	1,24	0,88	1,41	41,51	15,40	m
9	2,01	1,20	0,81	1,48	40,30	16,24	m
10	1,98	0,99	0,99	1,00	50,00	16,49	M
11	1,85	1,24	0,61	2,03	32,97	17,65	sm
12	1,84	1,06	0,78	1,36	42,39	17,74	m
13	1,62	1,00	0,62	1,61	38,27	20,15	m
14	1,57	0,84	0,73	1,15	46,50	20,80	m
			Cuscuta lupuliformis				
1	6,96	3,48	3,48	1,00	50,00	6,40	M
2	3,82	2,24	1,58	1,42	41,36	11,65	m
3	3,80	2,55	1,25	2,04	32,89	11,72	sm
4	3,20	1,60	1,60	1,00	50,00	13,91	M
5	3,14	1,82	1,32	1,38	42,04	14,18	m
6	3,07	1,83	1,24	1,48	40,39	14,50	m
7	2,98	1,76	1,22	1,44	40,94	14,94	m
8	2,94	1,80	1,14	1,58	38,78	15,14	m
9	2,76	1,70	1,06	1,60	38,41	16,13	m
10	2,52	1,56	0,96	1,63	38,10	17,67	m
11	2,43	1,33	1,10	1,21	45,27	18,32	m
12	2,40	1,20	1,20	1,00	50,00	18,55	M
13	2,30	1,26	1,04	1,21	45,22	19,36	m
14	2,20	1,10	1,10	1,00	50,00	20,24	M
			Cuscuta planiflora				
1	5,28	2,64	2,64	1,00	50,00	5,54	M
2	4,35	2,55	1,80	1,42	41,38	6,72	m
3	4,24	2,82	1,42	1,99	33,49	6,89	sm
4	4,08	2,04	2,04	1,00	50,00	7,16	M
5	3,96	2,26	1,70	1,33	42,93	7,38	m
6	3,78	2,15	1,63	1,32	43,12	7,73	m
7	3,54	2,18	1,36	1,60	38,42	8,26	m

province), was found as 2n=2x=28. The haploid karyotype formula of this species has 10 median regions (m) and 4 points median (M) regions. Metaphase chromosome length varies between 5.18-2.80 μm. Chromosome arm ratios vary between 1.03-1.15 μm. Its centromere index ranges from 50.00 to 44.98 μm and relative length from 11.08 to 20.49 μm. The intra-chromosomal asym-

metric index (A1) is 0.04, and the inter-chromosomal asymmetric index (A2) is 0.04 (Table 2, Figure 1).

Cuscuta kotshyana var. *caudata*: The chromosome number of this species was determined as 2n=2x=14. Haploid karyotype formula; It has 4 median regions (m), 2 points median (M) and 1 submedian region (cm) region. Metaphase chromosome length was measured in lengths ranging from 3.93-3.04 μm. Chromosome arm ratios vary between 1.77-1 μm. The centromere index is 50.00-36.13 μm. Its relative length was measured in the range of 6.22-8.04 μm. The intra-chromosomal asymmetric index (A1) is 0.15, and the inter-chromosomal asymmetric index (A2) is 0.07 (Table 2, Figure 1).

Cuscuta babylonica var. *babylonica*: The chromosome number of this species is mainly found in the Eastern Anatolia region of Turkey, at an altitude of 850-1200 m, whose stems are between thin filamentous and medium thickness, and which is yellowish-red is 2n=2x=14. The haploid karyotype formula of this species is 4 median regions (m), 2 submedian regions (cm), and 1 dotted median (M) region. Metaphase chromosome length varies between 6.23-3.80 μm. Chromosome arm ratios range from 1.64 to 1 μm. Its centromere index ranges from 50.00-30.92 μm, and its relative length ranges from 5.45 to 8.94 μm. The intra-chromosomal asymmetric index (A1) is 0.34, and the inter-chromosomal asymmetric index (A2) is 0.07 (Table 2, Figure 1).

Cuscuta europaea: C. europaea; has 2n=2x=14 chromosomes. The haploid karyotype formula has 5 median regions (m) and 2 submedian regions (cm). Metaphase chromosome length varies between 6.48-4 μm. Chromosome arm ratios vary between 2.08-1.25 μm. Its centromere index ranges from 44.44 to 32.50 μm, and its relative length ranges from 5.25 to 8.51 μm. The intrachromosomal asymmetric index (A1) is 0.33, and the inter-chromosomal asymmetric index (A2) is 0.07 (Table 2, Figure 1).

Cuscuta kurdica: The chromosome number of this species was found to be 2n=2x=14. The haploid karyotype formula has 3 median regions (m), 3 submedian regions (cm), and 1 dotted median (M) region. Metaphase chromosome length varies between 4.80-3.87 μm. Chromosome arm ratios vary between 2.27-1 μm. Its centromere index ranges from 50.00-30.59 μm and relative length is between 6.46 and 8.01 μm. The intra-chromosomal asymmetric index (A1) is 0.34, and the inter-chromosomal asymmetric index (A2) is 0.07 (Table 2, Figure 1).

Cuscuta brevistyla: The chromosome number of C. brevistyla species, which is annual, parasitic, and generally distributed in the mountains, was determined as 2n=6x=42. The haploid karyotype formula has 15 medi-
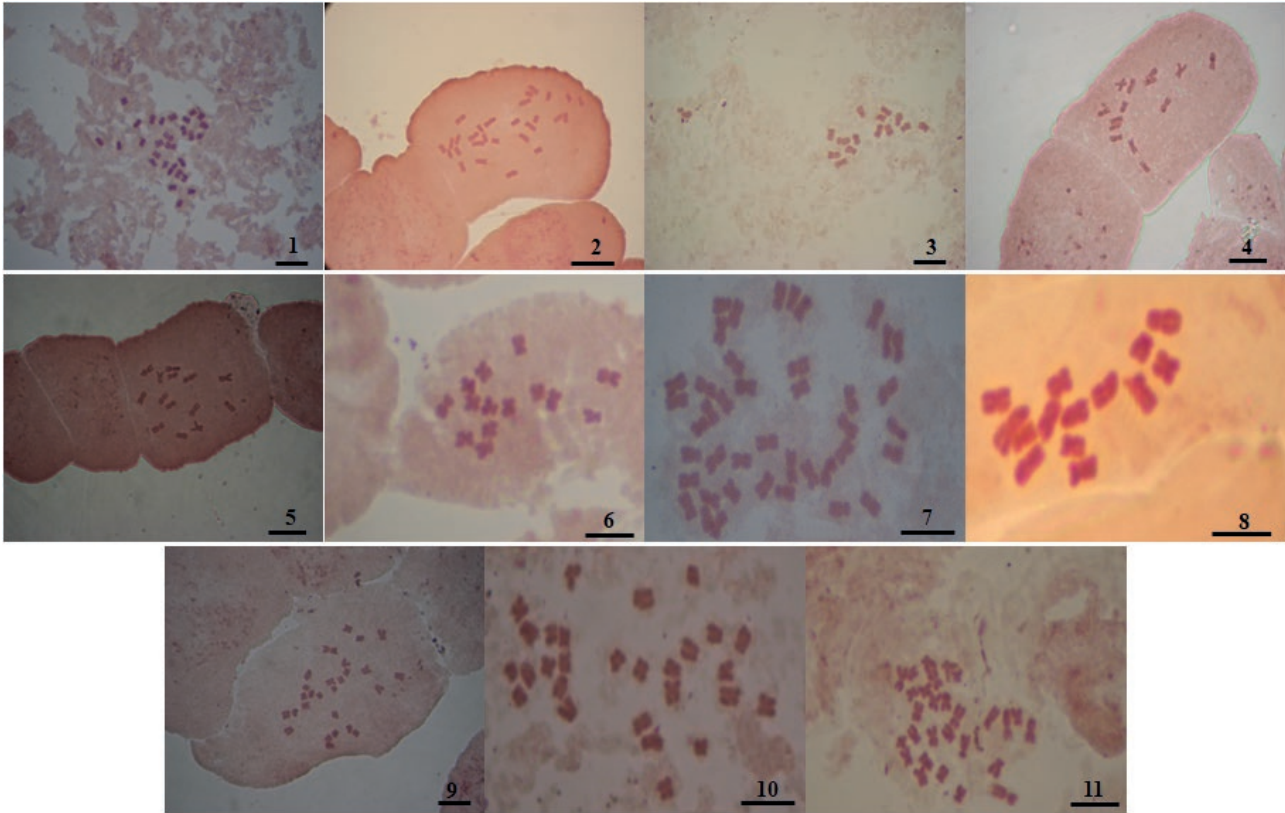
Figure 1. Mitotic metaphase chromosomes of *Cuscuta* taxa 1. *Cuscuta campestris*, 2. *Cuscuta hyalina*, 3. *Cuscuta kotschyana*, 4. *Cuscuta babylonica*, 5. *Cuscuta europaea* 6. *Cuscuta kurdica*, 7. *Cuscuta brevistyla*, 8. *Cuscuta planiflora*, 9. *Cuscuta approximata*, 10. *Cuscuta lupuliformis*, 11. *Cuscuta palaestina* (Scale:10 μm).

an regions (m), 3 submedian regions (cm), and 3 dotted median (M) regions. Metaphase chromosome length varies between 4.73-1.78 μm. Chromosome arm ratios vary between 1.97-1 μm. Its centromere index ranges from 50.00-33.63 μm, and its relative length varies between 12.63- 33.55 μm. The intra-chromosomal asymmetric index (A1) is 0.25, and the inter-chromosomal asymmetric index (A2) is 0.02 (Table 2, Figure 1).

Cuscuta planiflora: The chromosome number of this species was determined as 2n=2x=14. The haploid karyotype formula has 4 median regions (m), 1 submedian region (cm), and 2 dotted median (M) regions. Metaphase chromosome length varies between 5.28-3.54 μm. Chromosome arm ratios vary between 1.60-1 μm. Its centromere index ranges from 50.00 to 38.42 μm, and its relative length ranges from 5.54 to 8.26 μm. The intra-chromosomal asymmetric index (A1) is 0.24, and the inter-chromosomal asymmetric index (A2) is 0.07 (Table 2, Figure 1).

Cuscuta approximata: *C. approximata* has 2n=4x=28 chromosomes. The haploid karyotype formula has 10 median regions (m), 1 submedian region (cm), and 3

point median (M) regions. Metaphase chromosome length varies between 3.68-1.57 μm. Chromosome arm ratios vary between 1.60-1 μm. Its centromere index ranges from 50.00 to 32.97 μm and its relative length from 8.87 to 20.80 μm. The intra-chromosomal asymmetric index (A1) is 0.23, and the inter-chromosomal asymmetric index (A2) is 0.04 (Table 2, Figure 1).

Cuscuta lupuliformis: The chromosome number of this species was found to be 2n=2x=28. The haploid karyotype formula has 9 median regions (m), 1 submedian region (cm), and 4 point median (M) regions. Metaphase chromosome length varies between 6.96-2.20 μm. Chromosome arm ratios vary between 2.04-1 μm. Its centromere index ranges from 50.00-32.89 μm, and its relative length is 6.40-20.24 μm. The intra-chromosomal asymmetric index (A1) is 0.24, and the inter-chromosomal asymmetric index (A2) is 0.04 (Table 2, Figure 1).

Cuscuta palaestina: The chromosome number of this species was determined as 2n=4x=28. The haploid karyotype formula is 7 median regions (m), 4 submedian regions (cm), and 3 point median (M) regions. Metaphase chromosome length varies between 4.80-2.23 μm.

Table 3. Karyotype characteristics of *Cuscuta* taxa (TLC: Total Lenght of Chromosomes, MTLC (Mean of Total Length of Chromosomes, MAX: Maximum Length of Chromosome, MIN: Minimum Length of Chromosome, MLA: Mean of Long Arms, MSA: Mean of Short Arms, MrV: Mean of r Value, MdV: Mean of d Value, MAR: Mean of Arm Ratio, MCI: Mean of Chromosome Index, MRLC: Mean of Relative Length of Chromosomes, DRL: Difference of Range of Relative Length, TF%: Total Form Percentage, S%: Relative Length of Shortest Chromosome, A_1: Intrachromosomal Asymmetry Index, A_2: Interchromosomal Asymmetry Index).

Cuscuta Taxa	TLC	MTLC	MAX	MIN	MLA	MSA	MrV	MdV	MAR	MCI	MRLC	DRL	TF%	S%	A_1	A_2	A
C. campestris	27.11	0.97	1.46	0.48	1.14	0.78	1.92	0.36	1.51	40.69	14.37	7.39	0.41	0.33	0.32	0.04	0.19
C. hyalina	57.37	2.05	2.63	1.30	2.09	2.00	4.09	0.09	1.05	48.79	14.52	9.41	0.49	0.49	0.04	0.04	0.02
C. kotschyana	24.44	1.75	2.51	1.42	1.89	1.60	3.49	0.29	1.19	40.12	7.06	1.82	0.46	0.57	0.15	0.07	0.08
C. babylonica	33.96	2.43	3.5	1.45	2.93	1.92	4.85	1.01	1.59	39.49	7.16	3.49	0.40	0.41	0.34	0.07	0.21
C. europaea	34.03	2.43	3.6	1.30	2.90	1.95	4.85	0.95	1.53	40.01	7.17	3.26	0.40	0.36	0.33	0.07	0.20
C. kurdica	31.01	2.22	2.97	1.30	2.66	1.76	4.42	0.90	1.62	39.60	7.03	1.55	0.40	0.44	0.34	0.07	0.20
C. brevistyla	59.72	1.42	2.53	0.78	1.62	1.22	2.84	0.40	1.34	43.45	22.63	20.92	0.43	0.31	0.25	0.02	0.14
C. planiflora	29.23	2.09	2.82	1.36	2.37	1.79	4.16	0.58	1.38	42.76	7.01	2.72	0.43	0.48	0.24	0.07	0.14
C. approximata	32.65	1.17	1.84	0.61	1.31	1.01	2.32	0.30	1.37	43.87	14.89	11.92	0.43	0.33	0.23	0.04	0.13
C. lupuliformis	44.52	1.59	3.48	0.96	1.80	1.37	3.17	0.43	1.36	43.10	15.19	13.84	0.43	0.28	0.24	0.04	0.14
C. palaestina	51.76	1.85	2.97	1.01	2.14	1.55	3.69	0.59	1.43	42.48	14.80	12.43	0.42	0.34	0.28	0.04	0.16

Chromosome arm ratios vary between 2.39-1 μm. Its centromere index ranges from 50.00 to 44.84 μm and its relative length from 10.78 to 23.21 μm. The intra-chromosomal asymmetric index (A1) is 0.28, and the inter-chromosomal asymmetric index (A2) is 0.04 (Table 2, Figure 1).

Karyotypes in plants; According to the types of chromosomes, there are two types: symmetrical and asymmetrical. The symmetrical karyotype is characterized by the predominance of median and submedian chromosomes of approximately the same size. The increase in asymmetry caused by the centromere shift creates an asymmetric karyotype. Chromosomes change from the median and submedian type to subterminal and terminal (Babaarslan and Eroğlu, 2014). When the asymmetric indices of *Cuscuta* taxa were examined, it was seen that the TF% value changed between 0.41-0.49, the A index changed between 0.02 and 0.25, the A1 index between 0.21-0.38 and the A2 index between 0.09-0.31 (Table 3).

Statistical findings

Chromosome micromorphological features of 11 *Cuscuta* taxa were specified, and statistical analyses were performed using formulas created using various chromosome features. Mitotic metaphase chromosome images of *Cuscuta* taxa are given in Figure 1, and karyotype features are given in Table 2-3. One-way ANOVA test, which is one of the analyzes made according to the chromosome characteristics of the taxa, is given in Table According to the values obtained with the formulas using the micromorphological chromosome features

of taxa, the data show a normal distribution according to the Shapiro-Wilk test (p>0.05), and the residual plot graph is shown in Figure 2. Then, according to the one-way ANOVA test p-value, the difference between taxa was statistically significant (p<0.05) (Table 4).

Correlation analysis

According to the correlation analysis, there are relations between the r-values of chromosomal data according to the significance level less than p <0.05. Particularly a high relationship Although there was a strong positive relationship between MTLC and MIN, MAX, MLA, MSA, and MRV, it was observed that there was a strong negative relationship between MRLC and DRL. In addition, MAR and A1 and A characters are strongly positively correlated, while TF% is strongly negative; With MRLC, DRL is strongly positive while A2 is strongly negative; TF% was strongly negatively correlated with MAR, MDV, A1, A (Figure 3).

Principal Component Analysis (PCA)

According to PCA (Figure 4), the first two components explained most of the variation according to chromosome data between taxa. While the first two components explain 87.94 and 9.80% of the variance, these characters explained 97.75% of the total variation. The characters most affected by the variation were TLC, DRL%, MCl, and MRLC. The TLC value was the most influential one. The impact of other characters was very
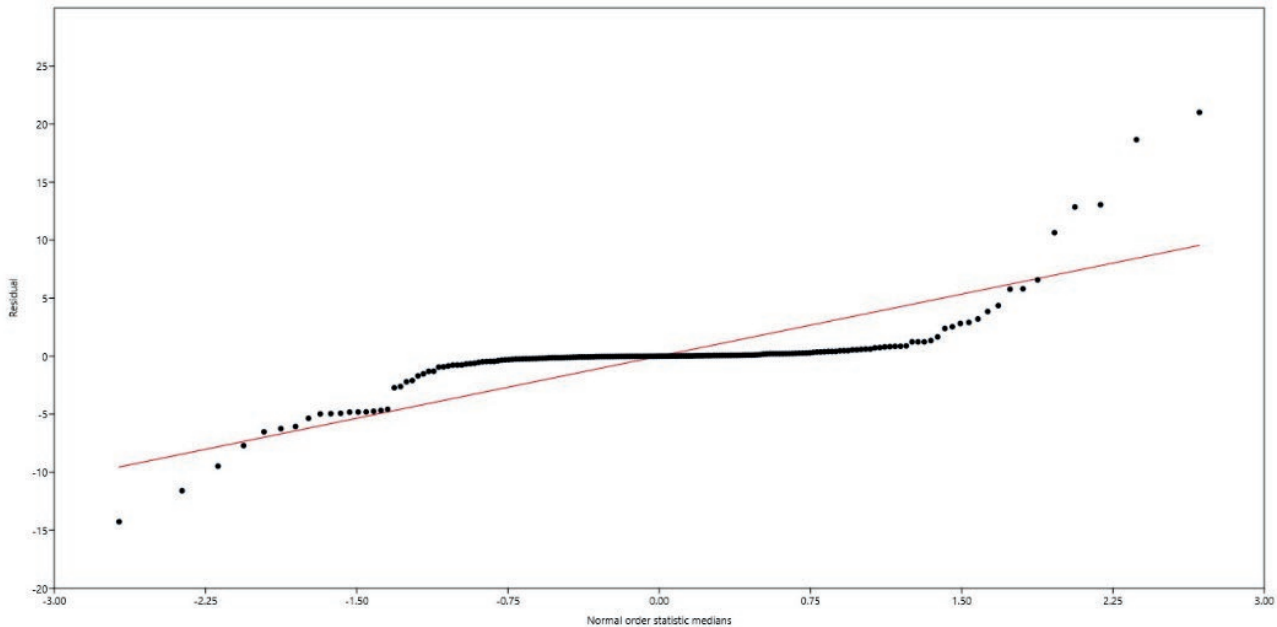
Figure 2. Shapiro - Wilk normality test(p=0.4809>0.05)-Residual plot.

Table 4. One way ANOVA test results.

Test for equal means					
	Sum of sqrs	df	Mean square	F	*p* (same)
Between groups:	45343.3	16	2833.96	351.6	8.149E-179
					Permutation
Within groups:	2329.64	289	8.06104		*p* (n=99999)
Total:	47672.9	305			1E-05
omega2:	0.9483				

low. While this TLC value was positively correlated with MCL, MRLC, and DRL characters in the correlation analysis, it was negatively correlated with MAR, A, A1, A2, and S% characters.

Cluster analysis

According to the Cluster analysis results of the UPGMA algorithm and Gower similarity index, the taxa are divided into three main groups (Figure 5). *C. brevistyla*, *C. lupuliformis*, *C. palaestina*, *C. approximata*, and *C. campestris* were group, *C. kotschyana*, *C. planiflora*, *C. babylonica*, *C. europea*, *C. kurdica* had created a group. The *C. hyalina* species wholly separated from these groups were a group. As stated before, the fact that *C. hyalina* species spread in a local area directly correlates with the analysis result.

DISCUSSION

Cuscuta species show wide variation in chromosome numbers ranging from 2n = 8 to 2n = 60. Therefore, the genus is generally a polyploid complex resulting from two basic chromosome numbers x = 7 and x = 15 (Pazy & Plitmann, 1995; Hunziker, 1949-50).

The first step in combating parasitic plants is their correct diagnosis, as with other weeds. Due to the lack of true root and leaf structure of dodder, diagnosis is mainly made according to flower and fruit characteristics. These features are sometimes insufficient for diagnosis. Diagnosis of this genus is problematic in the World and Turkey. Therefore, determining the chromosome number and chromosomal morphology of the species belonging to this genus is of great importance in determining the systematic location of the species, identifying the species, and, when necessary, agriculturally struggling with these species. According to the karyotype analysis results of *Cuscuta* taxa, the primary chromosome number was determined as x=7. Among the study samples, *C. brevistyla* is polyploid, *C. campestris*, *C. hyalina*, *C. approximata*, *C. lupuliformis, C. palaestina* tetraploid, and other taxa are diploid.

According to the total length of chromosomes, The species with the longest chromosome length is *C. lupuliformis,* with 6.96 Mμ lengths. This species was morphological; *C. campestris,* with a total chromosome length of 2.48 Mμ was determined to be the shortest chromo-
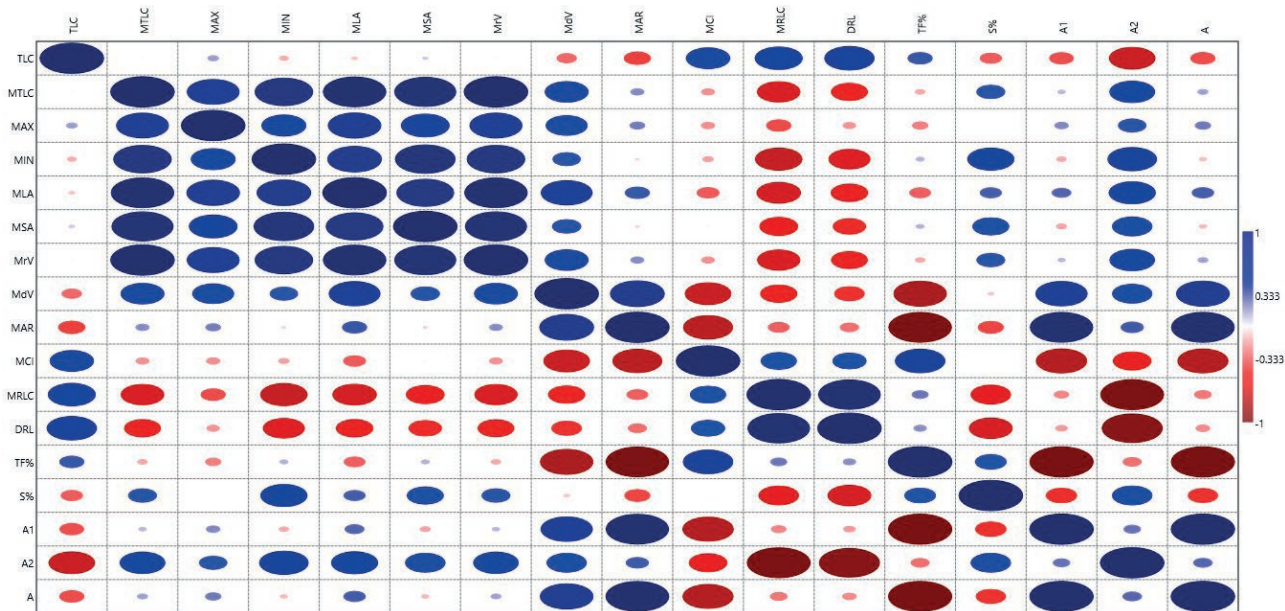
Figure 3. Correlation analysis between karyotype characteristics.
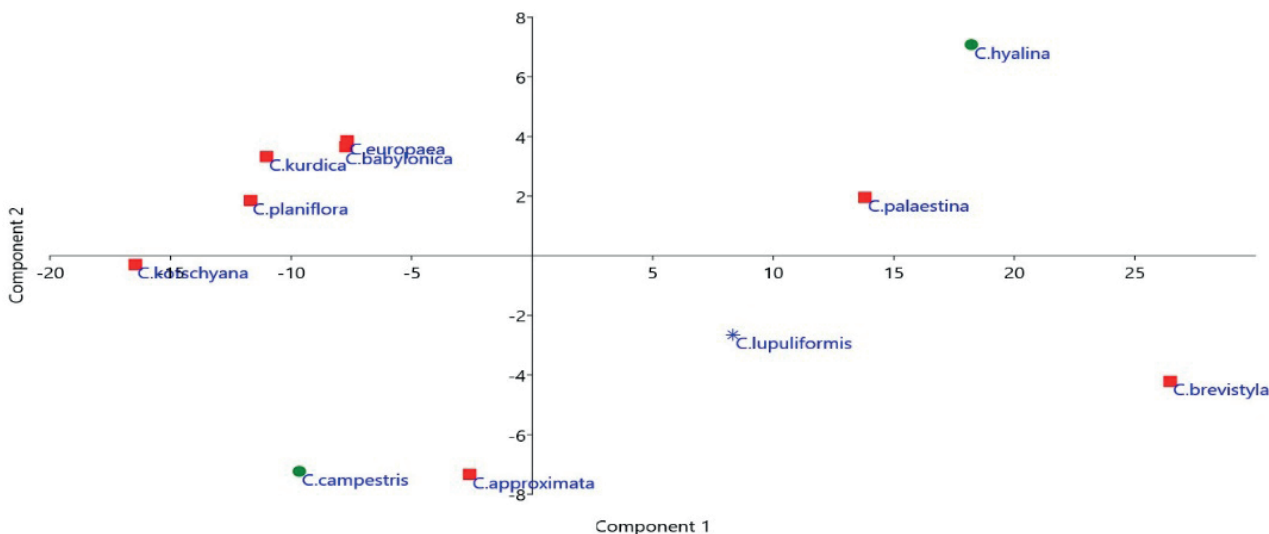

Figure 4. PCA analysis scatter plot (same colors are the same subgenus).

some length. The chromosome number of *C. campestris* was first determined by Ward(1984) as 2n=28; later, Aryavand and García & Castroviejo (1987) 2n=56; Khatoon & Ali(1993) determined it as 2n=14, 28. According to our research results, the chromosome number of the species is 2n=28. It has been shown that the haploid karyotype formula is 10m+2sm +2M. The morphometric characteristics of the species were first revealed in this study. Singh and Roy(1970). collected *C. hyalina* from

India; The chromosome number of the species is 2n=30; Vu et al. determined as 2n=28. According to our study results, the chromosome number of the species is 2n=28. The haploid karyotype formula is 10m+4M. This study first revealed the chromosome number and morphometric characteristics of C. *kotschyana* species. Chromosome number 2n=14; Haploid karyotype formula; It has 4 median regions (m), 2 points median (M), and 1 submedian region (cm) region (Figure 6).
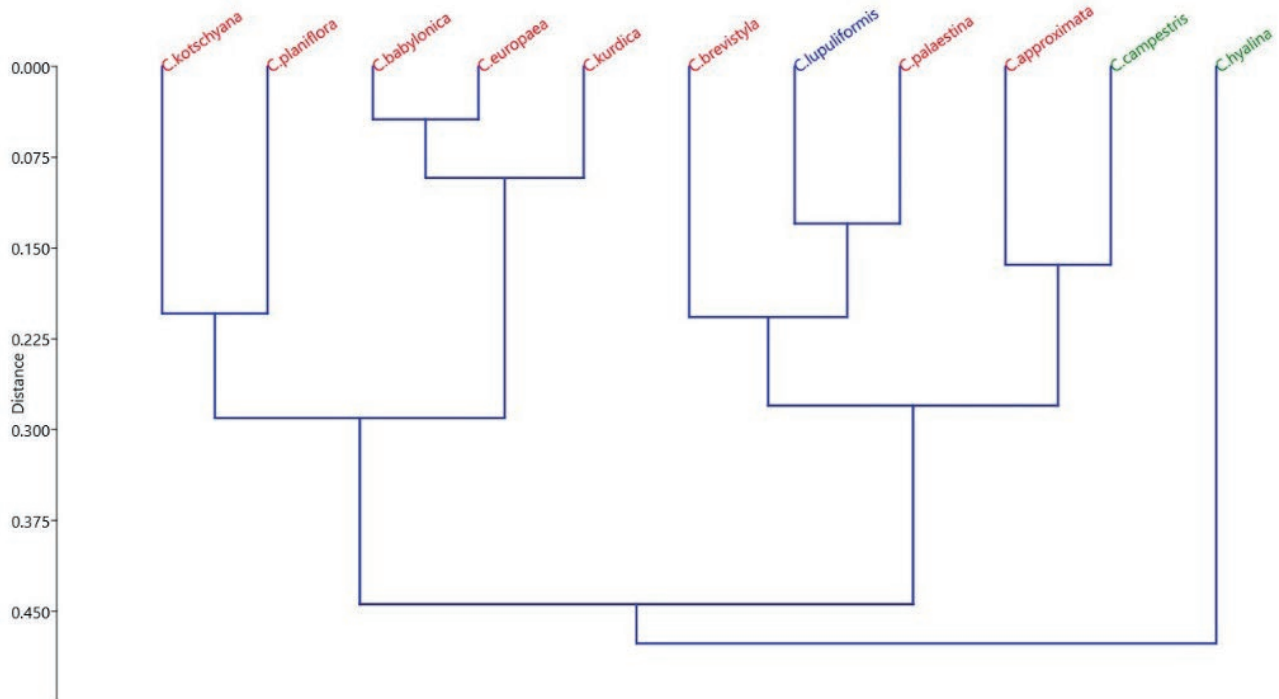
Figure 5. Cluster analysis according to karyotype characteristics Show that 3 main groups (Same colored taxa are located in the same section).

Pazy and Plitmann (2002) determined the chromosome number of *C. babylonica* as 2n=8, where they specified Israel as the locality. However, according to our research results, the chromosome number of the species is 2n=14, and the haploid karyotype formula is 4m + 2 cm + 1M.

The chromosome number of the *C. europaea* species was previously reported by Albers and Pröbsting(1998) and García and Castroviejo(2003) as 2n=14. Our research data also confirm this result. The haploid karyotype formula of the species, in which we found the chromosome number as 2n=14, is 5m + 2 cm.

Regarding chromosome number and morphology, the chromosome number of *C. kurdica* species, which was first discussed in this study, was determined as 2n=14. The haploid karyotype formula is 3m + 3 cm + 1 M.

Pazy and Plitman (1994) and Feinbrun and Taub(1978) found the chromosome number of *C. brevistyla* as 2n=42, where they specified Israel as a locality. According to our study results, the chromosome number of this species is 2n=42. The haploid karyotype formula is 15m + 3 cm + 3 M.

The chromosome number of *C. planiflora* has been determined by many researchers. Singh and Roy determined the chromosome number of this species as 2n=14; Pazy and Plitmann. (1991) 2n=14; García and Castroviejo.

(2003) 2n=26, 28; Aryavand(1987) reported 2n=28 and Vasudevan 2n=14. As a result of our research, the chromosome number of the species was determined as 2n=14. The haploid karyotype formula was 4m + 1 cm + 2 M.

C. approximata; García and Castroviejo (2003) and Guerra(2004). 2n=28 chromosomes have reported it. Our studies also confirm this result, and the chromosome number of this species is 2n=28. The haploid karyotype formula is 10m + 1 cm + 3M..

The chromosome number of *C. lupuliformis* was determined as 2n=28 by Vasudevan. According to our research results, the chromosome number of this species is 2n=28. The haploid karyotype formula is 9m + 1 cm + 4M.

Plazy and Plitmann (1991) showed the *C. palaestina* species as 2n=28 chromosomes. Our research confirms this result. We found the chromosome number of 2n = 28 of this species. The haploid karyotype formula is 7m + 4 cm + 3M.

Various karyological studies have been carried out on the chromosome number of species belonging to the *Cuscuta* genus. As a result of these studies, the Chromosome number of *Cuscuta japonica* Choisy. species is 2n= 32 (Leusova et al., 2005); the Chromosome number of *Cuscuta epithymum* L. species is 2n= 14 (Montgomery et al., 2003); the chromosome number of *Cuscuta australis* R. Br. species is 2n=56 (Yeh et al., 1995); Chromosome
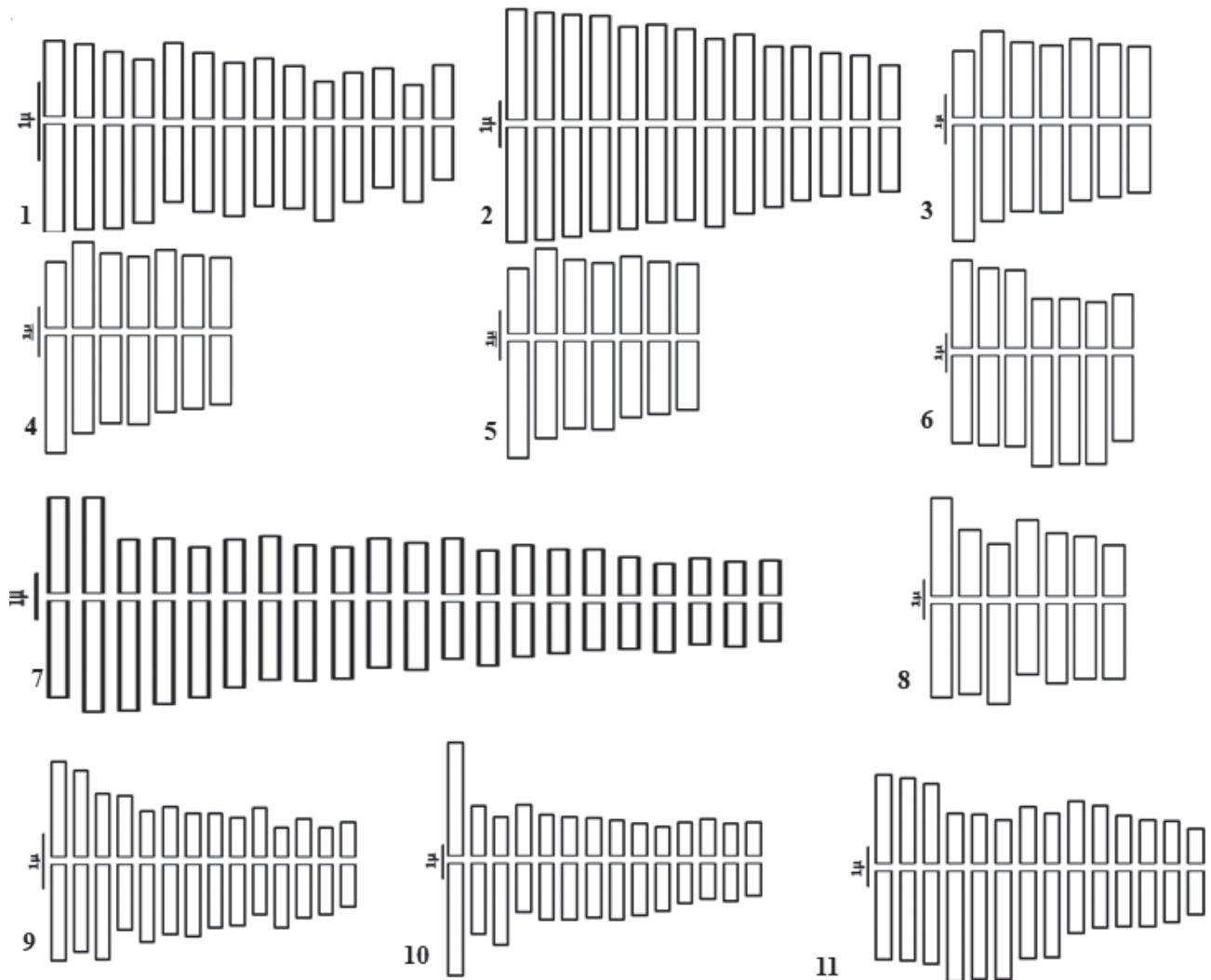
Figure 6. Haploid idiogram in *Cuscuta* taxa 1. *C. campestris,* 2. *C. hyalina*, 3. *C. kotschyana*, 4. *C. babylonica*, 5. *C. europaea* 6. *C. kurdica*, 7. *C. brevistyla*, 8. *C. planiflora*, 9. *C. approximata*, 10. *C. lupuliformis* 11. *C. palaestina..*

number of *Cuscuta triumvirati* Lange. Species 2n= 14 (García et al., 2003); Chromosome number of *Cuscuta pentagona* Engelm. is 2n= 44 (Pazy et al., 1995); The chromosome number of *Cuscuta pedicellata* Ledeb. species was determined as 2n= 10 (Pazy et al., 1991), and the chromosome number of *Cuscuta chinensis* Lam. species was determined as 2n= 60 (Mesǐcek et al., 1995).

According to cluster analysis, taxa were divided into 3 main groups. It is noteworthy that although *C. campestris* and *C. hyalina* are in the Grammica subgenus, they are in different groups according to chromosome micromorphological data. Here, it is estimated that some chromosomal features (According to PCA, such as TLC) may have differentiated over time, as the *C. hyalina* species was distributed in a local region in Turkey. It is seen

that *C. babylonica* and *C. europea* species in the *Cuscuta* subgenus and *C. kurdica* species are closely related. According to their morphological similarities, C. europea and *C. kurdica* species show very close similarities.

According to PCA, the most important character explaining the differentiation between taxa was seen as TLC (Total Lenght of Chromosomes) character. In addition, when the distribution of taxa in the diagram is examined, it is a compatible image with cluster analysis.

In this study, 11 species belonging to the genus *Cuscuta*, an essential part of Turkey's biological richness and consists of parasitic plants, were discussed in detail in terms of chromosome number and chromosome morphology and compared statistically. These karyological studies reveal the karyological differences and similari-

ties between the infrageneric and species. The results obtained increase our knowledge about these species. Thus, obtaining new data that can be used in the systematics of these species aims to reveal basic information about the systematics, karyology, and morphological features of taxa. In addition, it will form a fundamental step for future breeding and hybridization studies related to this genus and contribute to other biological research.

REFERENCES

Açar M, Satıl F. 2019. Distantes R. Bhattacharjee (Stachys L. /Lamiaceae) Altseksiyonu Taksonları Üzerinde Karşılaştırmalı Anatomik ve Mikromorfolojik Çalışmalar. [Comparative Micromorphological and Anatomical Investigations on the Subsection Distantes R.Bhattacharjee (Stachys L./Lamiaceae)]. Kahramanmaraş Sütçü İmam Üniversitesi Tarım ve Doğa Dergisi. 22(Ek Sayı 2): 282-295.

Açar M. & Taşar N. 2022. A statistical overview to the chromosome characteristics of some CentaureaL. taxa distributed in the Eastern Anatolia (Turkey). Caryologia. https://doi.org/10.36253/caryologia-1562

Adhikary AK. 1974. Precise determination of centromere location. Cytologia. 39: 11-16.

Albers F. & Pröbsting W. 1998. In R. Wisskirchen & H. Haeupler, Standardliste der Farn- und Blütenpflanzen Deutschlands. Bundesamt für Naturschutz & Verlag Eugen Ulmer, Stuttgart.

Arabaci T., Çelenk S., Özcan T., Martin E., Yazici T., Açar M., ... & Dirmenci T. 2021. Homoploid hybrids of *Origanum* (Lamiaceae) in Turkey: morphological and molecular evidence for a new hybrid. Plant Biosystems-An International Journal Dealing with all Aspects of Plant Biology, 155(3): 470-482.

Aryavand, A. 1987. The chromosome numbers of some *Cuscuta* L. (*Cuscuta*ceae) species from Isfahan, Iran. Iran. J. Bot. 3: 177–182.

Costea M, Stefanović S. 2009. Molecular phylogeny of *Cuscuta* californica complex Convolvulaceae and a new species from New Mexico and Trans-Pecos. Syst Bot., (34): 570-579.

Costea M, Tardif F.J. 2006. The biology of Canadian weeds. 133. *Cuscuta campestris* Yuncker, C. gronovii Willd. ex Schult., C. umbrosa Beyr. ex Hook., C. epithymum (L.) L. and C. epilinum Weihe. Canadian Journal of Plant Science, 86 (1): 293-316.

Davis P.H. (ed.) (1978). Flora of Turkey and the East Aegean Islands (Vol. 6). Edinburgh Univ. Press., Edinburgh.

Dawson J.H, Musselman L. J, Wolswinkel P, Dörr I. (1994). Biology and control of *Cuscuta*. Reviews of Weed Science, (6): 265–317.

Dirmenci T., Arabacı T., Özcan T., Yazıcı T. Martin E., Çelenk S., Açar M., Üzel D. (2020). Chapter 6: Homoploid Hybridization and Its Role in Emergence and Diversity of the Genus Origanum L. (Lamiaceae). In book: The Lamiaceae Family: An Overview. Alexander Adler (Editor). Series: Plant Science Research and Practices. Nova Science Publisher. ISBN: 978-1-53617-078-8.

Dirmenci T, Özcan T, Açar M, Arabacı T, Yazıcı T, Martin E. 2019. A rearranged homoploid hybrid species of Origanum (Lamiaceae): O. × munzurense Kit Tan & Sorger. Botany Letters. 166(2): 153-162.

Feinbrun-Dothan N., 1978. - Flora *Palaestina*, 3: 44-50, The Israel Acad. of Sci. and Humanit., Jerusalem.

García M. A. & S. Castroviejo. 2003. Estudios citotaxonómicos en las especies ibéricas del género *Cuscuta* (Convolvulaceae). Anales Jard. Bot. Madrid 60(1): 33–44.

Gedik O., Kıran, Y., Arabacı, T., Kostekci, S. 2014. Karyological studies on the annual members of the genus Carduus L. (Asteraceae, Cardueae) from Turkey. Caryologia, 67(2):135–139.

Genç H, Yildirim B, Açar M, Çetin T. 2021. Statistical evaluation of chromosomes of some Lathyrus L. taxa growing in Turkey. Caryologia. 74(3): 107-117. doi: 10.36253/caryologia1124

Guerra M., & García M. A. (2004). Heterochromatin and rDNA sites distribution in the holocentric chromosomes of *Cuscuta approximata* Bab.(Convolvulaceae). Genome, 47(1): 134-140.

Hammer Q, Harper DAT, Ryan, PD. 2001. Past: Paleontological Statistics Software Package for Education and Data Analysis. Palaeontologia Electronica. 4(1): 1-9.

Hunziker A.T., 1949-50. -Las especies de *Cuscuta* (Convolvulaceae) de Argentina y Uruguay. Trab. Mus. Bot. Univ. Nac. Cordoba, 1 (2): 1-358.

Huziwara Y. 1962. Karyotype analysis in some genera of Compositae. VIII. Further studies on the chromosome of Aster. American Journal of Botany. 49(2): 116-119.

Khatoon S. & S. I. Ali. 1993. Chromosome Atlas of the Angiosperms of Pakistan. Department of Botany, University of Karachi, Karachi.

Levan A., Fredga K., Sandberg A.A. 1964. Nomenclature for centromeric position on chromosomes. Hereditas, 52: 201–220.

Leusova. 2005. Karyological study of Cuscuta japonica Choisy. Pages 53–54 in Karyology, Karyosystematics and Molecular Phylogeny. St. Petersburg, Russia.

Mesĭcek, J. & J. Sojăk. 1995. Chromosome numbers of Mongolian angiosperms. II. Folia Geobot. Phytotax. 30: 445–453.

Montgomery, L., M. Khalaf, J. P. Bailey & K. J. Gornal. 1997. Contributions to a cytological catalogue of the British and Irish flora, 5. Watsonia 21: 365–368.

Pazy B. & U. Plitmann. 1991. Unusual chromosome separation in meiosis of *Cuscuta* L. Genome 34: 533–536.

Pazy B. & U. Plitmann. 2002. New perspectives on the mechanisms of chromosome evolution in parasitic flowering plants. Bot. J. Linn. Soc. 138(1): 117–122.

Pazy B., Plitmann, U., 1987. -Persisting demibivalents: a unique meiotic behaviour in *Cuscuta babylonica* Choisy. Genome, 29: 63-66.

Pazy B., Plıtmann, U., 1987: Persisting demibivalents: a unique meiotic behaviour in *Cuscuta babylonica* CHoIsY. Genome 29: 63-66. 1991: Unusual chromosome separation in meiosis of *Cuscuta* L. Genome 34: 533-536.

Pazy B., Plitmann, U., 1991. Unusual chromosome separation in meiosis of *Cuscuta* L. Genome, 34: 533-536.

Pazy B., Plitmann, U., 1994. Holocentric chromosome behaviour in *Cuscuta* (*Cuscuta*ceae). Pl. Syst. Evol., 191: 105-109.

Pazy, B. & U. Plitmann. 1995. Chromosome divergence in the genus Cuscuta and its systematic implications. Caryologia 48(2): 173–180.

Peruzzi L, Eroğlu HE. 2013. Karyotype asymmetry: again, how to measure and what to measure? Comparative cytogenetics. 7(1): 1-9.

Plitman S. 1978. *Cuscuta*, 222-237 in Davis PH. Flora Of Turkey and The East Aegean Islands. (6), Edinburgh Press MC, Scholes JD, Watling JR. 1999. Parasitic plants: physiological and ecological interactions with their hosts. In: Press, MC, Scholes, JD, Barker, MG, eds. Physiological Plant Ecology. Oxford, UK: Blackwell Science, 175–197

Rezaei M, Naghavi MR, Hoseinzadeh AH, Abbasi A, Jahangiri B. 2014. Study of Karyological Characteristics in Papaver bracteatum and Papaver somniferum. Cytologia. 79(2): 187-194.

Singh V.K and S.K. Roy. (1970). Sitology of *Cuscuta* Linn. Sci. Cult.36: 567-568

Stebbins GL. 1971. Chromosomal Evolution in Higher Plants. Edward Arnold. London.

Tasar N, Dogan G, Kiran Y, Rahman MO, Cakilcioglu U. 2018a. Morphologıcal, Anatomıcal and Cytologıcal Investıgatıons on three taxa of Centaurea L. (asteraceae) From Turkey. Bangladesh J. Plant Taxon. 25(2): 215-226.

Tasar N, Dogan G, Kiran Y. 2018b. Karyological Investigation on Seven Centaurea L. (Asteraceae) Taxa from Turkey. Cytologia. 83(3): 317–321.

Ward D. E. 1984. Chromosome counts from New Mexico and Mexico. Phytologia 56(1): 55–60.

Watanabe K, Yahara T, Denda T, Kosuge K. 1999. Chromosomal evolution in the genus Brachyscome (Asteraceae, Astereae): Statistical tests regarding correlation between changes in karyotype and habit using phylogenetic information. J. Plant Res. 112: 145-161.

Yeh, H. c. & J. l. Tsai. 1995. Karyotype analysis of the Convolvulaceae in Taiwan. Annual Taiwan Mus. 38: 58–61.

Yuncker T.G. 1932. The genus *Cuscuta*. Mem Torr Bot. Club., (18): 113-331.

Zarco RC. 1986. A new method for estimating karyotype asymmetry. Taxon. 35(3): 526-530.

Identifying potential adaptive SNPs within combined DNA sequences in Genus *Crocus* L. (Iridaceae family): A multiple analytical approach

Masoud Sheidai[1,*], Mohammad Mohebi Anabat[1], Fahimeh Koohdar[1], Zahra Noormohammadi[2]

[1] *Department of Plant Sciences and Biotechnology, Faculty of Life Sciences and Biotechnology, Shahid Beheshti University, Tehran, Iran*
[2] *Department of Biology, School of Basic Science, Science and Research Branch, Islamic Azad University, Tehran, Iran*
*Corresponding author. E-mail: msheidai@sbu.ac.ir

Abstract. The genus *Crocus* L. of Iridaceae family contains about 160 species and is considered as a complex group of plant taxa with regard to evolutionary and phylogenetic events. Inter-specific hybridization and gene flow contribute to species genetic homogeneity in one hand and high within species genetic variability and species genetic content overlaps caused species resolution a problem. In spite of extensive molecular phylogenetic studies in this genus, nothing is known about DNA sequences or Single nucleotide polymorphisms (SNPs) which are of adaptive nature. Moreover, nothing is known about which geographical or environmental factors plays role in species local adaptation and speciation events within *Crocus* L. genus. Therefore, the present study was conducted to answer the above said questions. We used a combined molecular data set of internal transcribed spacer (*ITS*) nuclear gene and trnL-F intergenic spacer (*trnL-F*) sequences of chloroplast genome. A multiple analytical method of Canonical correlation (CCA), Redundancy analysis (RDA), and Latent Factor Mixed Model (LFMM) identified a few potential adaptive SNPs. Moreover, population criterions like Tajimas' D, molecular clock test, as well as skyline-plot revealed a smooth and continuous genetic changes for most of the *Crocus* species, but the occurrence of a sudden deep nucleotide substitution for *Crocus* taxa of Iran. The impact of latitude was significantly higher on nucleotide changes compared to that of longitudinal distribution of *Crocus* species.

Keywords: *Crocus*, adaptive divergence, SNPs, speciation.

1. INTRODUCTION

The genus *Crocus* L. (family Iridaceae), has about 100 species and contains an economically important species *Crocus sativus* L., the edible saffron. The species of this genus are distributed from Western Europe and north-

western Africa to Western China. Though the Asia Minor is the center of genus diversity (Sheidai et al., 2017), many species grow in the Mediterranean region (Saxena, 2010).

Several studies were concerned with molecular phylogeny and DNA barcoding of this genus which produced valuable information on different molecular aspects of genus. Aghighiravan et al. (2019), reported that ITS barcode is the best molecular marker for phylogenetic investigation on *Crocus* L. genus. Similarly, Sheidai et al. (2017), reported a high degree of genetic variability both within and among the studied species in the genus and that ISSR molecular markers are useful in *Crocus* species delineation. Along with the species relationships, these authors also reported population fragmentation and inter-specific gene flow in these taxa.

In a recent investigation, Mohebi et al. (2021), presented both DNA barcode and chromosome number variation in the genus. These authors suggested that molecular events like horizontal gene transfer (HGT) and deep coalescence may be associated with geographical distribution and *Crocus* taxa diversification. Due to importance of this genus and also lack of knowledge on geographical association of the genetic differences in *Crocus* species, we carried out a detailed bioinformatic analyses of a combined molecular data set of ITS nuclear DNA sequences and *trnL-F* chloroplast sequences, to : 1- Identify discriminating nucleotide sequences among *Crocus* species, 2- Illustrate if these sequences are significantly associated with geographical coordinates, 3- Identify nucleotide sequences with phylogenetic importance.

For bioinformatic studies, we used different analytical approaches like discriminate analysis of principal components analysis (DAPC), which is suitable for SNP sequences, as well as both CCA (Canonical correspondence analysis), and RDA (Redundancy analysis). Moreover, some data on *Crocus* species expansion were also produced by using population genetics analysis methods of Tajimas' D value, molecular clock test, and mismatch nucleotide pair test. The findings of this research are new to *Crocus* science.

2. MATERIAL AND METHODS

In this study, ITS nuclear DNA and trnL-F sequences of 68 *Crocus* species were obtained from National Center for Bioinformatic Information (NCBI). In addition, we used two species of the genus *Romulea* as outgroup taxa because of the high similarity to *Crocus* (Goldblatt et al., 2006; Petersen et al., 2008) (Table 1).

2.1. Data analyses

Sequence alignment and curation was done by MUSCLE program implemented out in molecular evolutionary genetics analysis (MEGA) 7 program. Mismatch analysis and skyline plot was constructed in R package 4.2. These sequences were then used to construct Maximum likelihood phylogenetic tree (ML tree), by MEGA 7 program based on Kimura-Two parameters distance. The following analyses were performed to identify the SNPs which show association with geographical coordinates of *Crocus* species distribution. We should mention that these analytical approaches have different assumptions and may differ to some extent in their results. Therefore, comparing obtained results are important for drawing a solid conclusion.

2.2. Canonical correspondence analysis

In the first approach we used CCA (Canonical correspondence analysis). This method is based on regression of the SNPs and ecological features and uses an approach similar to principal components analysis (PCA), but it is utilized for discrete characteristics like SNPs (Podani, 2000; Sheidai et al., 2020). This method differs from PCA in the way that, PCA tries to maximize the variance of data in a reduced space, while CCA tries to maximize the association of data (SNPS), to ecological features studied (Podani, 2000; Sheidai et al., 2020). CCA was performed in PAST ver. 4., program.

2.3. Latent Factor Mixed Model (LFMM)

Latent factor mixed model is a method for testing associations between loci and environmental gradients using latent factor mixed models. LFMM implements an MCMC algorithm for regression analysis in which the confounding variables are modeled with unobserved (latent) factors. The program estimates correlations between environmental variables and allelic frequencies, and simultaneously infers the background levels of population structure (Frichot et al., 2013, Frichot and Francois, 2015). LFMM was performed by LFMM package in R. 4.2.

2.4. Redundency analysis (RDA)

Redundancy analysis (RDA), a form of constrained ordination which is fit for genomic data sets, where we are interested in understanding how the multivariate environment shapes patterns of genomic composition across geographical areas. RDA is based on multivariate

Table 1. The accession numbers and chromosome number of taxa in for the genus *Crocus* and outgroup representatives.

Number	Taxa	Accession number(ITS)	Accession number(trnL-F)	chromosome number	Country
1	*C. veneris*	HE801061.1	HE864222.1	2n= 16	cyprus
2	*C. etruscus*	HG518187.1	HG518216.1	2n= 8	Italy
3	*C. kosaninii*	HG518189.1	HG518206.1	2n= 14	Serbia
4	*C. baytopiorum*	LS398370.1	LT991646.1	2n= 28	Turkey
5	*C. scardicus*	HE663961.1	HE864166.1	2n= 36	Macedonia
6	*C. versicolor*	HE801142.1	HE864249.1	2n= 26	Italy
7	*C. malayi*	HE801170.1	HE864246.1	2n= 30	Croatia
8	*C. imperati*	HE801131.1	HE864231.1	2n= 26	Italy
9	*C. minimus*	HE801140.1	HE864247.1	2n= 24	Italy
10	*C. corsicus*	HE801096.1	HE864241.1	2n= 18	Italy
11	*C. cambessedesii*	HE801105.1	HE864228.1	2n= 16	Spain
12	*C. nudiflorus*	HE801146.1	HE864253.1	2n= 48	Spain
13	*C. serotinus*	HE801125.1	HE864225.1	2n= 22	Portugal
14	*C. niveus*	HE801081.1	HE864219.1	2n= 28	Greece
15	*C. goulimyi*	HE801130.1	HE864230.1	2n= 12	Greece
16	*C. ligusticus*	HE801167.1	HE864234.1	2n= 24	Italy
17	*C. kotschyanus*	HE664000.1	HE864256.1	2n= 8	Turkey
18	*C. scharojanii*	HE801135.1	HG518229.1	2n= 8	Russia
19	*C. vallicola*	HE801168.1	HE864238.1	2n= 8	Russia
20	*C. gilanicus*	HE801172.1	HE864255.1	2n= 24	Iran
21	*C. sativus*	HE801172.1	LT991682.1	2n= 24	Iran
22	*C. pallasii* sub sp. *hausknechtii*	LS398387.1	LT991663.1	2n= 14	Iran
23	*C. thomasii*	LS398411.1	LT991688.1	2n= 16	Italy
24	*C. cartwrightianus*	LS398376	LT991648.1	2n= 16	Greece
25	*C. moabiticus*	LS398392.1	LT991669.1	2n= 14	Jordan
26	*C. oreocreticus*	LS398397.1	LT991674.1	2n= 16	Greece
27	*C. asumaniae*	LS398366.1	LT991641.1	2n= 26	Turkey
28	*C. mathewii*	HE801089.1	HE864217.1	2n= 70	Turkey
29	*C. reticulatus*	LM993447.1	LM993633.1	2n= 10	Moldova
30	*C. cvijicii*	LT222444.1	HE864276.1	2n= 18,20,22	Albania
31	*C. dalmaticus*	HE801137.1	HE864242.1	2n= 24	Croatia
32	*C. sieberi subsp. sieberi*	HE663966.1	HE864171.1	2n= 22	Greece
33	*C. robertianus*	HE801134.1	HE864236.1	2n= 20	Greece
34	*C. cancellatus* subsp. *pamphylicus*	HE801128.1	HE864229.1	2n= 12	Turkey
35	*C. hermoneus*	HE801163.1	HE864268.1	2n= 12	Jordan
36	*C. abantensis*	HE664019.1	HE864239.1	2n= 8,16	Turkey
37	*C. angustifolius*	HE801136.1	LM993589.1	2n= 20	Russia
38	*C. ancyrensis*	HE663987.1	LM993597.1	2n= 10	Turkey
39	*C. gargaricus* sub sp. *gargaricus*	HE801138.1	HE864243.1	2n= 30	Turkey
40	*C. sieheanus*	HE801157.1	HE864263.1	2n= 16	Turkey
41	*C. rujanensis*	LT222441.1	HE864280.1	2n= 22	Serbia
42	*C. biflorus* sub sp. *biflorus*	HE801121.1	HE864220.1	2n= 8	Italy
43	*C. almehensis*	HE801162.1	HE864271.1	2n= 20	Iran
44	*C. danfordiae*	HE664007.1	HE864201.1	2n= 8	Turkey
45	*C. pestalozzae*	HE801141.1	HE864248.1	2n= 28	Turkey
46	*C. cyprius*	HE663962.1	HE864168.1	2n= 10	Greece
47	*C. hartmannianus*	HE801173.1	HE864264.1	2n= 20	Cyprus
48	*C. leichtlinii*	LN864711.1	HE864277.1	2n= 20	Turkey
49	*C. kerndorffiorum*	HE801159.1	HE864213.1		Turkey

Number	Taxa	Accession number(ITS)	Accession number(trnL-F)	chromosome number	Country
50	*C. nerimaniae*	HE663977.1	HE864181.1	2n= 10	Turkey
51	*C. korolkowii*	HE801139.1	HE864244.1	2n= 20	Uzbekistan
52	*C. michelsonii*	KY797650.1	HE864278.1	2n= 20	Iran
53	*C. caspius*	HE801171.1	HE864266.1	2n= 24	Iran
54	*C. alatavicus*	HE801116.1	HE864273.1	2n= 20	Uzbekistan
55	*C. naqabensis*	LS398395.1	LT997016.1	2n= 14	Jordan
56	*C. antalyensis*	HE664015.1	HE864209.1	2n= 8	Turkey
57	*C. olivieri*	HE8011	HE864216.1	2n= 6	Turkey
58	*C. candidus*	HE663981.1	HE864186.1	2n= 6	Turkey
59					
60	*C. hyemalis*	HE801060.1	HE864215.1	2n= 6	Plestin
61	*C. aleppicus*	HE801175.1	HE864267.1	2n= 16	Jordan
62	*C. veneris*	HE801062.1	HE864222.1	2n= 16	Cyprus
63	*C. carpetanus*	HE801071.1	HE864265.1	2n= 64	Turkey
64	*C. nevadensis*	HE663960.1	HE864170.1	2n= 28, 30	Spain
65	*C. fleischeri*	HE663983.1	HE864188.1	2n= 20	Turkey
66	*C. pulchellus*	HE801145.1	HE864252.1	2n= 12	Greece
67	*C. laevigatus*	HE801166.1	HE864233.1	2n= 30	Greece
68	*C. banaticus*	HE801147.1	HE864254.1	2n= 26	Romania
69	*Romulea ramiflora*	HE664012.1	HE864206.1	2n= 36	Turkey
70	*R. bulbocodium*	HE664012.1	HE864202.1	2n= 34,36,42	Turkey

regression, and models linear combinations of the environmental predictors that explain linear combinations of the SNPs. This method effectively identifies covering loci associated with the multivariate environmental features (Legendre and Legendre, 2012).

Redundancy analysis is a highly flexible framework, and produce answers on: 1- What environmental conditions cause genetic divergence among the studied taxa? and 2. What is the genetic basis of local adaptation to the environment? RDA identifies linear relationships among the response and predictor matrices; if non-linear relationships are expected, other statistical frameworks may be more suitable. RDA was performed in Paleontological statistics (PAST) ver. 4, program.

Mantel test was performed with 1000 times permutations as implemented in PAST ver. 4., program to study correlation between genetic distance and geographical distance of the studied species.

Phylogenetically important SNPs was determined by character mapping of 110 SNPs obtained based on parsimony criterion as performed in Mesquite 3.6 program. We performed Tajima's D test (Tajima, 1989) to reveal if *Crocus* species DNA sequences evolved randomly ("neutrally"), or under a non-random process, including directional or balancing selection, demographic expansion or contraction. Moreover, we also carried out the molecular clock test, to show if SNP changes occurred in accordance with a uniform clock rate model of evolution during *Crocus* genus speciation events. These tests were performed by MEGA 7 program.

3. RESULTS

3.1. The species genetic difference

The preliminary analysis of combined sequences obtained after sequence alignments and curation, produced a DNA segment of 110 base pair length. The average p dis of the studied species was 0.126. Based on Kimura 2-parameters, the studied taxa differed in genetic distance from 0. 01 to 0.30. The paired mismatch plot of nucleotide difference is presented in Fig. 1. This plot shows a normal distribution in genetic difference of these species, which indicates that genetic divergence occurred in a continuous and steady mode in evolution of the genus *Crocus* L. Skyline-plot (Fig. 2), of the same species also revealed a smooth and continuous species expansion in the genus *Crocus*, with two sudden changes in population demography and sequence change which are related to the speciation events in Iran *Crocus* taxa.
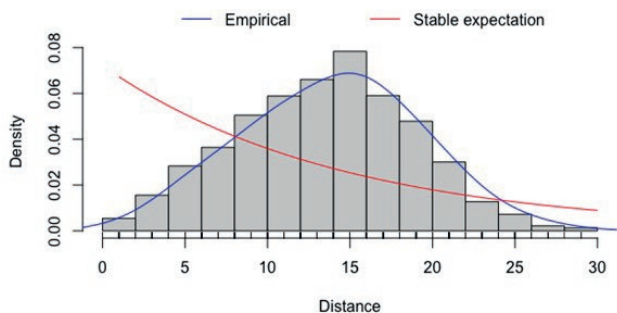
Figure 1. Mismatch plot of nucleotide difference among *Crocus* species.
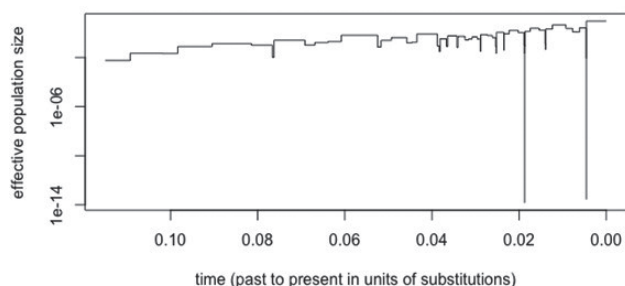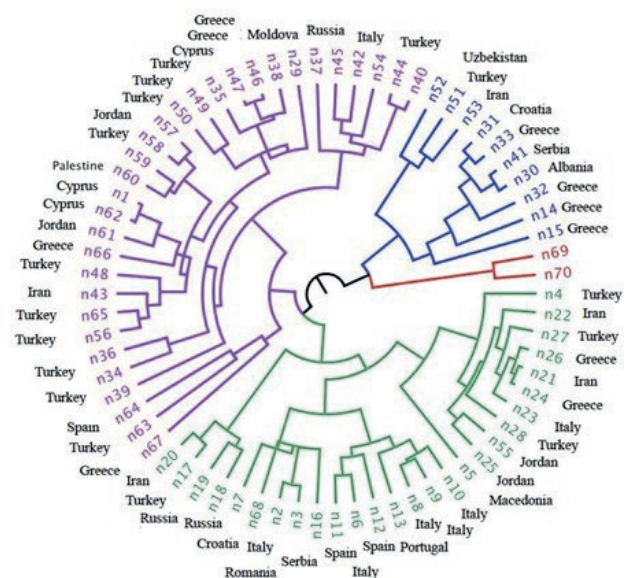

Figure 2. Skyline-plot of *Crocus* species based on combined sequence data set.

### 3.2. Genetic grouping of taxa

ML (Maximum likelihood) phylogenetic tree of the studied *Crocus* species based on combined molecular data set and the species geographical distribution, is presented in Fig. 3. We can place the studied species in three to four major clades. At the first glance, it is evident that species with Mediterranean distribution and those of South-West Asia (Iran, Iraq, and Afghanistan), and the neighboring regions, comprise adjacent clades, while the species growing in Europe are showing closer genetic affinity.

Genetic grouping of these species by Linear discriminating analysis (LDA), as performed in DAPC analysis is provided in Fig. 4. This plot also supports the presence of four genetic groups in the studied taa. The assignment test for the studied *Crocus* species based on DAPC analysis identified the species with genetic affinity (Fig. 5). The species n1-n68, are scattered in four major genetic groups as revealed by different cluster colors.

Linear discriminating analysis revealed that the first three discriminating analysis (DA) axes, comprise about 80% of total variation, and the first two axes have significant contribution with high Fst value (Fig. 6). DA loading obtained revealed that SNPs 74, 75 have the highest

Figure 3. ML phylogenetic tree of the studied *Crocus* species and their geographical distribution. (n1-n70, as in Table 1).
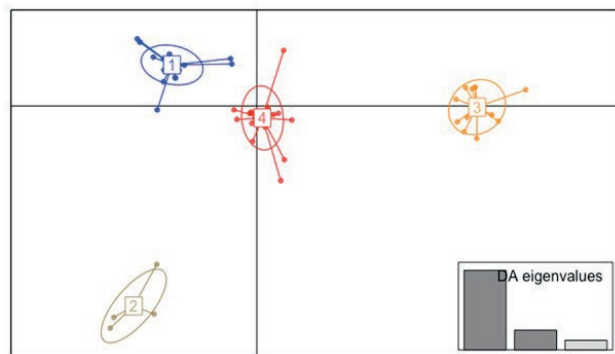
Figure 4. Genetic groups identified based on LDA analysis.
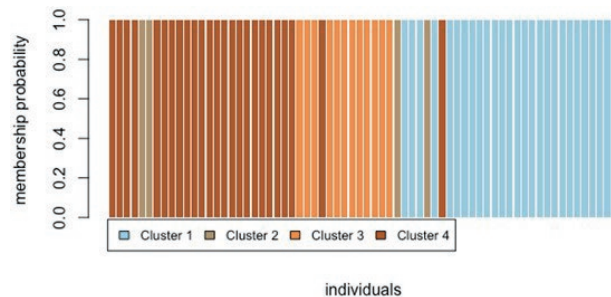
Figure 5. Assignment plot of *Crocus* species based on DAPC analysis (Individuals from left to wright are n1 to n 68 of Table 1).

discriminating power in the first LDA axis, followed by SNPs 31, and 109, in the second axis. Similarly, SNP 53 has high discriminating power in the third DA axis.

The following analyses were performed to identify the SNPs which show association with geographical coordinates of *Crocus* species distribution. We should mention that these analytical approaches have different assumptions and may differ to some extent in their results. Therefore, comparing obtained results are important for drawing a solid conclusion.

3.3. Canonical correspondence analysis

CCA plot of *Crocus* species and 110 SNPs used is provided in Fig. 7. The analysis produced two CCA axes with Eigenvalue% of 99.97and 0.028, respectively. Distribution of 110 SNPs used shows association between SNPS 31, 70, 71, 74, and 75, with latitude distribution of *Crocus* species of these three SNPS. viz. 31, 74, and 75, were identified as discriminating loci among *Crocus* taxa, by DAPC analysis. These SNPs have high association value as are placed in the first CCA axis. The SNPs

2, 93 and 94 of the second CCA axis, show a lower degree of association with longitude distribution of the studied *Crocus* taxa. From these results, we may conclude that, genetic changes of *Crocus* species towards latitude distribution was accompanied to these SNPs, which probably were associated with some important adaptive genes during *Crocus* speciation.

It becomes interesting when we plot the selected countries (geographical regions), by CCA (Fig. 8). We observe that countries like Iran, Russia, and Georgia, become separated from the other studied countries towards latitude. That means SNPs' changes occurred in these regions. The Skyline plot presented before also revealed a sudden change in nucleotide substitution and population size in Iran.

3.4. Latent Factor Mixed Model (LFMM)

Manhattan plot of LFMM analysis is presented in Fig. 9. It identified SNPs 2, 9, 63, and 79, showed a significant association with environmental features.

Figure 6. F-statistics of LDA analysis showing significant contribution of the first two axes in discriminating *Crocus* species.
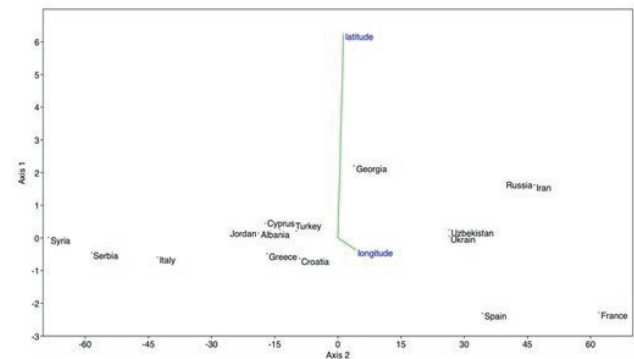
Figure 8. CCA plot of geographical regions showing separation of countries towards altitude and longitude *Crocus* species.

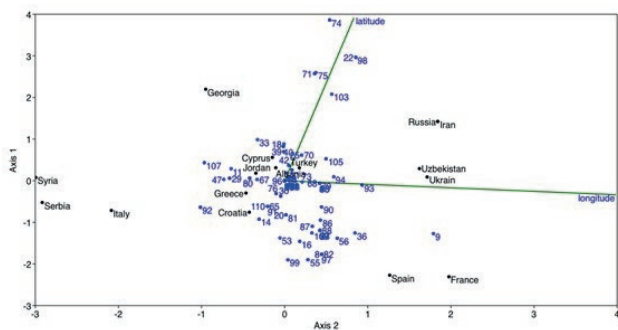**Figure 7.** CCA plot of *Crocus* species showing association of few SNPs with geographical factors.
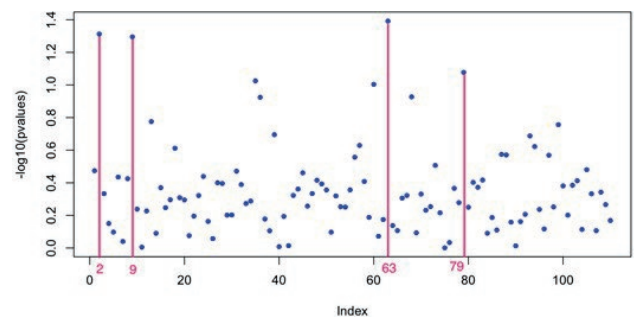
Figure 9. Manhattan plot of LFMM analysis identifying four SNPs associated with environmental features.
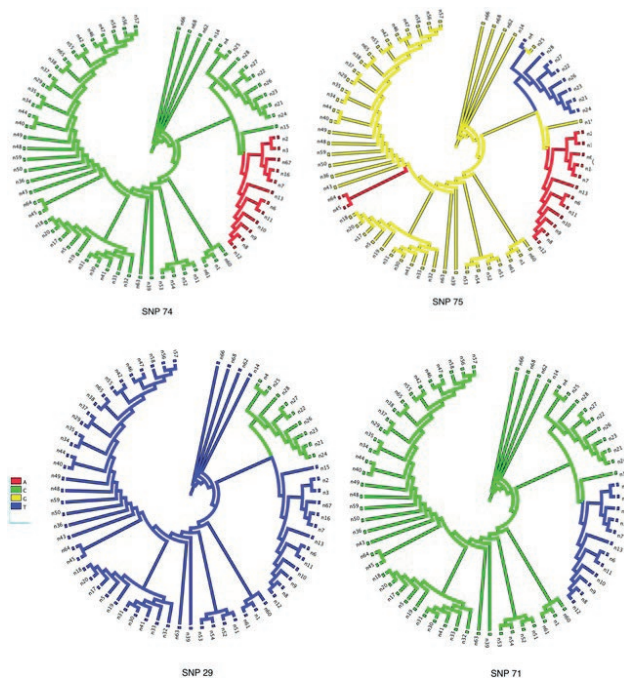
3.5. Redundancy analysis (RDA)

Redundancy analysis (RDA) was performed to detect the roles of geographical variables in *Crocus* species genetic subdivision, as well as the relative contribution of each variable to the population genetic structure. RDA plot is presented in Fig. 10. The SNPs 22, 71, 74, 75, 98, and 103, show association with latitude which occurs in RDA axis one with about 85% of total variance, followed by SNPs 9, 93 and 94, associated with longitude and second RDA axis with only 14% of total variance. Therefore, if we consider different association approaches utilized in this study, we can consider a few SNPs which are significantly associated with geographical factors studied. These SNPs occurred during species divergence within the genus *Crocus*.

A negative Tajima's D = -1.2, was obtained for the studied SNPs in *Crocus* species. This signifies an excess of low frequency polymorphisms relative to expectation, indicating population size expansion after a bottleneck or a selective sweep, which result in reduction in genetic diversity and formation of adaptive genotypes (species), in different geographical areas. The molecular test showed that SNP changes within the genes *Crocus* did not occurred under uniform rate of evolution and different phylogenetic clades differed in their genetic changes. This results also agree with the earlier result of skyline plot showing a deep change in SNP substitution and population size change in *Crocus* species of Iran and neighboring regions.

Mantel test performed after 1000 times permutations, produced non-significant correlation between genetic distance and geographical distance of the studied species (r = - 0.03, P = 0.7). This result indicates that nucleotide difference and change in *Crocus* taxa is not due to mere geographical distance and as indicated by different analyses reported here, genetic changes are. mainly associated with latitude distribution of these taxa.

Figure 11. Character mapping of SNPs by parsimony criterion showing that these SNPs can differentiate different phylogenetic clades.

3.6. Phylogenetically important SNPs

Character mapping of the SNPs (Fig. 11), based on parsimony criterion, revealed that some of these SNPs are of phylogenetic importance as they differentiate almost a particular clade of the studied species. Interesting enough, SNPs 74 and 75. are also among these phylogenetic important SNPs. These two SNPs were identified as discriminating SNPs among *Crocus* species and also they are associated with latitude distribution of taxa, particularly *Crocus* species of Iran and neighboring areas.

4. DISCUSSION

Speciation within the genus *Crocus* is complex. A combination of diploid and polyploidisation events as well as inter-specific hybridization have been postulated for *Crocus* genus evolution (Mosolygo-L et al., 2016). Complexity at the species level has been reported by Seberg and Petersen (2009), as these authors could not delineate *Crocus* species even by utilizing different barcoding markers. However, some authors, could resolve *Crocus* species of Balkan (Mosolygo-L et al., 2016) and Iran (Sheidai et al., 2018), by using different molecular markers.

Figure 10. RDA plot of *Crocus* species showing association of few SNPs with geographical factors.

Recently, Mohebi et al. (2020), provided DNA barcode of Chloroplast DNA (trnH-psbA) region, which differentiated saffron genotypes of Iran from the other imported genotypes. Moreover, the same authors (unpublished data), provided some DNA barcode which illustrate genetic differentiation between *Crocus* taxa growing in different geographical regions and not for a particular *Crocus* species.

Nine *Crocus* L. species have been reported from Persia and some adjacent areas (Wendelbo, 1977; Matine, 1978). Taxonomy of the genus is controversial as evidenced by difficulties in *Crocus* species delineation. In spite of extensive efforts on the phylogenetic aspects of *Crocus* genus, there has been now report on ecological or geographical association of the genetic or DNA sequence changes with speciation events in this genus. The present study revealed that DNA nucleotides of both nuclear and chloroplast origin can efficiently differentiate some of the phylogenetic clades of *Crocus* taxa. Moreover, some of these sequences may be associated with geographical distribution of *Crocus* species. Some nucleotide seems to be tightly associated with latitudinal distribution of these taxa.

Tajima's test of these sequences produced a negative Tajima's D, which indicates an excess of low frequency polymorphisms relative to a selective sweep and speciation events (Tamura and Nei, 1993). We also observed almost a continuous and gradual nucleotide substitution for most of the species growing in other parts of the world, but a sudden deep change in DNA sequences of Iran *Crocus* species, which may be related to geographical adaptation as also evidenced by CCA and RDA analyses.

Different approaches used to identify the nucleotides associated with geographical variables, revealed some degree of difference. It is due the fact that CCA and RDA methods are based on linear association (regression), with different approaches, while LFMM method is a Bayesian-Model approach (Podani, 2000; Frichot and Francois, 2015). It seems therefore, using different approaches may improve understanding of associated SNPs with geographical and ecological variables. Such combined data evaluations, give insights into contemporary processes, and may explain how environmental factors influence selective and neutral genomic diversity within and among related species or different geographical populations within a single species (Segovia et al., 2020).

Presence of heterogenous environmental conditions are known to cause changes in genetic diversity of plant species and result in local adaptations even in the populations of a single species (Segovia et al., 2020). Understanding the genetic basis of local adaptation is one of the main concern of evolutionary biologists, as identifying

adaptive genetic loci or SNPs improves our knowledge of the genetic mechanism of local adaptation and probably species diversification within a genus (Zhang et al., 2019).

Recent studies which are concerned with genetics of local adaptations try to answer two major questions: 1- which environmental variables play key role in the adaptive genetic divergence of a species or different species within a particular genus and shape its landscape genetic structure, and, 2-which genes or loci on the genome undergo adaptive genetic differentiation (Li et al., 2017, Zhang et al., 2019).

In general, populations' local adaptation which leads to speciation thing a genus is the act of natural selection in oppose to continuous gene flow. In plant groups such as *Crocus* genus in which species differentiation is vague due to inter-specific hybridization and a high degree of genetic affinity, local adaptation, may be expected to happen for a few genes or nucleotides, as also we demonstrated in this study. The latitude occurrence of nucleotide changes and species diversification in *Crocus* genus, may be related to a warmer and drier environmental conditions of Iran, and Afghanistan and neighboring regions in compare to those prevailing in Mediterranean countries and Europe.

In a similar study, Ingvarsson et al. (2006), characterized patterns of DNAsequence variation at the putative candidate gene phyB2 in 4 populations of European aspen (*Populous tremula*) and scored single-nucleotide polymorphisms in an additional 12 populations collected along a latitudinal gradient in Sweden. They utilized a sliding-window scan of phyB2 and identified six putative regions with enhanced population differentiation and four SNPs showed significant clinal variation. Therefore, they suggested that the clinal variation at individual SNPs is an adaptive response in phyB2 to local photoperiodic conditions. It has been suggesting that divergent selection enhances the levels of genetic differentiation not only for the sites that are the direct target of selection but also for neutral sites in the vicinity of the site(s) under selection (Charlesworth et al., 1997; Nordborg and Innan, 2003).

5. CONCLUSION

In conclusion, the present study provide data on DNA sequences changes in association with geographical variables in the genus *Crocus* and suggest that latitudinal distribution has a more profound effect on these genetic changes. Moreover, we also suggest utilizing a multiple analytical approaches for identification of both discriminating DNA nucleotides/ SNPs within a genus

and for illustrating SNPs association with geographical or ecological variables.

REFERENCES

Aghighiravan, F., Shokrpour, M., Nazeri, V., Naghavi, M.R., 2019. Phylogenetic assessment of some species of *crocus* genus using DNA barcoding. J. Genet. Resour. 5(2), 118-129.

Charlesworth, B., Nordborg, M., Charlesworth,D., 1997. The effects of local selection, balanced polymorphism and background selection on equilibrium patterns of genetic diversity in subdivided populations. Genet. Res. 70, 155–174.

Frichot, E., Schoville, S.D., Bouchard, G., Francois, O., 2013. Testing for associations between loci and environmental gradients using latent factor mixed models. Mol. Biol. Evol. 30 (7), 1687-1699.

Frichot, E., Francois, O., 2015. LEA: An R package for landscape and ecological association studies. Methods in Ecology and Evolution: 6 (8), 925-929

Ingvarsson, P. K., Garcı´a, M.V., David Hall, D., Luquez, V., Jansson, S., 2006. Clinal Variation in phyB2, a Candidate Gene for Day-Length-Induced Growth Cessation and Bud Set, Across a Latitudinal Gradient in. European Aspen (*Populus tremula*). Genetics. 172, 1845–1853. DOI: 10.1534/genetics.105.047522

Legendre, P., Legendre, L., 2012. Numerical ecology. 3 editions. Oxford, UK.

Li, Y., Zhang, X.X., Mao, R.L., Yang, J., Miao, C.Y., Li, Z., Qiu, X.Y., 2017 Ten years of landscape genomics: challenges and opportunities. Front. Plant. Sci. 8, 2136.

Matine, F., 1978. Liste des plantes de l'herbierd'. vine (Herbarium Ministerii Iranici Agriculturae). Iridaceae, Tehran.

Mohebi Anabat, M., Riahi, H., Sheidai, M., Koohdar, F., 2020. Population genetic study and barcoding in Iran saffron (*Crocus sativus* L.). Ind. Crop. Prod. 143, 111915.

Mohebi Anabat, M., Riahi, H., Sheidai, M., Koohdar, F., 2021. A new look at the genus *Crocus* L. phylogeny and speciation: Insight from molecular data and chromosome geography. Genet. Resour. Crop. Accepted paper.

Mosolygó-L, Á., Sramkó, G., Barabás, S., Czeglédi, L., Jávor, A., Molnár, A., Surányi, G., 2016. Molecular genetic evidence for allotetraploid hybrid speciation in the genus *Crocus* L. (Iridaceae). Phytotaxa. 258 (2), 121–136.

Nordborg, M., Innan, H., 2003 The genealogy of sequences containing multiple sites subject to strong selection in a subdivided population. Genetics. 163, 1201–1213.

Podani J., 2000. Introduction to the Exploration of Multivariate Data Backhuyes, Leiden.

Petersen, G., Seberg, O., Thorsoe, S., Jorgensen, T., Mathew, B., 2008. A phylogeny of the genus *Crocus* (Iridaceae) based on sequence data from five plastid regions. Taxon. 57, 487–499.

Segovia, N. I., González-Wevar, C. A., Haye, P. A., 2020. Signatures of local adaptation in the spatial genetic structure of the ascidian Pyura chilensis along the southeast Pacific coast. Sci. Rep. 10,14098.

Sheidai, M., Tabasi, M., Mehrabian, M.R., Koohdar, F., Ghasemzadeh-Baraki, S., Noormohammadi, Z., 2017. Species delimitation and relationship in *Crocus* L. (Iridaceae). Acta. Botanica. Croat. 77(1): 10-17 .

Sheidai, M., Tabasi, M., Mehrabian, M. R., Koohdar, F., Ghasemzadeh-Baraki, S., Noormohammadi, Z., 2018. Species delimitation and relationship in *Crocus* L. (Iridaceae). Acta Bot. Croat. 77 (1), 10–17.

Tajima, F (1989) Statistical method for testing the neutral mutation hypothesis by DNA polymorphism. Genetics. 123: 595-595.

Tamura K., Nei M., 1993. Estimation of the number of nucleotide substitutions in the control region of mitochondrial DNA in humans and chimpanzees. Mol. Biol. Evol. 10, 512-526.

Wendelbo, P., 1977. Tulips and Irises of Iran, and their relatives, Botanical Institute of Iran, Tehran.

Zhang, X. X., Liu, B. G., Li, Y., Liu, Y., He, Y. X., Qian, Z. H., Li, J. X., 2019. Landscape genetics reveals that adaptive genetic divergence in *Pinus bungeana* (Pinaceae) is driven by environmental variables relating to ecological habitats. BMC Evolutionary Biology. 19,160.

OPEN ACCESS POLICY

Caryologia provides immediate open access to its content. Our publisher, Firenze University Press at the University of Florence, complies with the Budapest Open Access Initiative definition of Open Access: By "open access" , we mean the free availability on the public internet, the permission for all users to read, download, copy, distribute, print, search, or link to the full text of the articles, crawl them for indexing, pass them as data to software, or use them for any other lawful purpose, without financial, legal, or technical barriers other than those inseparable from gaining access to the internet itself. The only constraint on reproduction and distribution, and the only role for copyright in this domain is to guarantee the original authors with control over the integrity of their work and the right to be properly acknowledged and cited. We support a greater global exchange of knowledge by making the research published in our journal open to the public and reusable under the terms of a Creative Commons Attribution 4.0 International Public License (CC-BY-4.0). Furthermore, we encourage authors to post their pre-publication manuscript in institutional repositories or on their websites prior to and during the submission process and to post the Publisher's final formatted PDF version after publication without embargo. These practices benefit authors with productive exchanges as well as earlier and greater citation of published work.

PUBLICATION FREQUENCY

Papers will be published online as soon as they are accepted, and tagged with a DOI code. The final full bibliographic record for each article (initial-final page) will be released with the hard copies of *Caryologia*. Manuscripts are accepted at any time through the online submission system.

COPYRIGHT NOTICE

Authors who publish with *Caryologia* agree to the following terms:

- Authors retain the copyright and grant the journal right of first publication with the work simultaneously licensed under a Creative Commons Attribution 4.0 International Public License (CC-BY-4.0) that allows others to share the work with an acknowledgment of the work's authorship and initial publication in Caryologia.
- Authors are able to enter into separate, additional contractual arrangements for the non-exclusive distribution of the journal's published version of the work (e.g., post it to an institutional repository or publish it in a book), with an acknowledgment of its initial publication in this journal.
- Authors are permitted and encouraged to post their work online (e.g., in institutional repositories or on their website) prior to and during the submission process, as it can lead to productive exchanges, as well as earlier and greater citation of published work (See The Effect of Open Access).

PUBLICATION FEES

Open access publishing is not without costs. *Caryologia* therefore levies an article-processing charge of € 150.00 for each article accepted for publication, plus VAT or local taxes where applicable.
We routinely waive charges for authors from low-income countries. For other countries, article-processing charge waivers or discounts are granted on a case-by-case basis to authors with insufficient funds. Authors can request a waiver or discount during the submission process.

PUBLICATION ETHICS

Responsibilities of *Caryologia*'s editors, reviewers, and authors concerning publication ethics and publication malpractice are described in *Caryologia*'s Guidelines on Publication Ethics.

CORRECTIONS AND RETRACTIONS

In accordance with the generally accepted standards of scholarly publishing, *Caryologia* does not alter articles after publication: "Articles that have been published should remain extant, exact and unaltered to the maximum extent possible".
In cases of serious errors or (suspected) misconduct *Caryologia* publishes corrections and retractions (expressions of concern).

Corrections

In cases of serious errors that affect or significantly impair the reader's understanding or evaluation of the article, *Caryologia* publishes a correction note that is linked to the published article. The published article will be left unchanged.

Retractions

In accordance with the "Retraction Guidelines" by the Committee on Publication Ethics (COPE) *Caryologia* will retract a published article if:

- there is clear evidence that the findings are unreliable, either as a result of misconduct (e.g. data fabrication) or honest error (e.g. miscalculation)
- the findings have previously been published elsewhere without proper crossreferencing, permission or justification (i.e. cases of redundant publication)
- it turns out to be an act of plagiarism
- it reports unethical research.

An article is retracted by publishing a retraction notice that is linked to or replaces the retracted article. *Caryologia* will make any effort to clearly identify a retracted article as such.
If an investigation is underway that might result in the retraction of an article *Caryologia* may choose to alert readers by publishing an expression of concern.

COMPLYNG WITH ETHICS OF EXPERIMENTA-TION

Please ensure that all research reported in submitted papers has been conducted in an ethical and responsible manner, and is in full compliance with all relevant codes of experimentation and legislation. All papers which report in vivo experiments or clinical trials on humans or animals must include a written statement in the Methods section. This should explain that all work was conducted with the formal approval of the local human subject or animal care committees (institutional and national), and that clinical trials have been registered as legislation requires. Authors who do not have formal ethics review committees should include a statement that their study follows the principles of the Declaration of Helsinki

ARCHIVING

Caryologia and Firenze University Press are experimenting a National legal deposition and long-term digital preservation service.

ARTICLE PROCESSING CHARGES

All articles published in *Caryologia* are open access and freely available online, immediately upon publication. This is made possible by an article-processing charge (APC) that covers the range of publishing services we provide. This includes provision of online tools for editors and authors, article production and hosting, liaison with abstracting and indexing services, and customer services. The APC, payable when your manuscript is editorially accepted and before publication, is charged to either you, or your funder, institution or employer.
Open access publishing is not without costs. *Caryologia* therefore levies an article-processing charge of € 150.00 for each article accepted for publication, plus VAT or local taxes where applicable.

FREQUENTLY-ASKED QUESTIONS (FAQ)

Who is responsible for making or arranging the payment?
As the corresponding author of the manuscript you are responsible for making or arranging the payment (for instance, via your institution) upon editorial acceptance of the manuscript.
At which stage is the amount I will need to pay fixed?
The APC payable for an article is agreed as part of the manuscript submission process. The agreed charge will not change, regardless of any change to the journal's APC.
When and how do I pay?
Upon editorial acceptance of an article, the corresponding author (you) will be notified that payment is due.
We advise prompt payment as we are unable to publish accepted articles until payment has been received. Payment can be made by Invoice. Payment is due within 30 days of the manuscript receiving editorial acceptance. Receipts are available on request.
No taxes are included in this charge. If you are resident in any European Union country you have to add Value-Added Tax (VAT) at the rate applicable in the respective country. Institutions that are not based in the EU and are paying your fee on your behalf can have the VAT charge recorded under the EU reverse charge method, this means VAT does not need to be added to the invoice. Such institutions are required to supply us with their VAT registration number. If you are resident in Japan you have to add Japanese Consumption Tax (JCT) at the rate set by the Japanese government.
Can charges be waived if I lack funds?
We consider individual waiver requests for articles in Caryologia on a case-by-case basis and they may be granted in cases of lack of funds. To apply for a waiver please request one during the submission process. A decision on the waiver will normally be made within two working days. Requests made during the review process or after acceptance will not be considered.
I am from a low-income country, do I have to pay an APC?
We will provide a waiver or discount if you are based in a country which is classified by the World Bank as a low-income or a lower-middle-income economy with a gross domestic product (GDP) of less than $200bn. Please request this waiver of discount during submission.
What funding sources are available?
Many funding agencies allow the use of grants to cover APCs. An increasing number of funders and agencies strongly encourage open access publication. For more detailed information and to learn about our support service for authors.
APC waivers for substantial critiques of articles published in OA journals
Where authors are submitting a manuscript that represents a substantial critique of an article previously published in the same fully open access journal, they may apply for a waiver of the article processing charge (APC).
In order to apply for an APC waiver on these grounds, please contact the journal editorial team at the point of submission. Requests will not be considered until a manuscript has been submitted, and will be awarded at the discretion of the editor. Contact details for the journal editorial offices may be found on the journal website.
What is your APC refund policy?
Firenze University Press will refund an article processing charge (APC) if an error on our part has resulted in a failure to publish an article under the open access terms selected by the authors. This may include the failure to make an article openly available on the journal platform, or publication of an article under a different Creative Commons licence from that selected by the author(s). A refund will only be offered if these errors have not been corrected within 30 days of publication.

Caryologia

2022
Vol. 75 – n. 3

International Journal of Cytology, Cytosystematics and Cytogenetics

Table of contents